ASSESSING THE FEASIBILITY OF COMBINING REFLECTANCE SPECTROMETRY WITH PHYTOGEOCHEMICAL EXPLORATION TECHNIQUES FOR THE DISCRIMINATION OF THREE GEOLOGIES ON THE WITWATERSRAND BASIN GOLD FIELDS, SOUTH AFRICA

Miranda Hanli Wilson
Student number: 0613700J

A Dissertation submitted to the Faculty of Science, University of the Witwatersrand, in fulfilment of the requirements for the degree of Master of Science

School of Computer Science and Applied Mathematics

University of the Witwatersrand, Johannesburg, South Africa

March 2017

Supervisor:

Professor Michael Sears, School of Computer Science and Applied Mathematics, University of the Witwatersrand

DECLARATION

I declare that this Dissertation is my own, unaided work. It is being submitted for the Degree of Master of Science at the University of the Witwatersrand, Johannesburg. It has not been submitted before for any degree or examination at any other University.

_____

(Signature of candidate)

29th Day of November 2017 in Johannesburg

ABSTRACT

Mineral exploration is expensive, logistically challenging and can be detrimental to the environment. In addition to the physical disturbed of geological sampling, artisanal miners, charcoal burners and poachers follow in the wake of geological exploration teams, resulting in severe environmental degradation. The remote sensing of geological features is used in conjunction with geophysics to help refine the amount of ground based sampling where the surface geology is exposed (e.g. deserts, barren surfaces and rocky outcrops). However, it is not feasible to use these geological remote sensing techniques the earth's surface is covered with vegetation. Studies have shown that plants respond to mineral nutrients or conversely toxicities in their growing environment, including metal concentrations in the soil, either through the presence or absence of particular species, or by exhibiting physiological or phenological changes in response to depleted or elevated substrate metal concentrations. The use of plant species composition and foliar elemental contents (methods known collectively as phytogeochemical exploration) have been successfully used to detect ore-bodies. Visible changes in leaf structure and chemical composition as a result of deficiencies in elemental nutrition or toxicities have been well-researched from botanical and soil science aspects, and are widely used for agronomic applications, but have yet to be exploited for mineral exploration.

This study assessed the feasibility of using remotely-sensed spectral reflectance signatures of tree foliage to detect changes in substrate elemental concentrations across three geologies on the Witwatersrand Basin. The study comprises of an outcropping metal-rich ore body, the Black Reef (quartzite), flanked by dolomite to the South East and Ventersdorp Lavas to the North West. The soils of these three parent geologies can be expected to exhibit differences in plant nutrient availability, as well as deficiencies or toxicities. Each geology on the study site was characterised and classified into landscape functional types to account for aspect, position on the catena and soils characteristics, all of which could mask, conflict or auto correlate with any observed changes in vegetation stress spectral signatures associated with the changing geology. Three tree species with continuous across the study

site were selected: *Searsia lancea* (L.f.) Moffet (previously *Rhus lancea*), *Euclea crispa* (Thunb.) Guerke var crispa and Acacia karroo Hayne.

The study determined how the foliar and substrate elemental concentrations and uptake ratios differed between the three tree species, the three geologies and the landscape functional types. The study then related plant spectral response of three tree species to geology, landscape function type and to the foliar and substrate elemental content. Soil elemental concentrations were analysed and it was found that the three parent geologies could be classified by their relative concentrations of Mn, Cr, Ti, Cu Cr, Pb, Ba, Fe, and Zr in the soils. The findings revealed that the plants showed changes in physiological status associated with geology which were detectable through the use of vegetation indices. The study made use of eight different vegetation indices (NDVI, NDWI, PSRI, Red-edge NDVI, red-edge position, red-edge inflection point, and the 725/702 ratio of the first and second derivative), derived from handheld hyperspectral data. The three species differed in their spectral response to the changes in geology and in their stress response to elevated metal content on the Black Reef ($p < 0.05$). Regression (linear and non-parametric) was used to identify which foliar and substrate elemental concentrations most affected spectral response. The *A. karroo* samples were found to be most affected by Mn, Ti, Fe and Sr. The *S. lancea* samples were found to be most affected by As, Cu, Pb and Sn and the *E. crispa* response was found to be most affected by Cu, Mn, Na, Ni, Rb, Zn, and Zr ($p < 0.01$). In order to identify the changes in geology, it was found to be necessary to first classify the spectral response of the three species, and then detect spectral variations within each species class, as the species-specific spectral responses to changes in geology were significantly different ($p< 0.05$). The study successfully classified the three tree species according to their spectral response through the combined use of the eight vegetation indices. However, it was found that a subset of the samples which had either much higher or much lower elemental concentrations in the leaves and soils than the remaining samples for that species, showed a plant stress response which affected the spectral response of the plants sufficiently to result in an incorrect species classification.

In conclusion, the finding of this study showed that VIs can be used to detect differences in spectral response between trees growing on different geologies. It was found that the combination of vegetation indices can be used to determine a “typical” spectral response per species, but that where the growing conditions were particularly stressful, the stress response could alter the plant spectral response sufficiently to result in a misclassification of the sample by species. Further work is required to validate this observation, and to investigate how more sophisticated spectral analysis could be used to distinguish between taxonomic and substrate induced spectral variation, before it would be possible to scale this work up to a canopy-scale remote sensing tool.

To my mother, as my father still has his brains

ACKNOWLEDGEMENTS

Firstly, I must thank Isabel Weiersbye, head of EEPP, for conceptualising this study, for her mentorship and not least, for the funding provided to me by the Ecological Engineering and Phytoremediation program (EEPP) and THRIP to complete this study. I owe another huge thank you to the EEPP team for their support and assistance and provision of facilities and technical lab assistance during the processing and analysis of the samples. To AngloGold Ashanti Ltd South Africa region for the use of their site to perform this study. Thank you to Bruce McLeroth and Kloppers from Red Earth cc for their assistance with the field work in the characterisation of the soils and to David Tongway for his assistance with the landscape function analysis and defining the landscape functional types. I received amazing support from Devlyn Hardwick during the initial supervision of this project, and vast amounts of support and patience from Michael Sears, who took over the supervision of this project from Devlyn.

Thank you to my loving family for all their support and sacrifices to ensure I had the best education, and to my wonderful husband for keeping me going through the long hours of fieldwork, lab work and writing up, and for being a fantastic sounding board and teacher.

TABLE OF CONTENTS

List of figures

LIST OF TABLES

1 12

1. INTRODUCTION

1.1. General Background

In recent years the amount of public pressure placed on mining companies to conduct environmentally acceptable operations has increased considerably. Historically, trends have shown that developing countries tend to have less stringent environmental legislation which allows for increased pollution throughout the mining lifecycle [1]. Multinational corporations may take advantage of these "pollution havens", which often offer the added benefit of having access to cheaper labour and resources [1]. There is, however, increased public pressure for responsible mining, particularly for large multinational corporations which are listed on international stock markets, and many governments and companies have realised the benefits of more sustainable and environmentally-friendly mining operations [2].

In South Africa, environmental legislation has become more stringent, and companies are held liable for the damage or disturbance caused by their operations [3]. This applies not only to the extraction of minerals from the earth, but to the exploration and post-mining stages too. Traditional methods of mineral exploration are both labour and energy-intensive and carry a high cost. They involve making paths and roads, clearing tracts of land in order to access sampling points, digging of soil pits and then drilling to collect samples [4]. Drill pads need to be level and large enough for the rig and compressors, which means that vegetation must be cleared for earthworks to be constructed. The areas that are cleared for drilling, and for roads to access sites become vulnerable to environmental degradation in the forms of erosion, and of colonisation by invasive plant species, and provide increased access to what may have been remote and pristine areas, allowing other parties access for activities such as hunting, logging and artisanal mining [4], [5]. Exploration activities can therefore compromise the availability of renewable natural resources and directly impact on the livelihoods of local peoples.

Invasion of previously undisturbed natural areas by artisanal miners, illegal access to protected resources such as ivory, animal trade, bush meat and rare plants, and trafficking of drugs and arms are detrimental impacts [5]–[7]. Forest carbon loss, erosion, local extinctions of flora and fauna may result in the loss of potential earning for countries under the new USAID and UN Policy REDD, which is designed to pay billions of Euros to those countries that can demonstrate forest conservation as opposed to exploitation [5]. In addition to this, conflict over land use has been a major contributing factor to a series of wars in Central African countries [8], [9]. By facilitating widespread and diffuse disturbance of natural areas through exploration for ore deposits, mining companies in such regions therefore expose themselves to the potential abuse of human rights and resources, and that can result in the loss of their social and legal license to operate [9]. As a result, for the early stages of mineral exploration, which involve the measurement of rocks and soils over vast tracts of remote landscapes, it is imperative that non-invasive and low disturbance methods are developed to detect anomalously high metal concentrations and reduce the impact of ground-based exploration activities.

Ground-based phytogeochemical exploration has long been used as a prospecting technique. Phytogeochemical exploration is the use of plants as an indicator of the presence of specific elements within the substrate. Both the health and distribution of vegetation may be indicative of underlying geological features or the presence of mineral ore bodies [10], [11]. Botanists acquire the information through the use of direct field observations, followed by chemical analyses [10]. This approach has been used successfully to identify the distinctive metallophyte flora associated with localized ultramafic outcrops with deposits of nickel, cobalt, copper and platinum group metals in many regions – such as the Katanga mining region of the D.R.C., New Caledonia, Australia and New Zealand [12]–[14]. Phytogeochemical exploration techniques have also been successful for gold prospecting for ore bodies at depths of up to 30m in the Tanami desert region of Australia and in Papua New Guinea, where the deep colluvial and alluvial cover makes soil sampling an inaccurate measure of underlying mineralized rock [15], [16]. However, while phytogeochemical exploration is less labour intensive and more efficient than traditional soil sampling techniques, it is still intrusive and dependent on extensive

ground-based surveys [16]. It would be more energy and cost-effective to reduce the amount of ground-based sampling required through the use of remotely sensed spectral reflectance data, associated with a restricted set of ground-truthing surveys for validation [4], [15], [17].

Currently, both multispectral and hyperspectral remote sensing of the characteristic reflectance spectra of minerals within soils and rocks are widely used for mineral exploration, but their utility is limited where cloud, mist or vegetation masks the earth's surface [10], [18]. In cases such as these, geologists would have to rely on traditional soil sampling techniques or geophysical surveys, but these again have challenges in terms of scale, cost and accessibility [10], [18]. As an alternative, the remote sensing of vegetation cover and plant health could be used as an indicator of changes to geology [10], [19]. A vast proportion of the Earth's land surface is covered in vegetation, snow and built up areas, and there is only approximately 30% of the Earth's surface which is suitable for the traditional geological remote sensing techniques. There would be value in increasing available exploration techniques by creating a deeper understanding the relationship between plant spectral characteristics and the underlying substrate conditions, and how to quantify this for a highly heterogeneous environment [19].

One of the ultimate outcomes of this study would be to develop a means of using remotely sensed measures of vegetation health and productivity as an indicator of the status of the underlying substrate as an alternative to invasive primary exploration techniques, or as a tool for the refining of broader scale exploration targets.

1.1.1. Plants and Heavy Metals

Records dating as far back as the early Sanskrit writings have noted that there is a relationship between plants and the underlying geology [10]. Over time, studies have expanded on this topic to the extent that plants are being considered as reliable indicators not only of the presence of certain minerals or elements, but of the relative concentrations of those elements present in the soils too

[20], [21]. Plants respond to changes in the geochemistry of the substrata in a number of ways. The most readily detectable of these is a taxonomic response: the absence or presence of a certain species, such as the Zambian Copper flower, *Becium centraliafricanum (B. homblei)* found on the copper barrens in the Copperbelt of Zambia and the Katanga region of the DRC [11], [22], or the presence of natural populations of *Senecio coronatus* as an indicator of serpentine soils in the Badplaas region of South Africa [23]. Plants have specific nutrient requirements, where a range of minerals is required for the successful completion of the lifecycle of the plant. These requirements differ between species. Plant species that have evolved the ability to tolerate concentrations of elements exceeding the range normally required for plant nutrition and which only occur in soils which contain those high concentrations are known as metallophytes [24], [25]. Geology has long been noted as a determinant of habitat preference in plant species, and certain plant species have been studied to the extent that their presence can be used as an indicator of both soils and underlying geology [11], [12], [26], [27]. The use of plants to determine information regarding the underlying geology and geochemistry is one of the established techniques used in phytogeochemical exploration [10], [12]. However, the field of phytogeochemical exploration has gone beyond the use of plant presence as an indicator of geology [28]. Plants respond to their growing conditions in a number of ways. A structural response to soil geochemistry can be expressed as morphological changes such as dwarfism. Phenological changes such as disturbances in the rhythmic patterns of seasonal senescence and flowering can occur. Physiological changes such as changes in nutrient allocation and water-use patterns may take place, and biochemical processes such as pigment synthesis may be altered [29], [30]. Any one of these changes may result in altered spectral responses in the plant [29]. Therefore, changes in pigment synthesis, flowering and senescence patterns and the presence or absence of particular plant species can all be used as indicators of variation in soil geochemistry [31]–[33].

Elemental composition of plants can also be affected by the changes in nutrient availability as a result of the substrate geochemistry, and therefore an assay of plant tissue can provide information on the elemental composition of the underlying substrata [4], [31], [34]. For example, Brooks *et al.*

(1977) analysed herbarium samples collected from around the world for Nickel, and used the results combined with the geographic locations of these samples to pinpoint areas rich in nickeliferous rocks ([12]. While these techniques still require optimisation, there have been several studies which have been successful in putting theory into practice [4], [11], [12], [16], [35].

1.1.2. The ability of plants to take up metals

It is possible to use certain plants to determine characteristics of the underlying geology because plants require certain elements for their physiological and metabolic processes. They have therefore developed mechanisms of acquiring the elements necessary for their nutrition by solubilising ions in the surrounding soils [10], [36], [37]. The uptake of elements is governed by the ionic size and charge of the element being taken up, and as a result, the methods of acquiring ions differ depending on the plants and elements in question. For example, some elements may be taken up actively, such as the divalent cations, Cu^{2+}, Zn^{2+} and Ni^{2+}, which are actively taken up through root cell membrane proteins, in exchange for H^{+} ions [36]. Other elements may only be taken up through passive diffusion, whilst others may be excluded, either through active exclusion or passive barrier mechanisms [38], [39]. Elements that have been absorbed through the roots may then be transported to the rest of the plant, although the rate at which this occurs is dependent on the presence of root-shoot translocation mechanisms, osmotic pressure and transpiration rates [36], [40].

While plants need certain concentrations of a variety of metals as macro and micronutrients for metabolic processes, some plants exceed the required uptake for these metabolic processes, which may result in the plant suffering metal toxicity, especially if the bioavailability of the element is increased by anthropogenic activities such as acid mine drainage (AMD) or a wide range of other factors [39], [41]. However, there are a select number of plant species which have the ability to tolerate exceptionally high concentrations of metals into their biomass without suffering from metal toxicity. There are three broad categories of metal tolerant plants.

The first category, metal *excluders* are plants that take up the amount of each metal that they require for their metabolic processes and no more. These plants have often evolved on metal rich sites, and have developed this adaptation so as to reduce the likelihood of suffering from metal toxicity from accumulating high concentrations of metals [39], [42] .

The second category is the *accumulators* which have the ability to take up high concentrations of metals in their biomass without suffering from metal toxicity. To qualify for this category, the plants must be able to continue all stages of the lifecycle without showing signs of plant stress or toxicity. The plants manage this by detoxifying the metals as they take them up into the cells [39], [42]. Hyperaccumulators are an extreme example of those species, as they are capable of accumulating metals to hundreds of times the levels of non-accumulator species, and often to hundreds of times the concentrations in the surrounding environment [42], [43]. In some cases this may present a problem when hyperaccumulator species are used in mineral exploration, as they may present a false indication of the underlying substrata [10]. Alternatively, hyperaccumulators have been used to identify very low concentrations of elements which may be difficult or expensive to detect in the soils.

A third category consists of the *indicators*, which are plants that have the ability to absorb some metals to the same concentrations as they exist in the rhizospheric soil. These plants appear to have little control over restricting the uptake of these metals from the soil, so while they may be able to take up high concentrations of a metal, they lack sufficient mechanisms for sequestering the metal within the cells, and so the plant will often suffer from physiological stress as a result of metal toxicity, and the least tolerant of the species will die [21], [42]. Because these plants accumulate metals to concentrations similar to those in the soil solution, one can measure the metal content within the plant to use as a biomarker of the metal content in the soil solution (although this soluble fraction of metal may not always reflect the total metal concentration of a soil). Fortunately for the field of phytogeochemical exploration, around 95 % of all plant species fall somewhere between the two extreme categories and are capable of accumulating metals to some extent [10], [25] .

In order for plants to accumulate metals, the metals must be in a bioavailable form, meaning that they are either present in the soil as free metal ions or soluble metal complexes, or they have been adsorbed to inorganic soil constituents at ion exchange sites [10], [39]. The bioavailability of metals within the soil depends on a number of factors. Foremost, some metals occur more readily in bioavailable forms, while others are typically less bioavailable. For example, lead (Pb) occurs as a soil precipitate which is not readily bioavailable. However, soil characteristics, pH and Eh in particular, affect the bioavailability of metals. The bioavailability of most elements is influenced by the pH of the environment that they are in. Many metals become more readily bioavailable in more acidic environments. This is due to increased competition with H_+ ions for soil binding sites, which causes the metal ions to break off into solution [10], [36]. The interactions between plant roots and soil microbes can also influence and increase the bioavailability of metals in the rhizosphere. This is achieved by the roots secreting protons, organic acids and other compounds which can solubilise minerals and mobilise metals and metalloids within the soil, thus enhancing uptake by plant roots. Root-colonising bacteria and mycorrhizae have also been known to catalyse redox transformations such as Pb^{2+},Hg^{2+}, Au^{3+}, Te^{4+}, Ag^{+}, increasing the bioavailability of these metals [10], [44]. The hyphae of mycorrhizae also increase the root absorption area, which allows for more nutrient uptake [44], [45]. However, regardless of the amount of root absorption area, metals cannot be taken up by plants without the correct transport proteins, due to the ionic charge of the metals which prevents them from moving freely across cellular membranes [36], [39]. This prevents the plant from taking up non-essential metals, or metals that would be harmful or toxic, although in some cases non-essential metals are still taken up in the roots when the transporters do not differentiate between two or sometimes more metals. For example, cadmium (Cd) is frequently absorbed instead of calcium (Ca), despite the fact that it is highly toxic to most plants [39]. Some plants have mechanisms which inhibit the stimulation of transporter activity when there is a high influx of metal ions from the soil, in order to prevent an over accumulation of a particular metal [39].

Even in plants which can tolerate metals, the increased concentrations of these metals inside the plant will affect important functions and processes [10]. Photosynthesis is one of the most metal sensitive metabolic processes, and as a result one of the indicators of plant metal stress is leaf chlorosis (yellowing of the leaves) due to the reduction of chlorophyll production. This is one of the structural changes mentioned above which is most easily measurable as a spectral change when there is a change in the geochemistry [10], [29].

1.1.3. Basic principles of Spectrometry

The plant spectral response to the leaf chlorophyll content is one of the most widely used measures in the remote sensing of vegetation. When combined with measures of plant water content, structure and other pigments, it is possible to derive volumes of information through the use of spectrometry [46]. To gain accurate results from spectral analysis, it is important to understand the basic principles of spectroscopy.

Spectroscopy is the study of the interaction between light and the object with which the light is interacting [47]. When light strikes an object, three possible interactions can occur: transmission, absorption or reflection [48]. Most remote sensing techniques focus on the fraction of the light that is reflected from the surface of an object, whereas for microscopy the absorbed and transmitted light are of key importance [49]. However, the absorbance and transmission of light is not disregarded completely in remote sensing. Materials such as water tend to absorb light at certain wavelengths. This is of particular importance as water vapour is a major constituent of the atmosphere. As incoming solar radiation passes through the atmosphere, the energy is scattered by atmospheric constituents. Further scattering occurs as light is reflected and this may influence the spectral reflectance of targets on the ground [48]–[51]. The wavelength at which light is scattered, absorbed or reflected is key.

Remote sensing focuses on measures of reflected light, using peaks and troughs in the reflectance spectrum to distinguish between different substances.

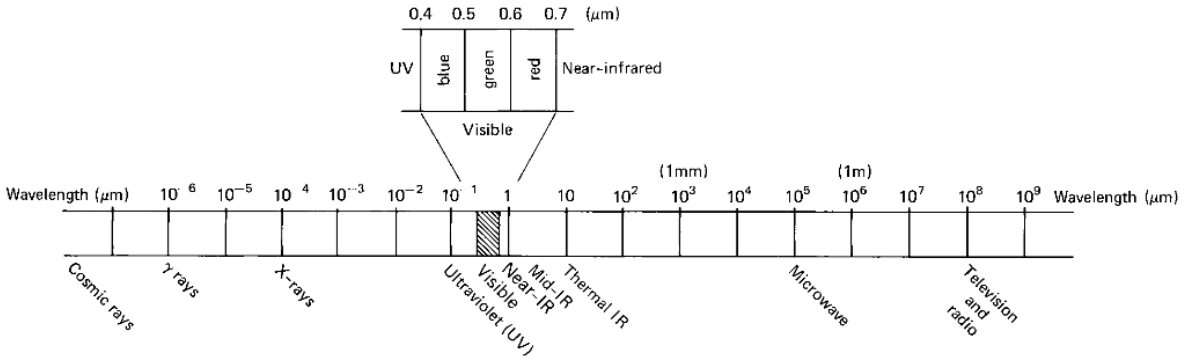

Figure 1-1 The electromagnetic spectrum (source: Lillesand et al, 2011, p 5)

The broad range of sensors that are used under the umbrella term of remote sensing encompasses a large portion of the electromagnetic spectrum shown in Figure 1-1. Applications for geophysics and geological mapping use a wider portion of the electromagnetic spectrum than that which is used for remote sensing of vegetation [52]. Remote sensing of vegetation focuses predominantly on the region of the electromagnetic spectrum from the blue wavelengths at 0.4 μm (400nm) to the Near Infrared (NIR) at 0.8 μm (800nm) where absorption and reflection of plant pigments is most pronounced. Water content and structure of plants is mostly detected in the Mid- and Shortwave-infrared bands (1200nm-2000nm), and limited use is made of the thermal or long wave length infrared wavelengths from 3 μm to 10μm for the purposes of the remote sensing of vegetation [53], [54]. The visible and near infrared portions of the electromagnetic spectrum are most commonly used, as this range gives sufficient information for basic analysis, and the sensors that are used to capture the light in this range are also simpler, cheaper and easier to use when compared to short-wave Infrared and thermal sensors [49]. By comparison, geological remote sensing makes extensive use of SWIR and Thermal IR data for the detection of geological features, which can also makes the collection of data more expensive [18].

Spectrometry, the actual physical measure of light, can be performed using a number of methods. Types of sensors that detect reflected light may be handheld devices which record reflected light as

spectral data, or image sensors which capture the information as pixels within an image. These sensors can be used at a range of scales [55]. Hand-held devices are usually used at the leaf or canopy scale, whilst image sensors are mounted on unmanned aerial vehicles (UAVs), normal aircraft and satellites. The type of analysis and resolution required and the available budget will often determine which sensor is used [48], [49], [55]. Three types of resolution are particularly significant for remote sensing: spatial resolution, which is the size of the pixels in the image; spectral resolution, which is the number of spectral bands and the width and position of those bands within the electro-magnetic spectrum; and the temporal resolution of the data, which is how frequently the data is collected. For satellite imagery, the options are much more limited [48], [55]. The temporal resolution of satellite imagery is determined by the revisit schedule for a given satellite and the cloud cover in an area, whereas a UAV has nearly unlimited capacity to revisit a site [56].

Spectral resolution can be broadly divided up into panchromatic, multispectral and hyperspectral data. Multispectral data is characterised by having a limited number of bands, each of which cover a fairly broad range of wavelengths (usually around 100nm-200nm but sometimes wider). The bands are usually for discrete sections of the EM spectrum, as opposed to hyperspectral imagery, which has narrow bands (usually between 2nm-10nm) which are contiguous in the range of the EM spectrum that is being covered. Panchromatic data covers a broad section of the EM spectrum i.e. from blue to red, in one single band [55]. For many years the minimum spatial resolution for satellite imagery was limited to 2m for multispectral imagery, and most commercial satellites were built at these specifications, which were guided by a legal requirement which stipulated that commercial satellite imagery could not be sold at a higher resolution than 2m for multispectral imagery and 50cm for panchromatic imagery [57]. A limited number of commercial satellites, such as Worldview 3, now have the capabilities to collect multispectral imagery at sub-metre resolution. Now that the regulations have changed, this higher resolution imagery comes at a premium price [57]. Non-commercial satellites such as LandSat and ESA Sentinel have a lower spatial resolution, but cover much larger areas with each pass and can be more easily accessed without cost barriers.

1.1.4. The remote sensing of vegetation

The use of a wide range of remote sensing tools has made it possible to evaluate reflectance spectra at a broad range of scales, from single leaves to the canopies of entire forests. The use of equipment such as a hand-held spectro-radiometer allows us to measure reflectance values at very narrow bands (1-2nm intervals), making it possible to detect small shifts in precise portions of the spectral signature for more refined remote sensing work [58]. In contrast, many of the commercial 4-band (Red, Green, Blue and Near infrared band) multispectral sensors, such as GeoEye, Pleiades, Spot 6 and Quickbird, collect the basic information required for more generalist remote sensing work where differentiating between different land cover surfaces is the main purpose [49]. It is possible to differentiate between surfaces such as concrete, bare soils, vegetation and water because they have very different spectral signatures, as discussed previously [47].

The dominant feature that is used to detect vegetation and distinguish it from other surfaces—such as green painted roofs—is the steep slope between the red and Near Infrared (NIR) portions of the EM spectrum. Vegetation has this feature due to the absorption of light in the red portion of the EM spectrum due to the chlorophyll content in plants, and the internal cellulose structure of the plant which reflects light in the NIR bands [54], [59], [60]. This steep slope is known as the Red-edge and is one of the most well-studied and well-used features in the remote sensing of vegetation [49].

There are numerous additional spectral features which have been associated with foliar structure and chemistry. Curran (1989) described the key spectral absorption features from 400nm to 2400nm that correspond with specific foliar chemical composition [53]. Table 1-1 provides a summary of the absorption features that are used in remote sensing for vegetation. These features can be used as indicators for a number of purposes, from differentiating vegetation from other materials, to differentiating between plant species and assessing plant health and nutritional status [61].

Table 1-1 Summary of absorption features used in remote sensing to assess vegetation between 400nm to 2400nm (after [53])

Chemical composition	Visible colour bands (400nm-700nm)				NIR (700nm – 1100nm)				Mid-IR (1200nm – 2000nm)				SWIR (2000nm-2400nm)	
Wavelength: (nm)	400	500	600	700	800	900	1000	1100	1200	1400	1600	1800	2000	2200
Chlorophyll a	430		660			900								
Chlorophyll b	460		640											
Carotenoids														
Anthocyanins		520												
Proteins						910	1020				1510, 1690	1980	2060, 2130, 2180	2240, 2300, 2350
Starch						970, 990			1200	1450, 1530, 1540, 1580	1690 1780	1900 1960	2000, 2080, 2100	2250, 2270, 2280, 2320
Oil						970	1040							2310
Water						970			1200	1400, 1450				
Lignin								1120	1200	1420, 1450	1690			
Cellulose									1200	1490, 1540	1780	1820		2100, 2270, 2280, 2340, 2350
Sugar										1450, 1490, 1580,	1780,	1960	2080,	2270
Nitrogen										1510,	1690		2060, 2180	2300, 2350

There are many techniques which can be used to perform analysis. One of the most commonly used techniques is that of Vegetation Indices (VIs). A vegetation index is a type of spectral index, a mathematical formula used to derive information from selected bands of spectral data relevant to a specific purpose. Vegetation indices are most frequently either a simple band ratio (R_x/R_y) or a normalised difference band ratio ($R_x - R_y)/(R_x + R_y$), where R_x is the reflectance at the given wavelength x, but may be calculated from more complex band combinations or derivatives of spectral data [61]. One of the most widely used VIs is the Normalised Difference Vegetation Index (NDVI) [61]–[63]:

$$\mathrm{NDVI} = \frac{(R_{800} - R_{680})}{(R_{800} + R_{680})}$$

This index estimates the slope from the absorption feature present in healthy vegetation in the red bands and the reflectance peak in the NIR related to chlorophyll content and leaf structure. Vegetation indices such as the NDVI detect plant productivity or stress by determining the relative leaf chlorophyll concentration, while the Normalised Difference Water Index, is used to determine plant leaf relative water content:

$$\mathrm{NDWI} = \frac{(R_{857} - \mathrm{R}_{1241})}{(R_{857} + R_{1241})}$$

Plants with low chlorophyll or water content may be showing signs of stress for a wide range of reasons, from drought stress or overgrazing to acid mine drainage (AMD) and consequent pH declines [64], [65]. Combining a number of vegetation indices (VIs) may provide more detailed information on causality. For example, it has been found that trees growing on AMD-polluted ground water at Highveld gold mines in South Africa show a high leaf water content (high NDWI) but low chlorophyll (low NDVI) content. Pollutants in the ground water are known to impair tree performance [66], [67] despite sufficient access to water, and this can be detected by comparing the two vegetation indices [68]. However, at higher salt concentrations in the groundwater, tree roots are unable to acquire the water due to its high osmotic potential, and thus suffer from `physiological drought'. This would be expected to result in a lower leaf water status and NDWI.

Derived vegetation indices (ratios) such as the Red-edge stress signature have been used to identify a number of different stressors in plants, and could be particularly useful in detecting vegetation stress related to pollution [64], [69]. These indices may be more sensitive to smaller shifts in the spectral signatures of plants than the NDVI, which has been shown not to be highly effective at determining exact quantitative assessments of chlorophyll content in plants [70]. Certain stressors, such as heavy metals, may cause either a shift of typical leaf signature towards the ultraviolent portion of the electromagnetic spectrum, known as a blue shift, or a shift towards the infrared portion of the electromagnetic spectrum, known as a red shift [59], [69], [71].

Vegetation indices have been found to be a quick method for collecting data about the physiological status of plants from the reflectance spectrometry of plant surfaces [64]. Vegetation indices have a broad application as they can be used for both multispectral and hyperspectral data. Many of the other techniques used in image and spectral data processing are more specific to either multispectral or hyperspectral data. Spectral indices have both the advantage of simplifying large amounts of data and only extracting key information, and the disadvantage of limiting the information analysed to a very small portion of the electromagnetic spectrum. They are often therefore valuable as a 'first pass' technique of assessing a scene before selecting more in-depth analytical techniques.

1.2. Research problem statement

The aim of this study was to determine whether it is feasible to use Vegetation Indices (VIs) and other spectral analytical techniques derived from reflectance spectrometry of tree leaves to infer substrate geochemistry, by assessing the relationship between the relative concentrations of metals in the substrate, and the spectral properties of the tree leaves. The study also identified constraints towards using this approach for mineral exploration. While this technique would be most applicable in ecologically sensitive and inaccessible areas such as the Congo Basin where vegetation cover prevents the use of certain other geological remote sensing techniques, it was too costly and logistically difficult to perform trials at such a location. This study was therefore based at a well characterised site situated on the Witwatersrand Basin. A central hypothesis in this study is that substrate geochemistry, in terms of the relative concentrations of heavy metals, results in structural and biochemical changes to plant leaves that are detectable from canopy or leaf reflectance signatures. The study assessed whether there is a difference in the presence or magnitude of the foliar stress response for plants growing on soils which are not metal-enriched and conspecific or congeneric plants that have evolved in metal-rich soils at the same locality.

The study is of value as a non-invasive preliminary mineral exploration tool, for contaminant mapping for risk assessment or remediation purposes, and for the identification of conservation priority areas such as habitats which may contain metallophyte flora, in order to plan how best to mitigate the damage related to mining activities.

1.3. Research Objectives

To test this hypothesis, the objectives that are addressed are as follows:

(i) To broadly characterise the physical characteristics of the study site in terms of (a) vegetation structure, (b) landscape functional types, and (c) soil characteristics, in order to account for environmental variables when selecting the study sampling plots.

(ii) To determine whether plants growing on metal-rich soils at the study site exhibit higher levels of foliar stress by comparison with conspecifics or congenerics on adjacent non-metal-enriched soils, and determine whether the responses inferred from leaf reflectance signatures and derived spectral products can be related to (a) foliar, and (b) substrate, metal concentrations.

1.4. Research Approach

This dissertation is divided into two content chapters structured systematically to address the research objectives discussed above. The study involved the collection of field samples and data, laboratory measurements and a combination of spatial and non-spatial statistical analysis of data to answer the research questions. The field work was completed over the period from January 2012 to March 2013. The research questions based on the spectral differences as a result of substrate geochemistry could not be answered without first understanding the effects that topography, localized vegetation distribution and surface cover may have on the spectral response of vegetation. Therefore, part of the first objective, the study site characterization, was completed before the sample and data collection for the remainder of the study could be completed. Soil samples that were collected were used to further validate the study site characterisation techniques, as well as provide background geochemistry information for the study of the plant material through elemental and spectral analysis. Chapter 2 further investigates whether the catenal effects play a role in determining plant spectral reflectance, or whether the underlying geology and geochemistry plays a stronger role. This chapter compared responses from vegetation indices and spectral derivatives to landscape function types within geologies and identified significant differences between geologies, but fewer differences between landscape functional types within the same geology, which indicates that the catenal effects played a lesser role in plant health than the substrate geochemistry.

Chapter 3 demonstrates how the preliminary findings in the previous chapter are further validated through the comparison of the soil elemental contents of the three geologies that have a strong influencing effect on the plant spectral response at a leaf level. Elemental ratios which are used as indicators of plant nutritional status, plant health, soil fertility and elemental bioavailability are all investigated to understand the influence of geology and soil geochemistry on plant metal uptake and spectral response. Regression analysis and grouping statistics were used to identify which elements accounted for the changes in spectral response most strongly. The concluding chapter summarises the findings and discusses the next steps for furthering this work.

1.4.1. Background of the Study Area

The study area is located on the Klerksdorp goldfields in the North West Province of South Africa. The physical study site is situated at AngloGold Ashanti Ltd.'s Vaal River Mining Operations near Orkney. The region is semi-arid, with the majority of the rain falling from December to March. The Mean Annual Precipitation (MAP) is less than 600 mm, and Mean Annual Potential Evapotranspiration of more than twice MAP. The Klerksdorp goldfields form the westernmost part of the West Rand Group of the Witwatersrand Supergroup located within the Kaapvaal Craton. The Klerksdorp goldfields have been an economically important gold-producing area since the late 1880's and are still being actively mined at present [73]. This study area is of interest due to the presence of three distinct geologies within a small geographic footprint. The formation of these features occurred between the late Archaean and early Proterozoic periods [73], [74]. Around 2714 Ma ago, the collision of the Kaapvaal and Zimbabwe cratons triggered the formation of the Ventersdorp Supergroup, which is composed of sedimentary rocks of the Witwatersrand Sedimentary Basin and the Lavas which erupted in the collision of the two micro-continents [74], [75]. The Ventersdorp Supergroup is the oldest formation in the study area. This period was followed by the rifting of the Kaapvaal craton at around 2650 Ma ago. This resulted in subsidence of the craton to below sea-level, resulting in the flooding and deposition within river systems which formed the Black Reef formation, a shallow ore body situated between the Ventersdorp Lavas and Malmani Dolomites. The reef is a narrow outcrop at surface, but is estimated to be 200-300m in width below the surface. The reef is enriched in S, Fe, Au, Co, Mn and U [74].

The formation of a shallow inland sea followed, and between 2600 and 2400 Ma ago the Malmani dolomites of the Chuniespoort group were formed by the accumulation of dolomite, iron and manganese precipitated by oxygen release from Cyano-bacteria [73]–[75]. The outcropping ridge of the Black Reef forms the main watershed across the mine site, and also forms the boundary of the dolomitic aquifer. The aquifer is relatively shallow, with the depth to ground water averaging 10m-30m. The vegetation type present on the dolomites, the Vaal Reefs Dolomite Sinkhole woodlands

(GH12), is dependent on access to the aquifer through fractures in the surface material. The majority of the trees found in this area grow in clusters in sinkholes and dolomitic or chert outcrops [72], [74].

Error! Reference source not found. shows the geology of the study site. Alternating bands of c hert-rich and chert-poor dolomites can be seen over the central and eastern portions of the mine, with the narrow outcrop for Black Reef to the west and, the Ventersdorp lavas further west. Alluvial deposits are found along the Schoonspruit and Vaal rivers.

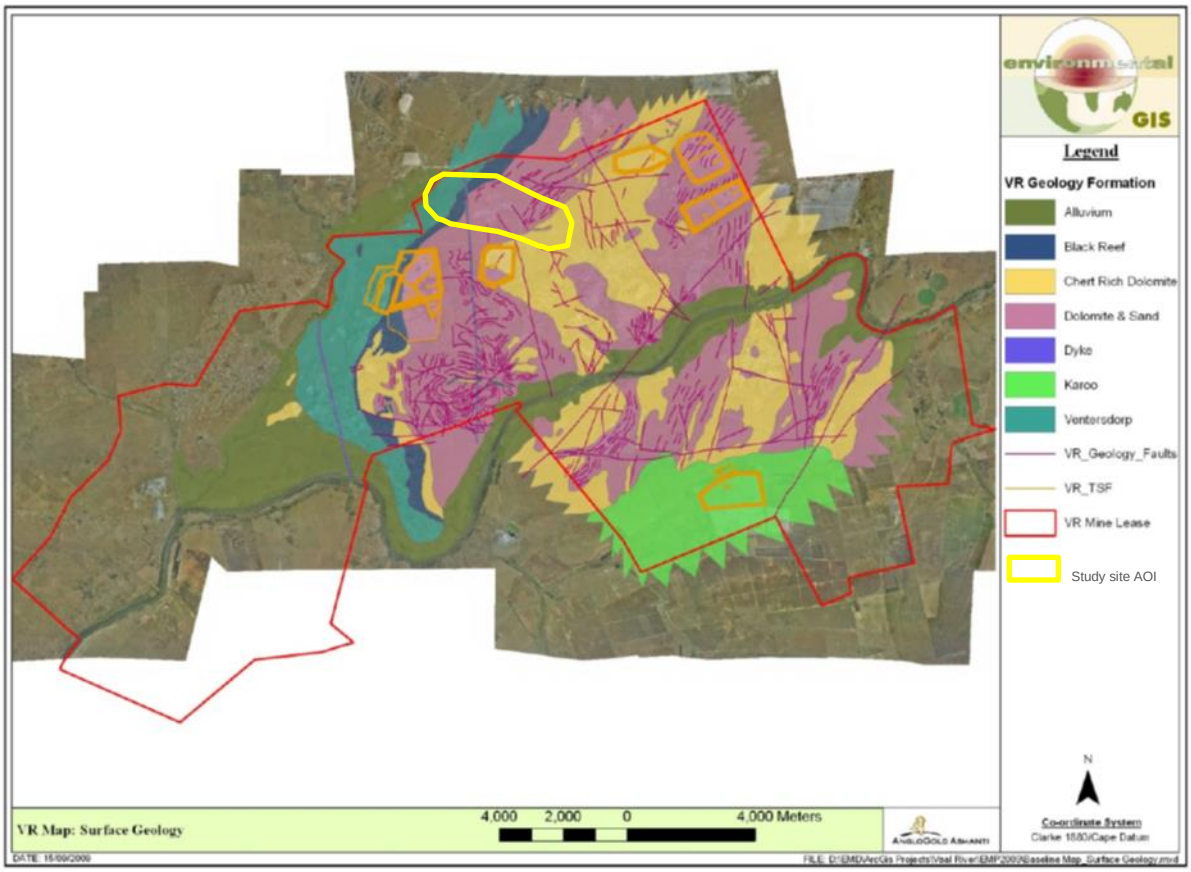

Figure 1-2 Surface Geology for the Vaal Reefs mine and study area shown in yellow. (After: ([74] **)**

2. SITE CHARACTERISATION

2.1. Introduction

This chapter covers the selection and characterisation of the study site based on geology and substrate geochemistry to account for additional variables that may also affect the plant spectral response such as catenal effects, soil types and surface roughness, plant species distribution and anthropogenic influences on the site such as historical mining. These variables need to be understood, in part because of the role that they play in potentially influencing plant spectral response, but also because they are in themselves a response to the geological features that are present in the study site. While the primary focus of this study is to understand the effects that the changes in soil geochemistry across different geologies have on plant spectral reflectance, other factors such a topography, plant species distribution, and evidence of historical or small scale mining are clues that are often used for the purposes of mineral exploration to differentiate between geologies and identify shallow ore bodies.

In order to select the site, a broad-brush approach was first used to identify a location with strongly contrasting geologies that would be of interest for mineral exploration. Once the location of the site had been narrowed down to focus on the Black Reef, an outcropping gold-bearing ore body situated between Malmani Dolomites and Ventersdorp Lavas, the next step was to identify a suitable location along this outcropping ore body which was relatively free of anthropogenic disturbance, assess the vegetation cover and identify the distribution of species across the three geologies. Landscape functional analysis (LFA) techniques were then used to characterise the selected site in terms of catenal effects and changes to soils and surface structure which may affect plant response. These results were used to divide the site up into different landscape functional types within each geology. A soils mapping exercise was completed to better understand the soils and account for variables such as in-situ versus transported material, anthropogenic contamination and interference

(dumping and borrow pits) and soil nutrient status. Soils were analysed for type, and taken to the lab for further analysis of Carbon, Nitrogen and Sulphur concentrations, and XRF and ICP-OES for the soil elemental content and bioavailability of selected elements. The dominant tree species across all landscape functional types were identified, and four phreatophyte tree species with dimorphic rooting systems (plant species with deep tap roots which access ground water for their water requirements, but obtain many of their nutrients from the surface soils through adventitious roots [67]) were selected to be used in the study. Leaf samples and leaf spectral reflectance data were collected from the selected trees.

This information is used for different purposes in this study, but the first stage of the analysis was to characterise the site and identify whether position within the catena affected the plant response. Basic vegetation indices were used to identify if there was any change to spectral response between the different geologies, and between different landscape function types within geologies, and whether catenal effects played a stronger role in determining plant spectral reflectance than changes to geology. This information was then used to justify the experimental design and analyses for the remainder of the study.

2.1.1. Target Plant Species

The plant species which have been chosen for this study are relatively evenly distributed across the different geologies at each study site. Many studies have looked at the presence of a species as an indicator of a particular geology [11], [23]. However, from a remote sensing perspective, this could limit the applicability to a much smaller suite of species and spatial range. It may be difficult to identify accurate indicator species as there are many other factors, such as water availability, topography and even habitat competition which may cause localised distributions of plant species [72]. While studies have successfully detected differences in spectral signatures between species, and even ecotypes,

using airborne hyperspectral remote-sensing, and Worldview 2 data, these techniques requires a greater understanding of plant and site-specific influences and extensive ground-truthing before they are applied on a broad scale [50], [65], [68], [76]. Using species which are ubiquitous should make it possible to detect differences in plant stress response across the study sites.

Table 2-1: List of species chosen for the study and characteristics of these species [77], [78],[79]

Species	Family	Preferred soils	Preferred habitat	Characteristics
Searsia lancea (L.f.) Moffet	Anacardiaceae	Lime soils associated with dolomites, but fairly widespread	Rocky, moist wooded slopes, open grasslands and riparian areas. Associated with sand-covered dolomitic sinkholes and underground watercourses.	Evergreen phreatophyte with a dimorphic rooting system. Leaves are rich in tannins
Ehretia rigida (Thunb.) Druce	Boraginaceae	Widespread	Generalist, grows in exposed or sheltered positions in woodlands, watercourses, rocky ridges	Deciduous, hardy
Euclea crispa (Thunb.) Guerke var *crispa*	Ebenaceae	Widespread	Exposed rocky areas and in sheltered wooded areas	Evergreen, hardy. By observation, not common on chert-poor dolomites. Similar observations in Siebert and Siebert (2005) where *E. crispa* was only present on Chert-rich dolomites.
Acacia karroo Hayne	Mimosaceae	Widespread	Generalist, but often found on grassy slopes of hills and may be found in rocky ridges	Deciduous, but may be evergreen in favourable conditions (as was found at the study site). Nitrogen fixing bacteria associated with the roots of this tree.

The first of the species which has been selected is the *Euclea crispa* (Thunb.) Guerke var *crispa,* which is part of the Ebenaceae family. The Ebenaceae family includes two genera, *Euclea* and *Diospyros,* which consist of between 500-600 species [80]. *Euclea* is a genus of sub-shrubs, shrubs or trees whilst *Diospyros* usually comprises small to medium sized tree species. A study conducted by White found 91 species of *Diospyros* and 12 species of *Euclea* in Africa [80]. However, *Diospyros* is far more prolific on the Asian continent, and much of the current research in the genus is performed in India on species which are found in the Asian tropics. *Diospyros melanoxylon* is one of the better researched species in this family [80]–[82]. It has been found that this species absorbs a number of heavy metals, both whilst in the active growth phase [82] and through activated carbon from leaf litter

[81]. Studies on the uptake of heavy metals in *D. melanoxylon* found that there was a strong correlation between soil Cu and Al and the Cu and Al content in the stems of the trees, but a negative and poor correlation respectively for the leaves. However, for Cr there was a strong correlation between soil and leaf Cr content [82]). Deo (2011) also found that the samples of leaves showed physiological signs of toxicity such as necrotic spots and leaf chlorosis. One of the first indicators of Fe and Mn toxicity is the appearance of necrotic spots on the leaves. Older leaves show the effects of toxicity more prominently as they have had longer to accumulate metals [83].

Ekosse (2008) conducted a study on the spatial distribution of vegetation on an abandoned manganese mine by sampling soil Fe content and pH and the Fe content of the leaves of *Combretum apiculatum*, *Euclea undulata* and *Terminalia sericea*. These three tree species and a number of *Acacia* species were the dominant tree species on the acidified soils around the mine. The results showed a relationship where areas with high soil Fe content and high leaf Fe content overlapped, as did areas with low soil Fe content and low leaf Fe content. Whilst the study did not display results for the individual species, this indicates that *Euclea* and *Acacia* were tolerant to high Fe content and show the potential to be used as indicator species for biogeochemical exploration.

Searsia lancea (L.f.) Moffet (previously included in the genus *Rhus)* is a common tree species found in the Witwatersrand Basin, and most notably in the region surrounding the Vaal River Mining operations study site. *S. lancea* has been found to be capable of withstanding high levels of anthropogenic contamination, and is found growing across the three predominant geologies at the site. *S. lancea* was found to take up elevated concentrations of sulphur (S), magnesium (Mg), aluminium (Al), iron (Fe), chromium (Cr), vanadium (V), manganese (Mn), zinc (Zn) and uranium (U) when growing on contaminated soils, and depressed concentrations of potassium (K) [84]. Similarly, the *Acacia karroo* Hayne which occur across a range of geologies in this region have also shown tolerance for anthropogenic contamination, as have several other *Searsia* and *Euclea* species [66], [85]. In a study of seed fate on contaminated land on the Highveld, the *A. karroo* showed tolerance for acid-rock drainage and the ability to regenerate on contaminated soils. The study also found that

Acacia species were some of the most common and dominant on disturbed and contaminated land and have shown an inherent tolerance to these conditions [66], [67].

2.1.2. Environmental Degradation, Remote Sensing and Vegetation Indices

It is established that growth in elevated concentrations of metals or metalloids, as well as osmotic stressors, results in biochemical and structural changes to leaves [86]. Hyperspectral remote-sensing of phreatophyte tree leaves was found to be a quick method for determining plant physiological status and the nature of the substrate. Changes in canopy spectral signatures occurred in response to seasonal drought, acid mine drainage (AMD), and high osmolality of groundwater [65], [68]. That these spectral responses were a consequence of stressful substrate conditions was supported by the findings that AMD-contaminated groundwater directly impaired viable seed production – a measure of fitness, in a range of phreatophyte species in a dose-dependent fashion [66], [67].

Leaves contain light-harvesting and photoprotective pigments that are sensitive indicators of growing conditions [87]. Anomalous plant water content is also detectable from the reflectance characteristics of foliage [58]. Remotely-sensed indices to estimate leaf water content and stress indices were used to determine where trees lacked access to groundwater, and where groundwater was contaminated by acid rock drainage (ARD) or acid mine drainage (AMD) resulting in osmotic stress [68]. In contrast, tree clusters and elevated leaf water indices in a dolomitic grassland during the dry season were used to identify probable dolines where roots access groundwater [88].

Furthermore, derived VIs can be useful in indicating substrate mineralisation and metal contamination by causing a shift in the typical leaf pigment signature towards the ultraviolet portion of the electromagnetic spectrum, known as a blue shift [69]. Detection of this shift has potential use in geobotanical exploration and has been successfully used in mapping of metal-polluted grasslands [89] and, used in combination with the Red-edge stress signature, to discriminate between plants grown in differing concentrations of $CuSO_4$ [29], [90].

2.1.3. Landscape functional analysis and landscape functional types

Remote sensing is a valuable tool because of the ability to collect information about large areas through the use of indicators and proxies for environmental conditions. Landscape function analysis is a similarly valuable technique, adapted to semi-arid environments, which allows the user to assess the functional status of the landscape through the use of selected indicators [91]. The model of Landscape function described by Tongway and Ludwig (1996) links terrain, soils and plant processes as key controllers in the functioning of a landscape. In order for a landscape to be functional, it needs to retain its resources and minimise leakiness of scarce resources such as nutrients and water [92]–[94]. Factors such as terrain and soil will play a role in determining how nutrients are transferred or retained within the landscape.

The concept of landscape functional types (LFT) was developed by David Tongway for a study of the Canberra Nature Parks. Tongway et al (2010) decided that differentiating a large area of land needed a coarser scale of assessment than the "hillslope" scale that LFA typically deals with. Nature parks and many mined lands are comprised of a number of local water catchments, so that terrain shape mixtures and vegetation structure, abundance and composition result in a highly complex landscape structure [95]. LFTs were designed to assist in making sense of larger sized natural landscapes. Many people are familiar with vegetation associations, which are largely decided with species composition and structure: there are well-decided rules about this. More traditional methods of delineating landscape patches depend heavily on the species composition and structure of the vegetation. LFTs are intended to have a more overt focus on the functional role of the vegetation, as well as reflecting geological, land-form and soil type/condition in a single classification (Pers. Comm. David Tongway, 16 Sept 2011). An LFT is determined based on soil surface and vegetation structure and disturbance factors [95].

LFTs therefore are in the order of at least hundreds of square metres in area, and differentiated from neighbouring LFTs. For example, "rocky grassland" characterised by a high rock cover would be distinguished from "grassland" where rocks play very little role in regulating the effect of rain on the

surface or in diverting run-off water. Each LFT would have several defining characteristics related to landscape function. Once mapped, the LFTs can be assigned sampling strategies based on the purpose of the research (Pers. Comm. David Tongway, 16 September 2011).

2.1.4. **Research objectives**

The overarching objective of this study is to determine whether it is possible to use the remote sensing of vegetation to distinguish between changes in the underlying geology. The aim of this chapter is to characterise the chosen study site to account for the variables which may have an influence on plant spectral reflectance and to identify whether position within the catena affected the plant response.

To address this aim, the following research objectives needed to be met:

1. Define and characterised the study sites in terms of vegetation patterns and structure, soils, and landscape functional types to account for changes in catena;
2. Identify whether there is any relationship between plant leaf spectral response, geology, soil types and landscape functional types.

Once these research objectives had been met, it was possible to identify whether catenal effects played a stronger role in determining plant spectral reflectance than changes to geology, by understanding whether there was a more significant change to spectral response between the different geologies, or between different landscape function types within geologies. This information was then used to justify the experimental design and analyses for the remainder of the study.

2.2. Site characterisation methods

The Vaal River Mining Operations was initially identified as a potential study site as this research forms part of a larger research project at the site. The site met with the basic criteria of having strongly contrasting geological features with similar vegetation across geologies. In order to narrow down the site selection and then to characterise the selected sites, three variables were used: vegetation, soils and geology, and landscape functional types.

2.2.1. Vegetation characterisation

Aerial photos and satellite imagery were used to initially characterise the site. Historical aerial photos from 1944 through to 2008 were used to visually interpret historical mining activities and impacts at the study site, and where there had been historical disturbances (eg. Old tailings storage facilities, processing plants and other direct sources of contamination). Land use and vegetation mapping data from the Vaal River Mine Environmental Management Plan was also made available for the purposes of the initial site characterisation. Visual interpretation of this data, combined with the geological and water quality data, was used to narrow down the site to the north western portion of the study site.

Vegetation transects (shown in Figure 2-3) across the proposed study site were walked. Transects were walked at 100m intervals across the "potential" study locations. Tree species and signs of historical disturbance were identified. The tree species data was used to narrow down the selection of the species that were most common across all geologies. The least disturbed portion of the study site was then selected as the final study area. Landscape functional analysis was performed on the study site to characterise the site in terms of changes in the landscape and catenal effects which may affect the vegetation response. By defining LFTs, it is possible to account for some of the landscape variables which could influence the spectral findings. For each LFT (two per geology), four sampling blocks of approximately 50m x 50m were selected. One tree of each of the chosen species was sampled per block. At each sampling point spectral reflectance measurements of the leaves of the

relevant *Searsia, Euclea*, *Ehretia* and *Acacia* spp., were taken using a hand-held spectro-radiometer (Field Spec-Pro, Analytical Spectral Devices (ASD) Inc., Boulder Colorado, U.S.A.) The spectro-radiometer has a spectral range of 350 nm to 2500 nm at 1.4 nm intervals in the 350-1000 nm range, and 2nm intervals at the 1000-2500 nm range. Leafy branches were cut from each tree and placed in labelled plastic bags immediately after cutting to reduce water loss, and kept in a cooler bag while they were transported to the spectral radiometer to be measured.

All spectra were collected using the internal halogen light source of the ASD. This ensured that the lighting conditions were identical for all samples, and atmospheric conditions did not affect the actual readings collected. For each tree (N=4 per species per LFT, total 74 samples), a minimum of 10 spectral readings were taken per tree from the abaxial surface of approximately 20 leaves per reading. A new selection of leaves was used for each reading, as the internal light source is hot, and in direct contact with the leaves, and may potentially damage the leaves, affecting subsequent readings. A white reference reading was taken between samples using the Spectralon® 100% reference panel.

2.2.2. Leaf elemental analysis

After measurement the sampled leaves were washed in distilled water, then frozen and lyophilised in preparation for elemental analysis together with composite site soil samples from the tree fine-root zone (0-50 cm) (data shown in Chapter 3).

2.2.3. Landscape functional types

The data used during the vegetation classification and vegetation transects was also used to understand the landscape in terms of topography and position within the catena. The vegetation mapping was used to understand the vegetation structure on a broad scale. The vegetation transect lines were used for the initial landscape functional analysis. Basic landscape function analysis techniques were used in the initial characterisation of the landscape functional types. At approximately 100m intervals along the transects, the following were noted for a 10m x 10m area:

vegetation structure, patch/interpatch zones and percentage vegetation cover, soil cover, potential nutrient flows (run off pathways) and disturbance status. Factors such as aspect and slope were also noted, but were validated using the LIDAR derived DEM.

This information was used to qualitatively determine the characteristics of the landscape functional types. Once the characteristics of the landscape functional types were determined, the boundaries of the landscape functional types were identified in the field and marked out using a GPS.

2.2.4. Soil characterisation

Soil sampling was done for a number of different purposes as part of the site characterisation. This included more detailed soils mapping to further the previous broad scale soils mapping work done as part of the EMP at the site. Soil samples were then collected and prepared for analysis in the lab.

In order to do the soil classifications, auger points were dug at the base of each of the selected trees used in the study. Where possible, soils were analysed at two depths, ±10cm below surface and at ±50cm below surface. Soil horizon depth and effective rooting depth were measured. Soils were analysed to colour, texture, parent material and organic carbon and clay contents. Depth limiting material and other relevant characteristics were noted during the fieldwork activities. This information was used to understand any anomalies in the results.

At each tree sampling location, soils samples were also collected for analysis in the lab. Composite soil samples of approximately 1 kg were taken from the upper profile of the soil (0-50 cm depth) after removal of surface litter. All samples were double bagged in plastic zip lock bags and immediately placed in a cooler box with ice. Labels were written in carbon pencil on paper and placed on the outside of the 2nd bag to avoid contamination of the soils. GPS co-ordinators of each sampling point were taken and notes were made on the landscape functional type and the surroundings. Features that were noted were approximate soil depth, slope aspect and steepness and position on the catena angle, and a broad description of the surrounding vegetation classes and density.

Samples were taken back to the laboratory for immediate measurement of pH, EC and Eh. To measure pH and EC, a soil paste was made up by mixing 1:2 soil in distilled water solution, stirring with a plastic rod until smooth (1 to 3 minutes), then measuring the sample.

The remaining soil samples were stored in a fridge until they could be analysed. The samples were subsampled and analysed as follows:

a) A representative subsample of +/-100g was dried in the forced-draught (fan) oven at room temperature in brown paper bags. This subsample was sent for analysis of organic carbon (C) and fertility (N) by LECO auto-analyser;

b) Another representative subsample of +/-50g was weighed, freeze-dried, weighed a second time to measure water content and then passed through a 2mm plastic sieve to remove any pebbles and vegetative matter. The samples were then ground using an agate mortar and pestle to break up soil aggregates. This subsample was further subsampled;

c) 10g sub-samples were weighed out, milled and pressed into pellets for analysis by XRF for major and trace elements.

The full list of elements that were analysed for all samples is shown in Table 2-2.

Table 2-2 Types of analysis used for samples, and elements analysed

Analysis type	Material	No of samples	Elements analysed
Leco Autoanalyser	Leaves	73	N, C
Leco Autoanalyser	Soils	73	N, C
XRF - Majors	Soils	57	SiO_2, Al_2O_3, Fe_2O_3, FeO, MnO, MgO, CaO, Na_2O, K_2O, TiO_2, P_2O_5, Cr_2O_3, NiO
XRF trace elements	Soils	57	Sc, V, Cr, Co, Ni, Cu, Zn, Ga, Rb, Sr, Y, Zr, Nb, Mo, Ba, Pb, Th, U
ICP OES*	Leaves	64	Al, Ba, Ca, Co, Cr, Cu, Fe, K, Mg, Mn, Na, Ni, P, S, Si, Ti, Zn, U
ICP-MS*	Leaves	64	V, Co, As, Ag, Cd, Sn, Sb, Au, Pb, U

* Shown in chapter 3

2.2.5. Analysis of data

A variety of analytical techniques and software packages were used in the processing of the data. Spectral data from the spectro-radiometer was processed using the RS^3 software package produced by Analytical Spectral Devices. 1^{st} and 2^{nd} derivatives were also calculated using this software. Statistical analysis of the data was completed using XLStat (Addinsoft), and spatial analysis was completed using ArcGIS 10.4.1 (ESRI).

2.2.6. Statistical analysis of soil samples

Descriptive statistics of the results of the XRF analysis of the soil samples by geology and by landscape functional type were calculated and interpreted to understand the distribution of the data. Data was also tested for normality. Once it was determined that the data was not normally distributed, a Kruskal Wallis test with a Dunn's post-test using a Bonferroni correction [96]–[98] was used to analysis the data and test for differences between elemental concentrations in soils per geology and elemental concentrations in soils per landscape functional type.

A further grouping analysis of the soil samples was performed in ArcGIS 10.4.1. The samples were plotted using GPS coordinates of the tree locations collected during sample collection.

The outliers were removed from the data set (e.g. Ash heap sample MMAK67) as the XRF results were significantly different from the remaining samples. The Grouping Analysis tool classifies the data into natural groupings based on selected attributes fields. The variables are standardised in order to compensate for the large variations in the range of the data being analysed. This analysis was performed without any spatial constraints. The tool used a K-Means algorithm to classify the data. This tool is predominantly used for exploratory analysis as the clustering is highly dependent on the combination of variables selected, seed locations and number of classes. Initially, all the elements which showed significant differences in the Kruskal Wallis test on the XRF data were used as variables in the analysis, and 3 classes were specified for the output. The grouping analysis provides an R^2 value as one of the outputs. This R^2 value represents the amount of the variation in the data retained after classifying the samples into groups.

The variables with the 10 highest R^2 values were selected for a second run of the analysis, using the same seed locations. The same analysis was run using 6 classes, and 3 additional seed locations which were randomly selected by the software. In addition to the 3 addition classes, an analysis was also run to identify the optimal number of classes for the data to be classified into.

Grouping effectiveness is measured using the Calinski-Harabasz pseudo F-statistic, which is a ratio reflecting within-group similarity and between-group difference [99]. The result with the highest solution value represents the optimal number of groups to classify your data. Using a higher or lower number of groups would indicate that there is either insufficient between group differences or limited within group similarity. This is calculated as shown below:

$$\frac{\left(\frac{(R^2)}{n_c - 1}\right)}{\left(\frac{1 - R^2}{n - n_c}\right)}$$

where:

$$R^2 = \frac{SST - SSE}{SST}$$

and *SST* is a reflection of between-group differences and *SSE* reflects within-group similarity defined by:

$$SST = \sum_{i=1}^{n_c} \sum_{j=1}^{n_i} \sum_{k=1}^{n_v} \left(V_{i_k}^{j} - \overline{V^k}\right)^2$$

$$SSE = \sum_{i=1}^{n_c} \sum_{j=1}^{n_i} \sum_{k=1}^{n_v} \left(V_{i_k^{j}} - \overline{V_i^k}\right)^2$$

n = *the number of features*

n_i = *the number of features in group* i

n_c = *the number of classes (groups)*

n_v = *the number of variables used to group features*

$V_{i_k^{j}}$ = *the value of the* k^{th} *variable of the* j^{th} *feature in the* i^{th} *group*

$\overline{V^k}$ = *the mean value of the* k^{th} *variable*

$\overline{V_i^k}$ = *the mean value of the* k^{th} *variable in the group* i

2.2.7. Analysis of spectral data

Vegetation indices are a rapid method of obtaining quantitative data from spectral data, and reducing the dimensionality of the data to only interrogate key spectral features. Vegetation indices were derived from the spectral data collected with the spectro-radiometer. Four vegetation indices were calculated for each sample to identify any broad differences in spectral response between the geologies or LFTs. The indices that were calculated were selected to assess the changes most likely to occur in plants growing in contrasting environmental conditions (underlying substrate or catenal effects). The selected indices were derived:

The Normalised Difference Vegetation Index [62]which estimates relative leaf chlorophyll content:

$$\text{NDVI} = \frac{(R_{800} - R_{680})}{(R_{800} + R_{680})},$$

the Plant Senescence Reflectance Index [100] calculates a ratio of estimated carotenoid and chlorophyll content in plants:

$$\text{PSRI} = \frac{(R_{680} - R_{500})}{(R_{680} + R_{500})},$$

the Normalised Difference Water Index [101] which estimates relative leaf water content:

$$\text{NDWI} = \frac{(R_{857} - \text{R}_{1241})}{(R_{857} + R_{1241})}$$

and the Red-edge NDVI [102] which has been designed for use with narrow band hyperspectral data to identify small changes in foliar chlorophyll content and leaf senescence :

$$\text{Red-edge} = \frac{(R_{750} - R_{702})}{(R_{750} + R_{702})}$$

In addition to these vegetation indices, a linear interpolation of the Red-edge was used to determine the inflection point and Red-edge wavelength[103]. This technique assumes that the Red-edge occurs around the midpoint of the slope from the absorption feature in the red band around 670nm and the peak of the Red-edge in the NIR at 780nm. A shift in the wavelength of the Red-edge

is indicative of plant stress. This is calculated through a two-step procedure, by first calculating the reflectance at the inflexion point (R_{re})

$$R_{re} = \frac{(R_{670} + R_{780})}{2}$$

where:

$R = reflectance$

and then calculating the Red-edge wavelength, also known as the Red-edge position (REP):

$$REP = 700 + 40\left(\frac{R_{re} - R_{700}}{R_{740} - R_{700}}\right)$$

where 700 and 40 are constants resulting from interpolation in the 700-740 nm interval

Further analysis was done by calculating the ratio at the double-peak reflectance feature at 702nm and 725nm. The 725nm/702nm ratio of the 1st and 2nd order derivatives of the reflectance data were used to detect a flattening of the double-peaked reflectance feature at 702nm and 725nm that has been associated with metal-related plant stress ([104]). This is one method which has been used previously to measure the blue shift of the plant spectrum

A Kruskal-Wallis non-parametric test with a Dunn's Post Test with a Bonferroni correction was used to detect significant differences between species, initially across the three geologies, and then across landscape functional types ([96]–[98]

2.3. Results

2.3.1. The Study Site

The study site was narrowed down to a smaller area by selecting an area that contained the outcropping Black Reef adjacent to the Ventersdorp Lavas and the Dolomite. It was also necessary for the study area to be relatively undisturbed. While there has been mining in the area for over 100 years, and finding completely undisturbed land is not possible, it was possible to locate a site which was not disturbed by recent or large-scale mining activities. There is evidence of historical mining activities around the study site such as old adits dug into the Black Reef, a small ash heap and old spoils heaps/dump rock, and the remnants of a tram line (shown as anthropogenic disturbance in Figure 2-1). Some other examples of anthropogenic disturbance were borrow pits on the dolomites, the mining area and Waste Rock Dump, water pumping stations, and on the lower portion of the Black Reef outcrop. Some old adits, identified by the Mine Health and Safety department as a potential safety risk, were backfilled with waste rock at the same time as this study took place.

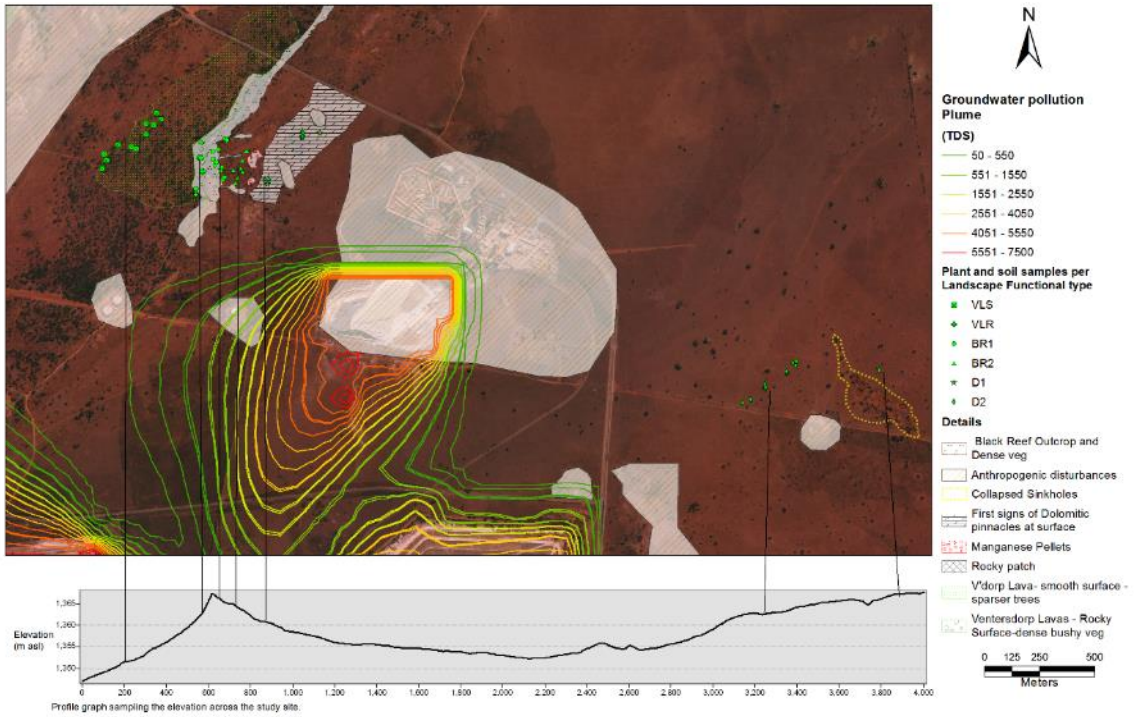

Figure 2-1 Landscape features identified during ground-based and aerial imagery investigation. Pollution plume modelled during development of EMP (data sourced from AGA, 2011)

The study site was intentionally situated up-gradient (i.e. beyond the influence) of the dominant groundwater pollution plumes (Figure 2-1), although historical contamination and natural leaching of the metalliferous rocks of the Black Reef has resulted in moderately elevated concentrations of certain elements in the soils of the study site [74]. The water quality based on borehole monitoring data across the full study area showed an acceptable water quality at the selected site, showing a pH range of 6.95-8.85, a TDS range 695-3293 ppm and a SO_4 range 52 – 291 ppm over a 10-year monitoring period (2001-2011).

Figure 2-2 below shows the digital elevation model (DEM) of the study site derived from LIDAR data. The ridge that is formed by the outcropping Black Reef Quartzite is visible. The ridge slopes gently to the west on the Ventersdorp Lavas, and to the east over the chert-poor Dolomites. There is a gentle increase in elevation over the chert-rich dolomites which are more resistant to erosion and soil loss, than the chert-poor dolomites. This elevation data combined with the geology, vegetation data, water monitoring data and land use data was used to narrow the focus for the ground-based site selection work.

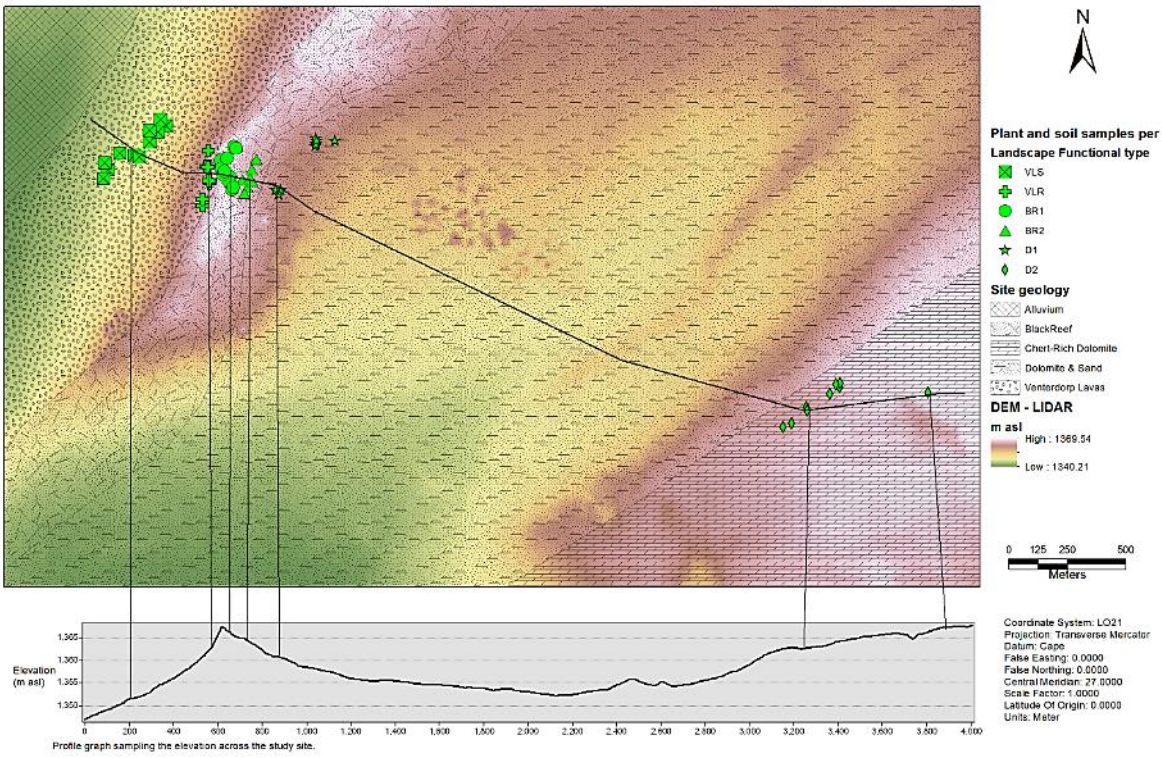

Figure 2-2 Geology and samples per landscape functional type (LFT) shown on a LIDAR based DEM of the study area

2.3.2. Vegetation characterisation

Historical photographs from the 1940's have shown that there was extensive clearing of trees, most likely for use within the mines. There has been a significant recovery of the Vaal Reefs Dolomite Sinkhole Woodlands and Klerksdorp Thornveld, which can be seen by comparing historical and recent aerial imagery [74]. The main vegetation unit is Vaal Reefs Dolomite Sinkhole Woodlands (Gh12) with a small area of Klerksdorp Thornveld (Gh13), rocky outcrops supporting trees and shrubs along the Black Reef [72]. The Vaal Reef Dolomite Sinkhole Woodlands are characterised by clumps of phreatophyte trees which may indicate dolines or sinkholes [88].

Figure 2-3 Land use and land cover classification based on 2008 imagery, provided by the Ecological Engineering and Phytoremediation program (EEPP) and field data. The vegetation transects completed for species identification are shown on this map. Collected plant samples are shown by species.

The aerial imagery and 2008 land cover classification supplied by the Ecological Engineering and Phytoremediation program (EEPP) were used to identify broad vegetation communities, and then transects were walked to identify dominant tree species found in the area (Figure 2-3). The most common species that were identified where *Searsia lancea, Euclea crispa and E. undulata, Acacia karroo, A. erioloba, A. caffra* and *Ehretia rigida*. It was not possible to identify all species as the vegetation transects and initial landscape functional analysis (LFA) fieldwork to define the LFTs was performed in winter (July - September 2011). The species that were most consistently and widely

spatially distributed (*S. lancea, E. crispa, A. karroo and E. Rigida*) were chosen to be used in the study. The species distribution was not consistent across the study site. The most consistently distributed tree species were the *S. lancea* and *A. karroo*, although *A. caffra* was more common on the chert-rich dolomites. Similarly, no *E. crispa* could be found on the chert-rich dolomites.

2.3.3. Definition of Landscape Functions Types (LFT's)

The site was characterised in terms of geological maps and soils, surface run-off pathways, vegetation structure, location within the catena, slope and soil characteristics, into the six LFTs. Table 2-3 below summarises the key characteristics identified within each landscape functional type. Vegetation structure and surface cover played a key role in determining the LFTs. Whilst the vegetation across the study site was predominantly woodland, there were distinctive differences in the structure of the woodlands between the LFTs. For example, on the Black Reef, the high lying outcrop (BR1) has dense woodlands, which are fairly continuous. Trees grow in sheltered crevices between the rocky outcrops. The trees are usually not large, standing at around 3-4 m, and the understory is mostly comprised of small thorny shrubs and very few grasses. Lower on the Black Reef (BR2) there was most grassy cover between the slightly more isolated tree clusters. There were small rocky outcrops and "boulder fields" comprised of quartzite derived material, which was presumably transported from the rocky outcrop. The transition to the chert-poor dolomites (D1) was visible. The first indication of the transition zone was the sparsely vegetated patches with manganese pellets and small pebbles at surface, interspersed with isolated dolomitic pinnacles forming outcrops. This transition zone was vegetated with grasses and very few trees or shrubs. The manganese pellets formed through oxidation which took place during the deposition period when the inland sea was still present, and during the formation of the dolomites. Table 2-3 summarises the characteristics that describe the chosen LFTs, and Table 2-4 provides a summary of the soil types and soil descriptions.

Table 2-3 Summary of key characteristics of each of the identified Landscape Functional types (LFTs) at the study site

	Ventersdorp Lavas Smooth	**Ventersdorp Lavas Rocky**	**Black Reef 1**	**Black Reef 2**	**Dolomite 1**	**Dolomite 2**
LFT description and Position in Catena	Gentle west-facing slope, mid-slope, grassland with dense isolated tree clusters	West facing upper slope, rocky surface, regular tree clusters and consistent grassy cover	Ridge scarp, large rocky outcrops. Trees growing between rocky outcrops with limited undergrowth. Old mining adits dug into the outcropping reef rock at some locations	South-east facing slope, upper slope, grassland with isolated tree clusters, Isolated dolomite pinnacles protruding in lower portion of LFT. Barren patches where manganese pellets have formed on lower slope near dolomite pinnacles. Some disturbance from historical mining evident.	South-east facing gentle slope. Large tree clusters and dense grassy undergrowth. Dolomite pinnacles evident and small mounds have formed around some pinnacles. Deep, dark brown soils evident between dolomite pinnacles	South-east facing gentle slope. Isolated tree clusters, often formed around collapsed sinkholes or deep fractures in the rock providing access to the aquifer for tree roots. Chert rich dolomite resulting in rockier, shallower soils. Some dolomite and chert outcrops evidence.
Soil parent material	T2 - **quartzite other,**	T2b - **black reef quartzite**	T2b/T2 - **black reef quartzite / quartzite other,**	T2b/T2 **- black reef quartzite/ quartzite other,**	L2/S - **Dolomite/ sand**	L2/T3 - **dolomite /chert**
Underlying geology	Ventersdorp lavas		Black reef quartzite		Dolomite	Chert-Rich Dolomite
Vegetation	Klerksdorp Thornveld		Vaal Reefs Dolomite Sinkhole Woodland		Vaal Reefs Dolomite Sinkhole Woodland	
Dominant tree species	*Searsia lancea, Acacia karroo, Euclea Crispa*	*Searsia lancea, Acacia karroo, Euclea Crispa*	*Searsia lancea, Acacia karroo, Euclea Crispa*	*Searsia lancea Acacia karroo, Euclea Crispa, Ehretia rigida*	*Searsia lancea, Acacia karroo*	*Searsia lancea, Ehretia rigida*
Soil Type (see explanation in Table 2-4**)**	Hu3100	Hu3100, Ms1100 and Ms2100	Ms1100, Ms2100	Hu3100 and Ms1100	Hu3100, Ms1100	Ms1100, Hu3100 and Gs
Slope (degrees)	2 degrees	4 degrees	2-8 degrees	2 degrees	2-4 degrees	2-4 degrees

Table 2-4 Summary of soil types found at the study site

Map Unit	Soil Forms	Broad Map Unit Description
Hu3	Hutton, Mispah	Shallow, red, sandy loam soils, flat to gently slopes, 1-10% exposed surface rock; Dolomite
Gs	Glenrosa, Mispah, Hutton	Shallow, reddish brown stony soils, flat to gently slopes, 1- 20% exposed surface stones; Chert rich dolomite
Ms1	Mispah, Glenrosa, Clovelly	Shallow, yellowish brown gravely soils, flat to gently slopes, 1-5% exposed surface stone; Andesite
Ms2	Mispah, Glenrosa, Clovelly	Shallow, yellowish brown stony soils, flat to slightly steep slopes, 1-30% exposed surface stone; Black Reef.

2.3.4. Soil characterisation

The soil characterisation exercise characterised the soils in terms of the soils' form and family, surface features, organic carbon range, effective rooting depth, presence of depth limiting materials, parent material and ground roughness. The full table of results can be seen in Appendix 2. This exercise was an essential part of characterising the site, as the presence of transported materials may mean that soils at surface and underlying geology may not correspond. Phytogeochemical exploration studies have shown that it is possible to use deeper rooted trees to detect underlying geology through regolith and transported materials as their root systems may penetrate deeper than the regolith. The results from the soils classification exercise show that there is transported material present across the different geologies. For example, Hutton3100 soil form is found across the Ventersdorp Lavas, the lower portion of the Black Reef and on the Dolomites, but was not found on the upper portion of the Black Reef. Soils on the Rocky Ventersdorp Lava show that they were derived from the Black Reef Quartzites, indicating that material has been transported off the rocky ridge by erosion (Table 2-3). The effective rooting depth of the soils was found to be much shallower on the Black Reef ridge, when compared to other areas, which supports the notion that weathered material has been transported from the top of the ridge to the lower lying areas. Figure 2-4 shows the effective rooting

depth range of each of the LFTs in relation to the terrain profile. The chert-poor dolomites (D1) had the deepest soils, where soils had formed between pinnacles. By contrast, the chert-rich dolomites were composed of much more rocky material which limited the depth of the soils.

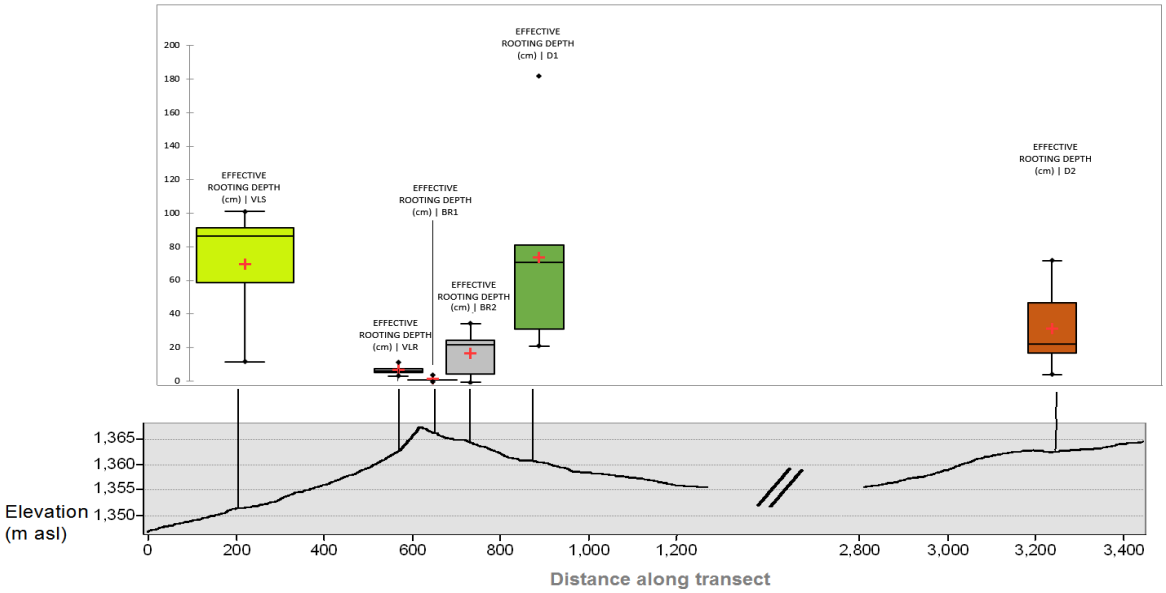

LFT	VLS	VLR	BR1	BR2	D1	D2
Mean of Ranks	59.7	21.5	10.9	40.5	57.4	41.9
Group	C	AB	A	BC	C	BC

Figure 2-4 Terrain profile across the study site and effective rooting depth shown in box plots above and results of the multiple pairwise comparison using Dunn's procedure below.

The clay content in the soils varied significantly ($p < 0.0001$) between the landscape functional types. The Black Reef outcrop (BR1) and the dolomites (D1 and D2) had the lowest clay content. The lower-lying Black Reef soils had higher clay content, and the Smooth Ventersdorp Lavas had the highest clay content, but also showed a large range in terms of clay content values. Clay content of the soils could have a significant effect on the soil moisture content and the bioavailability of many elements which could potentially be bound to the clays and therefore be less mobile.

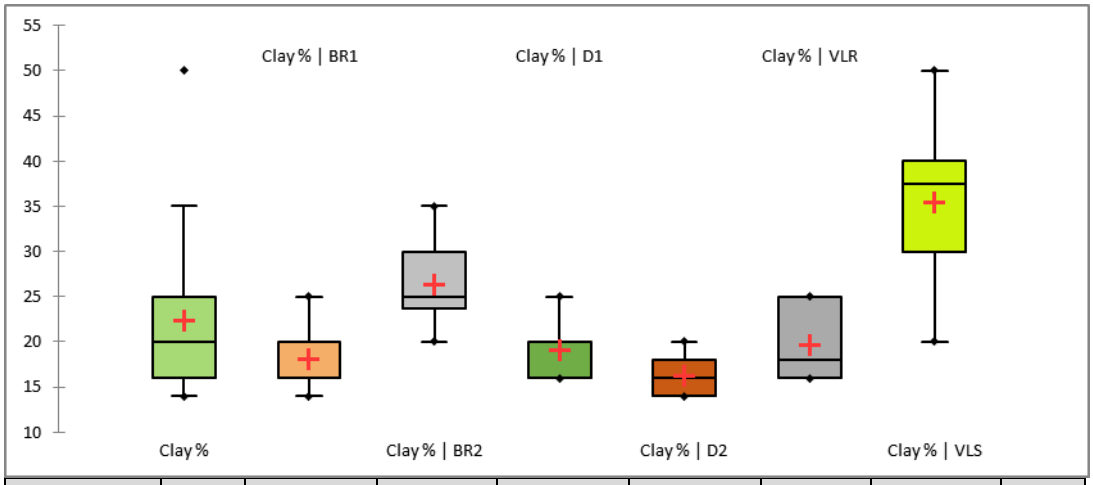

LFT		BR1	BR2	D1	D2	VLR	VLS	
Mean of ranks		26.5	53.667	31.833	16.318	32.333	65.333	
Group		A	BC	AB	A	AB	C	

Figure 2-5 Estimated clay content of soils. Box plots show range for the full sample and range per Landscape Functional type, and the results of the Kruskal Wallis test Pairwise comparisons using the Dunn's procedure are shown below.

The soil organic carbon range was ranked in terms of range. The most frequent category was Medium-high. The Black Reef outcrop (BR1) and Rocky Ventersdorp Lavas (VLR) had the highest Soil Organic Carbon results. This could potentially be due to shelter from fires in the rocky outcrops allowing longer times for decomposition of organic matter, or to the general erosion of soils resulting in higher humic content proportionally in the soils.

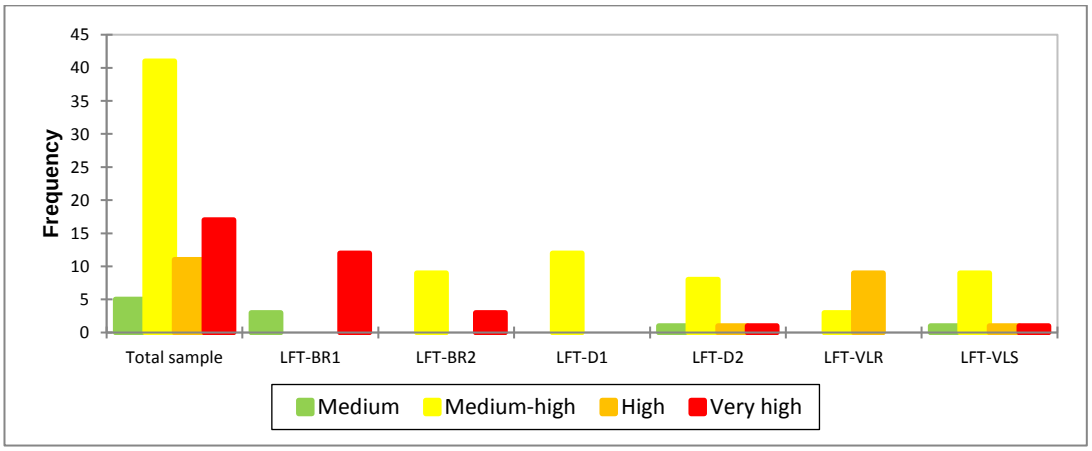

Figure 2-6 Histogram of the estimated organic carbon range where Medium was < 0.8%, Medium high 08% - 1.2%, High 1.3%- 1.7% and Very high was > 1.7%. Results are shown as the full sample and range per landscape functional type.

2.3.5. Soils sample analysis – pH and soil water content

This section contains the results obtained for the analysis of the soil water content and soil pH which were measured in the lab after sample collection. Table 2-5 shows the results of the Kruskal Wallis test and pairwise comparison of the data. There were no significant differences identified between either the soil water content or the soil pH between the three geologies.

Table 2-5 Results of the Soil water content and soil pH analysis by the Kruskal Wallis test and multiple pairwise comparison using the Dunn's procedure

Variable	K observed	p-value	Geology	Obs.	Min	Max	Sum of ranks	Mean of ranks	Group
Soil water content (%)	2.678	0.262	Ventersdorp Lava	24	1.080	6.300	972.00	40.500	A
			Black reef	25	0.980	6.080	778.00	31.120	A
			Dolomite	23	1.760	6.300	878.00	38.174	A
Soil pH	5.284	0.071	Ventersdorp Lava	24	5.080	7.370	686.50	28.604	A
			Black reef	25	5.200	7.230	982.50	39.300	A
			Dolomite	23	5.710	7.500	959.00	41.696	A

The range of the pH for the soils was also within a fairly neutral range of 5- 7.5. It was anticipated that the soil pH for the Black Reef would be lower than the other geologies, but the results indicated that while there was a broad range of values for the Black Reef, no obviously acidification of the soils was observed.

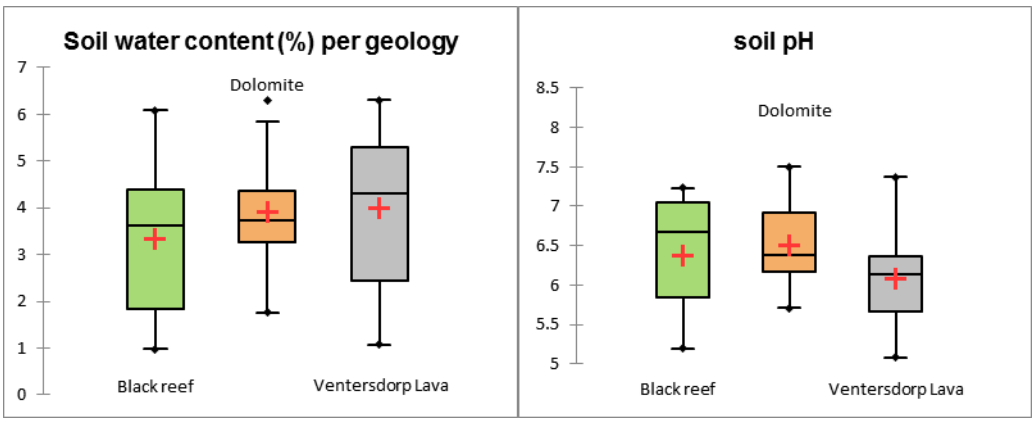

Figure 2-7 Box plots showing the range obtained for the measured soil water content (%) and soil pH for the three geologies at the study site

While no differences where observed between geologies, analysis per landscape functional type showed differences between some of the LFTs for the soil water content, as shown in Figure 2-8. The Smooth Ventersdorp Lavas (VLS) showed the highest water content and was significantly different to the Black Reef outcrop (BR1) and the Rocky Ventersdorp Lavas (VLR) which had the lowest water content in the soils. This result follows a similar trend for soil clay content in Section 2.3.4. There were no significant differences for the soil pH per landscape functional type, as shown in Figure 2-9.

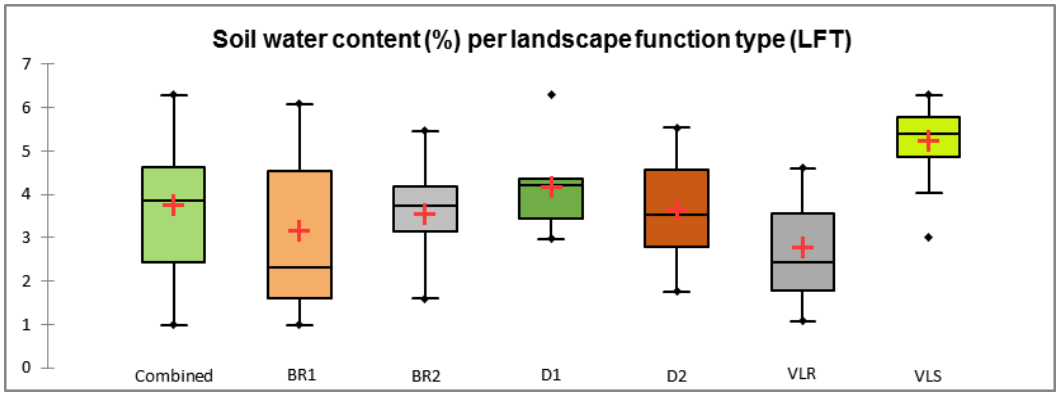

LFT		BR1	BR2	D1	D2	VLR	VLS	
Mean of ranks		29.154	33.250	41.125	34.955	23.50	57.00	
Group		A	AB	AB	AB	A	B	

Figure 2-8 Soil water content (%) per landscape function type. Box plots show range for the full sample and range per Landscape Functional type, and the results of the Kruskal Wallis test Pairwise comparisons using the Dunn's procedure are shown below the box plot.

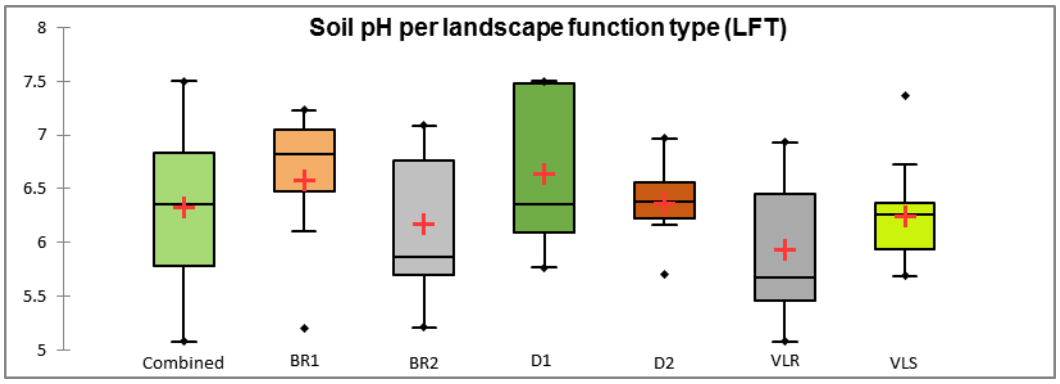

LFT		BR1	BR2	D1	D2	VLR	VLS	
Mean of ranks		45.692	32.375	45.167	37.909	24.167	33.042	
Group		A	A	AB	A	A	A	

Figure 2-9 Soil pH per landscape functional type. Box plots show range for the full sample and range per Landscape Functional type, and the results of the Kruskal Wallis test. Pairwise comparisons using the Dunn's procedure are shown below the box plot.

2.3.6. Exploratory analysis of soils sample XRF results

The descriptive statistics and initial interpretation of the data showed some expected trends and also helped to identify certain samples which showed anomalous results which were likely as a result of isolated anthropogenic contamination. The results also showed that there were overlaps in the ranges of concentrations of many of the elements between LFTs on the same geology (Box plots shown in Appendix 3). The majority of the elements were not normally distributed, as shown in the Shapiro Wilk test in Appendix 1. Results with a $p < 0.05$ were not normally distributed.

Al ($p = 0.1913$) and Ga ($p = 0.9391$) were the only two elements which did not have any significant differences in the Kruskal-Wallis test of soil elemental content per Geology (Table 2-6). For selected elements, such as Ba, Si and Sr, the Dolomites and Ventersdorp Lavas samples clustered together whereas the Black Reef samples fell into a separate class. Many of the samples formed three distinct classes for Black Reef, Dolomite and Ventersdorp lavas ($P < 0.05$). The analysis of the LFTs did not result in as many distinct classes, as for many of the elements there were only two groups. Ca ($p = 0.221$) was the only element for the analysis of soil elemental content per Landscape functional type that did not show any significant differences between samples. The element which showed the highest number of groups was Pb ($p < 0.0001$). There was one anomalously high sample on the Black Reef (2) which was identified as an ash heap during the soil mapping exercise. It is expected that this may account for the separate grouping of the BR2 LFT for Pb. This sample showed Pb values of 54.498 ppm compared to a background median of 17.785 ppm (Appendix 1). Zn values for this sample were 1380.2 ppm which was also a full order of magnitude higher than the next highest concentration (100.2 ppm).

Table 2-6 Results of Kruskal Wallis test with a Dunn's Post-test on the XRF analysis of the soil samples (N=72) per geology and LFT

Element	Mean per geology/LFT and Dunn's Post-test grouping						chi-squared	p-value (geology /LFT)	Df	Pairwise comparisons						
	Black Reef Quartzite		Dolomite		Ventersdorp Lava					Black Reef	Dolomite-Black Reef		Ventersdorp Lava - Black Reef		Ventersdorp Lava - Dolomite	
	BR1	BR2	D1	D2	VLR	VLS				BR1 - BR2	BR1-D1	BR1-D2	BR1-VLS	BR1-VLR	D1-VLS	D1-VLR
											BR2 - D1	Br2 - D2	BR2-VLs	BR2-VLR	D2-VLS	D2-VLR
Al2	30590.65(a)		30537.72(a)		28209.02(a)		3.3077	0.1913	2,		0.197622		0.345222		0.937944	
	27402.937	36804.927	32566.517	25490.605	24901.213	36222.752		**< 0.0001**		0.002	0.023	0.556	0.000	0.234	0.201	0.001
	AB	C	BC	AB	A	C					0.453	0.000	0.598	< 0.0001	< 0.0001	0.574
Ba	172.57(a)		333.57(b)		162.2(b)		445.8045	**0**	2,		0		0.892311		0	
	156.888	212.248	268.523	598.005	142.473	195.950		**< 0.0001**		0.074	< 0.0001	< 0.0001	0.054	0.364	0.038	< 0.0001
	A	AB	BC	C	A	AB					0.027	0.000	0.891	0.008	0.000	< 0.0001
Ca	964.83(a)		1429.38(b)		1214.98(ab)		11.5113	**0.003165**	2,		0.002367		0.4159		0.084244	
	1715.261	1762.907	1494.897	1331.926	1292.401	1256.667		0.221		0.015	0.743	0.388	0.267	0.269	0.443	0.446
	A	A	A	A	A	A					0.038	0.136	0.192	0.191	0.828	0.832
Co	12.68(a)		11.02(b)		14.95(c)		152.1371	**0**	2,		0		0.000044		0	
	13.576	16.834	12.224	9.593	13.484	15.249		**0.000**			0.468	0.002	0.101	0.865	0.020	0.380
	B	B	AB	A	B	B					0.482	0.002	0.105	0.861	< 0.0001	0.001
Cr	143.26(a)		123.68(b)		90.7(c)		520.6412	**0**	2,	0.000	0		0		0	
	141.905	147.023	127.778	105.339	90.474	91.723		**< 0.0001**			0.107	0.002	< 0.0001	< 0.0001	0.002	0.000
	C	C	BC	AB	A	A					0.033	0.000	< 0.0001	< 0.0001	0.107	0.048
Cr2	176.18(a)		117.68(b)		99.21(c)		452.0665	**0**	2,	0.000	0		0		0.0265	
	184.313	177.950	123.555	103.004	114.376	95.731		**< 0.0001**			0.000	< 0.0001	< 0.0001	< 0.0001	0.077	0.585
	B	B	A	A	A	A					0.003	< 0.0001	< 0.0001	0.000	0.489	0.613
Cu	22.14(a)		16.92(b)		28.87(c)		383.3555	**0**	2,	0.000	0		0		0	
	24.866	28.848	18.474	16.280	28.063	31.838		**< 0.0001**			0.045	0.006	0.016	0.113	< 0.0001	0.000
	ABC	BC	AB	A	C	C					0.008	0.001	0.097	0.396	< 0.0001	< 0.0001
Fe	19199.43(a)		20987.24(b)		24562.84(c)		220.2557	**0**	2,		0.002011		0		0	
	20359.412	20469.032	21492.483	20428.989	23532.909	26402.460		**< 0.0001**		0.944	0.407	0.959	< 0.0001	0.014	0.002	0.109
	A	A	A	A	AB	B					0.377	0.906	< 0.0001	0.013	0.000	0.021

Element	Mean per geology/LFT and Dunn's Post-test grouping						chi-squared	p-value (geology /LFT)	Df	Pairwise comparisons						
	Black Reef Quartzite		Dolomite		Ventersdorp Lava					Black Reef	Dolomite-Black Reef		Ventersdorp Lava - Black Reef		Ventersdorp Lava - Dolomite	
	BR1	BR2	D1	D2	VLR	VLS				BR1 - BR2	BR1-D1	BR1-D2	BR1-VLS	BR1-VLR	D1-VLS	D1-VLR
											BR2 - D1	Br2 - D2	BR2-VLs	BR2-VLR	D2-VLS	D2-VLR
Fe2	2098.28(a)		2308.11(b)		2727.76(c)		209.7767	**0**	2,		0.000767		0		0	
	2259.684	2273.135	2395.534	2269.955	2605.362	2931.761		**0.000**		0.925	0.341	0.987	< 0.0001	0.019	0.004	0.171
	A	A	AB	A	AB	B					0.305	0.915	< 0.0001	0.017	0.000	0.025
Ga	6.52(a)		6.03(a)		6.44(a)		0.1256	0.9391	2,		0.9946		0.938278		0.969144	
	5.833	8.087	7.370	5.696	5.371	7.980		**< 0.0001**		0.009	0.018	0.753	0.001	0.232	0.299	0.000
	AB	BC	BC	AB	A	C					0.807	0.005	0.427	0.000	0.000	0.403
K2	7969.42(a)		6807.21(b)		6226.11(c)		77.7991	**0**	2,		0		0		0.002122	
	6385.754	10951.036	8211.547	4973.341	6122.342	6094.670		**< 0.0001**			0.004	0.019	0.751	0.739	0.002	0.001
	AB	C	BC	A	A	A					0.591	< 0.0001	0.000	0.000	0.045	0.047
Mg	1386.98(a)		1386.98(b)		1326.68(b)		33.2724	**0**	2,	0.000	0.923989		0		0.000011	
	1373.067	1794.032	1673.425	1217.036	1236.224	1417.135		**0.001**			0.042	0.110	0.968	0.093	0.051	0.000
	AB	AB	B	A	A	AB					0.367	0.008	0.294	0.006	0.108	0.967
Mn	697.01(a)		3407.61(b)		542.12(c)		487.0272	**0**	2,	0.000	0		0.000856		0	
	583.821	709.919	3401.157	4097.582	471.128	651.835		**< 0.0001**			< 0.0001	< 0.0001	0.497	0.155	0.001	< 0.0001
	A	A	B	B	A	A					0.002	0.001	0.735	0.016	0.000	< 0.0001
Mo	0.86(a)		1.08(b)		0.72(c)		104.2542	**0**	2,	0.000	0		0.000011		0	
	1.020	0.925	1.160	1.153	0.698	0.781		**0.039**			0.335	0.478	0.086	0.143	0.009	0.017
	A	A	A	A	A	A					0.132	0.213	0.262	0.382	0.019	0.036
Na2	296.74(a)		148.37(b)		296.74(c)		33.4843	**0**	2,		0.011022		0.013144		0	
	313.863	309.107	98.914	532.788	352.382	426.568		**0.000**		0.474	0.002	0.295	0.216	0.535	< 0.0001	0.013
	B	AB	A	B	AB	B					0.016	0.086	0.055	0.925	0.874	0.105
Nb	6.75(a)		5.62(b)		5.61(b)		150.1868	**0**	2,		0		0		0.907078	
	6.705	7.057	6.180	5.163	6.284	4.975		**< 0.0001**		0.412	0.384	0.001	0.000	0.581	0.005	0.755
	C	C	ABC	AB	BC	A					0.097	< 0.0001	< 0.0001	0.178	0.747	0.006
Ni	28.22(a)		37.99(bc)		43.26(bc)		143.6471	**0**	2,		0		0		0.005067	
	14.386	27.082	43.415	38.758	33.724	39.053		**< 0.0001**		< 0.0001	0.001	0.006	< 0.0001	0.026	0.942	0.031
	A	A	B	BC	B	BC					0.000	0.012	< 0.0001	0.013	0.006	0.578

Element	Mean per geology/LFT and Dunn's Post-test grouping						chi-squared	p-value (geology /LFT)	Df	Pairwise comparisons						
	Black Reef Quartzite		Dolomite		Ventersdorp Lava					Black Reef	Dolomite-Black Reef		Ventersdorp Lava - Black Reef		Ventersdorp Lava - Dolomite	
	BR1	BR2	D1	D2	VLR	VLS				BR1 - BR2	BR1-D1	BR1-D2	BR1-VLS	BR1-VLR	D1-VLS	D1-VLR
											BR2 - D1	Br2 - D2	BR2-VLs	BR2-VLR	D2-VLS	D2-VLR
Ni	31.43(a)		33.79(b)		33.79(c)		28.4168	**0.00000**	2,		0.0001		0		0.685089	
	32.432	34.881	27.830	35.347	40.141	48.772		**< 0.0001**			0.654	1.000	0.143	0.563	0.037	1.000
	AB	AB	AB	AB	B	C					0.224	1.000	0.002	0.943	0.001	1.000
P2	414.6(a)		261.85(b)		305.49(c)		186.1955	**0**	2,	0.000	0		0		0	
	493.490	483.699	261.852	313.429	345.499	312.768		**< 0.0001**			< 0.0001	0.001	0.005	0.074	0.044	0.003
	C	ABC	A	AB	BC	ABC					0.006	0.190	0.460	0.789	0.556	0.116
Pb	28.35(a)		18.11(b)		10.19(c)		519.7743	**0**	2,	0.000	0		0		0	
	26.178	54.498	19.981	15.136	12.256	7.318		**< 0.0001**			0.131	0.004	< 0.0001	< 0.0001	< 0.0001	0.013
	CD	D	BCD	ABC	AB	A					0.032	0.001	< 0.0001	< 0.0001	0.007	0.274
Rb	33.87(a)		36.17(b)		31.58(c)		67.8275	**0**	2,	0.000	0.008789		0		0	
	29.708	41.990	41.370	32.089	25.772	36.106		**< 0.0001**			0.000	0.403	0.025	0.170	0.154	<
	AB	C	C	ABC	A	BC					0.711	0.018	0.292	< 0.0001	0.185	0.033
Sc	8.87(a)		8.31(b)		9(c)		41.2413	**0**	2,		0.000222		0.051944		0	
	8.636	10.095	8.314	7.426	7.894	10.947		**0.003**		0.482	0.763	0.258	0.008	0.472	0.004	0.682
	AB	AB	AB	A	A	B					0.325	0.074	0.053	0.163	0.000	0.675
Si	417068.9(a)		411950.5(b)		416017.1(b)		20.9062	**0.00002**	2,		0.000622		0.000122		0.9407	
	418124.203	408686.211	409387.364	419352.936	418151.770	405904.973		**0.000**		0.154	0.008	0.851	0.001	0.782	0.447	0.004
	B	AB	AB	B	B	A					0.228	0.121	0.049	0.095	0.001	0.935
Sr	17.07(a)		12.31(b)		16.22(bc)		135.9779	**0**	2,		0		0.7115		0	
	19.857	22.749	13.728	13.663	16.124	17.748		**0.003**		0.149	0.002	0.001	0.651	0.111	0.010	0.141
	B	AB	A	A	AB	AB					0.105	0.065	0.332	0.884	0.005	0.088
Th	2.87(a)		3.29(b)		1.8(c)		90.3018	**0**	2,		0.007122		0		0	
	3.095	3.322	4.683	2.676	1.802	2.139		**0.002**			0.061	0.464	0.221	0.022	0.002	<
	AB	AB	B	AB	A	A					0.096	0.374	0.169	0.015	0.649	0.139
Ti	3471.69(a)		2668.28(b)		3861.57(c)		468.0002	**0**	2,	0.000	0		0.001056		0	
	3762.998	3933.988	2913.107	2516.914	4455.116	3518.193		**< 0.0001**			0.000	< 0.0001	0.403	0.105	0.003	<
	C	BC	AB	A	C	C					0.012	0.001	0.647	0.004	< 0.0001	<

Element	Mean per geology/LFT and Dunn's Post-test grouping						chi-squared	p-value (geology /LFT)	Df	Pairwise comparisons						
	Black Reef Quartzite		Dolomite		Ventersdorp Lava					Black Reef	Dolomite-Black		Ventersdorp Lava -		Ventersdorp Lava -	
	BR1	BR2	D1	D2	VLR	VLS				BR1 - BR2	BR1-D1 BR2 - D1	BR1-D2 Br2 - D2	BR1-VLS BR2-VLs	BR1-VLR BR2-VLR	D1-VLS D2-VLS	D1-VLR D2-VLR
V	66.18(a)		69.32(ab)		80.83(b)		83.0575	**0**	2,	0.000	0.045267		0		0	
	62.682	83.572	78.041	64.710	72.273	91.004		**< 0.0001**			0.002	0.534	< 0.0001	0.049	0.033	0.285
	A	ABC	BC	AB	AB	C					0.880	0.030	0.022	0.359	< 0.0001	0.202
Y	12.88(a)		10.31(b)		13.09(ab)		294.1864	0	2,	0.000	0		0.767344		0	
	12.840	13.636	11.018	10.176	12.655	13.459		**< 0.0001**			0.003	0.000	0.474	0.654	0.000	0.012
	C	C	AB	A	BC	C					0.001	< 0.0001	0.766	0.399	< 0.0001	0.002
Zn	34.86(a)		18.78(b)		25.78(c)		196.6485	0	2,		0		0		0.002411	
	39.283	141.654	28.348	27.644	24.795	24.394		**0.000**		0.336	0.001	0.000	0.002	0.009	0.704	0.424
	B	AB	A	A	AB	A					0.016	0.006	0.042	0.107	0.441	0.238
Zr	303.92(a)		256.24(b)		291.69(c)		311.5375	0	2,		0		0		0	
	327.150	302.109	251.255	259.687	311.435	257.543		**< 0.0001**		0.579	< 0.0001	< 0.0001	< 0.0001	0.599	0.711	< 0.0001
	B	B	A	A	B	A					0.000	0.001	0.000	0.977	0.912	0.001

2.3.1. Grouping analysis of Geology and LFTs from soil XRF results

The grouping analysis was run using 3 and 6 classes, to determine how the elements varied over the different geologies and landscape functional types. The Kruskal Wallis test above looked at individual variables per Geology or LFT, whereas the grouping analysis compares the elemental data and forms clusters using a K-means test. The grouping analysis was first run on all the variables which showed significant differences ($p<0.05$) in the Kruskal Wallis test per geology. The 10 highest R values were then selected for a second analysis. As shown in Figure 2-10, the 3 groups classified in the first test fell almost exactly within the 3 geologies, with only one sample from the Black Reef falling into the incorrect class.

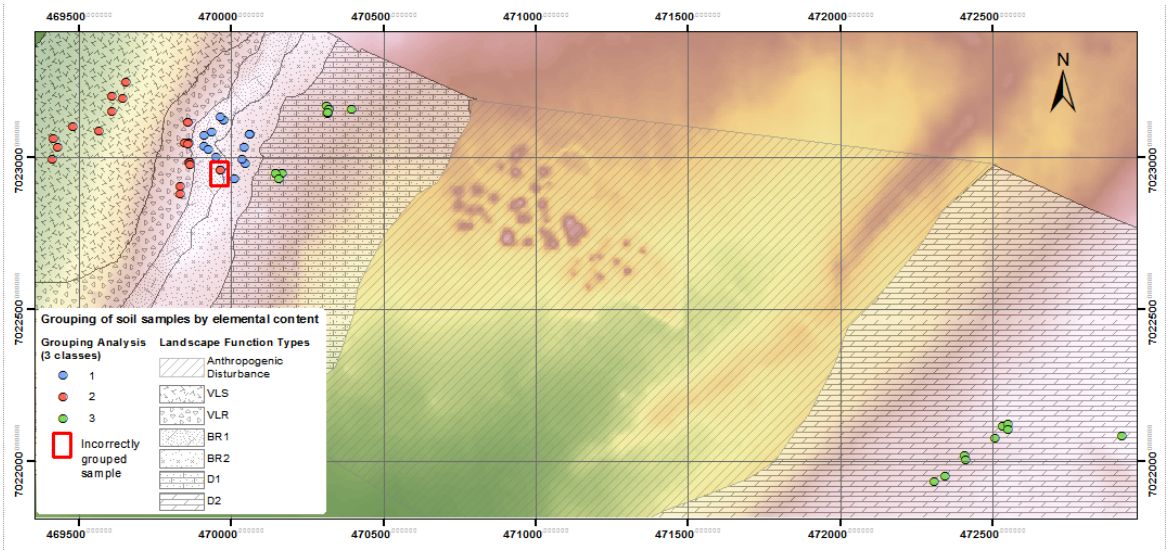

Figure 2-10 Spatially plotted results of the 3-class Grouping analysis of the soil elemental content and landscape functional types shown in background for reference purposes

The one sample for which the group did not match the geology had higher Fe, Fe_2, Cu, Ti and Zr values than were typically found on the Black Reef, which may indicate an anomaly/deviation in the geological features as the element content for this one sample more closely resembled the Ventersdorp Lavas in elemental makeup. Overall, the results indicated that there is a strong distinction between the elemental contents of the soils,

despite possible mixing of transported materials, and anthropogenic disturbance. The analysis showed that the variables that accounted for the largest proportion of the variance in the data were Mn, Cr and Ti. This relates strongly to the Dunn's post-test on the Kruskal-Wallis test which showed that these elements each fell into a separate class.

Table 2-7 Results of the grouping analysis for 3 classes based on the 10 variables which accounted for the most within class similarity and between class difference (shown by the R^2 value

Variable	*Mean*	*Std. Dev*	*Min*	*Max*	*R^2*
Mn	1590.616	1605.335	309.7828	6195.656	0.824116
Cr	115.7925	25.3424	80.51	167.09	0.692591
Ti	3457.552	760.9244	2113.883	5572.691	0.594537
Cu	23.92192	7.520388	10.45	50.25	0.577366
Cr2	131.2747	46.3602	45.84153	248.3653	0.55531
Pb	17.71385	8.62517	5.42	38.94	0.549092
Ba	246.9317	164.5889	101.56	1004.21	0.495279
Fe	21852.73	3411.537	16090.21	29848.51	0.436362
Fe2	2425.125	379.8165	1818.508	3287.302	0.42714
Zr	284.9246	48.95138	192.26	462.35	0.235256

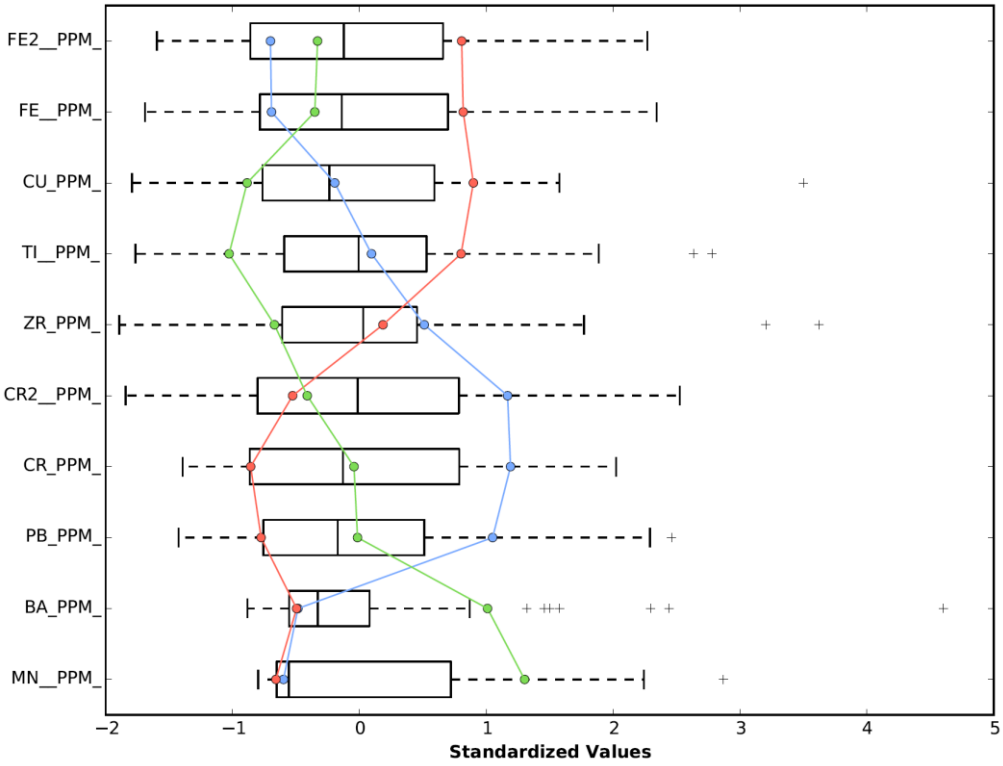

Figure 2-11 Box plot showing results of the 3-class Grouping analysis of the soil elemental content (Class 1 – Blue, Class 2 – Red, Class 3 – Green)

Table 2-8 Summary of Grouping Analysis classes (3 class analysis)

	Ventersdorp Lavas	Black Reef	Dolomites
Class 1	0	15	0
Class 2	19	1	0
Class 3	0	0	17

The distribution of data and the clustering of the different groups can be seen in Figure 2-11. Class 1 appears to be differentiated from Class 2 and Class 3 by higher Zr, Cr, CR_2, and Pb content. These elements were outside of the upper quartile for the full sample set. Class 2 was distinguished by elevated concentrations of Fe_2, Fe, Cu and Ti, and lower concentration of Cr_2, Cr and Pb. Class 3 was distinguished by lower concentrations of Cu, Ti and Zr, and elevated concentrations of Ba and Mn. These groups correlated strongly to the geologies, with all Class 1 samples falling within the Black Reef (n=15), the majority of the Class 2 samples falling within the Ventersdorp Lavas (n=19) and one sample appearing on the Black Reef, and all Class 3 samples appearing on the Dolomites (n=17).

The next stage of the analysis was to run the grouping analysis for 6 classes, using the same variables as defined in the 3 class analysis, and using the same 3 seed locations and randomly selecting another 3 seed locations (1 per class is required for the analysis). A further analysis tested the optimal number of classes by calculating the Calinski-Harabasz pseudo F-statistic [99]. The number of groups with the highest resulting F-statistic mean value represents the optimal number of groups to describe between class variation and within class similarity. The result of the optimal number of classes was three (mean = 402.7936). Table 2-10 displays the map of the results for the 6-class grouping analysis. The majority of the samples are still clustered into 3 classes which follow the three different geologies.

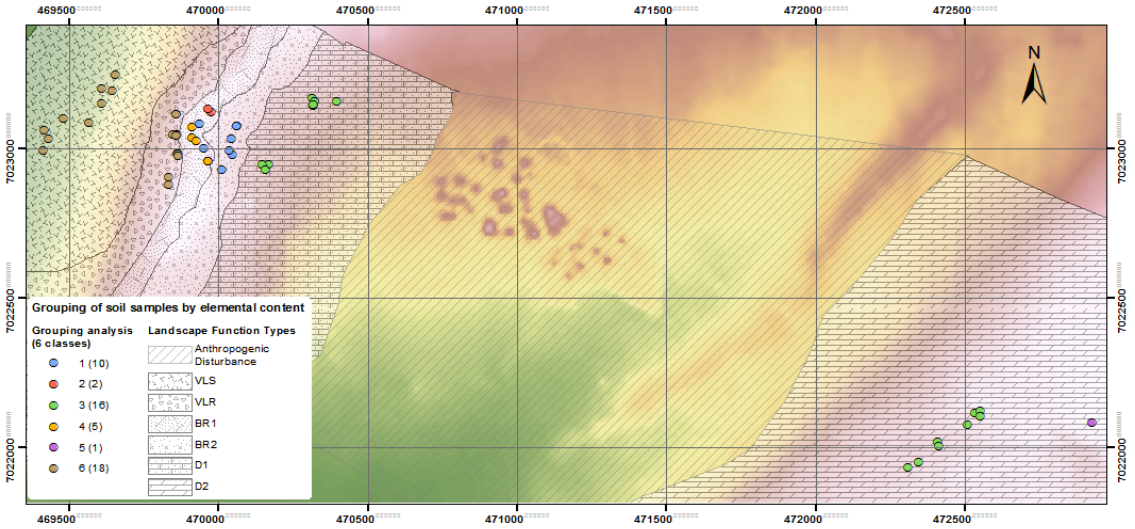

Figure 2-12 Spatially plotted results of the 6-class Grouping analysis of the soil elemental content and landscape functional types shown in background for reference purposes

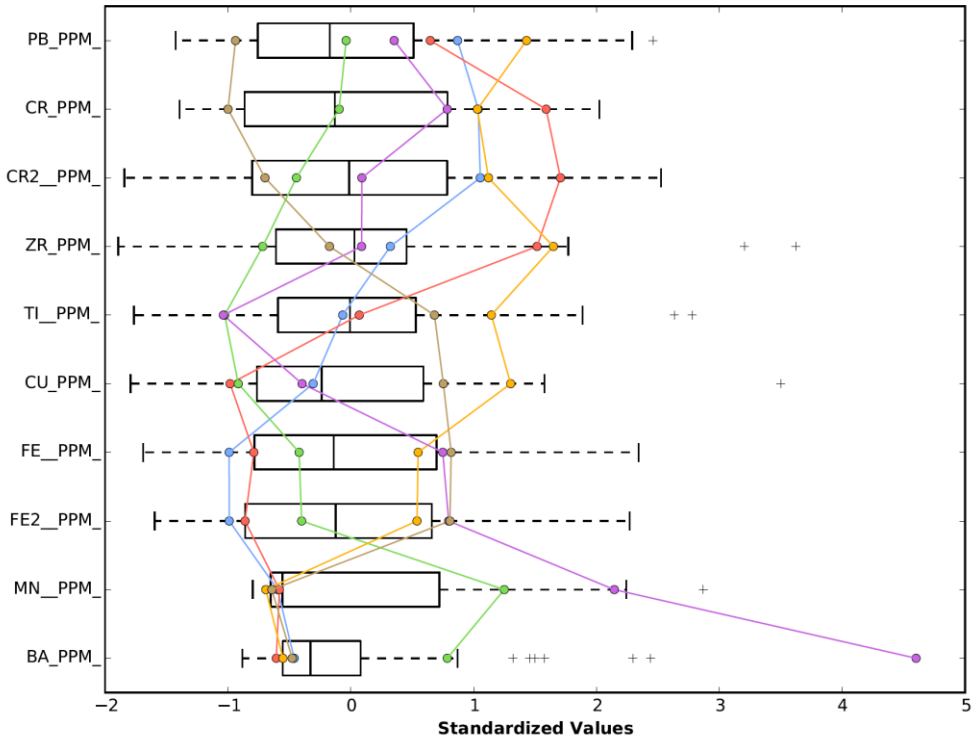

Figure 2-13 Box plot showing results of the 6-class Grouping analysis of the soil elemental content (Class 1 – Blue, Class 2 – Red, Class 3 – Green, Class 4 – Orange, Class 5 – Purple, Class 6 - Brown)

Table 2-9 Summary of grouping Analysis (6 classes) per Landscape functional Type per geology

	VLS	VLR	BR1	BR2	D1	D2
Class 1	0	0	3	7	0	0
Class 2	0	0	2	0	0	0
Class 3	0	0	0	0	8	8
Class 4	0	1	4	0	0	0
Class 5	0	0	0	0	0	1
Class 6	9	9	0	0	0	0

Class 1, 2 and 4 follow a similar distribution as Class 1 of the 3-class grouping analysis, with elevated Pb, Cr, Cr_2 and Zr values accounting for the majority of the difference from the other classes. Class 4 had elevated Ti and Cu values, which were identified as characteristics of the Ventersdorp Lavas samples in the 3 class analysis. There is however an overlap in range between the Class 1 and Class 2 values of the 3-class analysis which accounts for the variation in the 6-class analysis. Class 3 and class 5 are characterised by lower Zr, Ti and Cu values and elevated Mn and Ba values, which follows the same trend as Class 3 in the 3-class analysis. Class 5 has slightly elevated Fe, Fe_2 Mn and Ba concentrations when compared to class 3. Class 6 is characterised by elevated concentrations of Fe_2, Fe, Cu and Ti, and lower concentration of Cr_2, Cr and Pb, which follows the same trend as Class 2 of the 3-class analysis. .Most of the variation was accounted for on the Black Reef outcrop (BR1) which had samples which fell into classes 1 (n=3), 2 (n=2) and 4 (n=4). All BR2 samples fell into class 1 (n=7). The majority of Ventersdorp Lavas samples from both LFTS, VLS (n=9) and VLR (n=9) fell into class 6. As with the 3-class analysis, 1 sample from VLR fell into the class 4 which was predominantly BR1 samples. All dolomite samples from LFTS D1 (n=8) and D2 (n=8) fell into class 3, expect for one sample which fell into class 5. This analysis strongly supported the hypothesis that the underlying geology strongly influences the soil elemental content in the rooting zone of the plants, and indicated that the underlying geology is not obscured by transported materials at the rooting zone

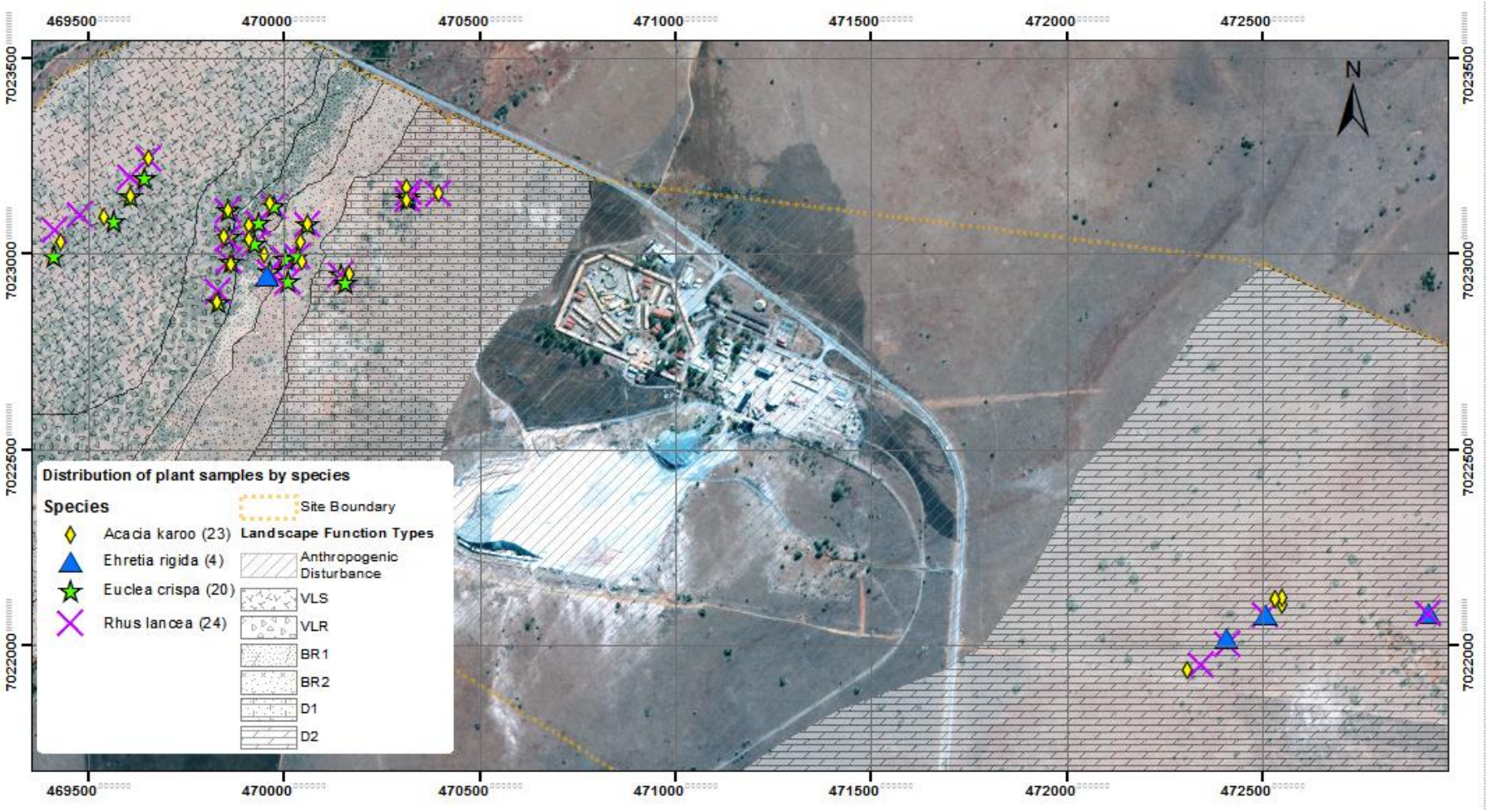

Figure 2-14 Map displaying the distribution of species collected during sampling

2.3.1. Vegetation sampling and leaf spectral analysis

Vegetation indices were derived from the spectral data collected with the spectro-radiometer. These spectral derivatives were used to test whether there was variation in spectral response per geology, per Landscape function type and per species. Figure 2-14 shows the locations of the plant samples collected and the distribution of the species. *Euclea crispa* trees were found to be less common on the dolomites, and did not occur within the boundaries of the study area on the Chert-rich dolomites (LFT D2). The *E. crispa* that occurred on the chert-poor dolomites were smaller and less vigorous than those occurring on the Black Reef and Ventersdorp Lavas. Similarly, the Ehretia rigida samples were less common on the Black Reef and Ventersdorp lava, and at the time of sampling, they were still dormant. Due to the fact that the Ehretia rigida samples were not adequately distributed across the site, these samples were omitted from the final analysis. Certain phenological differences were noted whilst performing the sample. The *S. lancea* and *A. karroo* obtained their first green flush after the dry season earlier on the Ventersdorp Lavas than on the Black reef or Dolomites. When sampling, only fully formed leaves were collected.

The ranges obtained for the eight spectral indices per species and for all four species combined are shown in Appendix 4. The data was tested for normality and the results of all 8 indices were found to be not normally distributed ($p < 0.05$). Based on this finding, the Kruskal-Wallis test with the Dunn post-test and Bonferroni correction were used for the analysis of the data.The Kruskal Wallis test for all species (*A. karroo, S. lancea and E. crispa*) combined showed significant differences per geology ($p < 0.05$) for all 8 spectral indices, as shown in Table 2-10 and Table 2-11. The strongest differences were for the NDVI, Red-edge NDVI, Red-edge inflection point and the 725/702 ratio of the 1st and 2nd

derivatives (Table 2-10). Pairwise comparisons showed that when combining data for the three species, only two groups per spectral index were formed. The NDVI, NDWI, Red-edge inflection point and Red-edge position found that the spectral response of plants on dolomites were significantly different to the Black Reef and Ventersdorp Lavas ($p < 0.05$). The Red-edge NDVI and the 725/702 ratios of the 1st and 2nd derivatives found that the spectral response of plants on Ventersdorp Lavas were significantly different to the Black Reef and Dolomites ($p < 0.05$), and the PSRI identified the Black Reef as being significantly different to the Dolomites and Ventersdorp Lavas ($p = 001$).

There were differences found in the results per species. For examples, there were no significant differences found between geologies for the NDWI ($p = 0.279$) and PSRI ($p=0.447$) for the *E. crispa* samples, and only a weak difference in the Red-edge inflection point ($p= 0.032$). There were significant differences between geologies for all indices for *A. karroo* and *S. lancea* samples, although in some cases, such as the Red-edge position ($p= 0.020$), the differences were only marginally significant at the 95% confidence interval. *S. lancea* samples also only showed a weak difference between geologies for the NDWI. The *E. crispa* samples had a highly significant result ($p < 0001$) for the Red-edge position, showing a blue shift on the dolomites. This result is in accordance with the observation noted that the *E. crispa* samples growing on dolomites were less vigorous than those growing on the Ventersdorp Lavas or Black Reef.

The indices that distinguished between the three geologies most successfully for the *A. karroo* were the NDVI ($p < 0.0001$) and the 725/702 ratio of the 1st derivative ($p < 0.001$), while the NDWI, Red-edge NDVI and the 725/702 ratio of the 2nd derivative were successful in distinguishing the Black Reef from the other two geologies. For the *E. crispa* samples, the NDVI ($p <0001$) and Red-edge NDVI were successful in distinguishing

between the three geologies. For the *S. lancea* samples, the Red-edge inflection point and 725/702 ratio of the 2nd derivative were most successful in distinguishing between the three geologies, but the PSRI results were significantly different for the Black Reef compared to the Ventersdorp Lavas and Dolomites. The *A. karroo* and *S. lancea* samples both showed higher NDVI values on the Black reef than on the surrounding geologies, and the *E. crispa* showed higher NDVI values on the Dolomites, despite also showing a blue shift, which is typically an indicator of plant stress. The variation in results between species has also shown that there is the potential for differences to be muted when combining data from all species as the three species respond differently to the changes in geology.

Pairwise comparisons of spectral indices per Landscape Functional type were also performed for the three species separately, and as a combined dataset. Table 2-11 shows the results of the Dunn's post test results for the spectral indices per Geology and per Landscape Functional Type. The results of the test per geology and the test per LFT have been compared to identify whether geology or position within the catena has a stronger effect on the plant spectral response. The results of **Soil characterisation** (sections 2.3.4-2.3.1) showed that there are differences in clay content, soil water content and rooting depth between the landscape functional types which could all potentially have an effect on the spectral response of the plant. The results of the XRF analysis showed that there was little difference in the soils elemental content for the landscape functional types within geologies (e.g. BR1 vs BR2, or VLS vs VLR). However, factors such as clay content could influence the uptake or bio-availability of the elements, which could also influence plant spectral response.

Table 2-10 Vegetation Indices (VI) for leaves of the three tree species. Data are ranges and mean of ranks and groups from the Dunn's procedure based on the mean of ranks. Significant differences between the three geologies (VL – Ventersdorp Lavas, BR – Black Reef, D – Dolomite) combined are indicated in bold. P-values and the observed K-value are given. The critical K-value is 5.991. (Kruskal-Wallis non-parametric test)

Spectral Index	Geology	*Combined (n= 682, D.f. = 2)*					*Acacia karroo (n= 223, D.f. = 2)*					*Euclea crispa (n= 209, D.f. = 2)*					*Searsia lancea n= 250, D.f. = 2)*				
		No of Obs.	Range	Mean of ranks (group)	p-value	K (observed)	No of Obs.	Range	Mean of ranks (group)	p-value	K (observed)	No of Obs.	Range	Mean of ranks (group)	p-value	K (observed)	No of Obs.	Range	Mean of ranks (group)	p-value	K (observed)
NDVI	**Black Reef**	244	0.714 - 0.92	329.95 (A)			81	0.714 - 0.87	138.44 **(C)**			81	0.717 - 0.856	74.21 **(A)**			82	0.767 - 0.92	120.1 (A)		
	Dolomite	202	0.64 - 0.909	411.89 **(B)**	**<0.0001**	40.808	80	0.64 - 0.863	109.61 **(B)**	**<0.0001**	28.466	42	0.767 - 0.873	163.07 **(C)**	**<0.0001**	59.730	80	0.67 - 0.909	151.06 **(B)**	**0.000**	16.032
	Ventersdorp Lava	236	0.642 - 0.919	293.19 (A)			62	0.642 - 0.874	80.53 **(A)**			86	0.68 - 0.848	105.64 **(B)**			88	0.674 - 0.919	107.3 (A)		
NDWI	**Black Reef**	244	0.02 - 0.108	318.98 (A)			81	0.041 - 0.108	84.67 **(A)**			81	0.036 - 0.097	113.25 (A)			82	0.02 - 0.08	108.99 **(A)**		
	Dolomite	202	0.026 - 0.112	386.93 **(B)**	**0.000**	15.408	80	0.064 - 0.112	134.64 (B)	**<0.0001**	25.016	42	0.026 - 0.094	97.45 (A)	0.279	2.552	80	0.027 - 0.072	142.41 **(B)**	**0.013**	8.652
	Ventersdorp Lava	236	-0.003 - 0.154	325.89 (A)			62	0.047 - 0.125	118.5 (B)			86	0.033 - 0.121	100.92 (A)			88	-0.003 - 0.154	125.51 (AB)		
PSRI	**Black Reef**	244	-0.102 - 0.129	378.18 **(B)**			81	-0.102 - 0.018	136.58 (B)			81	-0.037 - 0.075	105.69 (A)			82	-0.035 - 0.129	159.27 **(B)**		
	Dolomite	202	-0.101 - 0.094	330.8 (A)	**0.001**	14.084	80	-0.101 - - 0.009	134 (B)	**<0.0001**	75.575	42	-0.027 - 0.081	114.21 (A)	0.447	1.609	80	-0.052 - 0.094	122.64 (A)	**<0.0001**	32.027
	Ventersdorp Lava	236	-0.158 - 0.109	312.73 (A)			62	-0.158 - - 0.04	51.5 **(A)**			86	-0.113 - 0.109	99.85 (A)			88	-0.074 - 0.084	96.64 (A)		
Red-edge NDVI	**Black Reef**	244	0.392 - 0.717	368.93 (B)	**<0.0001**		81	0.514 - 0.717	153.09 **(B)**	**<0.0001**		81	0.392 - 0.632	106.7 **(B)**	**<0.0001**		82	0.403 - 0.704	117.4 (A)		
	Dolomite	202	0.419 - 0.715	398.79 (B)		58.237	80	0.419 - 0.639	95.7 (A)		53.827	42	0.478 - 0.648	149.71 **(C)**		35.945	80	0.482 - 0.715	160.78 **(B)**	**<0.0001**	30.185
	Ventersdorp Lava	236	0.381 - 0.704	264.1 **(A)**			62	0.381 - 0.642	79.35 (A)			86	0.417 - 0.597	81.56 **(A)**			88	0.447 - 0.704	100.98 (A)		

Spectral Index																				
	Geology	No of Obs.	Range	Mean of ranks (group)	p-value	K (observed)	No of Obs.	Range	Mean of ranks (group)	p-value	K (observed)	No of Obs.	Range	Mean of ranks (group)	p-value	K (observed)	No of Obs.	Range	Mean of ranks (group)	p-value	K (observed)
		Combined (n= 682, D.f. = 2)					*Acacia karroo (n= 223, D.f. = 2)*					*Euclea crispa (n= 209, D.f. = 2)*					*Searsia lancea n= 250, D.f. = 2)*			
Red-edge Inflection point	**Black Reef**	244	0.248 - 0.416	313.11 (A)			81	0.304 - 0.416	111.26 (AB)			81	0.253 - 0.401	99.26 **(A)**			82	0.248 - 0.336	85.38 **(A)**		
	Dolomite	202	0.275 - 0.454	411.77 **(B)**	**<0.0001**	13.502	80	0.301 - 0.454	127.29 **(B)**	**0.008**	7.869	42	0.275 - 0.398	126.88 **(B)**	**0.032**	31.667	80	0.277 - 0.38	164.18 **(C)**	**<0.0001**	7.789
	Ventersdorp Lava	236	0.095 - 0.434	310.7 (A)			62	0.269 - 0.434	93.24 **(A)**			86	0.212 - 0.404	99.72 (AB)			88	0.095 - 0.389	127.73 **(B)**		
Red-edge Position	**Black Reef**	244	727.701 - 736.447	349.14 (B)			81	728.537 - 734.345	95.98 **(A)**			81	729.353 - 736.447	117.86 (B)			82	727.701 - 735.392	131.15 (AB)		
	Dolomite	202	727.495 - 736.343	300.65 **(A)**	**0.001**	36.525	80	729.305 - 736.343	121.85 **(B)**	**0.020**	9.743	42	728.012 - 731.806	58.1 **(A)**	**<0.0001**	6.883	80	727.495 - 734.264	107.21 **(A)**	**0.020**	48.210
	Ventersdorp Lava	236	727.09 - 737.818	368.56 (B)			62	729.034 - 737.818	120.23 (AB)			86	729.22 - 734.675	115.79 (B)			88	727.09 - 734.063	136.86 **(B)**		
725-702 Ratio of the 1st derivative	**Black Reef**	244	0.557 - 2.087	385.24 (B)			81	0.994 - 2.087	160.73 **(C)**			81	0.591 - 1.524	118.16 (B)			82	0.557 - 1.723	116.71 (A)		
	Dolomite	202	0.643 - 1.758	406.27 (B)	**<0.0001**	95.462	80	0.873 - 1.493	100.08 **(B)**	**<0.0001**	83.646	42	0.643 - 1.586	134.33 (B)	**<0.0001**	30.505	80	0.879 - 1.758	163.44 **(B)**	**<0.0001**	34.867
	Ventersdorp Lava	236	0.531 - 1.558	240.84 **(A)**			62	0.721 - 1.378	63.73 **(A)**			86	0.531 - 1.388	78.28 **(A)**			88	0.626 - 1.558	99.2 (A)		
725-702 Ratio of the 2nd derivative	**Black Reef**	244	-21.165 - 6.386	391.73 (B)			81	-1.981 - - 0.197	159.7 (B)			81	-21.165 - 6.386	114.73 (B)			82	-4.297 - 1.201	125.05 **(B)**		
	Dolomite	202	-19.213 - -0.352	367.67 (B)	**<0.0001**	53.025	80	-17.146 - - 0.44	88.39 (A)	**<0.0001**	70.110	42	-19.213 - - 0.432	124 (B)	**0.001**	14.238	80	-2.168 - - 0.352	156.28 **(C)**	**<0.0001**	27.272
	Ventersdorp Lava	236	-23.568 - 165.363	267.16 **(A)**			62	-23.568 - 37.974	80.15 **(A)**			86	-20.513 - 165.363	86.56 **(A)**			88	-9.335 - - 0.495	97.94 **(A)**		

Table 2-11 Comparisons between groups obtained using the Dunn's procedure for the differences between the VIs results across the three geologies (VL – Ventersdorp Lavas, BR – Black Reef, D – Dolomite) and for the six landscape functional types (LFTs) for the three tree species. Significant differences between geologies and between LFTs within geologies are shown in bold (Kruskal-Wallis non-parametric test)

Dunn's Post test results	All species combined						Acacia Karroo						Euclea Crispa						Searsia Lancea					
Vegetation Index/Spectral analysis	Black Reef		Dolomite		Ventersdorp Lava		Black Reef		Dolomite		Ventersdorp Lava		Black Reef		Dolomite		Ventersdorp Lava		Black Reef		Dolomite		Ventersdorp Lava	
	BR1	BR2	D1	D2	VLS	VLR	BR1	BR2	D1	D2	VLS	VLR	BR1	BR2	D1	D2	VLS	VLR	BR1	BR2	D1	D2	VLS	VLR
NDVI	A		**B**		A		**C**		**B**		**A**		**A**		**C**		**B**		A		**B**		A	
	AB	A	BC	C	A	A	**B**	**A**	A	A	A	A	**A**	**B**	C		B	B	BC	AB	C	BC	ABC	A
NDWI	A		**B**		A		**A**		B		B		A		A		A		A		**B**		AB	
	AB	BC	C	C	**C**	**A**	**A**	**B**	B	B	**B**	**A**	A	A	A		A	A	A	A	A	A	A	A
PSRI	**B**		A		A		B		B		**A**		A		A		A		**B**		A		A	
	B	B	**B**	**A**	A	AB	**C**	**B**	BC	BC	A	A	A	A	A		A	A	C	C	BC	AB	A	AB
Red-edge NDVI	B		B		**A**		**B**		A		A		**B**		**C**		**A**		A		**B**		A	
	B	B	B	B	A	A	**B**	**A**	A	A	A	A	**A**	**B**	B		A	A	AB	AB	C	BC	AB	A
Red-edge Position	B		**A**		B		**A**		**B**		AB		B		**A**		B		AB		**A**		**B**	
	ABC	BC	A	AB	C	ABC	**A**	**C**	BC	BC	**C**	**AB**	**D**	**AB**	A		CD	BC	AB	BC	A	ABC	ABC	C
Red-edge Inflection point	A		**B**		A		AB		**B**		**A**		**A**		**B**		AB		**A**		**C**		**B**	
	B	AB	**B**	**C**	**B**	**A**	B	B	**B**	**C**	**BC**	**A**	A	A	A		A	A	AB	A	CD	D	BCD	BC
725-702 Ratio of the 1st derivative	B		B		**A**		**C**		**B**		**A**		B		B		**A**		A		**B**		A	
	B	B	B	B	A	A	D	CD	BC	AB	A	A	A	B	B		A	A	A	A	B	AB	A	A
725-702 Ratio of the 2nd derivative	B		B		**A**		**B**		A		A		B		B		A		**B**		**C**		**A**	
	B	B	B	AB	A	A	D	CD	**BC**	**A**	AB	AB	**AB**	**C**	BC		A	ABC	A	A	B	AB	A	A

Table 2-12 P-values for the Kruskal Wallis test for 8 spectral indices for three tree species individually and combined

Spectral index	Combined	A. Karroo	*S. lancea*	E. Crispa
NDVI	**< 0.0001**	**< 0.0001**	**< 0.0001**	**< 0.0001**
NDWI	**< 0.0001**	**< 0.0001**	0.055	0.182
PSRI	**< 0.0001**	**< 0.0001**	**< 0.0001**	0.739
Red-edge NDVI	**< 0.0001**	**< 0.0001**	**< 0.0001**	**< 0.0001**
Red-edge Inflection point	**< 0.0001**	**< 0.0001**	**< 0.0001**	0.132
Red-edge Position	**0.001**	**< 0.0001**	**0.000**	**< 0.0001**
725-702 Ratio of the 1st derivative	**< 0.0001**	**< 0.0001**	**< 0.0001**	**< 0.0001**
725-702 Ratio of the 2nd derivative	**< 0.0001**	**< 0.0001**	**< 0.0001**	**< 0.0001**

The first observation to be noted is that the pairwise comparisons of the LFTs (Table 2-11) frequently only resulted in 2-3 groups, and that the highest number of significant differences between groups was 4, which indicates that none of the spectral index results correlated directly to the LFT classifications. The VIs results which had the maximum number of groups for the Dunn's test were: *A. karroo* results for the 725-702 ratio of the 1st and 2nd derivatives; the Red-edge Position for the *E. crispa* samples; and the Red-edge inflection point for the *S. lancea*. Samples frequently fell into the same class for LFTS within Geologies. For example, with the combined data for the 725-702 Ratio of the 1st derivative, where the geologies were classified and Black reef (B), Dolomite (B) and Ventersdorp Lavas (A), the LFTS were categorised as BR1 and BR2 (B), D1 and D2 (B) and VLS and VLR (A), meaning that there were no differences between LFTs within the same geology. This trend can be seen for the 725-702 Ratio of the 2nd derivative, the PSRI and the Red-edge NDVI. For the PSRI and Red-edge inflection point, D1 and D2 fall into separate groups, and they also showed differences between the two Ventersdorp lavas LFTS. In the PSRI, this could be due to the fact that there were no samples for the *E. crispa* on D2 which may skew the results, but in the Red-edge NDVI, the *A. karroo* samples showed the same variation in groupings between the dolomites, which could reflect a plant response to the differences in soil characteristics between the Chert-rich and Chert-poor dolomites. In a number of cases the LFTs fell into more than one group, where at least one of the groups was the same for LFTS within the same geology.

For the *A. karroo* samples, there were frequently differences in the BR1 and BR2 LFTS, as seen for the NDVI, NDWI, PSRI and Red-edge NDVI. For the NDWI, the BR1 and VLR fall into group A, where all the other samples fall into group B. This could potentially be linked to the soil depth or effective rooting depth which was much shallower for these two LFTS. The other two species do not show the same trend. Similar results are shown for the Red-edge Position, although the VLR LFT also falls into the same group as the Dolomite LFTs. For the Red-edge NDVI, BR1 is the only LFT which is significantly different to the other LFTS.

For the *E. crispa* samples, a similar result is seen, where the BR1 LFT is significantly different from the remaining LFTS. In some cases, there are other LFTS which are also different. For the NDWI, PSRI and Red-edge Inflection point, there were no significant differences between LFTs. For the Red-edge Position and the 725-702 ratio of the 2nd derivative, there was overlap between groups. For the *S. lancea* samples, there were also a number of spectral indices which showed inconclusive results as the LFTs fell into several groups. For the NDVI, Red-edge NDVI, Red-edge inflection point and Red-edge Position, at least 4 of the 6 LFTS fell into more than one group. This poses a challenge when interpreting the data of linking it to trends in the soils and LFT characteristics.

Overall, the analysis of the spectral indices per geology showed much more distinct results in terms of the pairwise comparisons. Some differences were found between LFTs within geologies which means that one cannot rule out the role of the position within the catena entirely, but neither is it the most dominant factor in determining spectral response.

2.4. Discussion

2.4.1. Landscape functional analysis and soils characterisation

Landscape functional analysis was used to classify the landscape into function units (Landscape Function types) in an objective manner [91], [95], [105]. It is important to have a means of characterising or quantifying the environmental variables within the landscape as these will play a role in determining plant spectral response. In total, six landscape functional types were defined, with two landscape functional types per geology. In the analysis of the soils characteristics, some typical catenal effects were observed. The soils on the upper portions of the catena were shallower and rockier than the soils of the lower lying areas. The shallowness of the soils in the upper portion of the catena indicated that there is erosion and transport of materials down slope. Typically this transport of material would include the organic matter which leads to leaching of Soil Organic Carbon (SOC) higher in the catenal sequence and enrichment is downslope sediments [106], [107]. However, this was not noted in the results of the soils characterisation, where the highest positions in the catenal also showed the highest SOC results. It is suggested that the change in surface cover on the Rocky Ventersdorp Lavas and Black Reef outcrop, where there is a transition from grassland to woodland, and a decrease in understory vegetative cover combined with the increased rocky cover provides shelter from fires and allows more organic matter to be collected and broken down into the soils. It is well documented that fires, especially very hot or frequent fires will decrease the amount of soil organic matter present in the soils [108], [109]. This may account for the lower SOC in the soils lower in the catenal sequence which would otherwise have been expected to have higher SOC content than the upslope soils. It is not certain whether the SOC is of biogenic or lithogenic origin, but the distribution of the SOC indicates it may be of biogenic origin.

The differences identified between LFTs for SOC, clay content, soil water content and soil depth showed that there were distinct differences in landscape characteristics between the LFTS. These have been accounted for and will be considered when comparing results for the plant spectral analysis and the plant elemental uptake (leaf elemental content) analysis that will be performed in Chapter 3.

2.4.2. Analysis of soil elemental content

The soil elemental content correlated well with the expected values for the three geologies. There were a small number of samples which had results that exceeded the expected ranges for that geology. It is expected that these sampling sites have been exposed to anthropogenic contamination at some point in the past, which may account for the deviation from the expected range. The concentrations of Co, Cr, Cu, Pb, Ni and Zn in the soils were similar to the ranges detected in a baseline study of these elements in South African soils [110].

The grouping analysis that was used showed clearly how the soil elemental content was consistent across the geologies and did not differ significantly between Landscape function types. This is an important finding, as there is potential for the soils to be composed of regolith and transported materials and not to be a true reflection of the underlying geology.

2.4.3. Vegetation indices and spectral analysis

Significant differences in leaf spectral response to soil metal contents have been found in pot trials, with plants grown in varying concentrations of elements which are known to cause plant stress, such as As, Pb, Cd, Cu and SO4 [33], [111]. Rathod (2015) used spectral indices such as the NDVI and NDWI, to detect changes between different concentrations of As, Pb and Cd at 1-month and 3-months after dosing samples. The results of this study showed differences between the geologies for all the spectral indices (Appendix 4, $p<0.001$). The NDVI showed lower median values over the dolomites, when the expected result would have been that there were lower values for the Black Reef, which had

elevated Pb and Cr values. The NDWI did not differ across LFTs, which suggests that the observed stress spectral signature is not related to low water availability or physiological (osmotic) drought.

There was significant variation in Red-edge inflection point and Red-edge wavelength between the geologies (Table 2-10, $p < 0.0001$). Determining the Red-edge wavelength and inflection point is one method of measuring the blue shift, and these features may be used as indicators of plant stress. The Red-edge wavelength range for *S. lancea* growing on the Black Reef indicated a strong blue shift when compared to the Dolomite and Ventersdorp Lavas ($p < 0.0001$). Similar differences have been found for *S. lancea* growing on AMD-polluted versus unpolluted groundwater on the same geology (Dolomites) (Govender, 2011), and between ARD-tolerant versus sensitive ecotypes of *S. lancea* grown together in plots on polluted groundwater underlying dolomitic soils (Weiersbye *et al*., 2006).

In contrast there were no differences for *Euclea* sp. between the Black Reef and the Dolomite for the Red-edge wavelength calculations and the derivative ratios. *Euclea* sp. on both these geologies were however significantly different to those on the Ventersdorp Lavas. The features most likely to influence plant growth on soils derived from Dolomites include their higher Ca and Mg status and neutral to slightly basic pH, and on the Black Reef, factors associated with ARD and elevated metal concentrations, including lower pH and fertility, and increased osmolarity. However, no differences in the NDWI were found to support an osmotic effect which could result in osmotic drought stress.

It has been established that saline or acidic conditions associated with ARD in the study region inhibit nutrient cycling, in particular the mineralisation of nitrogen and phosphorus. A linear decline in tree seed production, mass and viability was observed for phreatophyte and riparian tree species growing in contaminated sites near the study area (Weiersbye and Witkowski, 2007). There was a possibility that similar effects may be observed on the Black Reef, and to confirm this, it would be necessary to acquire data and perform analyses relating to leaf pigments, oxidative indices, and bioavailability of elements in the soils. More in-depth spectral analysis could also be performed to identify possible nutrient deficiencies. However, many of the indices that have been developed for

identifying nutritional deficiencies are specific to selected types of crops, and may not be accurate for woodland tree species. It would be necessary to validate these indices before using them.

Both the *S. lancea* and *A. karroo* samples growing on the Black Reef, and particularly the Black Reef outcrop showed higher PSRI values. When plant leaves are senescent, the chlorophyll content degrades faster than the carotenoid content, resulting in a higher carotenoid/chlorophyll ratio. The PSRI correlates strongly to the carotenoid/chlorophyll ratio in plants [112]. This may correspond to the observation that the plants were experiencing their "green flush" at different times across the three geologies. The very young, immature leaves were not collected. On the Black Reef, many of the trees did not have mature leaves from the new season's growth and therefore leaves from the previous season were harvested. These were not visibly senescent, as all three species are evergreen/ semi-deciduous. None of the three species had lost their leaves over the dry season. The timing of the green flush could potentially be used as a valuable clue in delineating between geologies [113].

Smith *et al*. (2004) found that the use of the 702/725 ratio of the 2nd derivative was successful in detecting where plants were growing in the vicinity of leaks from gas pipelines [104]. However, this study found that the 702/725 ratio of the 1st derivative, rather than the 2nd derivative showed greater variation between the six LFTs, and supports the findings of Mutanga & Skidmore (2007), where the 1st derivative of the Red-edge was used to identify nitrogen deficiencies in pasture grasses [114].

Table 2-11 presents the results of the Dunn's multiple pairwise comparisons between geologies for each test, and between LFTs for each test. By comparing the results between geologies and LFTs one can determine how much of the variation in the dataset is due to topographic and landscape effects on the leaf spectral reflectance compared to effects as a result of parent geology. The LFTs were defined on the basis of physical factors such as shape, slope steepness, aspect, surface roughness, landscape heterogeneity and litter flow pathways, whereas the factors associated with parent geology would include salinity and osmotic potential, and metal deficiencies or toxicities. Both LFTs and geology would incorporate the influence of water availability and soil fertility to varying

extents, and factors such as clay content, pH and soil particle size could influence how the plant species respond to both landscape and geology, due to changes in elemental mobility and cation exchange capacity.

There were very few significant differences between LFTs within geologies, for all the VIs tested, which suggests that the topography (also a product of underlying geology) or physical landscape was playing a lesser role in tree spectral reflectance than the factors related to parent geology.

2.5. Conclusion

This chapter of the study focused on understanding the variables that could potentially affect plant spectral response. The study firstly characterised the landscape and soils characteristics to understand how these differed across the study site. The structure of the landscape is result of geomorphological processes which also determine the underlying geology, and as such, it is impossible to separate the geology and landscape entirely. There are certain variables however, as a result of subsequent processes such as weathering or the soils, transport of materials and biological processes that may have changed the soils characteristics in a non-uniform manner across geologies. The study needed to characterise these variables, and understand how they may affect spectral response of the plants. To do this, the site was divided up into landscape functional types, which were determined based of these variables. All subsequent analyses of the soils and spectral responses were performed at two levels – geology and landscape functional type.

Vegetation indices are an established method of detecting changes in plant physiology as a consequence of growing conditions. This study demonstrated significant disjunctions in foliar spectral data for three native phreatophyte tree species, which link to the changes in parent geology across a savannah in a semi-arid region. Whether the differences found in this study are directly related to substrate mineralogy and ARD, including changes in nutrient status or toxicities, will be investigated further in the next chapter.

This chapter identified that there are changes in spectral response between geologies, as well as selected spectral responses which are specific to a landscape functional type. Therefore it is important to incorporate both levels of analysis for the remainder of the study. It has also been observed that it is necessary to analyse the spectral data at a species level to gain the best understanding of the variables that are being analysed.

Further analysis should identify which aspects of the changes in geology account for the changes in spectral reflectance. As the plant species respond differently to the changes in the geology, it would also be valuable to investigate selected biophysical parameters in the plants such as oxidative indices and plant pigments to understand whether the observed responses, such as the red-shift in the *E. crispa* samples on the Black Reef are in fact stress responses with an atypical spectral response.

3. PLANT SPECTRAL RESPONSE TO SOIL AND LEAF ELEMENTAL CONTENT

3.1. Introduction

In Chapter 2, there were two key findings which were identified. The soil elemental content could be clustered together to classify the underlying geology. Secondly, the spectral response of the leaves changed with geology. This chapter demonstrates how the preliminary findings in the previous chapter are further validated through the comparison of the substrate and foliar elemental concentrations with plant spectral response. Studies have shown that elemental concentrations and changes in bioavailability of specific elements can cause a plant stress response which can be detected through the a change in the leaf spectral response [111], [115]. Much of the previous work on this topic has been performed in controlled environments such as laboratory trials, or in relatively homogenous landscapes with low species diversity, such as agricultural fields. These studies have successfully detected plant stress responses in elevated concentrations of species elements, such as Cu, As, Cd, Pb [111], [115]. There is evidence, however that the changes in geology can cause a sufficient shift in plant spectral response to be detectable, even in more heterogeneous environments [71], [90].

This study aimed to quantify how the many variables in a heterogeneous landscape could affect plant response, and to identify whether the factors which affected plant spectral response were also a factor of the changing geology. It had already been determined that the differences between the three geologies had an influencing effect on the plant spectral response at a leaf level. Analysis of soil and leaf elemental concentrations, bioconcentration factors and elemental ratios were used as indicators of plant nutritional status, plant health and soil fertility and elemental bioavailability. These variables were all investigated to understand the influence of geology and soil geochemistry on plant metal uptake and spectral response. In order to do this, the leaf elemental concentrations were first

compared to global mean concentrations [116] for each of the elements analysed to assess whether there were any excessively high or low concentrations found in the plant samples from the study site. The samples were then tested for significant differences in the soil, leaf and bioconcentration factors (BCF) between geologies, and between landscape functional types (LFTs). The soil, leaf and BCF concentrations were then correlated with each other to understand whether the differences in BCF between geologies were a product of leaf or soil elemental concentrations, or a combination of both. This provided insight in the bioavailability and potential elemental exclusion by the plants to control uptake or translocation of the metals to the leaves. The differences between the leaf elemental concentration and BCF and leaf and soils elemental ratios were also assessed at a species level to understand how the three species differed in their uptake of the elements in the soils, and to give more insight into plant nutritional status.

These analytical procedures provided valuable insight into the differences in soil conditions and uptake of elements in the samples. The next stage of the analysis was to understand how these differences in soil and leaf elemental concentrations affected plant health, determined by the selected set of vegetation indices (VIs). It was important to understand which of the variables caused the changes in spectral response so that future analyses can predict the substrate conditions based on the changes in spectral response. As it was found that the results differed significantly between species, the final step of the analysis tested the use combining VIs to first classify the species, and then look at the variation within species classes to assess metal concentrations. This final step of the analysis showed that it was possible to classify the majority of samples into their species classes, but that the stress response for a subset of samples which were growing in less favourable conditions altered the spectral signature significantly. The soil and leaf elemental concentrations of these subset samples were compared to the remaining samples and the differences that were detected indicate a strong correlation between leaf and substrate elemental concentrations and the plants spectral response.

3.2. Background

3.2.1. Plants and Soil elemental interactions

Certain elements are considered to be essential for plants to grow. There are seven elements in particular which are considered necessary for maintaining life processes in humans, animals and plants. These elements are chlorine (Cl), manganese (Mn), iron (Fe), zinc (Zn), boron (B), copper (Cu) and molybdenum (Mo). In addition to these elements, there are other elements which particular plant species have become dependent on for metabolic processes [117]. For example, Cobalt (Co) is essential for nitrogen fixing bacteria which are symbiotic with certain tree species [117]. Furthermore, certain plants have adapted to a specific suite of soil conditions. An example is *Senecio coronatus* which only occurs on serpentine soils [23] which are characterised by low calcium to magnesium ratios, a lack of essential nutrients and high concentrations of nickel and chromium. There is usually a preferred concentration range of elements in soils for the optimal growth of plants. Deficiencies in elements required for plant growth can result in stunted growth, disease, low seed germination or an incomplete lifecycle for a plant (inability to flower or produce viable seeds) [67]. Similarly, an excess of an element which is considered to be essential for plant growth can be equally detrimental, and sometimes extremely toxic [118]. Elements such as arsenic (As), cadmium (Cd), lead (Pb) and mercury (Hg) are generally considered to be non-essential elements for plant growth, and even extremely low concentrations in the soil can have a harmful effect on plants [117]. Often the mechanisms that are developed to take up essential nutrients also allow for the uptake of some non-essential elements [40], [118]. Even if the plant is not able to take up an element from the soil, it is possible for the element to be detrimental to plant growth by changing the ratios of essential elements available in the soils, or by causing osmotic stress, where the concentration of salts in the soil water is too high to allow for osmosis to take place at the root [66]. Mobility of the elements in the soils can also play an

important role in the effect of elemental concentrations in the soils on plant health. As discussed in Chapter 2, factors such as soil particle size and clay content will affect the mobility of certain elements in the soils, as will other factors such as porosity and homogeneity [119], [120] . Other critical factors to soil elemental mobility are pH and redox potential (eH), mineralogy and surface charge [119]. Changes in chemical species strongly influence bioavailability of elements or the compounds that are formed in the soils. Elements which form metal-organic complexes are relatively stable around pH 6-7, and not generally bioavailable [120]. Soil microbial activity and soil organic matter play a critical role in maintaining or establishing a healthy soil profile [121], [122]. In certain conditions, soil organic matter can have an immobilising effect on elements in the soil [120]. The interactions between plant roots and soil microbes may also influence and increase the bioavailability of metals in the rhizosphere. This is achieved by the roots secreting protons and organic acids which mobilise heavy metals within the soil and enhancing uptake by plant roots [117], [120]. Root-colonising bacteria and mycorrhizae have also been known to catalyse redox transformations such as Pb^{2+}, Hg^{2+}, Au^{3+}, Te^{4+}, Ag^{+}, thus increasing the bioavailability of these metals [44]. The hyphae of mycorrhizae also increase the root absorption area, which allows for more nutrient uptake [44]. However, regardless of the amount of root absorption area, metals cannot be taken up by plants without the correct transport proteins. This is due to the ionic charge of the metals which prevents them from moving freely across cellular membranes [39]. Transmembrane transporters have specialised binding sites that the metals bind to when being taken across the membrane. The binding domain of the transmembrane transporters is only receptive to the ions of specific metals and is responsible for transporter specificity. This prevents the plant from taking up non-essential metals, or metals that would be harmful or toxic. Some plants have mechanisms which inhibit the stimulation of transporter activity when there is a high influx of metal ions from the soil, in order to prevent an over-accumulation of a particular metal [39], [118]. Despite the specificity of the binding sites on many plants, some non-essential metals are still taken up in the roots when the transporters do not differentiate between two

or sometimes more metals. For example, Cadmium (Cd) is frequently absorbed instead of Calcium (Ca), despite the fact that it is highly toxic to most plants [123], [124].

Not all of the metals that are taken up by these transporter proteins are transported to the rest of the plant. Many of the metal ions become bound to the cell walls of the roots, and because they are bound, cannot be transported to other parts of the plants. Some metals, such as Pb are predominantly bound in the roots as there is very little translocation of Pb to the shoots [39], [125].

As with the transport of most nutrients from the root to the shoot, the transportation or translocation or metal-containing sap from the roots to the shoot of the plant is dependent on root pressure and transpiration, as well as a series of chemical interactions [40]. It is this stage of the uptake process that will determine how many metal ions will be bound to the root cell walls, and how many will be taken up into the shoots of the plant and sequestered, excreted or volatilised [40]. The vacuole is only one of the many sites where metals may be sequestered. The metals which are not bound in the vacuole, and are loaded into the xylem instead are transported to the leaves where the metals are reabsorbed into the leaf cells [39]. Many metals are distributed to apoplastic structures such as the cell wall or the trichone. It is estimated that for most Ni and Zn hyper-accumulating species, 60-70% of the metal is sequestered in the cell wall. Ligands and proteins are also largely responsible for the detoxification of metals. Complexation with ligands can happen either extra- or intra-cellularly [44], [126]. In a certain plant species, *T. goesingense*, the Ni was rendered inactive by histidine, a proteinogenic amino acid, which complexed the Ni is such a way that it was no longer toxic to the plant [39], [126]. Metallothioneins and phytochelatins are also responsible for intracellular complexation. While metallothioneins are gene-encoded, phytochelatins (PC) are enzyme synthesized. It is thought that PC synthase activities are only stimulated by the presence of metal ions. Phytochelatins have been found in a wide range of both higher and lower plants [44].

While there are numerous plant species that have evolved mechanisms to survive in high concentrations of metals in the soils, either through uptake and binding and rendering the metal inert

within the cell, or through the active exclusion of harmful elements, there are still elements which have been found to be toxic to all plants [127]. Resistance to metal stress is achieved in plants through one of two mechanisms: avoidance, which includes the active exclusion of uptake as one of the strategies to externally limit harm from metal stress, and tolerance, which describes internal mechanisms for limiting harm from metal stress [128]. Plants which are tolerant to metals still exhibit signs of stunted growth and poor productivity compared to congenerics growing in non-contaminated conditions. It is suggested that this is due to the energy expenditure required, as there is a high metabolic cost associated with the detoxifying harmful elements [25], [128]. Many plants are not fully tolerant to elevated metal concentrations, but can withstand slightly elevated concentration in the soils. These plants are considered to be associate metal-tolerant species, as opposed to metallophyte which are dependent on the elevated concentrations of metals in the soils for their survival [25]. When the concentrations in the soil exceed the tolerance limit for the metal tolerant species, toxic effects such as growth inhibition and leaf chlorosis are seen. Studies have found that metal toxicity can affect stomatal opening, which in turn affects plant respiration [40] Other findings have shown that plants growing in toxic conditions have poor root development, which limits nutrient and water uptake [122]. Metal toxicity has also been shown to cause oxidative stress, and to damage the photosynthetic apparatus [40], [129], [130]. In extreme cases, findings have even shown that the central Mg ion of the chlorophyll molecule can be replaced, essentially disabling the photosynthetic ability of that chlorophyll molecule [131], [132].

Metal toxicity is only one of the harmful effects that is experienced by plants growing in metal rich soils. Often, metalliferous soils are also characterised by a number of growth limiting characteristics. For example, findings have shown that on Serpentine soils, which are characterised by a low Ca:Mg ratio, the low availability of Ca and excess Mg availability which may cause toxicity, and specific adaptations to maintain a higher foliar Ca:Mg ratio, were limiting factors to plant health and distribution [133]. Serpentine soils also often contain elevated concentrations of elements such as Fe, Ni, Co and Cr, all of which have the potential to cause plant stress. However, they are typically also

characterised by poor physical characteristics such as steep rocky slopes which have poor nutrient holding capacity, and low clay contents which result in poor water holding capacity [25], [34]. These factors result in high erosion potential, which in turn reduces the likely of humic matter decomposing in the soils to form compost. The added presence of soil organic matter (SOM) can greatly reduce the levels of toxicity experienced by plants growing in metal rich soils [34], [120], [122], [133].

Species which have high tolerance to heavy metals have evolved on sites which either have naturally occurring heavy metal in the soils, or have been polluted for a long time [25]. These are often ecotypes that differ from the rest of their species in terms of resistance to harmful metals. Because only the most resistant of the species would have established themselves on the contaminated site, there is limited genetic diversity for some hyperaccumulators [44], [134], [135].

When investigating plant uptake on metal rich soils, one of the indicators of a hyperaccumulator is the percentage of the dry mass of the plant that is made of up a specific element [136]. Alternatively, the percentage or ratio of accumulation compared to the background concentrations found in the soils can be used [137]. Calculating a ratio between the soil elemental concentrations and the plant elemental concentration can also provide insight into the mobility of elements. This ratio is typically known as the bioconcentration factor [120], [137], and is calculated as:

$$BCF = \frac{Concentration\ in\ the\ plant}{Concentration\ in\ the\ soil}$$

The elemental concentration in plant biomass is not usually directly related to the elemental content of the soils. The BCF therefore gives a relative indication of mobility in the soils, and/or an indication of the plant ‘s ability for uptake of a specific element [120], [137].

3.2.2. Reflectance characteristics of plants

Studies on the use of remote sensing to determine foliar chemistry identified more than 40 absorption features which have been related to particular foliar chemical concentrations [53], shown in Chapter 1, **Error! Reference source not found.**. While it is possible to detect certain of these f eatures, such as overall chlorophyll or carotenoid content using less refined data sources such as multispectral satellite imagery, airborne hyperspectral sensors and hand-held spectroradiometers, which measure from 400nm to 2500nm at 1-2 nm intervals, will obviously detect a more exact spectral response [53], [138], [139]. Measuring spectral reflectance at the leaf scale with a hand-held spectroradiometer also allows one to eradicate a lot of the variability associated with canopy or landscape scale data (such as scattering from atmospheric dust or moisture). Ground-truthing is also easier when performed at the leaf/tree scale and this `clean' data can then be related back to the more `noisy' data acquired at the canopy or landscape scale using airborne or satellite-based sensors [58], [33]. Collecting spectral data is also a rapid process, and there is very little post-processing work required on the spectra to make them usable, compared to the orthorectification and atmospheric correction procedures require for aerial photography and satellite imagery.

Studies have shown that it is possible to detect the effects of plant stress through the plant spectral reflectance [33], [30], [65], [111]. Spectral reflectance values represent the amount of light reflected from a surface at a given wavelength. For vegetation, the spectral characteristics are determined predominantly by a range of pigments such as chlorophyll A and B, carotenoids and anthocyanins and the water, nitrogen, cellulose and lignin content of the plant [53], [111], [140], [141]. Green leafy vegetation has a particular spectral signature due to the leaf pigments, which reflect light in the visible wavelengths, whilst leaf water content reflects light in the shortwave infrared bands (SWIR), as shown in figure 1 [64], [142]. Chlorophyll is present in healthy, productive plants to absorb light energy during the photosynthetic process, but declines in concentration quickly when plants are under stress or during leaf senescence [69]. Chlorophyll has strong absorption peaks in the blue and

red bands. However, carotenoid absorption also peaks in the blue band and for this reason the red band is usually used for estimations of chlorophyll content. Carotenoids also dissipate less rapidly than chlorophylls when plants suffer stress or during leaf senescence, making carotenoids a useful indicator of plant stress [69]. Leaf senescence is one of the first indicators of metal toxicity as the photosynthetic process is extremely sensitive to the effects of metal toxicity [10]. This indicates that plants growing in metal rich soils will show signs of stress which should be identifiable through the Red-edge stress signature. However, as there are many other reasons for leaf senescence there needs to be a further indicator for metal specific stress. Studies have found that plants growing in metal rich soils show an exaggerated peak in the green (0.5-0.6 μm) wavelengths and depending on the species, a shift in the entire plant signature either towards the blue or red regions of the electromagnetic spectrum [33] (I.M. Weiersbye, unpublished PhD study). The blue shift is thought to occur as a result of the plant increasing the production of blue and UV absorbing pigments, which may have a biochemical protective function as antioxidants [143].

3.2.3. Methods for the remote sensing of vegetation

The use of a portable device to test spectral reflectance means that one can choose whether to conduct a study in a controlled or uncontrolled environment. It is also possible to collect data within a controlled environment, such as in a pot trial and then use that data to help interpret data collected in an uncontrolled environment, such as from satellite imagery of a landscape or forest canopy. For example [30] conducted pot trials to test the effects of metal contamination on red spruce, sorghum and mangroves. Results of this study showed an increase in the reflectance in the green band (0.5-0.6μm) for the plants growing in metal enriched soils. For the sorghum pot trial, the results showed a slight peak between 0.5-0.6μm for the control, an even greater peak in for the pots with a 100 ppm dose of $CuSO_4$ and the highest peak for the pots with a 400ppm dose of $CuSO_4$ [30], [115]. There was also a visible blue shift in the plants with the highest dose of Cu. Red Spruce, however, showed an increase in reflectance at the 0.5-0.6μm bands. There was a much lower peak in the reflectance in the

near infra-red (0.75-0.8µm) bands for the plants growing in Cu and Mo. This could be as a result of the addition of Mo to the soils as it is highly toxic to plants in higher concentration, resulting in a pronounced Red-edge stress signature [30], [115], [144]. Once the reaction of these plant species to Cu enriched soils has been established, the data can be used to interpret spectra collected from plants growing in natural, uncontrolled field conditions [30].

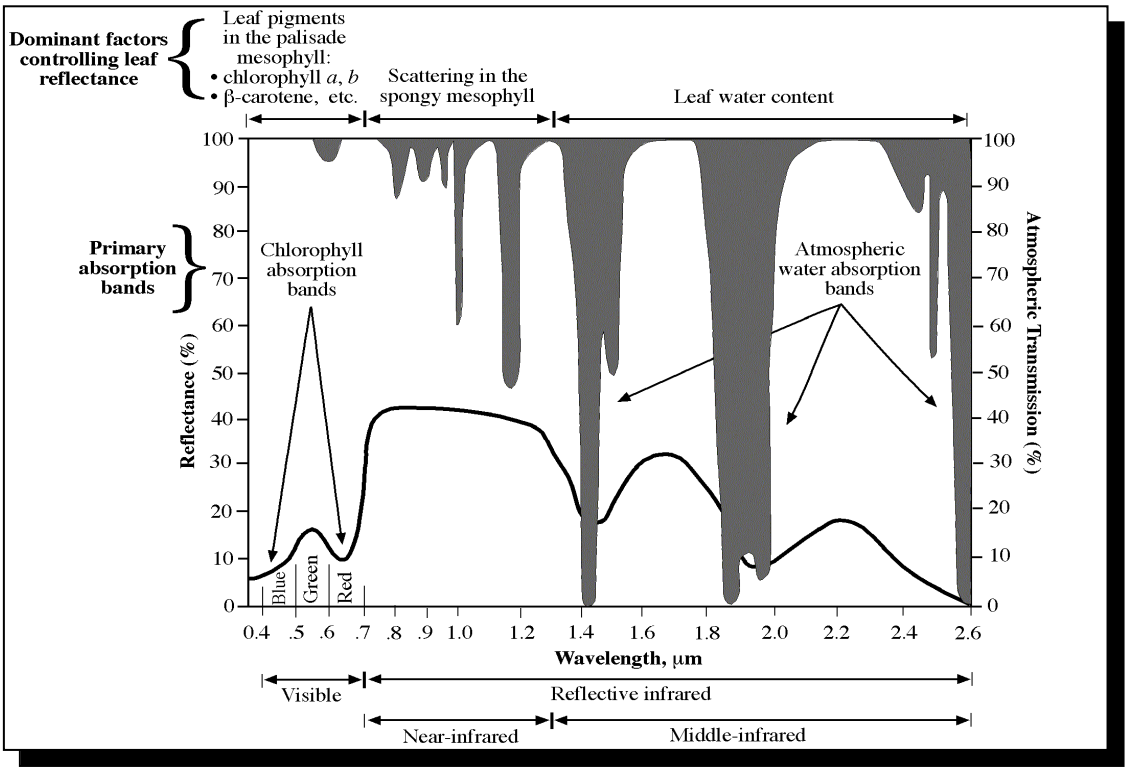

Figure 3-1 A typical spectral signature for green leafy vegetation and the particular plant structures that control leaf reflectance at given wavelengths (Jensen, 2007

The Red-edge stress signature has been used to detect gas leakages from underground pipelines. Studies found that gas leakages from underground pipes displace soil oxygen which disturbs the rhizospheric interactions, resulting in plant stress which is detectable through the use of the Red-edge stress signature [104]. The Red-edge and estimations of blue shift have been used on the Highveld gold mines to identify seepage plumes through the use of airborne hyperspectral imagery [65]. This study used the plant stress signatures to identify the extent of the seepage plumes from tailings facilities. The plumes have a high total dissolved solids (TDS) content, and low pH. The use of the modified Red-edge NDVI also allowed different ecotypes of different tree species of the same age to

be discriminated from each-other. The trees are being used for hydraulic control of the seepage plumes, as part of a site-species matching phytoremediation trial so the different ecotypes were planted in separate replicate plots. It was possible to identify the ecotypes that are more tolerant to AMD, which could be very useful for future monitoring programs from contaminated sites, and for identifying metallophyte flora.

Studies have found that the Mg^{2+} ion in chlorophyll of plants growing in heavy metal contaminated environments may be substituted by one of the metals present in the growth media [131], [145]. This change in the molecular structure of the chlorophyll affects the productivity of the plants and therefore the spectral signature. For metals such as Cu^{2+}, Zn^{2+}, Cd^{2+} and Ni^{2+} a spectral shift in the red band absorption feature towards the blue portion of the electromagnetic spectrum has been detected. In Mg^{2+}-Chlorophyll, the chlorophyll absorption for Chlorophyll a and b occur at 662nm and 641nm respectively. However, when the Mg^{2+} ion was replaced with Cu^{2+}, Zn^{2+}, Cd^{2+} and Ni^{2+} there was a blue-shift in the absorption feature ranging from 1nm-15nm. When the Mg^{2+} ion was replaced with Hg^{2+}, a red shift was detected [131].

Detection of these features was performed on the chlorophyll extracts from plants grown in metal-rich growth media, and not on the live leaves of the plants. Destructive methods of determining pigment concentrations in leaves, where the plant pigments are extracted from the leaf matter using organic solvents and analysed through a spectrophotometric assay are commonly used [146]. However, destructive methods of analysis are not always feasible, and are extremely labour-intensive if one is analysing a large sample set, compared to the rapid collection of spectral data [147]. Therefore it is preferable to make use of different techniques of hyperspectral analysis based on the spectra collected from fresh leaves, and referenced spectra from plants showing stress responses from known concentrations of metals. In order to determine the specific concentrations of chlorophyll a and b, and carotenoids from the spectral response, it is possible to make use of Ratio analysis of the spectra, which is essentially a simplified form of Spectral Unmixing [61], [146]

Without specifically separating out the chlorophyll response from the plant spectral reflectance spectrum, studies have successfully managed to measure a metal induced blue shift in plants.[111], [90] Detection of a blue shift in the electromagnetic spectrum, used in combination with the Red-edge stress signature has been successful in detecting contamination of mineral related in pot trials of sorghum grown in differing concentrations of $CuSO_4$ [30]. Leaf reflectance indices have been used to distinguish between different tree species and ecotypes of the same species planted for a site-species matching trial on AMD from adjacent gold mine tailings storage facilities on the Highveld. It was possible to differentiate between eight Eucalyptus species and hybrids, and between two Searsia lancea ecotypes, due to their varying tolerance to the pollutant-related stress, and possible tolerance to salinity [148]. This difference in tolerance within plant taxa may allow for a distinction between naturally mineralised substrata and anthropogenically contaminated land.

3.3. Research Objectives

The overarching objective of this study is to determine whether it is possible to use the remote sensing of vegetation to distinguish between changes in the underlying geology. The results of the previous chapter showed that there are significant differences in the elemental contents of the soils for the three geologies in question, but not between landscape functional types. There were differences between landscape functional types in landscape characteristics such as effective rooting depth, soil clay content, soil organic carbon, and soil moisture content. There were also differences in plant spectral response between the geologies and between landscape functional types. The differences were more distinct at a species level than for all species combined, as the different species responded differently to geology and landscape factors. The aim of this chapter is to further characterise the plant spectral response to the changes in elemental content, used as an indicator of changes in geology. This chapter will investigate whether specific elements determine the plant spectral response, or whether it is a factor of plant elemental uptake, or soil or plant elemental ratios which best describes the spectral response. This will give further clues as to the variables relating to changes in geology, or combination of variables, that influence plant spectral reflectance most strongly.

To address this aim, the following research objectives needed to be met:

a. Investigate trends in plant elemental content
b. Identify whether there are any relationships between plant and soil elemental content, through the use of bioconcentration factors
c. Compare a selected set of soils and leaf elemental ratios which are established indicators of nutrient deficiencies, metalliferous soils or plant stress
d. Test which factors control for the most variation in the calculated vegetation indices, which are used as a relative indicator of plant health

The outcome of these analyses will help us to understand how changes in soil elemental concentrations, and plant-soil interactions may affect plant spectral reflectance. Based on the findings, it may be possible to then further refine spectral analytical techniques to be able to reliably identify changes in geology at both a leaf and canopy scale.

3.4. Methods

This analysis builds on the work described in the previous chapter. Many of the same datasets will be used for this analysis. Site selection, sample collection and preparation are the same as described in Chapter 2. A brief recap of the data acquisition and preparation for analysis is given below for reference purposes.

3.4.1. Data acquisition and sample analysis

The study site is divided up into three geology types, the Black Reef Quartzites, which is the ore body of interest. This is an outcropping sulphide rich, gold-bearing ore body, which forms the catenal divide and watershed across the study site. The ore body runs roughly across the site from the north-east to south-west. To the north-west is the Ventersdorp Lavas and to the South-east are the Malmani Dolomites. Each geology was divided into 2 landscape functional types to better understand the effects of position within the catena. It was found in Chapter 2 that elemental content in the soils typically remained consistent between landscape functional types within geologies. This analysis looked at total elemental content using XRF, and did not investigate soil solutions or leachates for bioavailability/mobility. Three main tree species were used for this study (*Searsia lancea*, *Euclea crispa* and *Acacia karroo*). Four samples for each tree species were collected per landscape functional type. Soils samples were collected from the base of each sampled tree, and leaf samples were harvested and measured for spectral reflectance before being washed and frozen while waiting for further sample prep to take place.

All samples were processed as described in detail in Chapter 2 and the following analysis was performed:

Table 3-1 Types of elemental analysis used in this study

Analysis type	Sample type	No of samples	Elements analysed
Leco Autoanalyser	Leaf	73	N, C (insufficient leaf material from MMEC43)
Leco Autoanalyser	Soils	74	N, C
XRF - Majors	Soils	57	SiO_2, Al_2O_3, Fe_2O_3, FeO, MnO, MgO, CaO, Na_2O, K2O, TiO_2, P_2O_5, Cr_2O_3, NiO
XRF trace elements	Soils	57	Sc, V, Cr, Co, Ni, Cu, Zn, Ga, Rb, Sr, Y, Zr, Nb, Mo, Ba, Pb, Th, U
ICP OES	Leaf	70	Al, Ba, Ca, Co, Cr, Cu, Fe, K, Mg, Mn, Na, Ni, P, S, Si, Ti, Zn, U
ICP-MS	Leaf	70	Ag, As, Au, Cd, Co, Pb, Sb, Sn, U, V

3.4.2. Leaf sample analysis

Once the spectral readings of each set of leaves had been taken, the leaves were washed in distilled water. Excess water was shaken off the leaves and they were weighed and stored frozen in Ziploc bags. The samples were then freeze dried and reweighed to calculate water content, and milled to a fine powder using an agate mortar and pestle and liquid nitrogen. Samples were extremely resinous and needed to be sieved through a plastic “colander” made from a plastic sample weighing boat so that they could be discarded after use. This allowed the fines to be kept aside and the fibrous matter to be milled further. Samples were subsampled for further analysis and kept frozen. Samples were then analysed as follows:

- A 1g, homogenously ground sample was weighed out for microwave digestion and ICP-OES. Elements that were below detection levels for ICP-OES were then analysed using ICP-MS.
- A 1g sample was weighed out and analysed for Carbon and Nitrogen by LECO Autoanalyser.

Results of the elemental analysis of the leaf material was analysed at a species level per geology and per landscape functional type. Leaf elemental content was also compared to global average leaf elemental concentrations as described in [116].

3.4.3. Leaf and soil elemental ratios

The bioconcentration factor (BCF) was calculated for the following elements: Al, Ba, C, Ca, Co, Cr, Cu, Fe, K, Mg, Mn, N, Na, Ni, P, Pb, Si, Ti, U, and Zn. These were the elements which had elemental data available for both the soil samples and the leaf samples.

A number of elemental ratios were then calculated for the leaf and soil samples separately. Ratios between leaf results and soil results were calculated for selected elemental ratios to further understand how soil content may affect the leaf ratios.

Table 3-2 below shows the list of ratios that were created, the type of ratio and the purpose of the ratio. The source or reference that was used to determine the ratio and the purposes is shown in the final column.

Leaf elemental content and leaf and soil elemental ratios and BCF were analysed per species, and by geology and landscape functional type. The Kruskal Wallis test was used to initially determine the leaf and soil elemental contents and BCF per geology and LFT for each element. Correlations were determined between the leaf and soil elemental contents, and the leaf elemental content and BCF and soil elemental content and BCF. These correlations were used in conjunction with the Kruskal Wallis test data for the leaves, soils and BCF to understand the mobility of the elements in the soils.

The leaf and soil elemental ratios were calculated, and specific tests were performed for some of the elemental ratios, such as the Si:Ti ratio. The Si:Ti ratio was used to detect whether the ratio in leaves and soils was similar, as similarity between the two ratios can be an indicator of dust/soil contamination on the leaves as plants do not take up the Ti and Si in the same ratios that those elements are present in the soils (pers. Comm. I.M. Weiersbye)

Table 3-2 Leaf and soil elemental ratios that were used during the study

Elemental ratio	Leaf/Soil	Purpose	Reference
Si:Ti	Soil ratio	Si/Ti is used as a contamination index. Neither element is readily absorbed by plants. Plants do however take up small amounts of Si and Ti. Therefore, if Si/Ti ratio in the plant material does not differ significantly from that in the soil, it indicates that there may be surface contamination on the leaves from dust.	I.M Weiersbye (pers.comm.)
Si:Ti	Leaf ratio		
Al:P	Leaf ratio	Al is amphoteric, and in acidic soils (e.g. ARD-impacted, sandstones as Al^{3+}) or alkaline soils (e.g. dolomitic) becomes more available for plant uptake. In addition, P becomes less available in acidified soils (due to both inhibition of P-cycling organisms and to chemical precipitation reactions). This can result in Al-toxicity and P-deficiency in plants because Al^{3+} competes with P for uptake at the root membrane. Al-toxicity affects root development and P-uptake (as well as other nutrients such as Ca), so affects leaf anatomy. P-deficiency results in increased levels of foliar anthocyanins which may affect spectral response.	I.M Weiersbye (pers.comm.)
Ca:Mg	Soil ratio	Ca:Mg ratio in soils is a useful indicator of a metal rich soil. While this is generally used for the analysis of ultramafic soils, it has relevance to the Black Reef within a dolomitic matrix in this study. Plants on ultramafic soils can suffer from nutrient deficiencies, this is unlikely on the dolomitic Ca, Mg-dolomitic rich soils at VR, but there may be a marked difference in ratios between the 3 geologies which may result in lower chlorophyll response in the vegetation indices.	I.M Weiersbye (pers.comm.), [133], [34]
Ca:Mg	Leaf ratio		
Na:K	Leaf ratio	The ratio of an immobile element to a mobile element, is a useful indication of membrane damage and leakiness. The Na/K index is used to check integrity of red blood cells and plant or other biological tissues. Membrane leakiness can result from stresses to the living organism (e.g. heat, acid soils, metals, etc.), and from crude preparation of the dead sample (e.g. too slow to dry, freeze, etc.).	I.M Weiersbye (pers.comm.)
Ca:S	Leaf ratio	Ca:S is a ratio of two essential macronutrients, Ca which is immobile and not volatilised from the leaf, and the other mobile and volatilised as SOx compounds. S likely to be more available along the Black Reef.	I.M Weiersbye (pers.comm.)
N:P	Leaf ratio	Both N and P are critical for the growth of healthy plants. While the optimal ratio between N and P is highly variable between species and types of plants, studies have found that on average, plants with an N:P ratio <10 or >20 show signs of either N or P-limited biomass production. Often N:P ratios are negatively correlated with biomass production.	[149], [150]
Si:Mn	Soil ratio	At high concentrations, Mn is toxic to plants. Mn toxicity can cause growth stunting and brown/chlorotic spots on leaves. Elevated Si in soils has been shown to alleviate Mn toxicity. Increased Si content in the soils can reduce toxicity of Mn in plants. Studies have shown that where there is high Si, there is reduced translocation of Mn to the shoots of plants	[151], [152]
Si:Mn	Leaf ratio		
Si:Mn:	Leaf ratio: Soil ratio		
Sr:Ca	Soil ratio	Sr is considered a non-essential element, but it can substitute for Ca	I.M Weiersbye (pers.comm.)
Rb:K	Soil ratio	Rb is relatively rare, but has been found to substitute for K in silicate minerals. More weathered soils have been observed to have a higher Rb:K ratio as the Rb which was bond to the silicate minerals is more available.	[153]
Zn:Cd	Leaf ratio	There is often competition between ions for uptake in plants. Studies have shown that Cd accumulation can interfere with uptake of Fe and Mg, resulting in a decrease in photosynthesis. Cd uptake can be supressed by the uptake of divalent cations such as Zn^{2+}, Mn^{2+}, $Si^{2+}$and Ca^{2+}.	[124]

C:N	Soil ratio	The ratio of C:N is soils varies between soil types, but a usual range is from 8:1-to 17:1. When the carbon content in the soils is significantly higher than this, it can cause a leaching of the available nitrogen in the soils. The balance of the two is essential for plant growth and carbohydrate production. Studies have found that soils with high organic carbon content in their SOM may be limited in terms of P, N and S. C:N ratio can also be lowered as a result of higher temperatures, whilst higher rainfall and increased soil acidity increased soil C:N ratios.	[149], [154], [155]
Mg:Mn	Leaf ratio	Mn^{2+} has a similar ionic radius to Mg^{2+} and therefore could substitute Mg in plant uptake. As Mg is a critical component of the chlorophyll molecule, Mg deficiencies could be detrimental to plant health. Mn is also an essential element. Higher Mg content in the plant tissue has also been shown to increase Mn tolerance and prevent toxicity.	[86], [156]
Mg:Mn	Soil ratio		
Ca:Al	Leaf ratio	Studies have shown that high concentrations of bioavailable Al in the soils can inhibit the uptake of Ca to the plant.	[157]
Al:Ca	Soil ratio		
N:S	Leaf ratio	In agronomy, the N:S ratio is used extensively to monitor ultimate crop production. An optimal ratio is crop plants is from 11:1 to 15:1. Anything higher than 15:1 indicates a sulphur deficiency, whereas anything lower than 11:1 would indicate a nitrogen deficiency in plants. There are many interactions between soils elements which can affect this ratio, such as the availability of Ca in the soils. This is however a potentially useful indicator of Nitrogen deficiency.	[158]–[160]

3.4.4. Leaf spectral analysis

Spectral data was collected as described in Chapter 2. The same suite of vegetation indices has been used for the analysis in this chapter. In Chapter 2, the Kruskal-Wallis non-parametric test with a Dunn's Post Test with a Bonferroni correction was used to detect significant differences spectral response of all three species, across the three geologies, and then across landscape functional types. The results showed that there were significant differences between geologies and, to a lesser extent, between the landscape function types found for the vegetation indices. The findings showed that the spectral response across the geologies differed between species. When combining the data for all three species, the results appeared to be obscured by the opposing spectral responses between species. For example, where the S. lancea showed a blue shift on the Black Reef, the E. crispa tended towards a red shift. Therefore the trend across geologies was not as defined when combining all species data.

3.4.4.1. Analysis of response of vegetation indices to soil elemental content, leaf elemental content and soil and leaf elemental ratios

Plant spectral response can be driven by a wide range of variables and environmental factors. Chapter 2 showed that in some cases, the spectral response between landscape functional types did not differ, but that the response between geologies did differ, which indicates that the drivers for spectral change related to the geology. In other cases, the response between landscape functional types did differ, which indicates that other variables, possibly those relating to the structure of the landscape and to position within the catena, may have more influence on the spectral response than the geology. The bioavailability of the elements, which may be a factor of the soil characteristics, could also influence the spectral response quite strongly.

To understand which variables had the strongest influence on the vegetation index results, the data was analysed at a species level and per element for leaf and soil bioconcentration factor and for a range of soil: leaf elemental ratios. As there was a very wide range of variables to be analysed, the variables characterisation tool in XLStat was used to reduce the number of variables that would be used in the final analysis. The variables characterisation tool uses the correlation co-efficient to determine the power that each variable has on the spectral index being tested where the lower the p-value, the stronger the relationship between the two variables in question. A Spearman's correlation test was used to perform this analysis as many of the variables were not normally distributed. This test was performed for each vegetation index per tree species. This provided a reduced number of variables which could then be used for further analysis.

Following on from the variables characterisation, regression analysis was used to determine the relationship between the subset of elemental content data and each vegetation index per species. Each of the variables was tested for normality, and if all variables that were pre-selected during the variables characterisation for a given spectral index were normally distributed, then linear regression

was used. The “best-model” option was used to identify which combination of variables provided the best model.

Where there were variables that were not normally distributed, non-parametric regression was used. This test does not provide the same “best-model” for identifying the best combination of variables to use. For each test, to adapt the model to provide the best fit, the variables with the lowest correlation p-value were removed, and the test was run again to identify if this improved the R^2 value. This process was repeated as many times as was necessary to identify the combination of variables that resulted in the best model. For all tests, 3 observations were randomly selected to be used as validation points.

By following this process, the number of variables in use was reduced. These were the variables that corresponded most strongly to the changes in the spectral response. This gives rise to two further questions:

- How do these elements correspond to the geology, and can the shift in spectral response therefore be linked to geology, through the correlation with the elemental content?
- What are the likely biophysical effects on the plant that could be caused by these elements, resulting in the changes in spectral response?

The first question is addressed in this study, but the second question goes beyond the scope of this study as information on plant pigments and oxidative stress indices is not available.

3.4.5. Grouping of species through the use of vegetation indices

The optimal final outcome of this work would be to be able to identify changes in geology remotely, with limited ground-truthing. If the variation in spectral response between the different species can obscure the change in response to geology when looking at all species data together, then it may be necessary to use a 2-step approach which first classifies the species, and then looks at within

class variations in spectral response to identify geologies. This would be especially important when using satellite imagery. There have been a number of studies which have managed to characterise tree species using Worldview 2 8-band satellite imagery [161], [162]. While this study is focusing on the hand-held spectral data that was collected, it is still possible to investigate the potential for using the spectral data for extracting species information. It was noted during a preliminary investigation of the data that the differences between VI results between the different species was quite pronounced. The spectral response difference between species was further investigated. No single index accounted for differences in all three species, and therefore the possibility of using multiple indices to classify species was investigated. The grouping analysis in ArcGIS Desktop 10.4.1 was used to delineate the spectral results into groups. The analysis was performed using an iterative approach, starting with just two indices, the Red-edge position and the PSRI. Different combinations of indices were then tested, gradually adding additional indices. The Calinski-Harabasz pseudo F-statistic was used to identify the optimal number of groups for each test that was run.

Elemental content of the leaves and soils and the leaf and soils elemental ratios and BCF were then classified by group to further understand the results defined in the grouping analysis.

3.5. Results

The results of this study are shown below. The first part of the analysis looked at the results of the leaf elemental content and the bioconcentration factors calculated using the leaf and soil elemental content in order to gain a broader understanding of how the plants may be responding to the changes in geology.

3.5.1. Analysis of leaf elemental content compared to global mean leaf elemental content

A comparison of the leaf elemental content to global average leaf elemental content was performed to understand how the range of elements analysed compared to data from "normal" growing conditions [116]. Figure 3-2 shows three graphs with the range of elements that were analysed for in the leaf samples plotted along with the global averages. The max, min and mean values for the leaf elemental content are shown as vertical bars, and the global averages are shown as red crosses. Gold, uranium, cadmium, silver, selenium, chromium and nickel content are all higher than average. Even the lowest values found in the leaf samples for the study site were higher than the global average by close to a full order of magnitude. These elements are documented as being present in high concentrations on the Black Reef and surrounding soils and therefore this finding seems to be in line with expected results for the Black Reef, but indicates a possibility of enrichment of the surrounding soils too. Silica content was found to be lower than the global averages. The ranges for the remaining elements overlapped with the global averages.

The analysis was also performed for each geology independently, but there were only very small differences in the ranges found for each geology. These graphs have been included in for reference purposes.

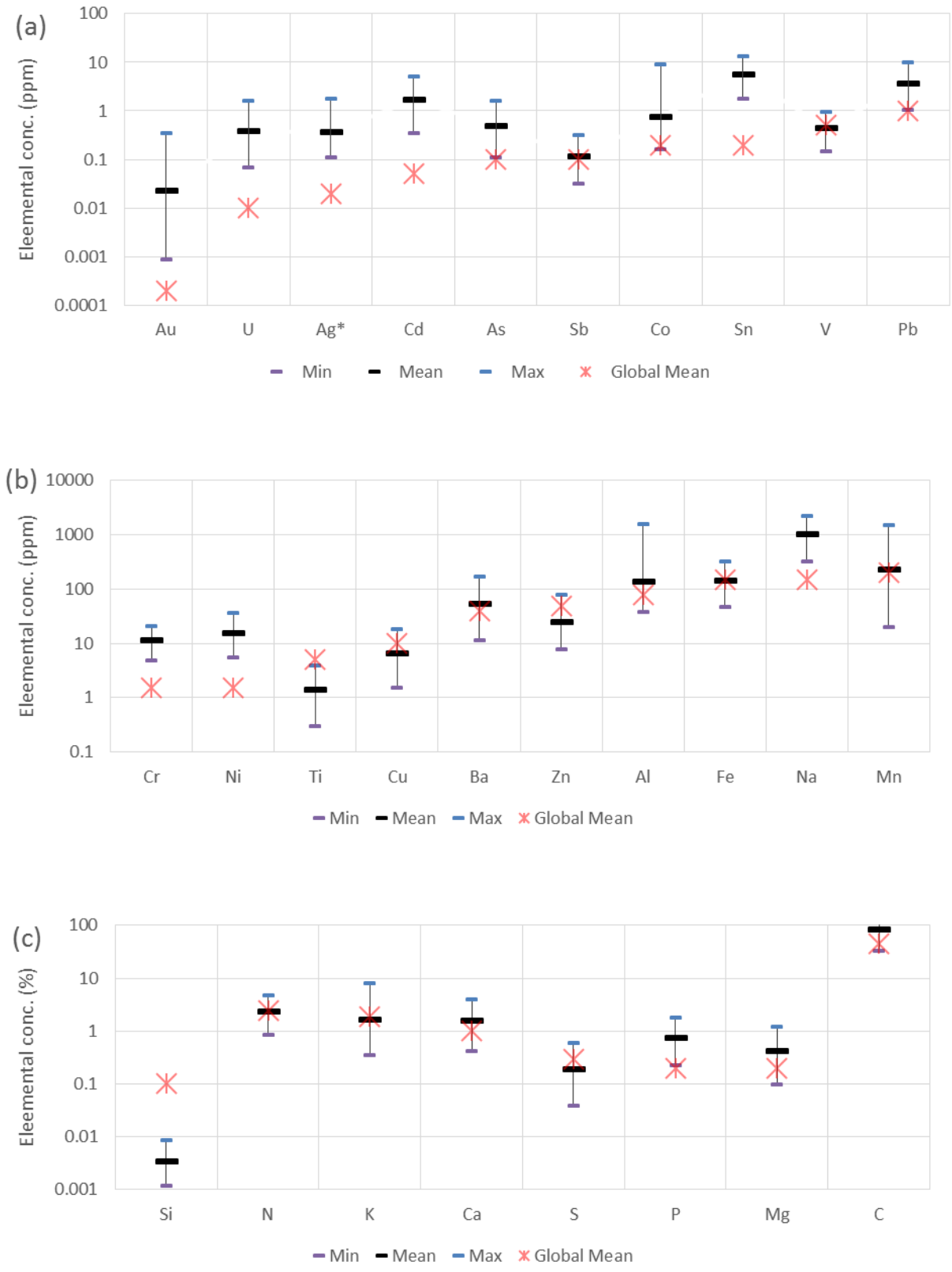

Figure 3-2 Graphs displaying the global average leaf elemental content as per Dunn 2007 and the ranges obtained for leaf elemental content for all analysed leaf samples. All geologies have been combined as there were very few differences between geologies[116]**. (a) shows elemental concentrations for Au, U, Ag, Cd, As, Sb, Co, Sn, V & Pb as ppm, (b) shows elemental concentrations for Cr, Ni, Ti, Cu, Ba, Zn, Al, Fe, Na and Mn as ppm, and (c) shows concentrations for major elements Si, N, K, Ca, S, P Mg, and C as percentage.**

3.5.2. Relationship between Leaf and soils elemental content and bioconcentration factors

Table 3-3 shows the results of the Dunn's procedure of the Kruskal Wallis test results for the soil elemental content, leaf elemental content and bioconcentration factors per geology and LFT. It also shows Spearman's correlation between the soil elemental concentration and the BCF, leaf elemental concentration and BCF, and soil and leaf elemental concentration for each element. Stronger correlations between BCF and leaves than the BCF and soils would imply that there is a possible change in the bioavailability of the soils, as the soils elemental content does not change significantly but the bioconcentration does. Strong correlation to soils and weak correlation to the leaf elemental content implies that either the elemental content is not bioavailable, not present in the soil solution or that the plants have excluder mechanisms to control the quantity of the element that is taken up. It should be noted that there were no significant correlations detected between leaf elemental content and soil elemental content.

While the Dunn's procedure on the Kruskal-Wallis test identified significant differences ($p< 0.05$) between geologies except for Al, Ca, Mg, Na and Si and for all elements per landscape functional type, there were, however, very few significant differences detected between leaf elemental content for the different geologies. Ca content on the Black Reef was significantly different to the Ventersdorp Lavas and Dolomites in the leaf samples, but not in the soils. There was no direct correlation between the leaf and soil element content for Ca. Ca uptake and concentration in plants plays an important role in metal tolerance. The fact that the plants growing on the Black Reef had significantly lower Ca content could indicate a much higher competition for binding sites and elemental uptake, as Co and Ni both had higher concentrations in the Black Reef leaf samples. Co is interesting in that the elemental concentration in the soils between the Ventersdorp Lavas and the Black Reef do not differ, and yet the leaf elemental content, and the bioconcentration factor was significantly higher on the Black Reef, and particularly at the Black Reef outcrop. This implies that the Co on the Black Reef is more bioavailable that on the other two geologies. Ni content in the soils is reportedly lower on the Black

Reef soils, than in the other two geologies, but was higher in the leaf samples of the Black Reef and Ventersdorp lavas, than in the leaf samples on the Dolomites. The bioconcentration factor was higher on the Black Reef than on the Dolomites or Ventersdorp Lava. Mn also showed a trend where there is a strong correlation between the leaf elemental content and the Bioconcentration factor ($R^2 = 0.720$) and a weaker negative correlation between the soil elemental content and the bioconcentration factor ($R^2 = -0.573$). For Mn, there was a significantly higher concentration of Mn in the dolomitic soils, and no differences observed between the Ventersdorp Lavas and the Black Reef soils, and no significant differences detected in the leaves, yet a significantly higher BCF in on the Black Reef outcrop and the Rocky Ventersdorp Lavas compared to the dolomites. The difference in bioconcentration factors between the Ventersdorp lavas and the Black Reef again indicates higher mobility or uptake of metals on the Black Reef than on the surrounding soils.

Pb concentration was significantly higher on the Black Reef soils compared to the other geologies, but there was no difference in leaf uptake. Pb is not usually transported to the leaf material, even when taken up by plants, and therefore this is not an unusual finding. Pb in the roots or surrounding soils could still potentially cause plant stress.

Table 3-3 Grouping results of the Kruskal-Wallis tests with a Dunn's procedure and Bonferroni correction for the soils elemental content, leaf elemental content and Bioconcentration factors (BCF) for the leaf samples by element per geology (in small letters) and landscape functional type (in CAPS). Spearmann's correlation between the BCF and soils,BCF and leaves and soil and leaf samples are also shown per element. Significant correlation ($p < 0.05$) are shown in bold.

Element	Dunn's Post-test grouping per geology (small letters) & LFT (CAPS)																		Correlations R^2 ($p < 0.05$)		
	Soil							Leaf							Bioconcentration factor								
	Ventersdorp Lavas		Black Reef		Dolomite		p-value	Ventersdorp Lavas		Black Reef		Dolomite		p-value	Ventersdorp Lavas		Black Reef		Dolomite		p-value	BCF/ Soil	BCF/ Leaf	Soil/ Leaf
	VLR	VLS	BR1	BR2	D1	D2		VLS	VLR	BR1	BR2	D1	D2		VLS	VLR	BR1	BR2	D1	D2				
Al_2/Al	a		a		a		0.844	a		a		a		0.396	a		a		a		0.186			
	A	C	AB	C	BC	AB	**< 0.0001**	A	A	A	A	A	A	0.179	A	A	A	A	A	A	0.288	**-0.397**	**0.855**	0.119
Ba	a		a		b		**< 0.0001**	b		ab		a		**0.011**	b		b		a		**< 0.0001**			
	A	AB	A	AB	BC	C	**< 0.0001**	B	B	B	AB	A	AB	**0.002**	ABC	C	C	BC	A	AB	**< 0.0001**	**-0.679**	**0.787**	-0.194
Ca	a		a		a		0.556	b		a		b		**0.003**	a		a		a		0.361			
	A	A	A	A	A	A	**0.2211**	A	A	A	A	A	A	**0.034**	A	A	A	A	A	A	0.477	**-0.678**	**0.582**	0.106
Co	b		b		a		**0.0000**	a		b		a		**< 0.0001**	a		b		a		**< 0.0001**			
	B	B	B	B	AB	A	**0.0003**	A	A	B	AB	A	A	**0.001**	A	A	B	AB	A	AB	**0.000**	**-0.419**	**0.733**	0.159
Cr	a		c		b		**< 0.0001**	a		a		a		0.183	c		a		b		**< 0.0001**			
	A	A	C	C	BC	AB	**< 0.0001**	B	AB	AB	AB	AB	A	**0.058**	C	C	AB	A	ABC	BC	**< 0.0001**	**-0.732**	**0.595**	-0.152
Cu	C		b		a		**< 0.0001**	a		a		a		1.000	a		a		a		**0.004**			
	C	C	ABC	BC	AB	A	**< 0.0001**	A	A	A	A	A	A	0.695	A	A	A	A	A	A	**0.025**	**-0.505**	**0.846**	0.003
Fe	b		a		a		**< 0.0001**	A		a		a		0.774	a		a		a		0.082			
	AB	B	A	A	A	A	**< 0.0001**	A	A	A	A	A	A	0.288	A	A	A	A	A	A	0.103	**-0.403**	**0.901**	0.055
K_2/K	a		b		ab		**0.0000**	A		a		a		0.987	a		a		a		0.219			
	A	A	AB	C	BC	A	**< 0.0001**	A	A	A	A	A	A	0.080	AB	AB	AB	AB	A	B	**0.011**	**-0.428**	**0.804**	0.085
Mg	a		a		a		0.178	A		a		a		0.939	a		a		a		0.818			
	A	AB	AB	AB	B	A	**0.0010**	A	A	A	A	A	A	0.774	A	A	A	A	A	A	0.283	**-0.342**	**0.903**	0.010

Element	Dunn's Post-test grouping per geology (small letters) & LFT (CAPS)																				Correlations R^2 ($p < 0.05$)		
	Soil							Leaf							Bioconcentration factor								
	Ventersdorp Lavas		Black Reef		Dolomite		p-value	Ventersdorp Lavas		Black Reef		Dolomite		p-value	Ventersdorp Lavas		Black Reef		Dolomite		p-value	BCF/ Soil	BCF/ Leaf	Soil/ Leaf
	VLR	VLS	BR1	BR2	D1	D2		VLS	VLR	BR1	BR2	D1	D2		VLS	VLR	BR1	BR2	D1	D2				
Mn	a		a		b		**< 0.0001**	A		a		a		0.065	b		b		a		**< 0.0001**			
	A	A	A	A	B	B	**< 0.0001**	A	A	A	A	A	A	0.097	ABC	C	C	BC	A	AB	**< 0.0001**	**-0.573**	**0.720**	0.062
Na_2/Na	a		a		a		0.262	a		a		a		0.057	a		a		a		0.244			
	AB	B	B	AB	A	B	**0.0002**	B	AB	AB	AB	A	AB	**0.011**	A	AB	AB	AB	B	A	**0.003**	**-0.898**	0.154	0.190
Ni	b		a		b		**0.000**	b		b		a		**< 0.0001**	a		b		a		**< 0.0001**			
	B	BC	A	A	B	BC	**< 0.0001**	BC	BC	C	C	A	AB	**< 0.0001**	A	A	C	B	BC	A	**< 0.0001**	**-0.709**	**0.812**	-0.188
P_2	b		b		a		**< 0.0001**	b		Ab		A		**0.007**	a		a		a		**0.043**			
	BC	ABC	C	ABC	A	AB	**< 0.0001**	B	B	AB	AB	A	AB	**0.006**	A	A	A	A	A	A	0.062	**-0.660**	**0.477**	0.220
Pb	a		c		b		**< 0.0001**	a		a		a		0.083	b		a		ab		**0.003**			
	AB	A	CD	D	BCD	ABC	**< 0.0001**	A	A	A	A	A	A	0.180	B	AB	A	AB	AB	AB	**0.015**	**-0.532**	**0.556**	0.216
Si	a		a		a		0.284	ab		a		b		**0.024**	Ab		a		b		**0.027**			
	B	A	B	AB	AB	B	**0.0002**	A	A	A	A	A	A	**0.040**	A	A	A	A	A	A	0.054	-0.084	**0.993**	-0.086
Ti	b		b		a		**< 0.0001**	a		a		a		0.375	ab		a		b		**0.007**			
	C	C	C	BC	AB	A	**< 0.0001**	A	A	A	A	A	A	0.845	A	A	A	A	A	A	**0.029**	**-0.426**	**0.867**	-0.002
V	b		a		ab		**0.005**	a		a		a		0.583	a		a		a		0.169			
	AB	C	A	ABC	BC	AB	**< 0.0001**	A	A	A	A	A	A	0.694	A	A	A	A	A	A	0.240	**-0.513**	**0.855**	-0.023
Zn	a		b		a		**< 0.0001**	a		a		a		0.535	b		a		b		**0.006**			
	AB	A	B	AB	A	A	**0.0005**	A	A	A	A	A	A	0.531	A	A	A	A	A	A	**0.035**	**-0.647**	**0.679**	0.015

3.5.3. Analysis of bioconcentration factors and soil and leaf elemental ratios

The bioconcentration factors and leaf and soils ratios were calculated and then analysed for significant differences and trends between species and geologies. Table 3-3 in the previous section showed the correlations between the leaf and soils elemental content and bioconcentration factors, and the differences between the three geologies and six LFTS for all species combined. This section takes a more in-depth look at the bioconcentration factors and soil and leaf ratios at a species level.

Table 3-4 describes the differences between leaf elemental uptake per species and bioconcentration factors per species. The leaf elemental content and the bioconcentration factors data was analysed to detected differences in the ranges of concentrations for each species to understand the differences in uptake between plant species. Overall, there were significant differences for most of the elements analysed for leaf elemental concentrations. Elements which did not show any significant differences for leaf elemental uptake were Au, C, Cd, N, Na, P, Si and U. Frequently, the *S. lancea* had the highest concentrations of elements in the leaves, and the *E. crispa* samples showed lower concentrations. Exceptions to this are K, Cr, Mg, Mn, Ni, S and Sn. Often *A. karroo* and *S. lancea* leaves showed similar concentrations. The bioconcentration factors results followed a similar trend to the leaf elemental content data. For example, E. *crispa* samples had significantly lower Ti and Zn, concentrations in the leaves, and a significantly lower bioconcentration factor compared to the *S. lancea* and *A. karroo* trees. The implication of this result is that the bioconcentration factors show a strong link to the leaf elemental content for the individual species which may be a result of plant specific abilities to take up or exclude specific elements and not purely a factor of the bioavailability of the elements in the soil solution. However, the fact that there were no *E. crispa* species on the chert-rich dolomites may skew these results slightly, as there were some differences in soil elemental

content (e.g. Mg and Na) on the chert-poor dolomites compared to the chert-poor dolomites, as is shown in Table 3-3.

Table 3-4 Kruskal-Wallis test results and Dunn's post-test procedure for the differences between leaf elemental concentration and bioconcentration factors per species

	Leaf concentration						Bioconcentration					
Element	p-value	Species	No of Obs	Sum of ranks	Mean of ranks	Groups	p-value	Species	No of obs	Sum of ranks	Mean of ranks	Groups
Ag	**0.01**	Acacia karroo	20	442	22.10	A						
		Euclea crispa	20	754	37.70	B						
		Searsia lancea	24	884	36.83	B						
Al	**<0.0001**	Acacia karroo	20	663	33.15	AB		Acacia karroo	20	721	36.05	B
		Euclea crispa	20	386	19.30	A	**< 0.0001**	Euclea crispa	20	375	18.75	A
		Searsia lancea	24	1031	42.96	B		Searsia lancea	24	984	41.00	B
As	**<0.0001**	Acacia karroo	20	778	38.90	B						
		Euclea crispa	20	322	16.10	A						
		Searsia lancea	24	980	40.83	B						
Au	0.27	Acacia karroo	20	702	35.10	A						
		Euclea crispa	19	500	26.32	A						
		Searsia lancea	24	814	33.92	A						
Ba	**0.01**	Acacia karroo	20	749	37.45	B		Acacia karroo	20	729	36.45	A
		Euclea crispa	20	445	22.25	A	0.162	Euclea crispa	20	520	26.00	A
		Searsia lancea	24	886	36.92	B		Searsia lancea	24	831	34.63	A
C	0.10	Acacia karroo	19	494	26.00	A		Acacia karroo	21	511	24.33	A
		Euclea crispa	20	753	37.65	A	**0.014**	Euclea crispa	20	829	41.45	B
		Searsia lancea	22	644	29.27	A		Searsia lancea	24	805	33.54	AB
Ca	0.05	Acacia karroo	20	800	40.00	B		Acacia karroo	20	844	42.20	B
		Euclea crispa	20	514	25.70	A	**0.011**	Euclea crispa	20	506	25.30	A
		Searsia lancea	24	766	31.92	AB		Searsia lancea	24	730	30.42	AB
Cd	0.25	Acacia karroo	20	687	34.35	A						
		Euclea crispa	20	730	36.50	A						
		Searsia lancea	24	663	27.63	A						
Co	**0.02**	Acacia karroo	20	745	37.25	B		Acacia karroo	20	864	43.20	B
		Euclea crispa	20	457	22.85	A	**< 0.0001**	Euclea crispa	20	406	20.30	A
		Searsia lancea	24	878	36.58	B		Searsia lancea	24	810	33.75	AB
Cr	**<0.0001**	Acacia karroo	20	758	37.90	B		Acacia karroo	20	667	33.35	A
		Euclea crispa	20	868	43.40	B	0.234	Euclea crispa	20	747	37.35	A
		Searsia lancea	24	454	18.92	A		Searsia lancea	24	666	27.75	A
Cu	**<0.0001**	Acacia karroo	20	451	22.55	A	**< 0.0001**	Acacia karroo	20	543	27.15	A
		Euclea crispa	19	456	24.00	A		Euclea crispa	20	428	21.40	A
		Searsia lancea	24	1109	46.21	B		Searsia lancea	24	1109	46.21	B
Fe	**<0.0001**	Acacia karroo	20	630	31.50	B		Acacia karroo	20	685	34.25	B
		Euclea crispa	20	310	15.50	A	**< 0.0001**	Euclea crispa	20	298	14.90	A
		Searsia lancea	24	1140	47.50	C		Searsia lancea	24	1097	45.71	B
K	**0.05**	Acacia karroo	20	663	33.15	AB		Acacia karroo	20	718	35.90	A
		Euclea crispa	20	793	39.65	B	0.258	Euclea crispa	20	701	35.05	A
		Searsia lancea	24	624	26.00	A		Searsia lancea	24	661	27.54	A

	Leaf concentration						Bioconcentration					
Element	p-value	Species	No of Obs	Sum of ranks	Mean of ranks	Groups	p-value	Species	No of obs	Sum of ranks	Mean of ranks	Groups
Mg	**<0.0001**	Acacia karroo	20	701	35.05	B	**<0.0001**	Acacia karroo	20	786	39.30	B
		Euclea crispa	20	1032	51.60	C		Euclea crispa	20	932	46.60	B
		Searsia lancea	24	347	14.46	A		Searsia lancea	24	362	15.08	A
Mn	**<0.0001**	Acacia karroo	20	296	14.80	A	**<0.0001**	Acacia karroo	20	404	20.20	A
		Euclea crispa	20	1032	51.60	C		Euclea crispa	20	959	47.95	B
		Searsia lancea	24	752	31.33	B		Searsia lancea	24	717	29.88	A
N_ppm	0.75	Acacia karroo	19	591	31.11	A	0.350	Acacia karroo	8	167	20.88	A
		Euclea crispa	20	663	33.15	A		Euclea crispa	15	271	18.07	A
		Searsia lancea	22	637	28.95	A		Searsia lancea	11	157	14.27	A
Na	0.57	Acacia karroo	20	719	35.95	A	0.954	Acacia karroo	20	614	30.70	A
		Euclea crispa	20	642.5	32.13	A		Euclea crispa	19	595	31.32	A
		Searsia lancea	24	718.5	29.94	A		Searsia lancea	23	744	32.35	A
Ni	**0.00**	Acacia karroo	20	478.5	23.93	A	**0.097**	Acacia karroo	20	615	30.75	A
		Euclea crispa	20	899	44.95	B		Euclea crispa	20	795	39.75	A
		Searsia lancea	24	702.5	29.27	A		Searsia lancea	24	670	27.92	A
P	0.65	Acacia karroo	20	648	32.40	A	0.688	Acacia karroo	20	628	31.40	A
		Euclea crispa	20	593	29.65	A		Euclea crispa	20	610	30.50	A
		Searsia lancea	24	839	34.96	A		Searsia lancea	24	842	35.08	A
Pb	**<0.0001**	Acacia karroo	20	563	28.15	A	**0.001**	Acacia karroo	20	525	26.25	A
		Euclea crispa	20	433	21.65	A		Euclea crispa	20	522	26.10	A
		Searsia lancea	24	1084	45.17	B		Searsia lancea	24	1033	43.04	B
S	**0.00**	Acacia karroo	20	865	43.25	B						
		Euclea crispa	20	661	33.05	AB						
		Searsia lancea	24	554	23.08	A						
Sb	**0.00**	Acacia karroo	20	378	18.90	A						
		Euclea crispa	20	716	35.80	B						
		Searsia lancea	24	986	41.08	B						
Si	0.10	Acacia karroo	20	781	39.05	A	0.198	Acacia karroo	20	757	37.85	A
		Euclea crispa	20	530	26.50	A		Euclea crispa	20	544	27.20	A
		Searsia lancea	24	769	32.04	A		Searsia lancea	24	779	32.46	A
Sn	**<0.0001**	Acacia karroo	20	829	41.45	B						
		Euclea crispa	20	840	42.00	B						
		Searsia lancea	24	411	17.13	A						
Ti	**<0.0001**	Acacia karroo	19	597.5	31.45	B	**<0.0001**	Acacia karroo	20	699	34.95	B
		Euclea crispa	18	295.5	16.42	A		Euclea crispa	20	348	17.40	A
		Searsia lancea	24	998	41.58	B		Searsia lancea	24	1033	43.04	B
U	0.06	Acacia karroo	20	648	32.40	A						
		Euclea crispa	20	508	25.40	A						
		Searsia lancea	24	924	38.50	A						
V	**<0.0001**	Acacia karroo	20	675	33.75	B						
		Euclea crispa	20	289	14.45	A						
		Searsia lancea	24	1116	46.50	B						
Zn	**<0.0001**	Acacia karroo	20	599	29.95	A	**0.000**	Acacia karroo	20	601	30.05	A
		Euclea crispa	20	366	18.30	A		Euclea crispa	20	417	20.85	A
		Searsia lancea	24	1115	46.46	B		Searsia lancea	24	1062	44.25	B

Table 3-5 Table showing p-values of the Kruskal Wallis test for the soil and leaf ratios per geology for all three tree species. Significant differences shown in bold. Dunn's post-test results for the significant results are shown below.

Variable	*S. lancea* p-value	*E. crispa* p-value	*A. karroo* p-value
Si:Ti soil ratio	**< 0.0001**	**0.013**	**< 0.0001**
Si:Ti leaf ratio	0.145	0.859	0.915
Ca:Mg soil ratio	0.439	0.783	0.560
Ca:Mg leaf ratio	0.606	**0.001**	**0.023**
Si:Mn Soil Ratio	**< 0.0001**	**0.004**	**< 0.0001**
Si:Mn leaf ratio	**0.001**	0.263	0.118
Al:P Leaf ratio	0.989	0.063	0.084
Sr:Ca soil ratio	0.159	0.056	0.110
Rb:K soil ratio	**0.006**	0.359	**0.036**
Zn:Cd leaf ratio	0.116	**0.048**	0.339
Na:K leaf ratio	0.532	0.446	0.201
Ca:S leaf ratio	0.191	**0.006**	0.385
C:N leaf ratio	0.129	**0.010**	**0.036**
Mg:Mn leaf ratio	**< 0.0001**	0.147	0.326
Mg:Mn soil ratio	**< 0.0001**	**0.003**	**< 0.0001**
Ca:Al leaf ratio	0.734	**0.025**	0.913
Al:Ca soil ratio	0.866	0.723	0.398
Leaf Ca:Al :soil Al	0.973	**0.014**	0.475
Ca BCF: soil Al	0.630	0.074	**0.045**
N:P leaf ratio	**0.003**	0.090	0.229
N:S leaf ratio	**0.003**	0.914	0.244
Mg:Al leaf ratio	0.588	0.327	0.171

Table 3-5 shows the results of the Kruskal Wallis test for the soil and leaf elemental ratios per geology. The Kruskal-Wallis test with a Dunn's post-test procedure and Bonferroni correction was run individually for each species. The results show that there are differences in the leaf and soils ratios between geologies, but that the ratios which showed significant results differed for the three tree species. This is particularly evident in the elemental ratios for leaf material. The soil elemental ratios for Si:Ti, Si:Mn and Mg:Mn showed significant differences between geologies across all three species, whereas the Ca:Mg, Sr:Ca, Al:Ca showed no significant differences between geologies for any of the three tree species. The leaf elemental data showed

no significant differences for the Si:Ti, Al:P, Na:K and Mg:Al ratios. None of the leaf elemental ratios showed significant differences between geologies for all three plant species, and many only showed differences in one of the three species, indicating differences in the ways in which the plants take up elements from the soils.

3.5.4. Analysis of soil and leaf ratios

The results shown in this section cover the analysis of the soil and leaf elemental ratios, and compare those as required to the leaf elemental concentrations for each species. The elemental ratios are used to give further information relating to the plant's growing conditions and nutrient status. In some cases the elemental ratios also provide further insight into the uptake or bioavailability of specific element.

3.5.4.1. Si:Ti leaf and soils ratios

One of the recommended checks to ensure that the leaf elemental content results were not skewed by the deposition of dust on the leaves was to compare the ratios of Si:Ti in the leaves and soils. Both of these elements are typically only taken up in small quantities, despite the fact that they are abundant in the environment, and especially abundant in mine tailings dust and soils near the study site. The Kolmogorov-Smirnov test was used to determine whether the leaf Si:Ti ratio followed the same distribution as the soil Si:Ti ratio. If the leaf samples had followed the soil samples, then there was likely to be dust contamination on the surface of the leaves. However, the results shown in Table 3-6 and Figure 3-3 showed that the two samples followed different distributions ($p < 0.0001$) indicating that the leaves were not coated in dust or were sufficiently well cleaned during the sample preparation phase.

Table 3-6 Kolmogorov-Smirnoff test results for the Si:Ti ratios in leaves and soils. Results show a significant difference in the two distributions

D	p-value	Variable	Obs.	Minimum	Maximum	Mean	Std. deviation
0.984	< 0.0001	Si/Ti Soil ratio	65	56.112	206.554	121.914	28.279
		Si/Ti leaf ratio	61	8.200	58.333	21.855	9.602

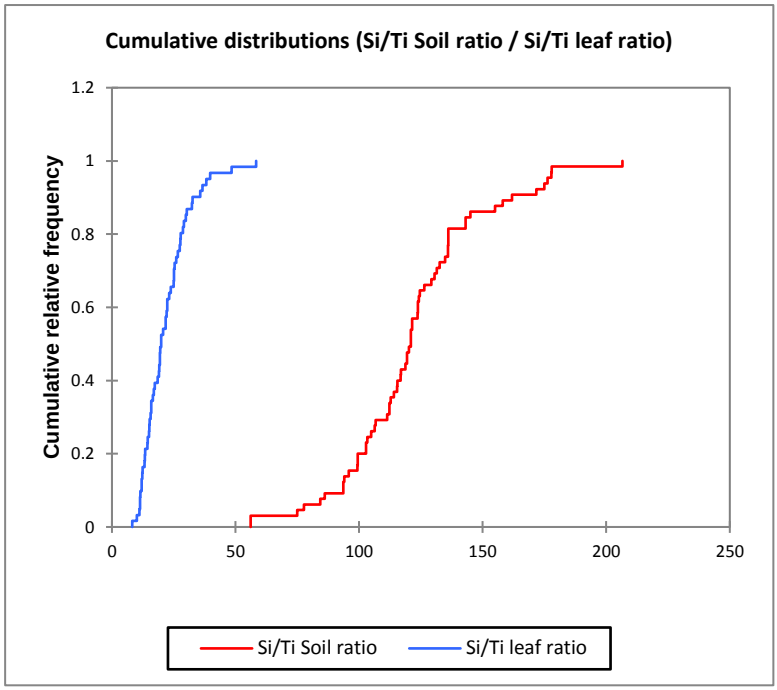

Figure 3-3 Cumulative distributions for Si:Ti ratios in leaves and soils

3.5.4.2. Ca:Mg ratios in leaves and soils

Ca:Mg ratio in soils is a useful indicator of a metal rich soil. While this is generally used for the analysis of ultramafic soils, it has relevance to the Black Reef within a dolomitic matrix in this study. While plants on ultramafic soils can suffer from nutrient deficiencies, this is unlikely on the dolomitic Ca, Mg-dolomitic rich soils at this study site. However, it was anticipated that there may be a difference in ratios between the 3 geologies. Table 3-7Table 3-12 shows the descriptive statistics and the Dunn's Post-test results for the Kruskal-Wallis non-parametric test used to differentiate between the Ca: Mg elemental ratio across the three geologies for leaves and soils. Overall only the *E. crispa* showed higher Ca:Mg ratios over the Black Reef and lower Ca:Mg ratios on the Ventersdorp Lavas and intermediate values for the dolomites.

Table 3-7 Summary statistics and multiple pairwise comparisons using Dunn's procedure for the Ca:Mg ratio analysis for leaf and soil samples . The Bonferroni corrected significance level was 0.0167

Species	Variable	Geology	No of Obs.	Min	Max	Mean	Std. dev.	Groups	
A. karroo	Soil ratio	Ventersdorp Lava	6	0.539	1.037	0.782	0.200	A	
		Black reef	7	0.451	1.185	0.796	0.310	A	
		Dolomite	8	0.451	1.494	0.962	0.377	A	
	Leaf ratio	Ventersdorp Lava	6	3.728	6.684	4.656	1.198	A	
		Black reef	7	2.147	4.851	3.027	0.980	A	
		Dolomite	8	3.124	7.239	4.740	1.567	A	
S. lancea	Soil ratio	Ventersdorp Lava	8	0.593	1.797	1.082	0.483	A	
		Black reef	8	0.379	1.778	0.899	0.593	A	
		Dolomite	8	0.464	1.718	1.001	0.497	A	
	Leaf ratio	Ventersdorp Lava	8	3.649	11.935	6.787	2.927	A	
		Black reef	8	2.256	7.993	5.208	1.720	A	
		Dolomite	8	4.298	6.422	5.341	0.751	A	
E. crispa	Soil ratio	Ventersdorp Lava	8	0.593	1.778	0.969	0.370	A	
		Black reef	8	0.409	1.778	0.940	0.562	A	
		Dolomite	4	0.593	1.086	0.902	0.214	A	
	Leaf ratio	Ventersdorp Lava	8	1.688	3.038	2.492	0.537	A	
		Black reef	8	1.064	2.144	1.551	0.312	A	B
		Dolomite	4	1.583	2.159	1.895	0.278		B

3.5.4.3. Leaf Al and P content, and Al: P leaf ratios

Al is amphoteric, and in acidic soils (e.g. ARD-impacted, sandstones as Al^{3+}) or alkaline soils (e.g. dolomitic) becomes more available for plant uptake. P however becomes less available in acidified soils due to both inhibition of P-cycling organisms and to chemical precipitation reactions. This can result in Al-toxicity and P-deficiency in plants because Al^{3+} competes with P for uptake at the root membrane. Table 3-8 shows the descriptive statistics and the Dunn's Post-test results for the Kruskal-Wallis non-parametric test used to differentiate between Al and P concentrations, and the Al:P elemental ratio in leaves across the three geologies. There were differences noted for the P content, with higher P content in *S. lancea* samples growing on the Black Reef, and in the *E. crispa* samples growing on the Ventersdorp Lavas. There were no differences noted between geologies for the Leaf Al content of the Al:P ratios for any of the three species.

Table 3-8 Summary statistics and multiple pairwise comparisons using Dunn's procedure for the Al:P ratio analysis for leaf and soil samples. The Bonferroni corrected significance level was 0.0167

Species	Variable	Geology	No of Obs.	Min	Max	Mean	Std. dev.	Groups	
A. karroo	Leaf Al	Ventersdorp Lava	6	44.287	1417.166	328.364	608.782	A	
		Black reef	8	52.400	95.371	67.882	16.512	A	
		Dolomite	7	49.202	181.954	100.703	48.362	A	
	Leaf P	Ventersdorp Lava	6	2293.989	5938.124	4747.234	1481.662	A	B
		Black reef	7	4186.651	6570.577	5692.333	810.102		B
		Dolomite	8	3261.952	5455.635	4317.831	707.029	A	
	Al:P Leaf ratio	Ventersdorp Lava	6	0.009	0.239	0.059	0.101	A	
		Black reef	8	0.008	0.019	0.012	0.004	A	
		Dolomite	7	0.010	0.049	0.024	0.013	A	
S. lancea	Leaf Al	Ventersdorp Lava	8	66.580	234.655	116.156	66.146	A	
		Black reef	8	65.763	110.644	85.188	16.853	A	
		Dolomite	8	58.647	220.212	102.321	55.437	A	
	Leaf P	Ventersdorp Lava	8	3518.593	10233.161	6156.370	2299.899	A	
		Black reef	8	4105.148	5862.345	4936.637	589.171	A	
		Dolomite	8	4047.049	7717.652	5016.694	1211.516	A	
	Al:P Leaf ratio	Ventersdorp Lava	8	0.009	0.058	0.022	0.016	A	
		Black reef	8	0.012	0.022	0.017	0.004	A	
		Dolomite	8	0.010	0.051	0.022	0.015	A	
E. crispa	Leaf Al	Ventersdorp Lava	8	38.269	138.745	61.189	32.642	A	
		Black reef	8	37.764	76.018	54.200	12.354	A	
		Dolomite	4	51.579	183.007	90.315	62.271	A	
	Leaf P	Ventersdorp Lava	8	4546.363	7623.901	5656.958	925.352		B
		Black reef	8	3013.972	6992.032	4389.831	1211.724	A	
		Dolomite	4	2858.856	4732.428	3905.889	867.888	A	
	Al:P Leaf ratio	Ventersdorp Lava	8	0.005	0.023	0.011	0.005	A	
		Black reef	8	0.006	0.019	0.013	0.005	A	
		Dolomite	4	0.016	0.039	0.022	0.011	A	

3.5.4.4. Leaf Na and K content, and Na:K leaf ratios

Table 3-9 Summary statistics and multiple pairwise comparisons using Dunn's procedure for the Na:K ratio analysis for leaf and soil samples. The Bonferroni corrected significance level was 0.0167

Species	Variable	Geology	No of Obs.	Min	Max	Mean	Std. dev.	Groups	
A. karroo	Leaf Na	Ventersdorp Lava	6	318.471	1187.625	775.029	333.563	A	
		Black reef	7	810.000	936.628	857.609	44.057	A	
		Dolomite	8	475.190	1089.129	675.293	240.449	A	
	Leaf K	Ventersdorp Lava	6	6329.618	16007.984	10404.857	3916.681	A	
		Black reef	7	10898.966	18395.850	13987.001	2644.186	A	
		Dolomite	8	7197.725	21747.805	12268.322	4454.575	A	
	Na:K Leaf ratio	Ventersdorp Lava	6	0.050	0.083	0.073	0.013	A	
		Black reef	7	0.044	0.078	0.063	0.012	A	
		Dolomite	8	0.026	0.080	0.058	0.019	A	
S. lancea	Leaf Na	Ventersdorp Lava	8	445.535	976.096	763.778	208.911	A	
		Black reef	8	424.660	808.061	591.403	130.248	A	
		Dolomite	8	563.198	946.215	703.141	134.103	A	
	Leaf K	Ventersdorp Lava	8	7287.085	19860.558	12397.435	5006.872	A	
		Black reef	8	6137.904	64925.970	15991.900	19984.587	A	
		Dolomite	8	7094.325	14396.965	10196.574	2823.778	A	
	Na:K Leaf ratio	Ventersdorp Lava	8	0.048	0.106	0.066	0.020	A	
		Black reef	8	0.010	0.104	0.061	0.027	A	
		Dolomite	8	0.057	0.093	0.071	0.013	A	
E. crispa	Leaf Na	Ventersdorp Lava	8	567.955	1119.552	840.441	187.935	A	
		Black reef	8	400.558	727.092	594.558	103.305	A	
		Dolomite	4	458.533	1098.243	734.287	274.063	A	
	Leaf K	Ventersdorp Lava	8	11206.552	21335.863	15378.372	3704.391	A	
		Black reef	8	3454.473	22785.315	12819.516	5967.093	A	
		Dolomite	4	9386.246	23482.428	15148.083	6422.601	A	
	Na:K Leaf ratio	Ventersdorp Lava	8	0.047	0.065	0.055	0.006	A	
		Black reef	8	0.028	0.158	0.060	0.042	A	
		Dolomite	4	0.042	0.065	0.050	0.010	A	

The ratio of an immobile element to a mobile element is a useful indication of membrane damage The Na/K is used to check integrity of plant cells and other biological tissues. Membrane leakiness can result from stresses to the living organism, and from crude preparation of the dead sample. Table 3-9 shows the descriptive statistics and the Dunn's Post-test results for the Kruskal-Wallis non-parametric test used to differentiate between Na and K concentrations, and the Na:K

elemental ratio in leaves across the three geologies. No significant differences in Leaf Na, Leaf K or the Na:K ratios were detected between geologies for any of the three species. The ranges that occurred for Na and K in the leaf samples was quite different between species.

3.5.4.5. Leaf Ca and S content and Ca: S leaf ratio

Table 3-10 Summary statistics and multiple pairwise comparisons using Dunn's procedure for the Ca:S ratio analysis for leaf and soil samples. The Bonferroni corrected significance level was 0.0167

Species	Variable	Geology	No of Obs.	Min	Max	Mean	Std. dev.	Groups	
A. karroo	Leaf Ca	Ventersdorp Lava	5	4707.404	22814.371	14101.643	6641.021	A	
		Black reef	8	6135.092	15403.739	10035.611	3700.352	A	
		Dolomite	7	8346.677	23842.315	16221.642	5338.572	A	
	Leaf S	Ventersdorp Lava	5	1247.505	2714.571	1658.430	604.314	A	
		Black reef	8	659.472	4047.335	2162.347	1335.504	A	
		Dolomite	7	1311.049	3590.637	1969.238	788.534	A	
	Ca:S Leaf ratio	Ventersdorp Lava	5	3.355	18.288	9.195	5.710	A	
		Black reef	8	2.523	15.141	6.603	4.778	A	
		Dolomite	7	5.071	14.924	8.738	3.200	A	
S. lancea	Leaf Ca	Ventersdorp Lava	8	7131.474	23860.456	13528.623	6440.079	A	
		Black reef	8	4656.275	13262.256	9612.655	3530.592	A	
		Dolomite	8	5520.000	13539.169	9858.260	3499.251	A	
	Leaf S	Ventersdorp Lava	8	389.844	2600.638	1519.727	835.991	A	
		Black reef	8	458.899	3581.433	1254.675	989.211	A	
		Dolomite	8	488.048	1020.817	699.652	200.655	A	
	Ca:S Leaf ratio	Ventersdorp Lava	8	3.103	61.205	15.767	19.358	A	
		Black reef	8	3.208	16.213	9.395	3.730	A	
		Dolomite	8	5.633	22.510	15.369	6.737	A	
E. crispa	Leaf Ca	Ventersdorp Lava	8	9909.326	24201.278	12627.626	4713.791		B
		Black reef	8	4119.171	8320.032	6496.711	1516.590	A	
		Dolomite	4	7660.486	13734.506	9814.052	2738.886	A	B
	Leaf S	Ventersdorp Lava	8	770.925	2747.802	1534.874	725.817	A	
		Black reef	8	1047.904	2768.924	1441.749	564.744	A	
		Dolomite	4	560.448	1345.694	946.018	346.046	A	
	Ca:S Leaf ratio	Ventersdorp Lava	8	3.942	14.714	9.626	4.132	A	B
		Black reef	8	2.115	7.794	4.919	1.727	A	
		Dolomite	4	5.693	17.615	11.694	5.442		B

This is a measure of two essential macronutrients: Ca, which is immobile and not volatilised from the leaf, and S, which is mobile and volatilised as SO_X compounds. Table 3-10 Table 3-9shows the descriptive statistics and the Dunn's Post-test results for the Kruskal-Wallis non-parametric test used to differentiate between Ca and S concentrations, and the Ca:S elemental ratio in leaves across the three geologies. S was expected to be more available along the Black Reef. However, no differences were found in the Ca:S ratios or leaf Ca or Leaf S content for the *A. karroo* or *S. lancea* samples. The *E. crispa* samples were found to have a higher leaf Ca concentration on the Ventersdorp Lavas and the lowest leaf Ca content on the Black Reef. Conversely the Ca:S ratio was lowest on the Black Reef, and highest on the Dolomites.

3.5.4.6. Leaf N and P content, and N:P leaf ratios by species

N and P are both essential elementals and are critical for the growth of healthy plants. Studies have found that N and P deficiencies can be identified through the N:P ratio [150]. While the optimal ratio between N and P is highly variable between species and types of plants, studies have found that on average, plants with an N:P ratio <10 or >20 show signs of either N- or P-limited biomass production. Often N:P ratios are negatively correlated with biomass production [47], [150]. Table 3-11 shows the descriptive statistics and the Dunn's Post-test results for the Kruskal-Wallis non-parametric test used to differentiate between N and P concentrations, and the N:P elemental ratio in leaves across the three geologies. For the *A. karroo*, the highest N concentrations in plant leaves were found on the Black Reef. This is also an interesting finding as the soil N concentrations for the *A. karroo* samples were below detection limits. Ventersdorp Lavas had the lowest N concentrations. P concentrations were also highest on the Black Reef. No differences in the ratio of N:P was found for the *A. karroo* samples. There were no differences in leaf N or P concentrations between geologies for the *S. lancea* samples, but there were differences between the Ventersdorp Lava and Dolomite samples, with the lowest ratios found

on the Ventersdorp Lavas and the highest ratio found on the Dolomites. The *E. crispa* samples were found to have the lowest concentrations of leaf N on the Dolomites and the highest on the Black Reef. The samples on the dolomites and Black Reef both had low concentrations of leaf P compared to the Ventersdorp Lavas. There were no differences between the geologies for the N:P ratio for *E. crispa* samples.

Table 3-11 Summary statistics and multiple pairwise comparisons using Dunn's procedure for the N:P ratio analysis for leaf and soil samples. The Bonferroni corrected significance level was 0.0167

Species	Variable	Geology	No of Obs.	Min	Max	Mean	Std. dev.	Groups	
A. karroo	**Leaf N**	Ventersdorp Lava	6	9721.700	16907.000	12830.450	2702.381	A	
		Black reef	7	14666.000	19394.000	17171.857	1610.964		B
		Dolomite	6	9958.400	17876.000	13161.733	3013.605	A	B
	Leaf P	Ventersdorp Lava	6	2293.989	5938.124	4747.234	1481.662	A	B
		Black reef	7	4186.651	6570.577	5692.333	810.102		B
		Dolomite	8	3261.952	5455.635	4317.831	707.029	A	
	N:P Leaf ratio	Ventersdorp Lava	5	1.891	5.995	2.929	1.731	A	
		Black reef	7	2.610	3.971	3.063	0.475	A	
		Dolomite	6	2.070	5.480	3.160	1.234	A	
S. lancea	**Leaf N**	Ventersdorp Lava	6	9671.400	14676.000	12857.733	1855.515	A	
		Black reef	8	11558.000	16697.000	15179.175	1880.451	A	
		Dolomite	8	10601.000	21815.000	14849.500	4351.212	A	
	Leaf P	Ventersdorp Lava	8	3518.593	10233.161	6156.370	2299.899	A	
		Black reef	8	4105.148	5862.345	4936.637	589.171	A	
		Dolomite	8	4047.049	7717.652	5016.694	1211.516	A	
	N:P Leaf ratio	Ventersdorp Lava	6	1.434	3.088	2.204	0.561	A	
		Black reef	8	2.343	3.833	3.117	0.558	A	B
		Dolomite	8	2.368	4.424	2.983	0.696		B
E. crispa	**Leaf N**	Ventersdorp Lava	8	10549.000	23474.000	15795.250	4208.729	A	B
		Black reef	8	14820.000	19734.000	16719.375	1776.950		B
		Dolomite	4	8316.400	13931.000	10541.025	2412.958	A	
	Leaf P	Ventersdorp Lava	8	4546.363	7623.901	5656.958	925.352		B
		Black reef	8	3013.972	6992.032	4389.831	1211.724	A	
		Dolomite	4	2858.856	4732.428	3905.889	867.888	A	
	N:P Leaf ratio	Ventersdorp Lava	8	1.916	4.777	2.891	1.086	A	
		Black reef	8	2.239	5.033	4.001	0.840	A	
		Dolomite	4	2.123	3.937	2.790	0.843	A	

3.5.4.7. Si:Mn ratios in leaves and soils

At high concentrations, Mn is toxic to plants. Mn toxicity can cause growth stunting and brown/chlorotic spots on leaves. Elevated Si in soils has been shown to alleviate Mn toxicity in plants by causing a reduction in the translocation of Mn to the shoots of plants.

Table 3-12 Summary statistics and multiple pairwise comparisons using Dunn's procedure for the Si:Mn ratio analysis for leaf and soil samples . The Bonferroni corrected significance level was 0.0167

Species	Variable	Geology	No of Obs.	Min	Max	Mean	Std. dev.	Groups	
A. karroo	Soil ratio	Ventersdorp Lava	6	572.448	1360.284	908.545	278.782		B
		Black reef	7	544.959	923.152	724.879	149.016		B
		Dolomite	8	92.557	220.446	152.566	47.582	A	
	Leaf ratio	Ventersdorp Lava	5	0.445	2.103	0.915	0.705	A	
		Black reef	7	0.187	0.842	0.407	0.231	A	
		Dolomite	8	0.264	0.699	0.444	0.132	A	
S. lancea	Soil ratio	Ventersdorp Lava	8	468.366	916.413	753.114	159.655		B
		Black reef	8	497.612	1382.767	696.852	289.238		B
		Dolomite	8	79.842	143.306	108.037	25.149	A	
	Leaf ratio	Ventersdorp Lava	8	0.226	0.677	0.422	0.176		B
		Black reef	8	0.052	0.291	0.112	0.084	A	
		Dolomite	8	0.117	0.680	0.260	0.181	A	B
E. crispa	Soil ratio	Ventersdorp Lava	8	572.448	1095.953	740.483	185.718		B
		Black reef	8	497.612	1331.917	691.754	271.540		B
		Dolomite	4	87.245	138.788	117.228	21.894	A	
	Leaf ratio	Ventersdorp Lava	8	0.021	0.212	0.079	0.071	A	
		Black reef	8	0.022	0.122	0.060	0.045	A	
		Dolomite	4	0.039	0.372	0.155	0.148	A	

Table 3-12 shows the descriptive statistics and the Dunn's Post-test results for the Kruskal-Wallis non-parametric test used to differentiate between the Si:Mn elemental ratio across the three geologies for leaves and soils. The soil ratios for all three species showed the same trend with the Si:Mn content on the dolomites being significantly lower than the Black Reef or Ventersdorp Lavas. This trend is due to the significantly higher Mn content for the dolomites compared to the other two geologies. Only the *S. lancea* samples showed any significant

differences in the leaf Si:Mn ratio, where the ratio on the Ventersdorp Lavas was significantly higher than that on Black Reef.

3.5.4.8. Leaf Zn and Cd content, and Zn:Cd leaf ratio

There is often competition between ions for uptake in plants. Studies have shown that Cd accumulation can interfere with uptake of Fe and Mg, resulting in a decrease in photosynthesis. Cd uptake can be supressed by the uptake of divalent cations such as Zn^{2+}, Mn^{2+}, $Si^{2+}$and Ca^{2+}. Zn, while toxic in high concentrations is an essential element in trace concentrations, while Cd can be toxic, even in low concentrations. Table 3-13 shows the descriptive statistics and the Dunn's Post-test results for the Kruskal-Wallis non-parametric test used to differentiate between Zn and Cd concentrations, and the Zn:Cd elemental ratio in leaves across the three geologies. For the *E. crispa* and *S. lancea* samples, there were no differences detected in the leaf uptake of Zn or Cd. There were no differences in the Zn:Cd ratios between geologies for either of the three species. There were differences in the leaf elemental content for Zn and Cd in the *A. karroo* samples. Both were highest on the Black Reef, and leaf Zn content was lowest on the Ventersdorp Lavas, and Cd was lowest on the Dolomites

Table 3-13 Summary statistics and multiple pairwise comparisons using Dunn's procedure for the Zn:Cd ratio analysis for leaf and soil samples. The Bonferroni corrected significance level was 0.0167

Species	Variable	Geology	No of Obs.	Min	Max	Mean	Std. dev.	Groups	
A. karroo	Leaf Zn	Ventersdorp Lava	6	10.379	22.691	16.653	4.742	A	
		Black reef	7	11.038	19.852	15.004	3.212		B
		Dolomite	6	10.479	15.563	13.018	2.063	A	B
	Leaf Cd	Ventersdorp Lava	6	0.608	1.674	1.219	0.555	A	B
		Black reef	7	0.719	3.314	1.793	0.768		B
		Dolomite	8	0.605	1.697	1.139	0.555	A	
	Zn:Cd Leaf ratio	Ventersdorp Lava	5	6.795	31.113	16.832	9.795	A	
		Black reef	7	4.312	27.626	10.562	7.873	A	
		Dolomite	6	6.239	23.720	14.228	7.054	A	
S. lancea	Leaf Zn	Ventersdorp Lava	6	14.194	36.269	24.087	7.953	A	
		Black reef	8	13.484	23.543	19.726	3.420	A	
		Dolomite	8	10.354	27.078	18.147	5.235	A	
	Leaf Cd	Ventersdorp Lava	8	0.624	2.243	1.358	0.557	A	
		Black reef	8	1.424	1.893	1.574	0.151	A	
		Dolomite	8	0.560	1.672	1.070	0.497	A	
	Zn:Cd Leaf ratio	Ventersdorp Lava	6	8.868	57.224	21.677	15.370	A	
		Black reef	8	8.680	15.791	12.578	2.191	A	
		Dolomite	8	7.602	29.779	19.932	8.566	A	
E. crispa	Leaf Zn	Ventersdorp Lava	8	8.393	23.662	14.534	4.814	A	
		Black reef	8	7.884	14.665	10.127	2.288	A	
		Dolomite	4	10.108	11.663	10.787	0.691	A	
	Leaf Cd	Ventersdorp Lava	8	0.635	2.087	1.428	0.497	A	
		Black reef	8	1.297	1.769	1.615	0.148	A	
		Dolomite	4	0.613	2.534	1.326	0.897	A	
	Zn:Cd Leaf ratio	Ventersdorp Lava	8	6.016	19.708	11.202	4.566	A	
		Black reef	8	4.906	8.288	6.259	1.180	A	
		Dolomite	4	3.989	17.947	11.286	6.474	A	

3.5.4.9. C:N ratios in leaves and soils

The ratio of C:N is soils varies between soil types, but a usual range is from 8:1 to 17:1. When the carbon content in the soils is significantly higher than this, it can cause a leaching of the available nitrogen in the soils. The balance of the two is essential for plant growth and carbohydrate production. Studies have found that soils with high organic carbon content in their SOM may be limited in terms of P, N and S. C:N ratio can also be lowered as a result of higher temperatures, whilst higher rainfall and increased soil acidity increased soil C:N ratios.

Table 3-14 Summary statistics and multiple pairwise comparisons using Dunn's procedure for the C:N ratio analysis for leaf and soil samples . The Bonferroni corrected significance level was 0.0167

Species	Variable	Geology	No of Obs.	Min	Max	Mean	Std. dev.	Groups	
A. karroo	Soil ratio	Ventersdorp Lava	2	25.897	42.366	34.132	11.646	A	
		Black reef	0						
		Dolomite	6	19.480	86.438	48.654	22.372	A	
	Leaf ratio	Ventersdorp Lava	6	18.493	49.792	38.195	11.700	A	
		Black reef	6	18.493	49.792	38.195	11.700	A	
		Dolomite	7	25.326	32.239	28.802	2.409	A	
S. lancea	Soil ratio	Ventersdorp Lava	3	18.557	41.623	26.401	13.185	A	
		Black reef	4	15.898	89.705	42.619	33.885	A	
		Dolomite	4	18.557	19.866	18.966	0.618	A	
	Leaf ratio	Ventersdorp Lava	6	32.807	49.433	38.406	5.945	A	
		Black reef	8	29.514	42.249	33.091	4.644	A	
		Dolomite	8	21.121	48.445	35.440	10.350	A	
E. crispa	Soil ratio	Ventersdorp Lava	6	16.820	62.824	30.599	17.958	A	
		Black reef	5	20.508	61.686	35.498	16.180	A	
		Dolomite	4	17.612	40.591	26.952	9.938	A	
	Leaf ratio	Ventersdorp Lava	8	20.777	46.059	32.764	8.055	A	B
		Black reef	8	26.321	33.262	30.216	2.492	A	
		Dolomite	4	36.548	62.616	50.646	10.985		B

Table 3-14 shows the descriptive statistics and the Dunn's Post-test results for the Kruskal-Wallis non-parametric test used to differentiate between the C:N elemental ratio across the three geologies for leaves and soils. Results showed that there were numerous Soil N samples which were below detection limits, particularly on the Black Reef. No significant differences were identified for the soil N content for the samples. It was particularly interesting to note that none of the *A. karroo* samples growing on the Black Reef had detectable levels of N present, despite the fact that *A. karroo* is a nitrogen-fixing tree species. There were differences identified for the *E. crispa* leaf samples, with a significantly higher leaf C:N ratio on the Dolomites than was found for the Black Reef samples.

3.5.4.10. Leaf N and S content, and N:S leaf ratios

In agronomy, the N:S ratio is used extensively to monitor ultimate crop production. An optimal ratio in crop plants is between 11:1 and 15:1. Anything higher than 15:1 indicates a sulphur deficiency, whereas anything lower than 11:1 would indicate a nitrogen deficiency in plants. There are many interactions between soils elements which can affect this ratio, such as the availability of Ca in the soils. This is however a potentially useful indicator of Nitrogen deficiency. Table 3-15 shows the descriptive statistics and the Dunn's Post-test results for the Kruskal-Wallis non-parametric test used to differentiate between N and S concentrations, and the N:S elemental ratio in leaves across the three geologies. *A. karroo* and *E. crispa* samples had the highest nitrogen content in their leaf matter, but showed no other differences. The N:S ratio for the *S. lancea* samples showed significant differences between the dolomites and Ventersdorp Lavas, with the higher N:S ratios found on the Dolomites. While the *S. lancea* samples had the highest N:S ratio on the dolomites, the *A. karroo* and *E. crispa* had the lowest mean values for the N:S ratio on the dolomites which is interesting to note from an uptake perspective.

Table 3-15 Summary statistics and multiple pairwise comparisons using Dunn's procedure for the N:S ratio analysis for leaf and soil samples. The Bonferroni corrected significance level was 0.0167

Species	Variable	Geology	No of Obs.	Min	Max	Mean	Std. dev.	Groups	
A. karroo	**Leaf N**	Ventersdorp Lava	6	9721.700	16907.000	12830.450	2702.381	A	
		Black reef	7	14666.000	19394.000	17171.857	1610.964		B
		Dolomite	6	9958.400	17876.000	13161.733	3013.605	A	B
	Leaf S	Ventersdorp Lava	5	1247.505	2714.571	1658.430	604.314	A	
		Black reef	8	659.472	4047.335	2162.347	1335.504	A	
		Dolomite	7	1311.049	3590.637	1969.238	788.534	A	
	N:S Leaf ratio	Ventersdorp Lava	5	5.343	9.801	7.658	1.812	A	
		Black reef	7	3.902	27.663	12.052	8.634	A	
		Dolomite	6	4.422	10.155	6.872	2.181	A	
S. lancea	**Leaf N**	Ventersdorp Lava	6	9671.400	14676.000	12857.733	1855.515	A	

Species	Variable	Geology	No of Obs.	Min	Max	Mean	Std. dev.	Groups	
		Black reef	8	11558.000	16697.000	15179.175	1880.451	A	
		Dolomite	8	10601.000	21815.000	14849.500	4351.212	A	
	Leaf S	Ventersdorp Lava	8	389.844	2600.638	1519.727	835.991	A	
		Black reef	8	458.899	3581.433	1254.675	989.211	A	
		Dolomite	8	488.048	1020.817	699.652	200.655	A	
	N:S Leaf ratio	Ventersdorp Lava	6	5.168	18.658	9.655	5.476	A	
		Black reef	8	4.614	36.096	16.900	9.637	A	B
		Dolomite	8	11.283	34.682	22.353	7.454		B
E. crispa	Leaf N	Ventersdorp Lava	8	10549.000	23474.000	15795.250	4208.729	A	B
		Black reef	8	14820.000	19734.000	16719.375	1776.950		B
		Dolomite	4	8316.400	13931.000	10541.025	2412.958	A	
	Leaf S	Ventersdorp Lava	8	770.925	2747.802	1534.874	725.817	A	
		Black reef	8	1047.904	2768.924	1441.749	564.744	A	
		Dolomite	4	560.448	1345.694	946.018	346.046	A	
	N:S Leaf ratio	Ventersdorp Lava	8	5.689	20.530	12.201	5.256	A	
		Black reef	8	5.654	16.276	12.756	3.741	A	
		Dolomite	4	9.447	17.025	11.873	3.474	A	

3.5.4.11. Mg:Mn ratios in leaves and soils

While Mn is an essential element in trace concentrations, in high concentrations can be toxic to plants. Mn^{2+} has a similar ionic radius to Mg^{2+} and therefore could substitute Mg in plant uptake. As Mg is a critical component of the chlorophyll molecule, Mg deficiencies could be detrimental to plant health. Higher Mg content in the plant tissue has also been shown to increase Mn tolerance and prevent toxicity. Table 3-16 shows the descriptive statistics and the Dunn's Post-test results for the Kruskal-Wallis non-parametric test used to differentiate between the Mg:Mn elemental ratio across the three geologies for leaves and soils. As seen with the Si:Mn ratios in the soils (Table 3-12), there was a significantly higher concentration of Mn in the soils on the Dolomites than was found on the other two geologies. There were no differences identified between geologies for Mg in Table 3-3. This has contributed in part to the results which show that the Ventersdorp and Black Reef had significantly higher soils Mg:Mn ratios than the Dolomites for all three species. The only difference for the leaf ratio for Mg:Mn was identified

for the *S. lancea* samples, with the lowest Mg:Mn ratio for the Black Reef. The Mn concentration on the *S. lancea* samples on the Black Reef was higher than on the Ventersdorp Lavas, despite soil concentrations being significantly higher on the Dolomites.

Table 3-16 Summary statistics and multiple pairwise comparisons using Dunn's procedure for the Mg:Mn ratio analysis for leaf and soil samples . The Bonferroni corrected significance level was 0.0167

Species	Variable	Geology	No of Obs.	Min	Max	Mean	Std. dev.	Groups	
A. karroo	Soil ratio	Ventersdorp Lava	6	2.225	3.115	2.634	0.355		B
		Black reef	7	1.817	2.985	2.322	0.394		B
		Dolomite	8	0.317	0.561	0.442	0.094	A	
	Leaf ratio	Ventersdorp Lava	5	28.555	166.518	109.485	55.522	A	
		Black reef	7	38.742	139.819	66.542	40.783	A	
		Dolomite	8	26.861	100.000	65.478	26.298	A	
S. lancea	Soil ratio	Ventersdorp Lava	8	1.990	3.115	2.435	0.330		B
		Black reef	8	1.699	5.353	2.632	1.142		B
		Dolomite	8	0.240	0.519	0.388	0.108	A	
	Leaf ratio	Ventersdorp Lava	8	18.921	51.034	34.140	10.030		B
		Black reef	8	5.576	34.086	11.804	9.250	A	
		Dolomite	8	8.865	28.763	18.381	6.439	A	B
E. crispa	Soil ratio	Ventersdorp Lava	8	1.990	2.628	2.363	0.232		B
		Black reef	8	1.699	5.353	2.746	1.249		B
		Dolomite	4	0.492	0.566	0.518	0.035	A	
	Leaf ratio	Ventersdorp Lava	8	5.408	46.031	18.132	12.900	A	
		Black reef	8	5.744	28.200	14.236	9.942	A	
		Dolomite	4	14.630	37.118	26.951	10.589	A	

3.5.4.12. Ca:Al ratios in the leaves and soils

Studies have shown that high concentrations of bioavailable Al in the soils can inhibit the uptake of Ca to the plant. As Ca is an essential element, and the uptake of Ca important for tolerance to many elements, the inhibition or competition for uptake could have detrimental effects on plant health, particularly if there are very high concentrations of other metals present in the soils. Table 3-17 shows the descriptive statistics and the Dunn's Post-test results for the Kruskal-Wallis non-parametric test used to differentiate between the Al:Ca elemental ratio for across the three geologies for leaves and soils. There were no differences identified for the total

Al:Ca ratio in the soils across the three geologies for any of the three species. There was a difference in leaf Ca:Al ratio, where the highest ratio values were found on the Ventersdorp Lavas. As shown in Table 3-10, there was a significantly higher concentration of Ca in the leaves of plants growing on the Ventersdorp Lavas which accounts for this difference in Ca:Al ratio.

Table 3-17 Summary statistics and multiple pairwise comparisons using Dunn's procedure for the Al:Ca ratio analysis for leaf and soil samples . The Bonferroni corrected significance level was 0.0167

Species	Variable	Geology	No of Obs.	Min	Max	Mean	Std. dev.	Groups	
A. karroo	Soil ratio (Al:Ca)	Ventersdorp Lava	6	0.026	0.050	0.035	0.010	A	
		Black reef	7	0.017	0.057	0.036	0.016	A	
		Dolomite	8	0.021	0.081	0.049	0.023	A	
	Leaf ratio (Ca:Al)	Ventersdorp Lava	5	11.923	437.931	194.513	159.649	A	
		Black reef	7	78.920	232.764	153.661	57.474	A	
		Dolomite	8	95.533	484.584	193.258	127.511	A	
S. lancea	Soil ratio (Al:Ca)	Ventersdorp Lava	8	0.021	0.091	0.052	0.028	A	
		Black reef	8	0.015	0.111	0.049	0.039	A	
		Dolomite	8	0.020	0.087	0.050	0.026	A	
	Leaf ratio (Ca:Al)	Ventersdorp Lava	8	34.395	265.160	135.732	69.164	A	
		Black reef	8	61.872	196.515	117.501	53.215	A	
		Dolomite	8	50.068	175.553	108.777	47.067	A	
E. crispa	Soil ratio (Al:Ca)	Ventersdorp Lava	8	0.027	0.091	0.044	0.021	A	
		Black reef	8	0.019	0.111	0.050	0.038	A	
		Dolomite	4	0.030	0.063	0.047	0.014	A	
	Leaf ratio (Ca:Al)	Ventersdorp Lava	8	77.810	353.869	232.450	81.663		B
		Black reef	8	76.190	169.857	123.077	31.410	A	
		Dolomite	4	52.537	266.279	142.923	89.574	A	B

Overall, there were relatively few significant differences between the leaf elemental concentrations between geologies, even at a species level. There was less evidence to indicate that there are severe nutrient limitations on the Black Reef than expected. The ranges observed between species differed more than the ranges between geologies for each species. The high Mn uptake in the *S. lancea* leaf samples was interesting to note from a bioavailability perspective. The finding that the *A. karroo* samples had the highest leaf content for N on the Black Reef but that the soils on the Black Reef had extremely low N also bears further investigation.

3.5.5. Determining the effects of leaf and soil elemental content on spectral derivative results

The Kruskal Wallis test results for each species identified significant differences between the geologies for selected vegetation indices. There were some results which showed that even when all species data was combined, there were differences between geologies which could be identified using the vegetation indices. The PSRI values for plants growing on the Black Reef were generally higher (as was also observed for the *A. karroo* samples on the Black Reef most notably), but not all spectral responses were consistent with the geology. Therefore, it is also necessary to look at how the spectral response relates to the leaf and soil elemental content, bioavailability of the elements and the nutritional status of the plants.

3.5.5.1. Selecting a subset of significant variables through variables characterisation

There were a large number of variables to be considered (soil elemental content, leaf elemental content, BCFs and soil and leaf elemental ratios), and therefore a variables characterisation test was run in XLStat. The variables characterisation tool used the correlation coefficient to identify the variables that showed the strongest correlation between the variable and the vegetation index. This process was repeated for each vegetation index per species. The summarised results of the variables characterisation are shown in Table 3-18. The full table of results with correlation coefficients and p-values is included in Appendix 8. For each vegetation index, the variables that showed the strongest correlation to the VI results were identified. Values which showed the strongest relationships are shown in the table ($p < 0.01$). The results were divided up into the 5 categories, soil elemental content (analysis by XRF), leaf elemental content (analysis by ICP-OES/ICP-MS), bioconcentration factors, soil and leaf elemental ratios and soil and plant characteristics.

Table 3-18 Summarised results of the variables characterisation analysis, per vegetation index and per for each individual species, and all species combined. Columns show the variables that showed a significant correlation to the vegetation index

VI	Species	Soils elemental content	Leaf elemental content	Bio-concentration Factors (BCF)	Soil:leaf ratios	Soil & plant characteristics
725-702 Ratio of the 1st Derivative	*A. karroo*					
	E. crispa	Rb			Na:K leaf ratio	
	S. lancea		Ba	Ti		
NDVI	*A. karroo*		Ti	Ti		
	E. crispa	Zr	Cu, Mn, Ni, S	Mn, Ni	Mg:Mn leaf ratio, Si:Mn leaf:soil ratio	
	S. lancea		Ba	Cu, Zn		
NDWI	*A. karroo*		Si	Si	Leaf ca: al:ca Soil, Al BCF: Ca BCF	
	E. crispa					
	S. lancea		Ba, Pb	Cu, Zn		Leaf Water content %
PSRI	*A. karroo*	Cu	Mn	Fe, Fe_2		soil pH
	E. crispa					
	S. lancea		As			Leaf Water content %
Red-edge NDVI	*A. karroo*		Ti	Ti	Si:Ti leaf:soil ratio,	
	E. crispa	K_2, Rb	Mn	Mn, Na	Na:K leaf ratio, Mg:Mn leaf ratio, Si:Mn leaf:soil ratio	
	S. lancea		Ba, Sn	Cu		
Red-edge position	*A. karroo*	Sr			Si:Ti leaf:soil ratio	
	E. crispa	V		Mn, Ni	Si:Mn leaf:soil ratio	
	S. lancea		Ba, Cu, Zn	Zn		
Red-edge inflection point	*A. karroo*		As, Fe, U			
	E. crispa					
	S. lancea		As, Ba, U	Ba, Mn, Zn	Si:Mn leaf:soil ratio, Rb:K soil ratio	

There were very few soil elements, or soil or plant characteristics such as soil pH and Leaf water content that correlated well with the spectral indices The leaf elemental content, bioconcentration factors and leaf and soil element ratios categories had more variables with strong correlations with the spectral indices. For the NDWI, PSRI and Red-edge inflection points, the *E. crispa* samples did not show any significant correlations to any of the leaf or soil variables. The *A. karroo* samples also did not show any significant correlations with the variables for the 725/702 ratio of the 1st derivative. The significant variables differed between the species. There was some overlap between variables for the individual species for the different indices, showing

a trend of sensitivity to specific elements. The variables that were identified as having significant correlations to the spectral indices for each species were then used for the regression analysis.

3.5.5.2. Identifying the substrate and foliar constituents with the strongest influence on vegetation index results

In order to be able to achieve the ultimate aim of this research, which would be to predict the changes in geology through the use of spectral response of the plants, it is first necessary to understand the influence that the changes in soil and foliar constituents have on the spectral response. To understand this relationship, a series of regression analyses for each VI and the subset of variables selected in section 3.5.5.1. was done.

The parametric multiple regression using a best model selection option was used when the variables that were being analysed were normally distributed. At a species level there were many variables that were normally distributed. If any of the variables for a given subset were not normally distributed then the non-parametric regression analysis was used. For the non-parametric tests, if the result of the regression was not significant, the least significant variable was removed to test if that improved the model. This process was repeated until the highest R^2 value was obtained for the set of variables thus simulating the best model procedure for the parametric test. For all tests, 3 validation samples were randomly selected to test the model.

For many of the vegetation indices, the regression results were relatively weak. The VIs per species which did not have any significant results in the variables characterisation were not included in the regression analysis. Only results for VIs with significant results are shown below.

3.5.5.3. Regression analysis of vegetation indices and elemental results for A. karroo

The subset of variables that correlated with the NDVI results for *A. karroo* were all normally distributed, and therefore a best model linear regression was used. The results for the regression of the NDVI results for *A. karroo* against the selected bioconcentration factor for Ti turned out to be the variable that generated the best fit model (Table 3-19). The adjusted R^2 value for the model was 0.158, which is quite low. However, the randomly selected three validation samples fitted the model well (Figure 3-4).

Table 3-19 *A. karroo* linear regression of variables against NDVI: Summary of the variables selection

No. of variables	Variables	MSE	R^2	Adjusted R^2	Mallows' Cp	Akaike's AIC	Schwarz's SBC	Amemiya's PC
1	Ti BCF	0.000	0.214	**0.158**	1.218	-130.714	-129.168	0.884
2	Leaf Ti (ppm) / Ti BCF	0.000	0.227	0.108	3.000	-128.980	-126.662	0.979

The best model for the selected selection criterion is displayed in blue

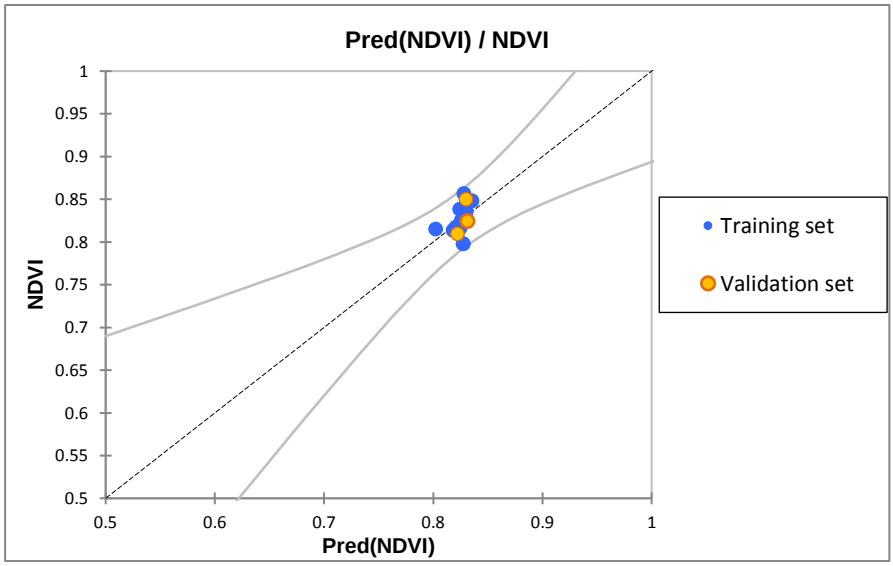

Figure 3-4 *A. karroo* linear regression of variables against NDVI: Predicted vs actual values

The variables which correlated with the NDWI for *A. karroo* were not all normally distributed and therefore a non-parametric regression was used. The combination of all variables identified in the variables classification did not show any significant trends, and there the lowest

correlation variables were removed until a significant result was identified. The final selection of variables is shown in Table 3-20 . The R^2 value for the relationship between the NDWI and the Leaf Si, Si BCF and Al BCF: Ca BCF ratio was low but significant (Table 3-21). The randomly selected validation samples followed the model (Figure 3-5).

Table 3-20 *A. karroo* non parametric regression results for NDWI: Correlation matrix

Variables	Leaf Si	Si BCF	Al BCF : Ca BCF	NDWI
Leaf Si	**1.000**	0.999	-0.625	-0.471
Si BCF	0.999	**1.000**	-0.625	-0.482
BCF Al:BCF Ca	-0.625	-0.625	**1.000**	0.683
NDWI	-0.471	-0.482	0.683	**1.000**

Table 3-21 Non-parametric regression of variable NDWI: Goodness of fit statistics

R^2	0.063
SSE	0.004
MSE	0.000
RMSE	0.015

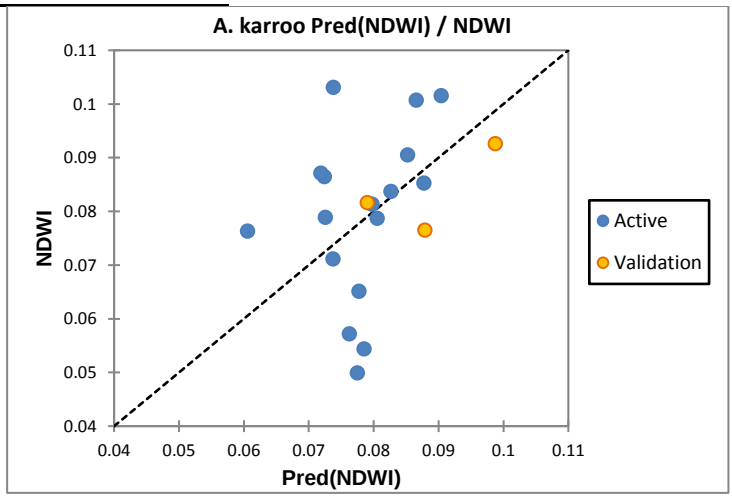

Figure 3-5 *A. karroo* Non-parametric regression of variables to NDWI: Predicted vs actual values

The *A. karroo* shows a fairly strong regression R^2 value (R^2=0.531) and strong correlations to Fe BCF (major and trace readings) and soil pH. All *A. karroo* PSRI values were found to be negative. The lower the PSRI value, the healthier the plant. The predicted values for the validation samples did not, however fit the model as well as the observations used to develop the model.

Table 3-22 *A. karroo* PSRI non-parametric regression correlation matrix:

Variables	Leaf Mn (ppm)	Fe BCF	Fe_2 BCF	Soil pH	PSRI
Leaf Mn (ppm)	**1.000**	0.491	0.503	0.591	0.659
Fe BCF	0.491	**1.000**	0.999	0.656	0.832
Fe_2 BCF	0.503	0.999	**1.000**	0.655	0.833
Soil pH	0.591	0.656	0.655	**1.000**	0.779
PSRI	0.659	0.832	0.833	0.779	**1.000**

Table 3-23 Non-parametric regression of variable PSRI: Goodness of fit statistics

R^2	0.531
SSE	0.005
MSE	0.000
RMSE	0.017

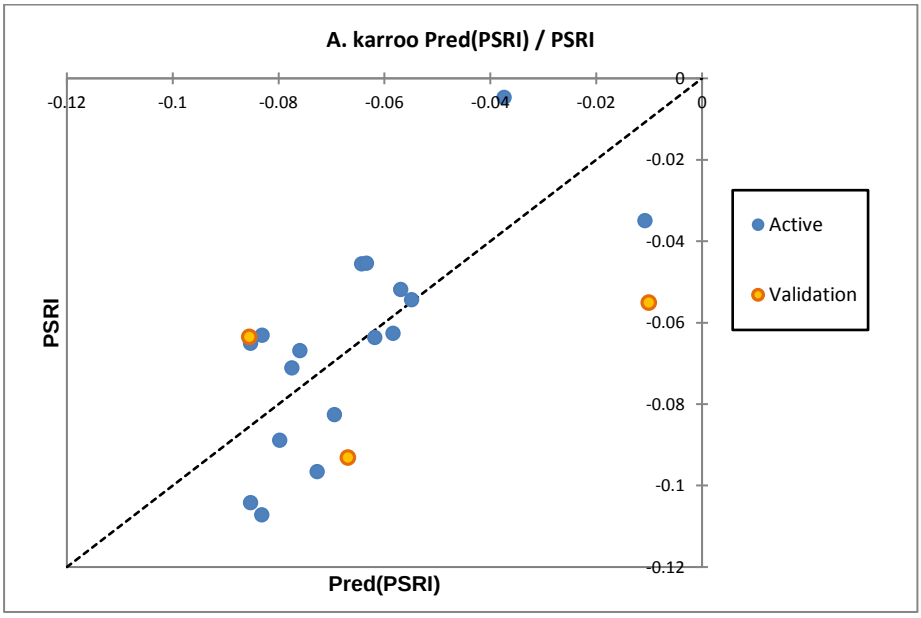

Figure 3-6 *A. karroo* Non-parametric regression of variables to PRSI: Predicted vs actual values

The best fit linear regression of Red-edge NDVI for *A. karroo* selected Ti BCF / Leaf Ti (ppm)*Si :Ti leaf/soil ratio as the best combination of variables for the model (Table 3-24). It was interesting to note that the variables with the strongest correlation to the Red-edge NDVI were linked to Ti uptake by the *A. karroo* samples. The adjusted R^2 value of 0.637 shows a good fit for

the model. When plotting the predicted against actual values (Figure 3-7), the validation samples also showed a good fit to the model.

Table 3-24 Summary of the variables selection for the linear regression for the *A. karroo* Red-edge NDVI

No. of variables	Variables	MSE	R^2	Adjusted R^2	Mallows' Cp	Akaike's AIC	Schwarz's SBC	Amemiya's PC
1	Ti BCF	0.001	0.208	0.151	11.543	-104.449	-102.904	0.891
2	Ti BCF / leaf Ti (ppm)*Si :Ti leaf/soil ratio	0.001	0.686	**0.637**	-0.654	-117.232	-114.915	0.398
3	leaf Ti (ppm)/ Si:Ti leaf/soil ratio / leaf Ti (ppm)*Si :Ti leaf/soil ratio	0.001	0.689	0.611	1.240	-115.413	-112.323	0.444

The best model for the selected selection criterion is displayed in blue

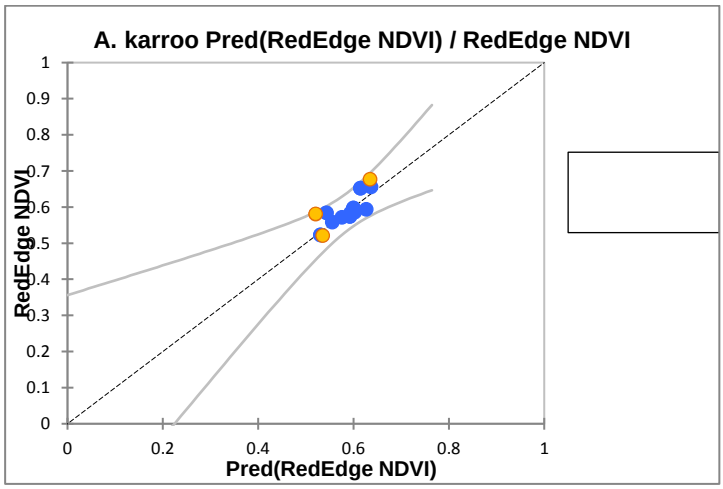

Figure 3-7 *A. karroo* linear regression of variables to Red-edge NDVI: Predicted vs actual values

The linear regression was used for the *A. karroo* Red-edge position. The best model for the regression used the soil Sr content and Si:Ti leaf/soil ratio. An adjusted R^2 value of 0.610 was obtain which shows a relatively good fit to the model (Table 3-25). The validation samples also showed a good fit to the model (Figure 3-8).

Table 3-25 Summary of the variables selection *A. karroo* Red-edge Position

No. of variables	Variables	MSE	R^2	Adjusted R^2	Mallows' Cp	Akaike's AIC	Schwarz's SBC	Amemiya's PC
1	Soil Sr (ppm)	0.243	0.535	0.502	5.870	-20.749	-19.204	0.523
2	Soil Sr (ppm)/ Si:Ti leaf/soil ratio	0.191	0.662	**0.610**	3.000	-23.840	-21.522	0.429

The best model for the selected selection criterion is displayed in blue

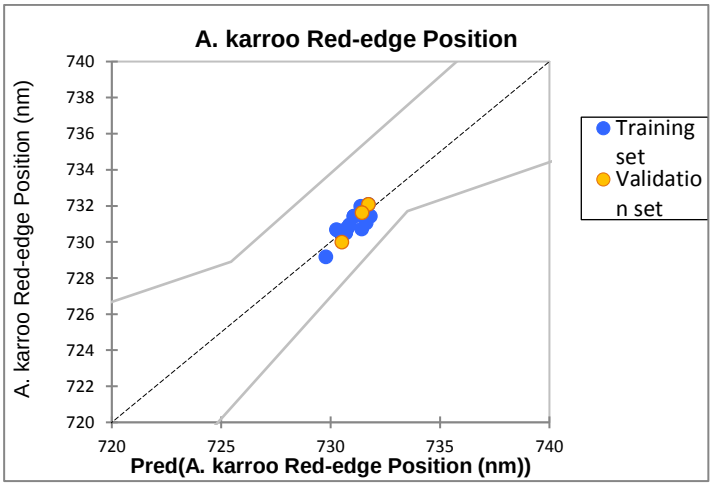

Figure 3-8 *A. karroo* linear regression of variables to Red-edge Position: Predicted vs actual values

Table 3-26 shows the results for the initial non-parametric regression for the Red-edge inflection point (Rre) for *A. karroo*. The correlation R^2 values were low and the regression result was poor, thus the variables were removed individually to see which gave the best regression result (highest R^2). The final test used the linear regression for the Leaf As content which gave a R^2 value of 0.410 (**Error! Reference source not found.**). The validation samples fitted the model, as shown in Figure 3-9.

Table 3-26 *A. karroo* Red-edge inflection point (Rre) – initial non-parametric regression – correlation matrix

Variables	Leaf Fe	Leaf U	Leaf As	Red-edge inflection point
Leaf Fe	**1.000**	0.834	0.759	-0.378
Leaf U	0.834	**1.000**	0.629	-0.413
Leaf As	0.759	0.629	**1.000**	-0.393
Red-edge inflection point	-0.378	-0.413	-0.393	**1.000**

Table 3-27 Final linear regression for the Red-edge inflection point (Rre): Summary of the variables selection

No. of variables	Variables	MSE	R^2	Adjusted R^2	Mallows' Cp	Akaike's AIC	Schwarz's SBC	Amemiya's PC
1	Leaf As (ppm)	0.000	0.447	**0.410**	2.000	-133.445	-131.778	0.619

The best model for the selected selection criterion is displayed in blue

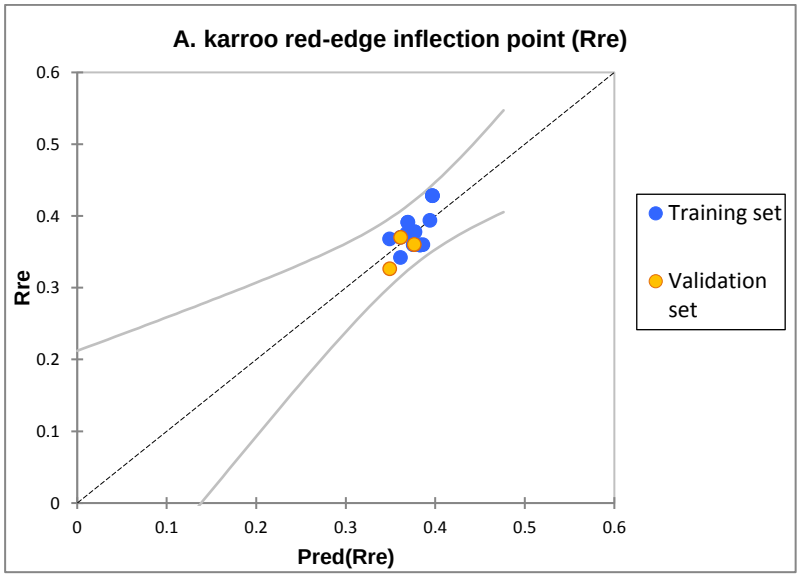

Figure 3-9 *A. karroo* linear regression of variables to Red-edge inflection point: Predicted vs actual values

3.5.5.4. Regression analysis of Vegetation indices and elemental results for E. crispa

This section presents the results for the regression analysis of the vegetation indices and elemental results for *E. crispa*. For the *E. crispa* there were no significant results in the variables correlation for the NDWI, PSRI and Red-edge inflection points and therefore no regression analysis was done for those vegetation indices. Table 3-19 shows the correlations from the NDVI regression results. There were a number of variables which were found to have significant correlations, and removing the variables with the lowest correlations did not improve the fit of the model. There was a significant result for the model and an R^2 value of 0.537 (Table 3-19). The predictions for the validation samples were within a similar range of error to the training samples (Figure 3-10)

Table 3-28 *E. crispa* non-parametric regression for NDVI : Correlation matrix

Variables	Ni BCF	Mn BCF	Soil Zr (ppm)	Ni2 BCF	Zn BCF	Leaf Cu (ppm)	Si:Mn leaf/soil ratio	Leaf Ni (ppm)	NDVI
Ni BCF	**1.000**	0.230	0.262	0.565	-0.426	-0.394	-0.350	0.469	-0.489
Mn BCF	0.230	**1.000**	0.494	0.384	-0.223	-0.422	-0.536	0.328	-0.558
Soil Zr (ppm)	0.262	0.494	**1.000**	0.451	-0.576	-0.409	-0.322	0.311	-0.680
Ni2 BCF	0.565	0.384	0.451	**1.000**	-0.240	-0.354	-0.462	0.747	-0.653

Zn BCF	-0.426	-0.223	-0.576	-0.240	**1.000**	0.451	0.065	-0.069	0.666
Leaf Cu (ppm)	-0.394	-0.422	-0.409	-0.354	0.451	**1.000**	0.251	-0.337	0.644
Si:Mn leaf/soil ratio	-0.350	-0.536	-0.322	-0.462	0.065	0.251	**1.000**	-0.550	0.431
Leaf Ni (ppm)	0.469	0.328	0.311	0.747	-0.069	-0.337	-0.550	**1.000**	-0.677
NDVI	-0.489	-0.558	-0.680	-0.653	0.666	0.644	0.431	-0.677	**1.000**

Table 3-29 *E. crispa* non-parametric regression of variable NDVI: Goodness of fit statistics:

R^2	0.537
SSE	0.004
MSE	0.000
RMSE	0.016

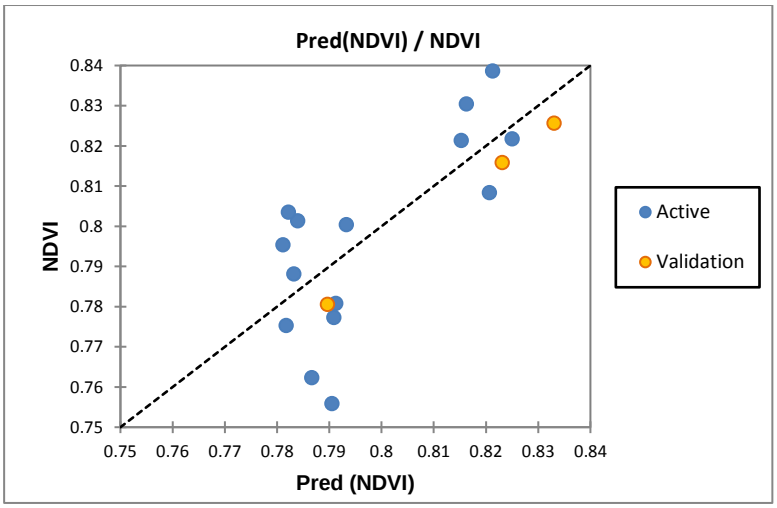

Figure 3-10 *E. crispa* non-parametric regression of variables to NDVI: Predicted vs actual values

Similar results were seen for the Red-edge NDVI as for the NDVI results for *E. crispa*, although for different variables. However, the uptake of Mn featured quite strongly as a common element between the NDVI and Red-edge NDVI. The Red-edge NDVI model was also not improved through the removal of variables in the initial correlation matrix (Table 3-21). The R^2 value shown in Table 3-22 and predictions plotted in Figure 3-11 showed a moderate fit to the model.

Table 3-30 *E. crispa* non-parametric regression for Red-edge NDVI : Correlation matrix:

Variables	Soil Rb (ppm)	Mn BCF	Leaf Mn (ppm)	Mg:Mn leaf ratio	Na BCF	Na:K leaf ratio	Si :Mn leaf/soil ratio	Red-edge NDVI

Soil Rb (ppm)	**1.000**	-0.692	-0.438	0.553	0.102	-0.195	0.615	0.648
Mn BCF	-0.692	**1.000**	0.736	-0.736	-0.273	0.613	-0.464	-0.729
Leaf Mn (ppm)	-0.438	0.736	**1.000**	-0.844	-0.361	0.338	-0.373	-0.758
Mg:Mn leaf ratio	0.553	-0.736	-0.844	**1.000**	0.135	-0.303	0.449	0.636
Na BCF	0.102	-0.273	-0.361	0.135	**1.000**	-0.233	0.349	0.487
Na:K leaf ratio	-0.195	0.613	0.338	-0.303	-0.233	**1.000**	-0.174	-0.366
Si :Mn leaf/soil ratio	0.615	-0.464	-0.373	0.449	0.349	-0.174	**1.000**	0.456
Red-edge NDVI	0.648	-0.729	-0.758	0.636	0.487	-0.366	0.456	**1.000**

Table 3-31 *E. crispa* non-parametric regression of variable Red-edge NDVI: Goodness of fit statistics:

R^2	0.469
SSE	0.016
MSE	0.001
RMSE	0.032

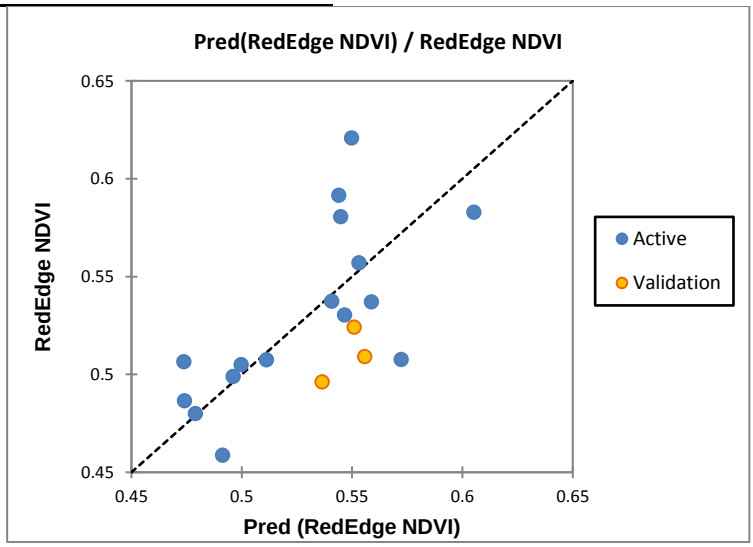

Figure 3-11. *E. crispa* non-parametric regression of variables to Red-edge NDVI: Predicted vs actual values

The regression for the Red-edge position was done using the non-parametric regression, which presented a result with a moderate R^2 value of 0.420. Again, the Mn BCF had a strong correlation with the Red-edge Position. Ni (trace and major) BCF and the Si:Mn leaf/soil ratio had less strong correlations. The overall fit of the model, as shown by the predicted vs actual results in Figure 3-12 showed a relatively good fit for more samples. Some of the training samples showed higher residuals and did not fit the model adequately.

Table 3-32 Initial *E. crispa* non-parametric regression for Red-edge position (REP): Correlation matrix:

Variables	Mn BCF	Ni BCF	Si:Mn leaf/soil ratio	Ni2 BCF	Soil V (ppm)	REP
Mn BCF	**1.000**	0.291	-0.557	0.431	-0.087	0.678
Ni BCF	0.291	**1.000**	-0.367	0.492	-0.442	0.433
Si:Mn leaf/soil ratio	-0.557	-0.367	**1.000**	-0.450	0.224	-0.435
Ni2 BCF	0.431	0.492	-0.450	**1.000**	-0.674	0.537
Soil V (ppm)	-0.087	-0.442	0.224	-0.674	**1.000**	-0.427
REP	0.678	0.433	-0.435	0.537	-0.427	**1.000**

Table 3-33 *E. crispa* non-parametric regression of variable Red-edge Position (REP): Goodness of fit statistics:

R^2	0.420
SSE	9.749
MSE	0.609
RMSE	0.781

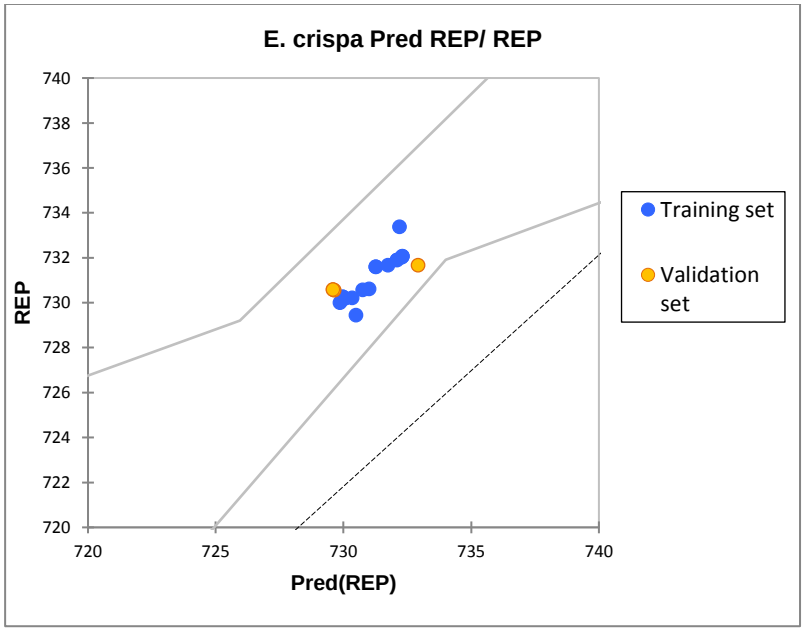

Figure 3-12 *E. crispa* linear regression of variables to Red-edge position: Predicted vs actual values

3.5.5.5. Regression analysis of Vegetation indices and elemental results for S. lancea

For the variables characterisation of *S. lancea*, most of the VIs had correlations with either Ba or Cu leaf concentrations or BCF. Only the NDWI showed correlations with any soil elemental contents and the Red-edge inflection point was the only index to have correlations with the soil elemental ratios.

The best model linear regression was used to determine the relationship between leaf Ba and Ti BCF and the 1st derivative 725/702 ratio. The model had a low R^2 value of 0.184 (Table 3-34) which can also been seen in the poor fit of the predicted vs actual values in Figure 3-13. The validation samples, however, did fit within the model fairly well.

Table 3-34 *S. lancea* linear regression of the 1st derivative 725nm/702nm ratio: Summary of the variables selection

No. of variables	Variables	MSE	R^2	Adjusted R^2	Mallows' Cp	Akaike's AIC	Schwarz's SBC	Amemiya's PC
2	Leaf Ba (ppm)/ Ti BCF	0.019	0.270	**0.184**	3.000	-76.363	-73.376	0.883

The best model for the chosen selection criterion is displayed in blue

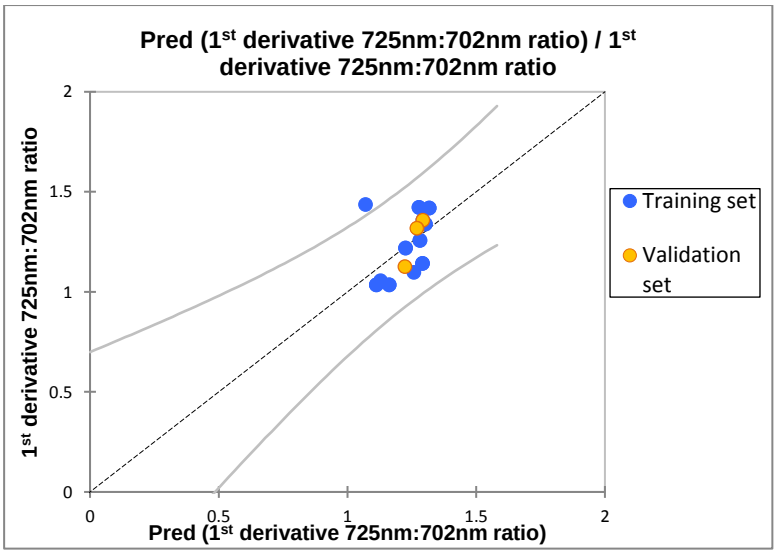

Figure 3-13 *S. lancea* linear regression of variables to 1st derivative 725nm/702nm ratio: Predicted vs actual values

The non-parametric regression did not produce any significant results, despite fairly strong correlations between the Cu BCF and Zn BCF with the NDWI (Table 3-35). The process was repeated until only the Leaf Pb and Cu BCF remained, and a linear regression was used to determine the relationship between these two variables and the NDWI. An R^2 value of 0.472 was obtained (Table 3-36). Figure 3-14 shows the predicted vs actual values and the validation samples which followed a similar distribution to the training samples.

Table 3-35 Initial *S. lancea* non-parametric regression of NDWI- correlation matrix:

	Leaf Water content (%)	Leaf Ba (ppm)	Leaf Pb (ppm)	Cu BCF	Zn BCF	NDWI
Leaf Water content (%)	**1**	0.303	-0.275	-0.309	-0.405	-0.125
Leaf Ba (ppm)	0.303	**1**	0.197	-0.468	-0.604	-0.295
Leaf Pb (ppm)	-0.275	0.197	**1**	0.082	0.096	-0.304
Cu BCF	-0.309	-0.468	0.082	**1**	0.933	0.602
Zn BCF	-0.405	-0.604	0.096	0.933	**1**	0.526
NDWI	-0.125	-0.295	-0.304	0.602	0.526	**1**

Table 3-36 Regression of variable NDWI: Summary of the variables selection NDWI:

No. of variables	Variables	MSE	R^2	Adjusted R^2	Mallows' Cp	Akaike's AIC	Schwarz's SBC	Amemiya's PC
2	Leaf Pb (ppm) / Cu BCF	0.000	0.488	**0.427**	0.356	-225.782	-222.795	0.620

The best model for the chosen selection criterion is displayed in blue

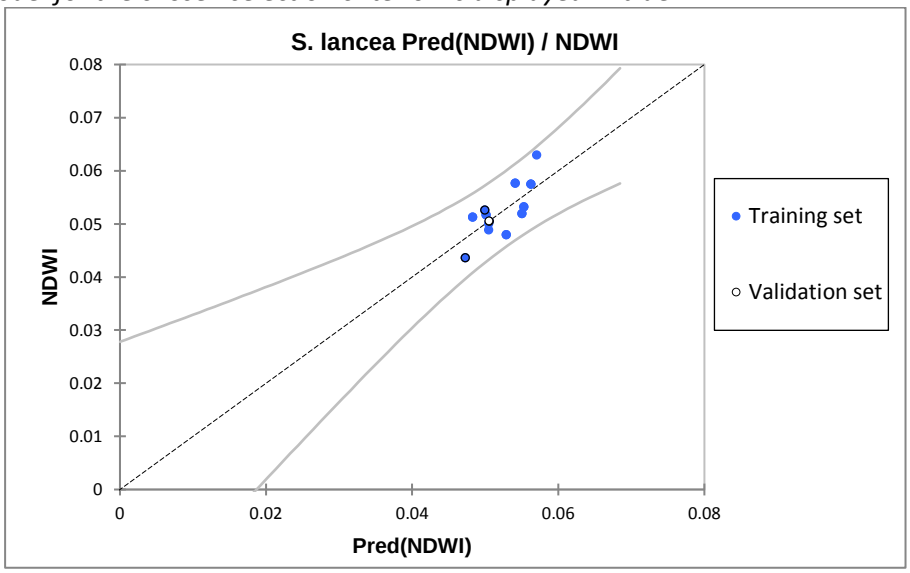

Figure 3-14 *S. lancea* linear regression of variables to NDWI: Predicted vs actual values

All variables identified as having a strong correlation with the *S. lancea* Red-edge NDVI were normally distributed and the best model linear regression was used to determine the relation between the selected variables and the Red-edge NDVI. As with the NDVI, there was a strong relationship with leaf Ba content, but this model found the best fit by incorporating Cu BCF and the leaf Sn content in the model. The resulting Adjusted R^2 value was 0.657 (Table 3-37). The predicted vs actuals plotted in Figure 3-15 shows a good fit and fairly low residuals for the validation samples.

Table 3-37 *S. lancea* linear regression of Red-edge NDVI: Summary of the variables selection

No. of variables	Variables	MSE	R^2	Adjusted R^2	Mallows' Cp	Akaike's AIC	Schwarz's SBC	Amemiya's PC
1	Leaf Ba (ppm)	0.000	0.573	0.549	7.695	-156.908	-154.916	0.470
2	Leaf Ba (ppm) / Leaf Sn (ppm)	0.000	0.688	0.651	3.331	-161.163	-158.176	0.378
3	Cu BCF / Leaf Ba (ppm) / Leaf Sn (ppm)	0.000	0.712	**0.657**	4.000	-160.761	-156.778	0.385

The best model for the selected selection criterion is displayed in blue

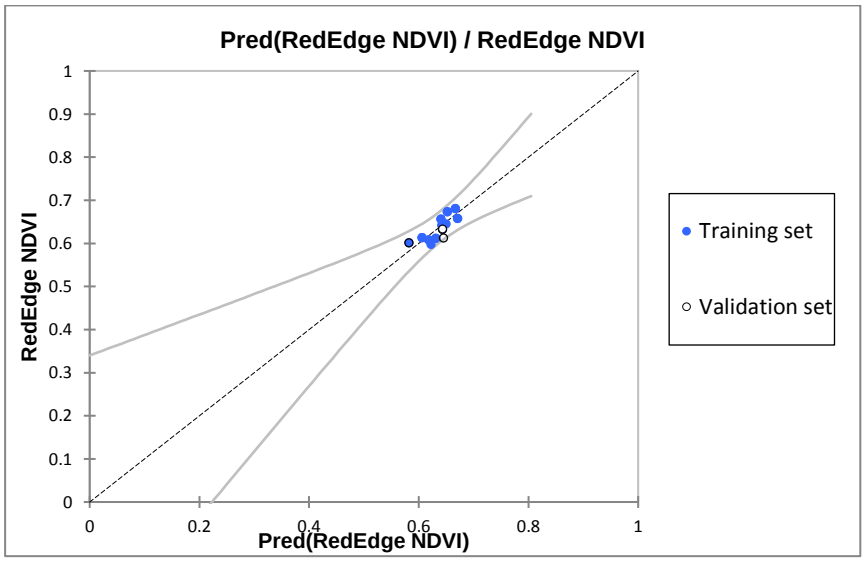

Figure 3-15 *S. lancea* linear regression of variables to Red-edge NDVI: Predicted vs actual values

The results of the PSRI found the best fit for the model using both the leaf water content and the Leaf As content. An adjusted R^2 value of 0.283 was obtained (Table 3-38) and the weak fit of the model is shown by the high residuals for narrow range of data shown in Figure 3-16.

Table 3-38 *S. lancea* linear regression of variable PSRI: Summary of the variables selection

No. of variables	Variables	MSE	R^2	Adjusted R^2	Mallows' Cp	Akaike's AIC	Schwarz's SBC	Amemiya's PC
1	Leaf water content (%)	0.000	0.221	0.177	4.660	-150.473	-148.482	0.857
2	Leaf water content (%)/ Leaf As (ppm)	0.000	0.359	**0.283**	3.000	-152.373	-149.386	0.776

The best model for the selected selection criterion is displayed in blue

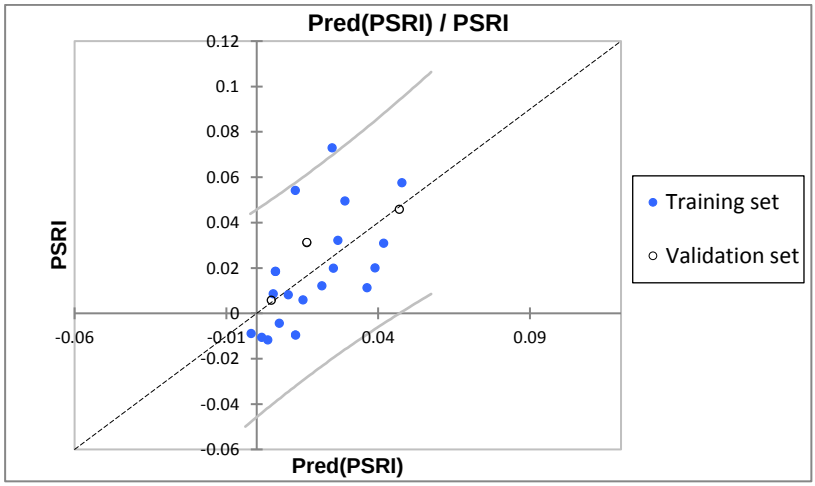

Figure 3-16 *S. lancea* linear regression of variables to PSRI: Predicted vs actual values

The variables characterisation again identified Leaf Ba, Leaf Cu and Leaf Zn as having a strong correlation with a vegetation index for the *S. lancea* samples. For the Red-edge Position (REP) the best model used the Leaf Ba and Leaf Zn contents. The R^2 value was 0.345 (Table 3-39). Some of the residuals were found to be a bit high within the training samples, but the validation samples fitted the model closely (Figure 3-17).

Table 3-39 *S. lancea* Regression of variable Red-edge Position (REP): Summary of the variables selection

No. of variables	Variables	MSE	R^2	Adjusted R^2	Mallows' Cp	Akaike's AIC	Schwarz's SBC	Amemiya's PC
1	Leaf Ba (ppm)	0.447	0.187	0.142	7.402	-14.222	-12.231	0.894
2	Leaf Ba (ppm) / Leaf Zn (ppm)	0.341	0.414	**0.345**	2.879	-18.758	-15.771	0.710
3	Leaf Cu (ppm)/ Leaf Ba (ppm) / Leaf Zn (ppm)	0.344	0.444	0.340	4.000	-17.827	-13.844	0.741

The best model for the selected selection criterion is displayed in blue

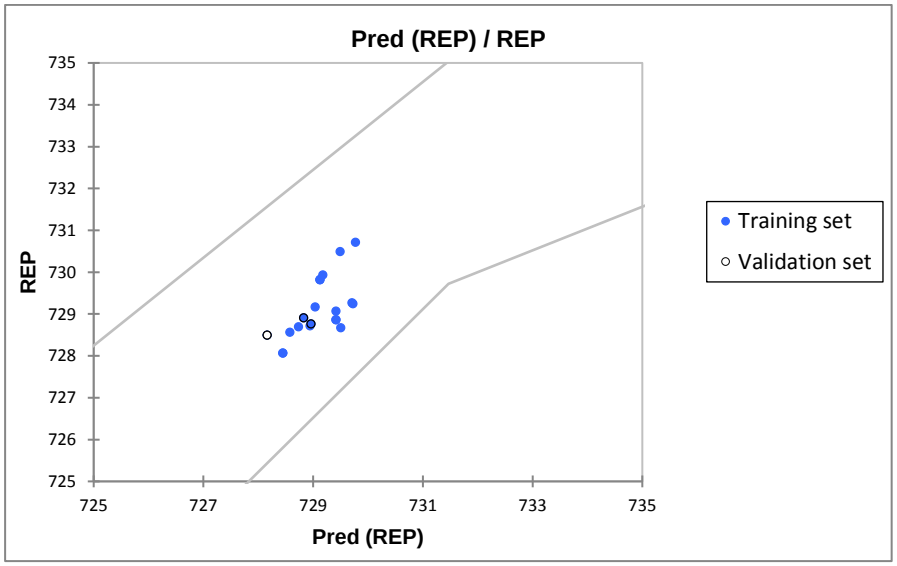

Figure 3-17 *S. lancea* linear regression of variables to Red-edge Position (REP): Predicted vs actual values

Table 3-40 *S. lancea* Regression of variable Red-edge inflection point: Summary of the variables selection

No. of variables	Variables	MSE	R^2	Adjusted R^2	Mallows' Cp	Akaike's AIC	Schwarz's SBC	Amemiya's PC
1	Leaf Ba (ppm)	0.000	0.506	0.479	6.910	-167.648	-165.656	0.543
2	Leaf As (ppm)/ Leaf Ba (ppm)	0.000	0.652	**0.612**	2.129	-172.667	-169.680	0.421
3	Leaf As (ppm) / Leaf Ba (ppm)/ Rb:K soil ratio	0.000	0.671	0.609	3.277	-171.752	-167.769	0.439
4	Leaf As (ppm) / Leaf Ba (ppm)/ Ba BCF / Rb:K soil ratio	0.000	0.677	0.591	5.000	-170.118	-165.140	0.475

The best model for the selected selection criterion is displayed in blue

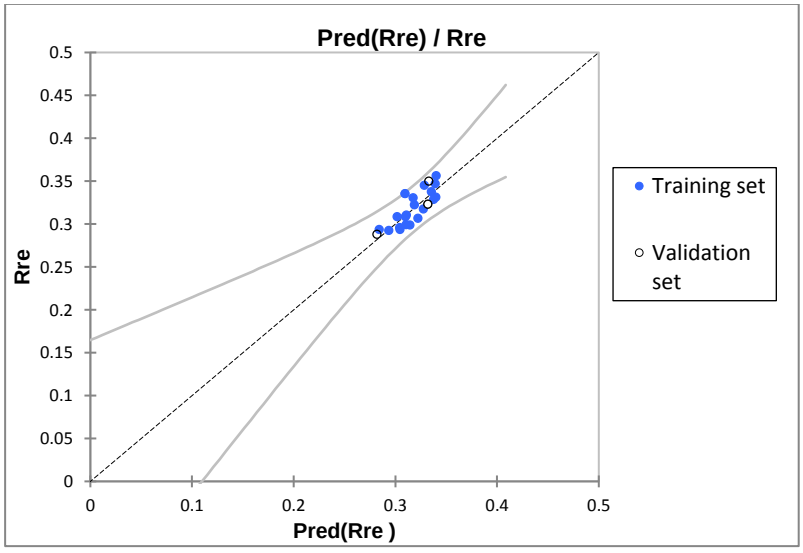

Figure 3-18 *S. lancea* linear regression of variables to Red-edge inflection Point (Rre): Predicted vs actual values

The Red-edge inflection point linear regression found the best fit using the leaf As and leaf Ba contents. The adjusted R^2 value was 0.612 (Table 3-40). The predicted vs actual values plotted well (Figure 3-18) and the validation samples were also found to fit the model well.

3.5.6. Species classification using vegetation index responses

The previous chapter showed some differences in vegetation index results between the three geologies and six LFTs for the three species. An important observation was that when combining the data for all three species to perform the analysis, the differences between geologies were obscured as the plants' spectral responses to changes in geology were not consistent across all three species. Therefore is it necessary to differentiate between species before attempting to differentiate between geologies, unless the growing conditions are extreme enough to cause a stress response, even in species which have adapted to their environment.

It was initially observed that there were certain spectral responses consistent with a particular species. For example, on average the PSRI values for *A. karroo* samples were lower than for the *E. crispa and S. lancea,* and the NDWI and Red-edge inflection point were higher, whereas the *S. lancea* samples showed higher NDVI and Red-edge NDVI results and lower Red-edge position and Red-edge inflection point. The *E. crispa* samples showed a lower 725/702 ratio of the 1st and 2nd derivatives, as shown in Figure 3-19. None of these spectral indices independently classified the species as being different from the other two species, but it was possible to use a combination of the vegetation indices to perform a grouping analysis in ArcGIS desktop which accounted for the majority of the variation between species.

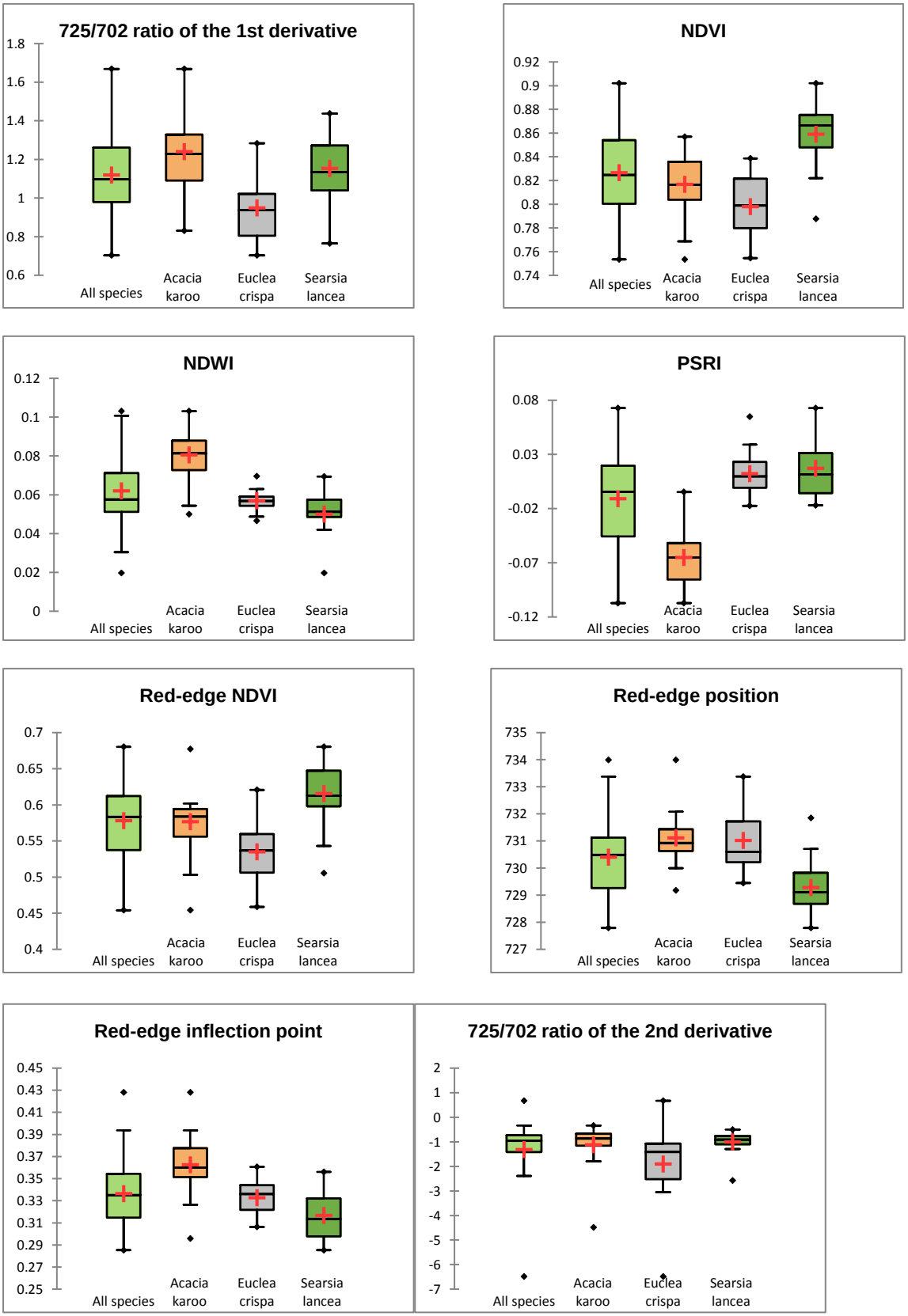

Figure 3-19 Box plots showing the results for all eight vegetation indices per species, and for all species combined

The grouping analysis tool was run using the results of the vegetation indices. An iterative approach was used to test multiple combinations of the vegetation indices. Results were similar for various combinations, but a combination of all eight indices produced the best results. Figure 3-20 shows the box plot using standardised values for the ranges of vegetation indices and the values which described each class. As with the soil elemental concentration grouping analysis in chapter 2, the Calinski-Harabasz pseudo F-statistic was used to identify the optimal number of groups, and the result returned was three.

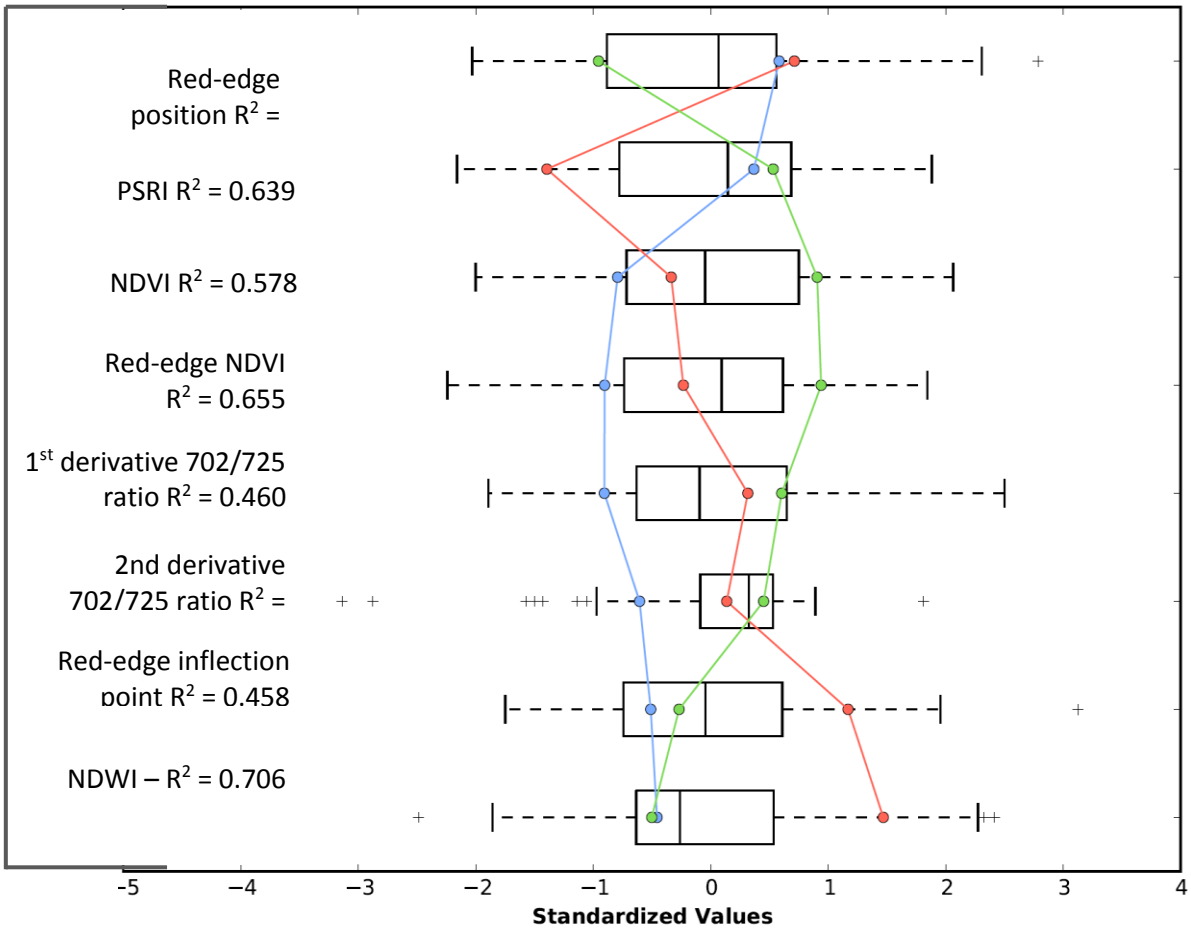

Figure 3-20 Grouping analysis using all eight vegetation indices. The Pseudo F-statistic identified 3 groups as the optimal number of groups (maximum mean F-statistic = 33.0270 (Class 1 – Blue, Class 2 – Red, Class 3 – Green). R^2 values are shown for each vegetation index in the axis labels.

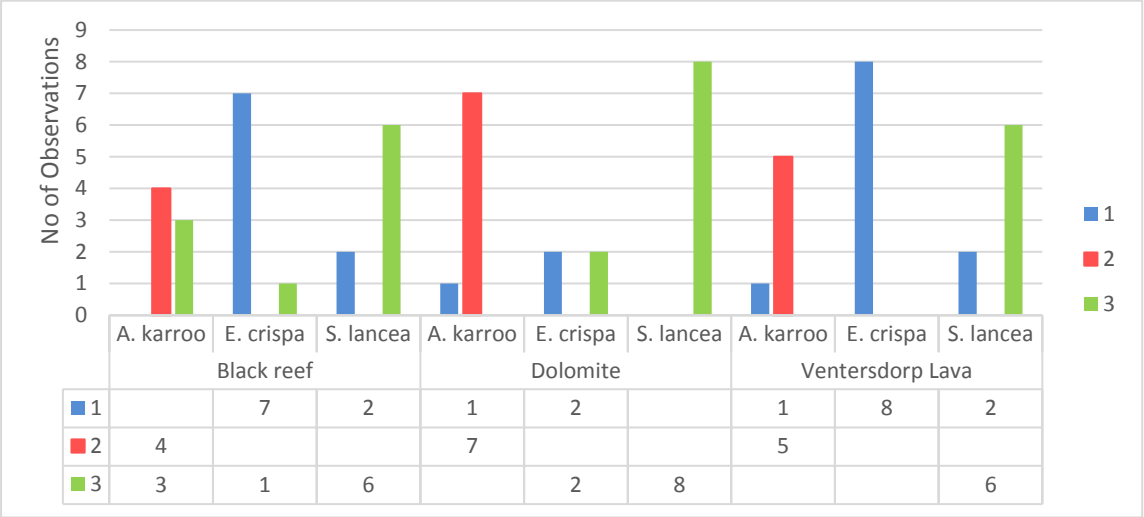

Figure 3-21 Graph showing the distribution of the grouping analysis results by species per geology. Class 1 accounted for most of the *E. crispa* samples, class 2 contained only *A. karroo* and class 3 accounted for the majority of the *S. lancea* samples. Samples which did not fall into the same group as the rest of their species were showing higher or lower than average VI results for that species.

It was observed that the three groups in the grouping analysis result corresponded strongly with the three species used in the analysis. Overall, group 1 contained 23 observations, of which 17 were *E. crispa*, group 2 contains 16 observations which were all *A. karroo* and group three contained 26 observations, of which 20 were *S. lancea*. In group 3, four of the observations which were not *S. lancea* occurred on the Black Reef, and two other *E. crispa* samples from the Dolomites also fell into group three. It is possible that these samples were showing stress responses which may account for their classification. Group 3 was characterised by a lower Red-edge Position, which is an indication of a blue shift, higher PSRI, an indicator of high carotenoid content and high NDVI and Red-edge NDVI, which are usually indicators of high chlorophyll content, and low NDWI. There were four *S. lancea* samples which fell into group 1, two on the Black Reef and two on the Ventersdorp Lavas. Group 1 was characterised by a higher Red-edge position, indicating a red shift, but a low Red-edge inflection point, high PSRI and low NDVI and Red-edge NDVI results, as well as a lower 1st and 2nd derivative 725/702 ratios. *A. karroo* samples in group 2 were differentiated by low PSRI values, high Red-edge inflection points and high NDWI values.

These results could provide indications as the variables which control for the more extreme spectral responses for each species. To verify this, the elemental data was classified by group from the above results, species and geology and descriptive statistics were used to investigate the differences between the mean and median values for the species by group. There were insufficient replicates to do further statistical analysis but the box plots shown in Figure 3-22 provided extremely valuable insight. Often the elements that showed marked differences for the "outliers" of the grouping analysis were not detected as being significantly different in the Kruskal Wallis tests for soils and leaf elemental contents, nor were they detected as having significant correlations with the spectral results in the analysis in Section 3.5.4.2. It is possible that these results have been obscured in the tests mentioned above as non-parametric tests are typically designed to compensate for extreme results by using median values and ranks for the analyses.

Initially, box plots were drawn using only the group result and species. A subset of the boxplots are shown in Figure 3-22, and the additional is displayed in Appendix 9. From the box plots it would be seen that there were differences in results between the different groups per species, particularly the *A. karroo* samples, where the majority classified into group 2, but three of the Black Reef samples classified into group 3, and the two Ventersdorp Lava and single dolomite sample fell into group 1. The blue shift in the Red-edge position and the higher PSRI values of the *A. karroo* samples was quite marked. For those samples, there were strong differences between the Co content in the Group 3 *A. karroo* samples compared to group 1 and 2 *A. karroo* samples. Group 3 *A. karroo* samples were found to have a lower soil water content, whilst the group 1 *S. lancea* samples has the lowest leaf water content of all group, but particularly compared to other *S. lancea* samples. Leaf Al content for the Group 1 *A. karroo* samples was an order of magnitude higher than all other samples. This may be a driver of the lower NDVI and Red-edge NDVI results of the group 1 *A. karroo* samples. The soil Cr and Mn

samples between group 1 and group 3 *E. crispa* samples were different, although there were some outliers in Group 1 which were similar to Group 3 results. It should be noted that the ranges of Mn values in the group 3 *A. karroo* samples and group 1 *S. lancea* samples were very small compared to their respective remaining groups.

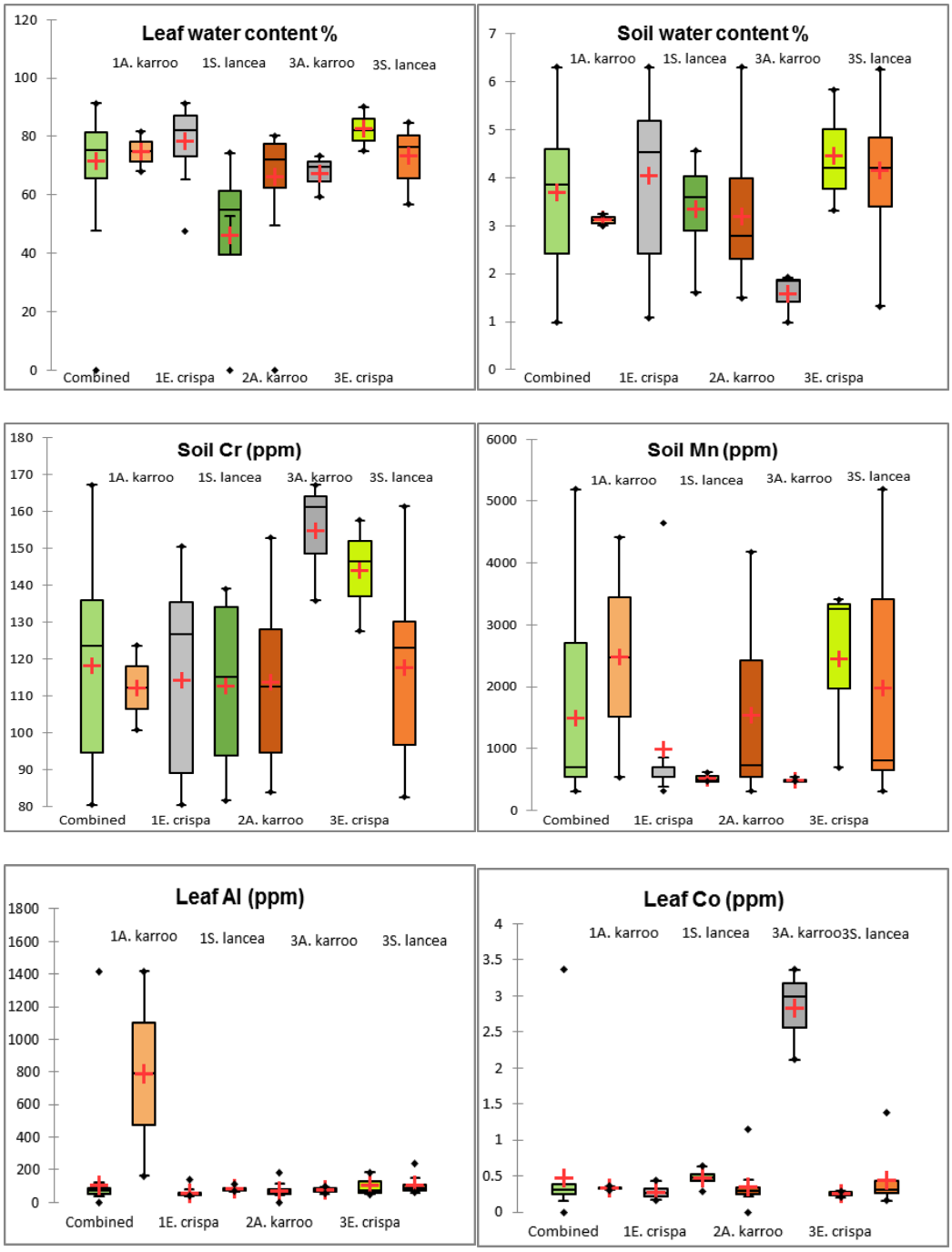

Figure 3-22 Box plots categorised by group and species, showing selected elements with marked differences between elemental content between groups for the three species (outliers shown by small black dots)

The group 3 *A. karroo* samples all occurred on the Black Reef, whereas the group 1 *S. lancea* samples and the group 3 *E. crispa* samples were distributed across the three geologies. As it was observed that there were not as many clear differences between groups for the *S. lancea* and *E. crispa* when categorising the descriptive stats by group and species, further analysis was done to differentiate between geology in addition to group and species.

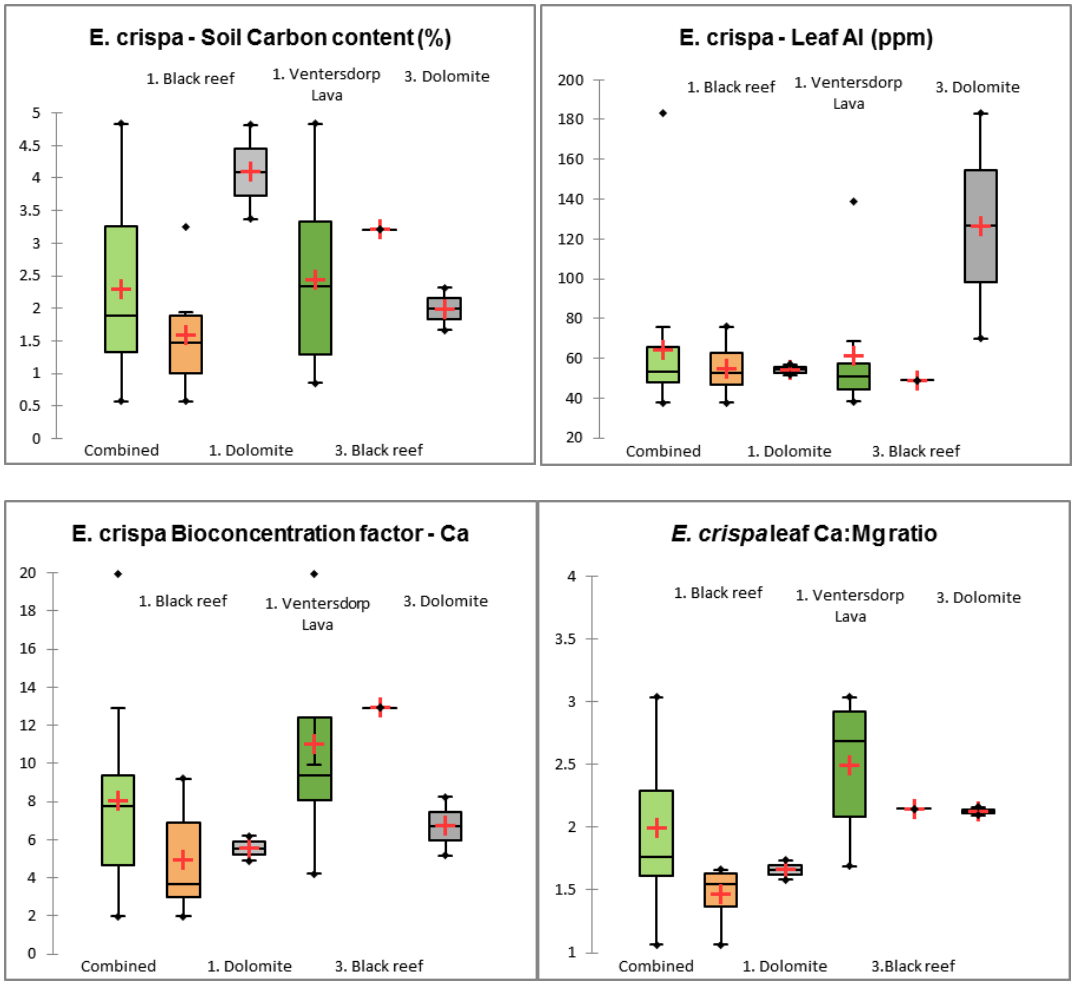

Figure 3-23 Box plots of the *E. crispa* samples categorised by group and geology. Full results of the descriptive statistics are shown in Appendix 5

Figure 3-23 shows the box plots categorised by group and geology for the *S. lancea* samples. There were differences noted between the group 1 and group 3 *E. crispa* samples, but these differences were more pronounced when the samples were further categorised by geology. There were no group 3 *E. crispa* samples on the Ventersdorp lavas. The group 1 *E. crispa* samples

on the Black Reef had lower soil carbon, and a lower Ca BCF and lower Ca:Mg leaf ratio than the group 3 *E. crispa* samples on the Black Reef. By contrast, the group 1 *E. crispa* samples on the dolomites had higher soil carbon content. Group 1 *E. crispa* samples on the dolomites show similar trends for the Ca BCF and Ca:Mg ratios to the Black Reef samples. The group 3 *E. crispa* samples had the highest concentrations of leaf Al compared to all other groups or subsamples.

The box plot results for the *S. lancea* samples are shown in Figure 3-24. The first two plots show the soil and leaf concentrations for Co. It is particularly interesting to note that the Group 1 samples on the Black Reef had the highest Co content in the soils, but the Group 3 samples on the Black Reef had the highest leaf Co content. The bioconcentration factor values for Group 3 were also higher than for group 1 on the Black Reef. While the ranges of the Co content of the leaves for the group 1 and group 3 samples on the Black Reef do overlap, this is still an indication of the differences in bioavailability of Co on certain parts of the Black Reef, as was observed with the *A. karroo* samples. Soil Fe content for the Group 3 Ventersdorp Lavas samples was higher than the Group 1 Ventersdorp lavas samples, whereas the reverse was seen for the Black Reef samples. Leaf S content was higher for the Group 1 Black Reef samples. This trend is also seen in other results such as the N:S ratios.

There were a limited number of samples in some of the groups, such as the *E. crispa* samples on the Black reef in Group 3, and the Group 1 *S. lancea* samples. Therefore this approach would benefit from more extensive sampling to validate the approach. However, even with limited samples, there are visible differences in the ranges of values obtained for specific elements for different groups for each species, which has the potential to describe the main controlling factors on spectral response of these three species.

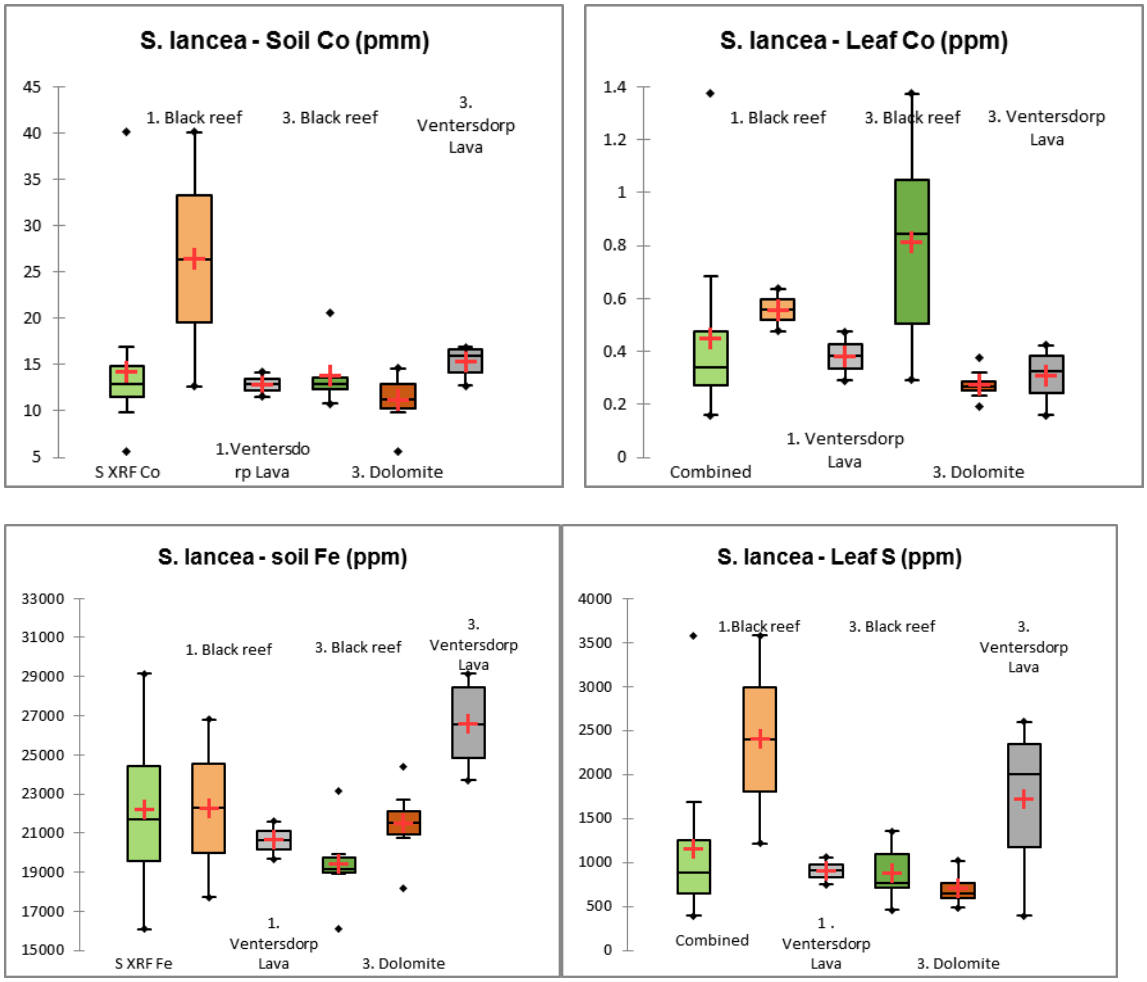

Figure 3-24 Box plots of the *S. lancea* samples categorised by group and geology. Full results of the descriptive statistics are shown in Appendix 6

3.6. Discussion

The results of the study showed that plant spectral reflectance is affected by differences in soil composition which are indicative of differing geologies. However, the relationship is neither simple nor straightforward. Bioavailability of elements in the soils, assessed through the BCF, varied between different sampling areas within the same geology, and even within the same landscape functional type. This variation in turn affected plant spectral reflectance, meaning that the change in spectral response could not be viewed as a graduated or linear change moving across geologies, but rather in clustered peaks or dips in spectral response. The spectral response between tree species was also significantly different, which further obscures spectral responses when grouping results by geology alone

3.6.1. Analysis of leaf and soil elemental concentrations and bioconcentration factors

To understand the relationship between plants and spectral reflectance, the chapter 2 characterised the landscape and soils across the study site and used these findings to define landscape function types (LFTs), and identified the changes in soil elemental content between the geologies and the LFTS. The findings showed that the total elemental content differed between geologies, but rarely differed between LFTs within the same geology.

This chapter investigated the changes in elemental content of the soils and leaves in more detail. Initially, the range of concentrations of the elements found in the leaves was compared to a global guideline of mean leaf elemental contents which was developed to guide studies on biogeochemical exploration [116]. Typically this guide would be used as a reference as to whether plants were in exceedance of the normal range for specific elements in order to identify good indicator plants for use in phytogeochemical exploration. While there is value in doing that, this study also wanted to understand where there may be very high or low concentrations that

may influence plant spectral responses. It has been established that saline or acidic conditions associated with ARD in the study region inhibit nutrient cycling, in particular the mineralisation of nitrogen and phosphorus [163]. A linear decline in tree seed production, mass and viability has been observed for phreatophyte and riparian tree species situated on or near ARD, and these changes could be expected to affect spectral response [67].

The results shown in Figure 3-2 found that Au, U, Ag, Cd, Sn, Cr, Ni and Na content in the leaves of all the samples analysed were in exceedance of the global mean sample data, often by a full order of magnitude. Si content was found to be an order of magnitude lower than the global mean average. As, Co, Pb, Al and Mn had fairly broad ranges which overlap with the global mean values, but had ranges that exceeded an order of magnitude over the global mean. While Co, Al, Mn, Ni, Na and Si are all known to be essential elements, they can be potentially toxic in high concentrations. Cd, Pb and As have no known nutritional benefits and can be detrimental to plant health even in low concentrations [117], [23]. The fact that these elements are present in relatively high concentrations in certain plants, or all samples in the case of Cd, indicates that there may be plant stress that may be detectable in the leaf spectral response. Cd regularly exists in soils as Cd^{2+}, which can easily be taken up by plants in place of other divalent cations such as Ca^{2+}, Zn^{2+}, or Fe^{2+}.[40]. Si content was lower than the global mean for all samples. Concentrations of Si were lower than 0.01% of the plant's dry mass. Agricultural nutrition guidelines classify plants with lower the 0.5% dry mass Si as excluders [164]. The role of Si as a beneficial nutrient has not been well defined in plants, but studies have shown that fertilisation with Si can help remediate signs of toxicity from other elements such as Mn [151], [165].

In chapter 2, it was noted that many of the soils were within acceptable ranges for plant tolerance. There were some exceptions, for example, the normal range for Zinc in soil is between 10ppm – 300ppm. Anything above this range can be expected to cause toxicity in plants. All soil

samples, except for sample no. MMAK67, which was growing in the ash-heap, were well below this level [166]. The range for all other samples was between 14.6ppm-100.8ppm, whereas MMAK67 was 1380ppm. This sample was removed from the analysis because the results were not reflective of the surrounding geology but were affected by anthropogenic contamination which was only detected during the sample analysis.

The soil elemental content, leaf elemental content and bioconcentration factors were analysed to investigate how uptake differed across the three geologies and their respective LFTs. To understand the relationships, the Kruskal-Wallis non-parametric tests with Dunn's post-hoc test with a Bonferroni correction was used to determine how the three sets of data grouped by geology and LFT. Then correlations between the Leaf and Soil elemental concentrations, leaf elemental content and BCF and Soil elemental content and BCF were used to further understand the relationships. The results, as shown in Table 3-3, did not pick up any direct significant correlations between the leaf and soil elemental content. There are many possible explanations for this result. The total soil elemental content, as analysed by XRF is not a good indicator of what is present in the soil solution [117], [120]. Sorption of the elemental content of the soils was also not specifically tested in this study [117]. In addition to this, the flora of this area may well have developed successful excluder (tolerance) mechanisms. Weiersbye et al. (2006) found that local ecotypes of the tree species used in mine rehabilitation on contaminated sites surround the study site were more tolerant than ecotypes harvested from non-metal enriched environments [65], [143]. The Si results support this hypothesis, as the soil Si content changed significantly between geologies, but the leaf elemental content and BCF showed no differences. There was a strong correlation between the leaf content and BCF, but a non-significant correlation between the soil content and BCF. This also supports the literature indicating that plants with lower than 0.5% Si in their leaf matter are excluders.

There were essentially three trends seen with the analysis of the leaf and soil elemental content and BCF. Some elements, such as Al, Si, Cu, Fe, Mg and V showed changes in soil elemental content which corresponded to the changes in geology, but these differences were not reflected in the leaf content or bioconcentration factor, and the BCF correlated to the leaf elemental content. In such cases, it is suggested that either the elements were not mobile, or were only partly mobile within the soil solution, or that the plants actively excluded them, or did not translocate these elements from roots to shoots or finally that there may have been competition for other ions which competed for uptake, as is common with Mg [117], [120], [164]. The second trend was where the BCF strongly reflected the changes in the elemental content of the soils as was seen with Ca, Cr, Pb and Ti. In the case of Ca, it is possible that competition with other ions inhibited uptake, or that the plant takes up an optimal amount to maintain an ionic balance. Cr, Pb and Ti may be excluded or only taken up in small amounts even when the concentrations in the soils are higher.

The third trend was seen as a balance between the changes in soil elemental content and leaf elemental content in the BCF. In these cases there was a significant correlation between both soil content and BCF and leaf content and BCF, but that the grouping of the BCF Dunn's Post test results reflected more of a combination of trends from the leaves and the soil elemental data, or that the elemental content alone did not describe the uptake well and the BCF showed differences in the uptake ratio where no differences were seen in the leaves or soils. This set of results, was seen for Co, Mn, Ba, K, Na, Ni, P and Zn. For P, what was observed, was a high soil content and high leaf content across one geology, and a low soil content and low leaf content on another geology, meaning there was no difference in the BCF between geologies. For Co, there were no differences between the soils contents on the Black Reef and Ventersdorp Lavas, even when comparing LFTs, but the leaf uptake was higher on the Black Reef outcrop (BR1). On the Black Reef and Ventersdorp Lavas, the BCF reflected the leaf uptake, but on the dolomites, where

there was a difference in soil elemental content between the chert-rich and chert-poor dolomites this was seen in the BCF as well. For Mn and Ni, there were no differences between the soils content between LFTs or for the leaf content between LFTs within the Black Reef, and for the Ventersdorp Lavas with the Mn results, but the BCF was different for the Black Reef outcrop which indicates a difference in the bioavailability of the elements between the LFTs. These differences between LFTs could be related to changes in SOC, Clay content, Redox potential and particle size of the soil materials[120], [167]. Other factors which affect tree growth such as rooting depth and soil water content may also affect the plant-soil interactions and resultant uptake of elements [117].

3.6.2. Analysis of leaf and soil elemental ratios

Elemental ratios are used broadly across geological, biological and ecological studies as rapid and easy to analyse indicators of processes [168]. Geological processes such as formation of soils and degrees of weathering can be determined through the use of elemental soil elemental and isotopic ratios [169], [170]. Soil elemental ratios have also been used to distinguish between natural soil enrichment and contamination of soils by certain elements [169]. Elemental ratios in soils and in leaves are used extensively in agriculture as proxy measures for plant performance and nutritional status. Many of the leaf ratios used in this study have been derived from agricultural practices [151], [164], [171]. Elemental ratios between root and shoot material in plants have also been used to determine the nutritional status of plants based on the understanding that plants withdraw much of their nutrients to their roots during periods of nutrient deprivation [172]. Root to shoot ratios were not assessed in this study however. This study assessed a number of soil and leaf elemental ratios to understand nutritional status of the plants at the study site and to test indicators of dust contamination and plant stress through toxicity caused by high concentrations on potentially toxic elements.

Elemental ratios such as the Si:Ti ratio and the Na:K ratios were useful indicators of potential weaknesses in the sample preparation. The Si:Ti ratio is used to identify whether there is dust contamination on the leaf surface. Often insufficient washing of samples can skew the elemental analysis through dust contamination. As Si and Ti will be taken up by the plant in different ratios relatively to their concentrations in the soils, comparing the soil and leaf ratios for Si and Ti gives an indication of whether there is dust contamination on the leave (Pers. Comm. I.M Weiersbye). The results for this study showed that the Si:Ti ratios for leaves and soils were significantly different, which confirms that if there was any dust present on the leaf samples, it was sufficiently well washed to remove the residue and not affect the analytical results. The Na:K ratio can be used to give an indication of whether plants started to degrade before analysis (Pers. Comm. I.M Weiersbye). This could happen if the freeze drying process was too slow or if samples were damaged in transport or prior to processing. There were no differences identified for the Na:K ratios between samples which indicates that there were no differences between the batches of samples that were processed.

Many of the elemental ratios used to assess plant nutritional status were based on indices used for agriculture, and therefore the ranges of fast growing leafy crops may not be the same as the ratios for hardy, slow growing trees which have adapted to their environment and are not managed and fertilised. Studies have already shown that the ranges of the N:P ratio can vary by up to fifty fold for a single species across different sites [150], [173]. While some suggested ranges are given, and these ranges were compared to the results obtained for the study, focus was placed on the relative values obtained and comparisons between geologies, rather than purely on absolute values. N:P is exactly such an example. The suggested ranges of the N:P ratio are between 10 and 20, and the literature suggests that any values lower than 10 may indicate a nitrogen deficiency [150], [173]. The maximum N:P ratio value that was obtained was 5.480, and the mean values for all three species were between two and four, which would suggest that

all the trees sampled were suffering nitrogen deficiencies. However, compared to the global mean data (Figure 3-2), the mean value observed for nitrogen in these samples was similar to the global mean data [116]. It is therefore suggested that it was rather the elevated P concentrations which are resulting in the lower N:P ratios found in these plant samples.

The *E. crispa* samples showed lower concentrations of many of the elements analysed when compared to the *A. karroo* and *S. lancea* samples. One of the exceptions was Mn. This was interesting to note. The soil elemental concentrations of Mn on the Black Reef and Ventersdorp Lavas were significantly lower than the Dolomites. There were no significant differences Mn content in the leaves between geologies. However, when looking at the bioconcentration factors, they were lowest on the Dolomites. The highest BCF for all samples were found on the VLR and BR1 LFTs. This indicates a possible change in the bioavailability of the Mn found on the Black Reef and rocky Ventersdorp Lavas, particularly as there was no elevated uptake associated with the high soil concentrations of Mn on the dolomites. The *E. crispa* that were found on the dolomites were small and much less vigorous than the trees growing on the Ventersdorp Lavas and Black Reef, and no *E. crispa* were found on the chert-rich dolomites. A similar trend has been noted in research in the Sterkfontein area [79]. This may indicate that the habitat preference may be a preference for exposed rocky areas and sheltered wooded areas [77], [78] is not just a physical preference, but that there may be specific mineral requirements for *E. crispa*, including the bioavailability of Mn.

Certain leaf elemental rations were used as indicators of potential ion competition for uptake, such as the Zn:Cd ratio and the Ca:Al. There were no differences observed between geologies for the Zn:Cd ratios for any of the three species (Table 3-14). The Kruskal Wallis test result for the E .crispa samples was slightly significant ($p= 0.048$), but once the Bonferroni correction on the Dunn's Post-test procedure was applied, there were no significant differences

observed. Cd levels for all the plant samples were elevated and Zn concentrations were slightly lower than the global average (Figure 3-2). Other studies have shown that the presence of bioavailable Zn can reduce the uptake and resultant toxicity of Cd [40]. Only the *A. karroo* samples showed differences between leaf elemental content for either Cd or Zn. The *A. karroo* leaf samples showed higher concentrations of both Zn and Cd on the Black Reef. Soils information on the Cd content is not available, but the Zn content of the soils was significantly higher on the Black Reef (Table 3-3). It is therefore possible that plants were also exposed to a degree of Cadmium-induced plant stress [40]. There was significantly higher Ca uptake for the *E. crispa* samples, but the other two species did not have any differences in Ca uptake. The difference in Ca uptake is reflected in the differences in Ca:Al and the Ca:Mg ratios in the leaves, where only the *E. crispa* samples showed differences. The Black Reef consistently had the lowest Ca concentrations and Ca* ratios. There were no differences in Al content in the leaves for any of the species. The differences in Al in soil were only detectable at a LFT level as there was quite a wide range in Al content for each geology. Studies have shown that for Ca, which also competes with Cd for uptake, high concentrations of Ca can reduce the uptake of Cd. In cases where there is low Ca availability in the soils, the Cd uptake to the roots is higher, but that uptake to shoots does not increase [124]. Essentially this indicates that while there may be competition of ions at the root-soil interface, there are additional mechanisms that may prevent translocation to the shoots [39], [44], [124].

3.6.3. Analysis of plant spectral response to changes in soil and leaf elemental contents

The aim of this chapter was to understand how the elemental concentrations of the soils and uptake to plant leaves affected spectral response. The results above have shown that there are differences to both the soil elemental content, and to a slightly lesser extent, the leaf elemental

content which correlate with geology. The next step was to identify which elements were responsible to the changes in leaf spectral response. The results of the initial spectral analysis in Chapter 2 showed that there were significant differences in the leaf spectral reflectance between geologies. However, there were also differences in the vegetation indices (VIs) between the three species. In some cases, the change in VI results to geology was opposite for two species, such as the *E. crispa* samples showing a red shift in the Red-edge inflection point and the *S. lancea* samples showing a blue shift over the Black Reef. It is not clear whether the red shift on the Black Reef for the *E. crispa* samples is a product of healthier plants, or the presence of other pigments which may be causing a shift towards the red wavelengths, as has been observed in *Amaranthus tricolor* [69]. However, due to the size and vigour of the *E. crispa* growing on the Black Reef compared to those growing on the Dolomites, it is likely that the Dolomites do not provide a hospitable habitat for *E. crispa* trees.

There have been a number of studies which have shown strong correlations between elemental content in the growth media and the change in spectral response [30], [111], [90], [174]. Many of these studies have been performed on pot trials in controlled environments. Rathod et al (2015) showed that plant spectral reflectance changed in response to spiking the soils with As, Cd and Pb. The individual trials for each element showed a measurable change in response, and the trails which combined all three elements showed the strongest response. The ratio of the 725/702nm 1st derivative spectrum showed a significant change in response to the metal treatments. Another interesting finding of this study is that while As was translocated to the shoots, there was very little translocation of Cd or Pb from the soil to the leaves, but there was still a detectable change in the spectral response [111]. Smith et al. (2004) found that the use of the 702/725 ratio of the 2nd derivative was successful in detecting where plants were growing in the vicinity of leaks from gas pipelines, and Mutanga & Skidmore (2007) used the 1st derivative of the Red-edge to identify nitrogen deficiencies in pasture grasses [114], [104].

These studies all look at a limited number of variables or stressors, whereas this study still needed to determine what the actual elements that caused a change in spectral response would be, particularly considering that the plants may have adapted to their environment and the potentially harmful concentrations of elements such as Pb, Cd, As and U [13], [25], [26]. There are many factors, or a combination of factors which could control for the plant spectral response across geologies, such as the soil geochemistry, the bioavailability plant uptake and resulting toxicity, poor nutritional status of the soils, and the soil biophysical parameters. To identify which of these had the most influence over spectral response, a subset of soil and plant characteristics and elemental concentrations was selected for each VI using the variables characterisation tool in XLStat, which used a Spearman's correlation co-efficient ($p< 0.01$) to select the variables which corresponded most strongly to the dependant variable, the vegetation index. This process was repeated for each vegetation index, per species, as it was previously established that the spectral analysis should be performed at a species level.

The results for the variables helped to reduce the number of variables to those that showed a relationship to the vegetation index under investigation. The analysis was not performed using geology as a grouping variable, but by directly correlating the soil or leaf characteristics to the VI. One of the observations was that there were very few of the soils elemental concentrations that were selected. This reiterates the importance of understanding the bioavailability of the elements, and presence of elements in the soil solution, rather than only looking at total elemental concentrations, as well as factors such as sorption of elemental to SOM [40], [117], [120]. Leaf elemental concentration and BCF variables were most frequently selected, and the soil and leaf elemental ratios had a number of significant results. Elements which are taken up and transported to the leaves are more likely to cause damage to the photosynthetic apparatus, so the fact that leaf elemental concentration correlated more strongly with the VI results than the soil elemental concentrations makes sense [40]. Very few of the VIs correlated with the leaf

or soil water content or soil pH or other physical characteristics. It was noted however, that many of the elements that were identified as having significant correlations in the BCF were the same elements that described geology through the grouping analysis of the soils in Table 2-7. This does indicate a relationship between the soil elemental concentrations and resulting bioconcentration factors and the spectral response of the leaves.

The *E. crispa* results showed no significant correlations for the NDWI, PSRI and Red-edge inflection point. These three indices also showed no significant differences in the case of the NDWI (p= 0279) and PSRI (p=0.447), and a very weak significant difference for the Red-edge inflection point (p= 0.032) in the Kruskal-Wallis test for differences between geologies (Table 2-11). The *A. karroo* results for the 1st derivative 725/702 ratio did not find any significant correlations with the variables tested. This index did have a significant difference ($p < 0.0001$) between geologies. This raised a small concern that there may be additional elements or factors which affect the response of the *A. karroo* to geology that may have been overlooked. Regression analysis was used to model the relationships between the subsets of variables and the VIs. A summary of the results is included in Table 3-41.

Table 3-41 Summary of the regression analysis results for the Vegetation Indices and leaf and soil elemental content and biophysical characteristics

VI	R^2 value	Species	Elemental content		Bioconcentration factors	Soil:leaf ratios	Soil & plant characteristics
			Soils	Leaves			
725-702 Ratio of the 1st Derivative		*A. karroo*					
		E. crispa					
	0.184	*S. lancea*		Ba	Ti		
NDVI	**0.158**	*A. karroo*			Ti		
	0.537	*E. crispa*	Zr	Cu, Ni,	Mn, Ni, Zn	Si:Mn leaf:soil ratio	
		S. lancea					
NDWI	**0.063**	*A. karroo*		Si	Si	BCF Al: BCF Ca	
		E. crispa					
	0.427	*S. lancea*		Pb	Cu		
PSRI	**0.531**	*A. karroo*		Mn	Fe, Fe2		soil pH
		E. crispa					
	0.283	*S. lancea*		As			Leaf Water content %

Red-edge NDVI	**0.637**	*A. karroo*		Ti	Ti	Si:Ti leaf:soil ratio,	
	0.469	*E. crispa*	Rb	Mn	Mn, Na	Na:K leaf ratio, Mg:Mn leaf ratio, Si:Mn leaf:soil ratio	
	0.657	*S. lancea*		Ba, Sn	Cu		
Red-edge position	**0.610**	*A. karroo*	Sr			Si:Ti leaf:soil ratio	
	0.420	*E. crispa*	V		Mn, Ni	Si:Mn leaf:soil ratio	
	0.345	*S. lancea*		Ba, Zn			
Red-edge inflection point	**0.410**	*A. karroo*		As, Fe, U			
		E. crispa					
	0.612	*S. lancea*		As, Ba			

The regression analysis showed some good regression results, and others which were quite weak. Mostly there were between two to three variables that provided the best fit for the regression model. However, the vegetation indices are quite strongly focused around the leaf chlorophyll content and Red-edge characteristics. It was expected that there would be more consistency in the variables that related to the VIs, where as many of the variables only occurred for one VI for one species. Studies on the change in spectral reflectance with exposure to As, Cd and Pb showed similar relationships between multiple VIs including the NDVI, derivative ratios and the Red-edge position and Red-edge inflection point [111]. There were some elements which occurred multiple times, such as Ti, where the bioconcentration factors, leaf Ti content and Si:Ti leaf:soil ratios occurred more than once for *A. karroo*. Mn also seems to relate strongly to the *E. crispa* samples, and Ba was found to have a significant relationship with spectral response for the *S. lancea*. The results here are not sufficiently conclusive to determine that any specific combination of elements explains the variation in spectral response determined through vegetation indices. It might be possible to develop this further through factor analysis, or to use alternative spectral analytical procedures, such as the use of spectral endmembers for hyperspectral data.

The next stage of the analysis was to look at how combinations of VIs could be used together to identify trends that may closely correlate to the changes in geology. It was noted when

visualising the VI results that there also seemed to be some trends which were specific to particular species, such as the PSRI values for the A .karroo samples were all negative, but that they increased on the Black Reef. The lower the PSRI value, the healthier the plant [100]. Combining the VI results using the grouping analysis tool in ArcGIS produced an unexpected result, which was the clustering of the sample data into three groups which mostly described the samples by species. Where the clustering did not work for a species was where the plant showed an abnormal spectral response compared to the total population. For example, for the *A. karroo* samples, the majority of the samples fell into group 2, and a small subset fell into group 3. The samples that fell into group 3 were those which had significantly higher PSRI results, and lower Red-edge position. Similar trends were seen for the *E. crispa* samples and the *S. lancea* samples. These coincided with the Rocky Black Reef (BR1). To investigate this trend further, descriptive statistics and box plots were drawn up to visualise the trends in the soil and leaf elemental data by species and group number. As some of the species only had 1 sample in a particular group, there were not sufficient replicates to do further statistical analyses. However the box plots described some strong visible trends, such as with the Co content of the group 2 vs group 3 *A. karroo* samples.

Even with limited replicates, the fact that the group analyses corresponded with the marked differences in soil and leaf elemental concentrations is strong evidence that plants do respond to the changes in geology. For example, the soils Co concentration on the Black Reef and Ventersdorp lavas was significantly higher than that on the Black Reef ($p < 0.0001$), and the leaf elemental content was also found to be significantly higher on the Black Reef (Table 3-3).The group 3 *A. karroo* samples were found to have very high Co content in the leaves compared to all other samples. The range of the group 3 *A. karroo* samples was higher than even the outliers for all other groups. The group 3 samples were characterised by high PSRI values, low Red-edge and Red-edge Inflection point values. Overall the *A. karroo* samples had low PSRI and high Red-

edge inflection point values. When using the Kruskal Wallis test, designed to normalise non-parametric data, the outliers, both in terms of the spectral response and in terms of the leaf and soils elemental content were not detected as having significant differences. Co was not one of the elements that was selected through the variables characterisation, yet the results from the descriptive statistics by group and species show a strong relationship to spectral response for *A. karroo*. The group 3 *A. karroo* samples were also found to have a high soil Cr content, low soil Mn concentrations and low soil water content. The Group 3 *E. crispa* samples also had a high soil Cr content when compared to the other samples. The Group 1 *A. karroo* samples had higher Al content compared to all other groups and species, and the Group 1 *S. lancea* samples on the Black Reef had high S content, and overall lower leaf water content and soil Mn content compared to other samples.

While further sampling would be required to investigate these findings and draw full conclusions as to the changes in leaf and soils elemental contents that affect plant spectral response, these preliminary findings show that there does appear to be a relationship with soil and leaf elemental content that affects leaf spectral reflectance, which can be detected through the use of vegetation indices. There have been several studies which have demonstrated this relationship in controlled laboratory studies [30], [111], [175], [90], and a number of studies which have identified metal contamination in relatively homogenous environments in the northern hemisphere [104], [176], [177]. There have been many studies which have investigated species nutrient deficiencies in pot-trials, grasslands and agricultural fields, but these lack the heterogeneity of a mixed savannah/wooded grassland found at the study site [178]. Another important finding is that it is not possible to ignore the differences in the spectral response of the different species. Cho et al (2012) succeeded in delineating tree species in an African savannah using airborne imagery [76]. This study came close to delineating tree species through the use of the eight vegetation indices, but identified that the changes in geology cause such a

significant shift in the spectral response of the leaves that it resulted in an incorrect species classification. While this opens up many opportunities for further understanding of the response of vegetation to changes in geology, it also presents a challenge in terms of scaling this technique up to airborne or satellite imagery.

3.7. Conclusion

This chapter investigated the changes in elemental content in the leaves and plant uptake of minerals from the soils across the three different geologies, and further investigated how leaf spectral reflectance is affected by these changes in the soil composition. To achieve this objective, the study followed a process of first identifying how soil elemental content, leaf element content and the uptake of these elements changed across the three geologies and six landscape functional types. The study then investigated how the elemental uptake differed between the three plant species being studied. Soil and leaf elemental ratios were used to further understand how the nutritional status of the plants differed. Further analysis of the spectral indices was done to identify, at a species level, which elements affected plant spectral response most strongly. The final part of this chapter explored the differences in spectral response between the three species, and how this was consistent except for the most extreme plant responses. These outlier responses were found to be associated with either elevated or very low concentrations of selected elements in the leaves or soils. These relationships need to be investigated further.

These outlier spectral response groupings for the combined indices were associated with elevated concentrations of different elements to those that were correlated with the total sample set for the individual vegetation indices for a given species. The reason for this could be that within a “normal” range of soil conditions, the spectral response does relate to the variables identified through the regression analysis, but that when samples are growing in conditions that are not within the normal range, the spectral response pattern and VI results are affected. The residuals for the regression analyses were often higher for the highest and lowest results in the model which could further substantiate this hypothesis. There were trends in the leaf and soils

analysis which linked the elemental results which had relationships for both types of spectral analysis to the geology.

The findings of this chapter suggest that plant spectral response to soil composition as a result of parent geology could be used for the purposes of discriminating between different geologies, however, due to the fact that the type and nature of the spectral response is complex and species dependent, further work will need to be performed in order to develop a methodology for the identification of geological features from the spectral response of selected tree species. This would need to be applicable to technologies such as airborne hyperspectral sensing, or ideally multispectral sensing from satellites as the primary objective is to be able to detect changes in geology without having to perform extensive ground sampling in order to verify results.

4. CONCLUSION

The cost of soil sampling for geological exploration is very high, and can be dangerous and logistically challenging. Exploration activities also have an impact on the environment, and can impact surrounding communities. One of the drivers of this study was the need to develop a tool that could be used for non-invasive preliminary mineral exploration in conjunction with traditional geophysics and geological remote sensing techniques to refine targets for further exploration activities in order to reduce the footprint of sampling that is required on the ground. A tool such as this would also have value in identifying habitats which contain metallophyte flora which are priority areas for conservation due to the high levels of endemism and specialisation of the species that have adapted to those environments. This would be highly valuable in mapping potentially contaminated areas from anthropogenic activities for monitoring purposes. This study has reported a number of findings which will assist in the development of such a tool.

The aim of this study was to determine whether it is possible to infer substrate geochemistry through the use of vegetation indices, by assessing the relationship between the relative concentrations of metals in the leaves and substrate with the leaf spectral properties. The central hypothesis in this study is that substrate geochemistry, in terms of the relative concentrations of heavy metals, results in structural and biochemical changes to plant leaves that are detectable from canopy or leaf reflectance signatures.

To test this hypothesis and address the aim of the research, there were two broad objectives that were met. Firstly, it was necessary to characterise the study site to understand and account for any environmental variables that may influence the spectral response and conflict or obscure the change in spectral response related to the changes in substrate geochemistry. Broadly, the study site was characterised by vegetation structure, landscape form and function and soils

characteristics. The differences in spectral response to contrasting geologies was compared to the landscape functional types which characterised the landscape form and function. The findings indicated that there were changes to spectral response that corresponded to geology, but that as the landscape is a product of the underlying geologies, there were features in the landscape which also influences spectral response and that these could not be ignored.

Secondly, it was necessary to determine how the levels of foliar stress differed between plants growing on metal-rich soils at the study site compared with conspecifics or congenerics on adjacent non-metal-enriched soils, and whether the leaf spectral responses could be related to either foliar or substrate, metal concentrations and plant nutritional status. To do this, firstly the substrate and foliar elemental concentrations were analysed, and then the relationships between these concentrations and the leaf spectral reflectance of the selected sample trees was modelled. The findings showed that there are correlations with spectral response to substrate geochemistry in terms of total elemental concentrations and to the changes in the bioavailability of selected elements, determined through uptake ratios.

Overall, the key findings of this study were that:

- There were differences in the soil characteristics such as SOC, soil rooting depth, soil water content and clay content which were identifiable between landscape functional types. These changes in soil characteristics could be a product of the underlying geology, but correlated more strongly to landscape function types than geologies. There were no differences between characteristics such as pH which were expected as a result of the changes in the parent materials of the different soils.
- The soil elemental content was significantly different between geologies, and it was possible to accurately classify the soils into their respective geologies based on the concentrations of Mn, Cr, Ti, Cu Cr, Pb, Ba, Fe, and Zr.

- There were significant differences in the bioavailability of certain elements which affected the uptake and leaf elemental concentrations, despite there being no differences in total elemental concentrations in the soils. These differences in bioavailability were often seen between LFTs within the same geologies, and could be a result of mineralisation and chemical speciation combined with/linked to changes to SOC, Clay content, pH and redox potential.
- There were significant differences between the three species that were analysed in terms of leaf elemental concentrations, bioconcentration factors and uptake ratios, and in the spectral response patterns.
- There were significant differences in the vegetation indices between the three geologies. The three species responded differently to the changes in the geologies and when combining the three species' data, the change in response across geologies was muted. When combining the data there were still detectable significant differences, but where there had been significant differences between all three geologies for the individual species, usually only one geology would be different from the other two when all species were combined. For example, the PSRI values were significantly higher on the Black Reef, compared to the Dolomites and Ventersdorp Lavas, and the Red-edge position was significantly lower on the Dolomites compared to the Black Reef and Ventersdorp lavas.
- When analysing the individual species and correlating their VI results to the soils and leaf elemental data, the *A. karroo* samples were found to have the strongest relationships with Mn and Ti Leaf content and Fe and Ti BCF, the Si:Ti leaf:Soil ratio and Sr content in the soils, the *S. lancea* samples were found to have the strongest relationships with the As, Pb and Sn in the leaves and the Cu BCF. *E. crispa* showed

the strongest relationships with Zr and Rb in the soils, Cu and Ni in the leaves, Mn, Na, Ni and Zn BCF and the Si:Mn leaf:soil ratio.

- The grouping analysis tool was used to test whether combinations of VIs could be used to differentiate between geologies. The findings showed that when clustering the combination of results for all 8 VIs, the resultant group followed species more closely than geology. The samples that did not cluster into the correct group for their species were found to have a combination of either or lower VI results than were typical for that species. It was found that this altered spectral response can be associated with either higher or lower elemental concentrations in the leaves or soils than the remaining samples for that species. These elevated concentrations corresponded with changes in geology.

From these findings, it is possible to conclude that the foliar and substrate elemental concentrations do influence the spectral response of the leaves of the plants selected for analysis. Further to this conclusion, the findings showed that the spectral response to changes in geologies differs between species, and that the typical spectral response for a given species may also be affected by changes in the substrate geochemistry to the extent that it no longer fits the classification criteria for that species. This finding provides a possible reason for the challenges that many previous researchers have encountered when attempting to apply remote sensing techniques for phytogeochemical exploration in the field, particularly when using airborne or satellite imagery with limited ground control data [30].

4.1. Recommendations for further research

This study covered a wide range of analyses in order to characterise the variables that may contribute to changes in spectral response across the study site. Based on the finding and the identified gaps in the data following on from the analyses of the data there are four main topics for further research that are recommended.

Further analysis of the leaf pigments and oxidative indices would assist in understanding the spectral response. This may also assist in understanding some of the metabolic processes which are ongoing in the plant samples. For example, there is evidence for heavy metals replacing the central Mg ion in the chlorophyll molecule in plants. When this occurs in shady conditions, the plant may remain green and the chlorophyll molecule is no longer functioning, but does not degrade. There could be an implication for spectral response were this to occur. In some cases, the plant response did not follow an expected pattern, such as where the *E. crispa* samples showed a red shift on the Black Reef. It would be valuable to relate these unexpected responses to pigment concentrations and oxidative indices to better validate whether this is a genuine "healthy" shift in the spectral response, or an altered stress response.

The BCF and selected soil and leaf elemental ratios were used as proxy indicators for bioavailability and changes in soil geochemistry between samples. It would be more valuable to use a sequential leaching procedure to better understand the bioavailability of the elements, and the concentrations likely to be found in the soil solution, rather than only using the total elemental content as measured by XRF and deriving proxies for bioavailability. There is an opportunity for comparing the actual bioavailable fraction of the elements to the leaf elemental content and spectral response. Similarly, additional information on the elemental content of the roots and woody biomass as compared to the leaves may give additional information about the

plant status and further explain stress responses identified through the spectral data, and potentially through the chlorophyll content and oxidative indices discussed above.

The finding on the relationship between the grouping analysis results for the VIs and the soil and plant elemental concentrations shows the strongest potential correlations between spectral response and changes in geology. Additional sampling to acquire sufficient replicates to test these findings and draw a more complete conclusion would be desirable.

Finally, the overarching aim of this research is to develop a tool which would enable non-invasive remote investigation of the changes in geology and substrate geochemistry, with limited ground-based sampling. This would imply that the spectral analyses should be using airborne or satellite derived imagery. Based on the findings above, accurate analysis of this data could present a challenge without the prior classifications of the species. However, the use of vegetation indices is a superficial analysis of the spectral data and there are more sophisticated remote sensing techniques that could be applied in order to quantify the variations in species, in order to first classify the species, and then analyse for changes within species to identify the changes in the substrate.

5. REFERENCES

[1] L. Maltby, A. Paetzold, and P. Warren, "Sustaining industrial activity and ecological quality: The potential role of an ecosystem serivces approach," in *Ecology of Industrial Pollution*, L. C. Batty and K. B. Hallberg, Eds. Cambridge: Cambridge University Press, 2010, pp. 327–343.

[2] G. Hilson, "Sustainable development policies in Canadas mining sector : An overview of government and industry efforts Sustainable development policies in Canada ' s mining sector : an overview of government and industry efforts," *Environ. Sci. Policy*, vol. 3, pp. 201–211, 2000.

[3] M. W. Sutton and I. M. Weiersbye, "South African Legislation Pertinent to Gold Mine Closure and Residual Risk," in *Mine Closure 2007*, A. Fourie, M. Tibbett, and J. Wiertz, Eds. Perth: Austalian Centre for Geomechanics, 2007, pp. 89–102.

[4] N. Reid, "Phyto-exploration in arid subtropical , arid mediterranean and tropical savanna environments : Biogeochemical mechanisms and implications for mineral exploration," University of Adelaide, 2008.

[5] N. Garrett, H. Mitchell, M. Lintzer, and S. Gilbert, "Promoting Legal Mineral Trade in Africa'S Great Lakes Region Resource Consulting Services Promoting Legal Mineral Trade in Africa'S Great Lakes Region," no. May, 2010.

[6] H. Fonseca, "Social and Environmental Impacts," Montevideo, 2004.

[7] N. Wielaard and M. Vissers, "Mining , forest change and conflict in the Kivus , eastern Democratic Republic of Congo Mining , forest change and conflict in the Kivus , eastern Democratic Republic of Congo," The Hague, The Netherlands, 2008.

[8] J. Botha, "Sustainable Development in Concession 40: A literature Review, Uncorrected Draft,. Ashanti Goldfields Kilo –Environmental Audit & Strategic Environmental Assessment, October 2011," Johannesburg, 2011.

[9] I. M. Weiersbye, "Environmental audit, GIS and strategic environmental assessment of Concession 40 in Ituri District, Province of Orientale, Democratic Republic of Congo," Johannesburg, 2011.

[10] C. E. Dunn, *Biogeochemistry in Mineral Exploration*, vol. 9. Oxford: Elsevier Ltd, 2007.

[11] B. B. M. Nkoane, G. M. Sawula, G. Wibetoe, and W. Lund, "Identification of Cu and Ni indicator plants from mineralised locations in Botswana," *J. Geochemical Explor.*, vol. 86, no. 3, pp. 130–142, Aug. 2005.

[12] R. R. Brooks, J. Lee, R. D. Reeves, and T. Jaffre, "Detection of nickeliferous rocks by analysis of herbarium specimens of indicator plants," *J. Geochemical Explor.*, vol. 7, pp. 49–57, 1977.

[13] B. Leteinturier, A. J. M. Baker, and F. Malaisse, "Early stages of natural revegetation of metalliferous mine workings in South Central Africa : a preliminary survey," vol. 3, no. 1, pp. 28–41, 1999.

[14] B. G. Lottermoser, P. M. Ashley, and N. C. Munksgaard, "Biogeochemistry of Pb–Zn gossans, northwest Queensland, Australia: Implications for mineral exploration and mine site rehabilitation," *Appl. Geochemistry*, vol. 23, no. 4, pp. 723–742, Apr. 2008.

[15] N. Reid and S. M. Hill, "Biogeochemical sampling for mineral exploration in arid terrains: Tanami Gold Province, Australia," *J. Geochemical Explor.*, vol. 104, no. 3, pp. 105–117, Mar. 2010.

[16] B. I. A. McInnes, C. E. Dunn, E. M. Cameron, and L. Kameko, "Biogeochemical exploration for gold in tropical rain forest regions of Papua New Guinea," *J. Geochemical Explor.*, vol. 57, no. 1–3, pp. 227–243, 1996.

[17] N. Reid, S. M. Hill, and D. M. Lewis, "Tanami geobotany and biogeochemistry: Towards its characterisation, role in regolith evolution and implications for mineral exploration," in *Regolith 2005- Ten Years of CRC LEME*,

2005, pp. 256–259.

[18] T. V. V King, M. R. Johnson, B. E. Hubbard, B. J. Drenth, and B. H. and B. D. King, T., M. Johnson, "Identification of Mineral Resources in Afghanistan--Detecting and Mapping Resource Anomalies in Prioritized Areas Using Geophysical and Remote Sensing (ASTER and HyMap) Data," *U.S. Geol. Surv. Open-File Rep.*, no. 7, p. 327, 2011.

[19] A. F. H. Goetz and B. N. Rock, "Remote Sensing for Exploration: An Overview," *Econ. Geol.*, vol. 78, no. 4, pp. 573–590, 1983.

[20] P. Madejon, T. Maranon, J. M. Murillo, and B. Robinson, "White poplar (Populus alba) as a biomonitor of trace elements in contaminated riparian forests," *Environ. Pollut.*, vol. 132, pp. 145–155, 2004.

[21] B. H. Robinson, G. Banuelos, H. M. Conesa, M. W. H. Evangelou, and R. Schulin, "The Phytomanagement of trace Elements in Soil," *Crit. Rev. Plant Sci.*, vol. 28, pp. 240–266, 2009.

[22] J. J. Ł. Brummer and G. D. Woodward, "A history of the ' Zambian copper flower ', Becium centraliafricanum (B . homblei)," *J. Geochemical Explor.*, vol. 65, no. 1999, pp. 133–140, 1999.

[23] R. S. Boyd, M. A. Davis, and K. Balkwill, "Elemental patterns in Ni hyperaccumulating and non-hyperaccumulating ultramafic soil populations of Senecio coronatus," *South African J. Bot.*, vol. 74, no. 1, pp. 158–162, Jan. 2008.

[24] S. N. Whiting, R. D. Reeves, D. Richards, M. S. Johnson, J. A. Cooke, F. Malaisse, R. Johns, T. Mcintyre, O. W. Purvis, D. E. Salt, H. Schat, F. J. Zhao, and A. J. M. Baker, "Research Priorities for Conservation of Metallophyte Biodiversity and their Potential for Restoration and Site Remediation," *Restor. Ecol.*, vol. 12, no. 1, pp. 106–116, 2004.

[25] A. J. M. Baker, W. H. O. Ernst, A. van der Ent, F. Malaisse, and R. Ginocchio, "Metallophytes : the unique biological resource , its ecology and conservational status in Europe , Central Africa and Latin America," in *Ecology of Industrial Pollution*, 1st ed., L. C. Batty and K. B. Hallberg, Eds. Cambridge: Cambridge University Press, 2010, pp. 7–40.

[26] F. Malaisse, A. J. M. Baker, and S. Ruelle, "Diversity of plant communities and leaf heavy metal content at Luiswishi copper/cobalt mineralization, Upper Katanga, Dem. Rep. Congo," *Biotechnol. Agron. Soc. Environ.*, vol. 3, no. 2, pp. 104–114, 1999.

[27] F. Malaisse, R. R. Brooks, and A. J. M. Baker, "Diversity of vegetation communities in relation to soil heavy metal content at the Shinkolobwe copper / cobalt / uranium Mineralization, Upper Shiba, Zaire," *Belgian J. Bot.*, vol. 127, no. 1, pp. 3–16, 1994.

[28] S. L. Ustin, M. O. Smith, S. Jacquemoud, M. Verstraete, and Y. Govaerts, "Geobotany: Vegetation Mapping for Earth Sciences," in *Remote Sensing for the Earth Sciences*, 3rd ed., R. A. Ryerson and A. N. (Geological S. of C. Rencz, Eds. New York: John Wiley & Sons, Inc., 1999, pp. 189–249.

[29] J. H. Schellekens, F. Gilbes, R. D. Garymar, Y. C. Ysa, S. Chardon, and Y. Fong, "Reflectance of Veg in response to copper deposits in Puerto Rico.pdf," *Caribb. J. Earth Sci. Trans. 16th Caribb. Geol. Conf. Barb.*, vol. 39, pp. 9–12, 2005.

[30] J. H. Schellekens, F. Gilbes-Santaella, A. Rodriguez-Roman, and Y. Roma-Colon, "Developing a protocol to use remote sensing as a cost effective tool to monitor contamination of mangrove wetlands," 2006.

[31] B. H. Robinson, R. R. Brooks, J. H. Kirkman, P. E. H. Gregg, and P. Gremigni, "Plant-available elements in soils and their influence on the vegetation over ultramafic ('serpentine') rocks in New Zealand," *J. R. Soc. New Zeal.*, vol. 26, no. 4, pp. 457–468, 1996.

[32] R. R. Brooks, "Biogeochemical parameters and their significance for mineral exploration," *J. Appl. Ecol.*, vol. 10, no. 3, pp. 825–836, 1973.

[33] J. H. Schellekens, F. Gilbes, R. D. Garymar, Y. C. Ysa, S. Chardon, and Y. Fong, "schellekens_etal_05 Reflectance

of Veg in response to copper deposits in Puerto Rico.pdf," *Caribb. J. Earth Sci. Trans. 16th Caribb. Geol. Conf. Barb.*, vol. 39, pp. 9–12, 2005.

[34] K. U. Brady, A. R. Kruckeberg, and H. D. J. Bradshaw, "Evolutionary Ecology of Plant Adaptation to Serpentine Soils," *Annu. Rev. Ecol. Evol. Syst.*, vol. 36, pp. 243–266, 2005.

[35] M. Akcay, A. Lermi, and A. Van, "Biogeochemical exploration for massive sulphide deposits in areas of dense vegetation : an orientation survey around the Kankoy Deposit (Trabzon , NE Turkey)," *J. Geochemical Explor.*, vol. 63, pp. 173–187, 1998.

[36] K. A. Hulme and S. M. Hill, "River Red Gums as a biogeochemical sampling medium in mineral exploration and environmental chemistry programs in the Curnamona Craton and adjacent regions of NSW and SA," in *Advances in Regolith*, 2003, pp. 205–210.

[37] N. Reid, S. M. Hill, D. M. Lewis, and L. Worrall, "Geobotanical and biogeochemical associations of Snappy Gum (Eucalyptus brevifolia): Tanami Region, W.A.," in *Regolith 2006 - Consolidation and Dispersion of Ideas*, 2006, pp. 288–290.

[38] A. L. Kovalevsky, "Chapter one: Fundamentals principles of biogeochemical exploration for mineral deposits," in *Biogeochemical Exploration for Mineral Deposits*, R. R. Brooks, Ed. Utrecht: VNU Science Press, 1987, pp. 8–23.

[39] M. M. Lasat, "Phytoextraction of metals from contaminated soil: A review of plant/soil/metal interaction and assessment of pertinent agronomic issues," *J. Hazard. Subst. Res.*, vol. 2, no. 5, pp. 1–25, 2000.

[40] S. Clemens, "Toxic metal accumulation, responses to exposure and mechanisms of tolerance in plants.," *Biochimie*, vol. 88, no. 11, pp. 1707–19, Nov. 2006.

[41] D. Peakall and J. Burger, "Methodologies for assessing exposure to metals : speciation, bioavailability of metals, and ecological host factors," *Ecotoxicol. Environ. Saf.*, vol. 56, pp. 110–121, 2003.

[42] A. J. M. Baker, "Accumulators and Excluders - Strategies in the response of plants to heavy metals," *J. Plant Nutr.*, vol. 3, no. 1–4, pp. 643–654, 1981.

[43] G. Serbin, C. S. T. Daughtry, R. E. Hunt, J. B. Reeves, and D. J. Brown, "Effects of soil composition and mineralogy on remote sensing of crop residue cover," *Remote Sens. Environ.*, vol. 113, no. 1, pp. 224–238, Jan. 2009.

[44] X. Yang, Y. Feng, Z. He, and P. J. Stoffella, "Molecular mechanisms of heavy metal hyperaccumulation and phytoremediation.," *J. Trace Elem. Med. Biol.*, vol. 18, no. 4, pp. 339–53, Jan. 2005.

[45] I. M. Weiersbye, C. J. Straker, and W. J. Przybylowicz, "Micro-PIXE mapping of elemental distribution in arbuscular mycorrhizal roots of the grass, Cynodon Dactylon, from gold and uranium mine tailings," *Nucl. Instruments Methods Phys. Res. Sect. B Beam Interact. with Mater. Atoms*, vol. 158, pp. 335–343, 1999.

[46] S. L. Ustin, D. A. R. A. Roberts, J. A. Gamon, P. Gregory, and R. O. Green, "Using Imaging Spectroscopy to Study Ecosystem Processes and Properties," vol. 54, no. 6, pp. 523–534, 2004.

[47] R. N. Clark, "Spectroscopy of Rocks and Minerals , and Principles of Spectroscopy," in *Manual of Remote Sensing, Volume 3, Remote Sensing for the Earth Sciences*, A. N. Rencz, Ed. New York, 1999, pp. 3–58.

[48] T. M. Lillesand and R. W. Kiefer, *Remote sensing and image interpretation*. New York: Wiley & Sons, 2000.

[49] O. W. Liew, P. C. J. Chong, B. Li, and A. K. Asundi, *Signature Optical Cues: Emerging Technologies for Monitoring Plant Health*, vol. 8, no. 5. 2008.

[50] N. Y. Kiang, J. Siefert, Govindjee, R. E. Blankenship, Govinjee, R. E. Blankenship, and V. S. Meadows, "Spectral Signatures of Photosynthesis. I. Review of Earth Organisms," *Astrobiology*, vol. 7, no. 1, pp. 222–251, 2007.

[51] C. Hui, "The Possibility of Assessing Heavy Metal Concentrations in reed along Le An River (China) using

Hyperspectral Data," Wuhan University, China, 2008.

[52] R. J. Boulding, "Remote Sensing and Surface Geophysical Methods," in *Subsurface Characterization And Monitoring Techniques A Desk Reference Guide: Solids And Ground Water Appendices A And B*, Environmental monitoring Systems Lab, 1996, pp. 1–82.

[53] P. J. Curran, "Remote sensing of foliar chemistry," *Remote Sens. Environ.*, vol. 30, no. 3, pp. 271–278, Dec. 1989.

[54] S. L. Ustin, A. a. Gitelson, S. Jacquemoud, M. Schaepman, G. P. Asner, J. a. Gamon, and P. J. Zarco-Tejada, "Retrieval of foliar information about plant pigment systems from high resolution spectroscopy," *Remote Sens. Environ.*, vol. 113, pp. S67–S77, Sep. 2009.

[55] W. H. Bakker, W. Feringa, A. S. M. Gieske, B. G. H. Gorte, K. A. Grabmaier, C. A. Hecker, J. A. Horn, N. Kerle, G. C. Huurneman, L. L. F. Janssen, F. D. van der Meer, G. N. Parodi, C. Pohl, C. V. Reeves, K. Tempfli, F. J. E. M. S. van Ruitenbeek, T. Woldai, M. J. C.Weir, and E. Westinga, *Principles of Remote Remote Sensing - An introductory text book*, Fourth Edi. Enschede: The international Institute for Geo-Information Science and Earth Observation, 2001.

[56] E. Frantz and S. Jefferys, "Automated Drones - A Giant Step in the Mining Value Chain," 2016.

[57] DigitalGlobe, "WorldView-3 DATASHEET." p. 2, 2014.

[58] M. Govender, P. J. Dye, I. M. Weiersbye, E. T. F. Witkowski, and F. Ahmed, "Review of commonly used remote sensing and ground-based technologies to measure plant water stress," *Water SA*, vol. 35, no. 5, pp. 741–752, 2009.

[59] F. Boochs, K. Dockter, G. Kupfer, and W. Kuhbauch, "Red-edge shift as vitality indicator for plants?," in *Proceedings of the 16th Congress of the International Society for Photogrammetry and Remote Sensing, held in Kyoto, Japan, on 1-10 July 1988*, 1988, pp. 742–749.

[60] P. J. Curran, J. L. Dungan, and H. L. Gholz, "Exploring the relationship between reflectance Red-edge and chlorophyll content in slash pine.," *Tree Physiol.*, vol. 7, no. 1_2_3_4, pp. 33–48, Dec. 1990.

[61] R. Main, M. A. Cho, R. Mathieu, M. M. O'Kennedy, A. Ramoelo, and S. Koch, "An investigation into robust spectral indices for leaf chlorophyll estimation," *ISPRS J. Photogramm. Remote Sens.*, vol. 66, no. 6, pp. 751–761, 2011.

[62] C. J. C. Tucker, "Red and photographic infrared linear combinations for monitoring vegetation," *Remote Sens. Environ.*, vol. 8, no. 2, pp. 127–150, 1979.

[63] J. W. Rouse, R. H. Haas, J. A. Schell, and D. W. Deering, "Monitoring the vernal advancement and retrogradation (green wave effect) of natural vegetation," Texasx, 1973.

[64] M. Govender, K. Chetty, V. Naiken, and H. Bulcock, "A comparison of satellite hyperspectral and multispectral remote sensing imagery for improved classification and mapping of vegetation," *Water SA*, vol. 34, no. 2, pp. 147–154, 2008.

[65] I. M. Weiersbye, N. Margalit, T. Feingersh, G. Revivo, R. Stark, Y. Zur, D. Heller, O. Braun, and E. Cukrowska, "Use of Airborne Hyper-spectral Remote Sensing (HSRS) to Focus Clean-up and Monitor Progress : Measurement of Contamination and Vegetation Processes Associated with Gold Mining in South Africa," in *Mine Closure 2006*, 2006, pp. 601–618.

[66] I. M. Weiersbye and E. T. F. Witkowski, "Acid Rock drainage (ARD) from gold tailings dams on the Witwatersrand Basin impacts on tree seeed fate, viability, inorganic content and morphology," in *Impacts of Acid Mine Drainage on the Environment , Proceedings of the 8 th International Mine Water Association (IMWA)*, 2003, pp. 311–330.

[67] I. M. Weiersbye and E. T. F. Witkowski, "Impacts of acid mine drainage on the revegetation potential of highveld phreatophytes," in *Multiple Use Management of Natural Forests and Woodlands : Policy*

Refinements and Scientific Progress IV . Department of Water Affairs and Forestry of South Africa, 2007, pp. 224–237.

[68] M. Govender, "Assessing Groundwater Access by Trees Growing above Contaminated Groundwater Plumes Originating from Gold Tailings Storage Facilities," University of the Witwatersrand, 2011.

[69] D. A. Sims and J. A. Gamon, "Relationships between leaf pigment content and spectral reflectance across a wide range of species, leaf structures and developmental stages," *Remote Sens. Environ.*, vol. 81, no. 2–3, pp. 337–354, Aug. 2002.

[70] M. A. Cho, A. Skidmore, F. Corsi, S. E. van Wieren, and I. Sobhan, "Estimation of green grass/herb biomass from airborne hyperspectral imagery using spectral indices and partial least squares regression," *Int. J. Appl. Earth Obs. Geoinf.*, vol. 9, no. 4, pp. 414–424, 2007.

[71] W. Collins and S. Chang, "Airborne Biogeophysical Mapping of Hidden Mineral Deposits," *Econ. Geol.*, vol. 78, pp. 737–749, 1983.

[72] L. Mucina, *The vegetation of South Africa, Lesotho and Swaziland*, Strelitzia. Pretoria: South African National Biodiversity Institute, 2006.

[73] N. Norman and G. Whitfield, *Geological Journeys*, First. Cape Town: Struik Publishers, 2006.

[74] S. Ngigi, "Chapter 3 : Baseline Description," 2009.

[75] T. S. Mccarthy and B. Rubidge, *The story of Earth and life: A southern African perspective on a 4.6 billion-year journey*. Cape Town: Struik Publishers, 2005.

[76] M. A. Cho, R. Mathieu, G. P. Asner, L. Naidoo, J. Van Aardt, A. Ramoelo, P. Debba, K. Wessels, R. Main, I. P. J. Smit, and B. Erasmus, "Mapping tree species composition in South African savannas using an integrated airborne spectral and LiDAR system," *Remote Sens. Environ.*, vol. 125, pp. 214–226, 2012.

[77] Tree Society of Southern Africa, *Trees and Shrubs of the Witwatersrand*, Third. Johannesburg: Witwatersrand University Press, 1974.

[78] V. Thomas and R. Grant, *Sappi Tree Spotting - Highveld and the Drakensberg*, 1st ed. Johannesburg: Jacana, 1998.

[79] F. Siebert and S. J. Siebert, "Dolomitic vegetation of the Sterkfontein Caves World Heritage Site and its importance in the conversation of Rocky Highveld Grassland," *Koedoe*, vol. 48, no. 1, pp. 17–31, 2005.

[80] B. Wallnöfer, "The Biology and Systematics of Ebenaceae : a Review," pp. 485–512, 2001.

[81] P. C. Mane, A. B. Bhosle, P. D. Deshmukh, and C. M. Jangam, "Chromium Adsorption onto Activated Carbon Derived from Tendu (Diospyros melanoxylon) Leaf Refuse : Influence of Metal/Carbon ratio , time and pH," *Adv. Appl. Sci. Res.*, vol. 1, no. 3, pp. 212–221, 2010.

[82] B. Deo, G. Nahak, and R. K. Sahu, "Studies on the uptake of heavy metals by selected plant species growing on coal mine spoils in sub-tropical regions of India," *J. Am. Sci.*, vol. 7, no. 1, pp. 26–34, 2011.

[83] G.-I. E. Ekosse, "Spatial distribution of Iron in soils and vegetation cover close to an abandoned Manganese Oxide Ore mine, Botswana," *J. Appl. Sci.*, vol. 8, no. 1, pp. 14–25, 2008.

[84] P. J. Dye, I. M. Weiersbye, and J. Xaba, "Annual water-use and elemental content of Rhus lancea (Karee) trees growing on acid mine drainage in South Africa," *Water SA*.

[85] I. M. Weiersbye, E. T. F. Witkowski, and M. Reichardt, "Floristic composition of gold and uranium tailings dams, and adjacent polluted areas, on South Africa's deep-level mines," *Bothalia*, vol. 36, no. 1, pp. 101–127, 2006.

[86] H. Marschner, "Functions of Mineral Nutrients," *Miner. Nutr. High. Plants*, pp. 313–404, 1995.

[87] F. Baret, S. Jacquemoud, G. Guyot, and C. Leprieur, “Modeled analysis of the biophysical nature of spectral shifts and comparison with information content of broad bands,” *Remote Sens. Environ.*, vol. 41, no. 2–3, pp. 133–142, Aug. 1992.

[88] M. H. Muller, D. Hardwick, and I. M. Weiersbye, “Using spatial distribution and leaf vegetation indices (VIs) of evergreen phreatophyte trees to identify potential sinkholes on dolomitic grasslands within the Witwatersrand Gold Fields - Manuscript,” 2012.

[89] L. Kooistra, R. S. E. W. Leuven, R. Wehrens, P. H. Nienhuis, and L. M. C. Buydens, “A comparison of methods to relate grass reflectance to soil metal contamination,” *Int. J. Remote Sens.*, vol. 24, no. 24, pp. 4995–5010, Jan. 2003.

[90] S.-H. Chang and W. Collins, “Confirmation of the Airborne Biogeophysical Mineral Exploration Technique Using Laboratory Methods,” *Econ. Geol.*, vol. 78, pp. 723–736, 1983.

[91] D. J. Tongway and N. L. Hindley, “Landscape Function Analysis: procedures for monitoring and assessing landscapes - with special reference to minesites and rangelands,” Canberra, 2004.

[92] D. J. Tongway and J. A. Ludwig, “Rehabilitation of Semiarid Landscapes in Productive Soil Patches,” *Restor. Ecol.*, vol. 4, no. 4, pp. 388–397, 1996.

[93] J. A. Ludwig, R. W. Eager, G. N. Bastin, V. H. Chewings, and C. Liedloff, “A leakiness index for assessing landscape function using remote sensing,” *Landsc. Ecol.*, vol. 17, pp. 157–171, 2002.

[94] D. Tongway and J. a Ludwig, “The conservation of water and nutrients within landscapes,” *Landsc. Ecol. Funct. Manag. Princ. from Aust. Rangelands*, pp. 13–22, 1997.

[95] D. J. Tongway and N. L. Hindley, “Canberra Nature Parks Review - DRAFT,” 2010.

[96] Wallis and Kruskal, “Use of ranks in one-criterion variance analysis,” *J. Am. Stat. Assoc.*, vol. 47, pp. 583–621, 1952.

[97] O. J. Dunn, “Multiple contrasts using rank sums,” *Technometrics*, vol. 5, pp. 241–252, 1964.

[98] C. E. Bonferroni, “Teoria statistica delle classi e calcolo delle probabilita,” *Pubbl. del R Ist. Super. di Sci. Econ. e Commer. di Firenze*, vol. 8, pp. 3–62, 1936.

[99] T. Caliński and J. Harabasz, “A dendrite method for cluster analysis,” *Commun. Stat.*, vol. 3, no. 1, pp. 1–27, Jan. 1974.

[100] M. N. Merzlyak, A. a Gitelson, O. B. Chivkunova, and V. Y. U. Rakitin, “Non-destructive optical detection of pigment changes during leaf senescence and fruit ripening,” *Physiol. Plant.*, vol. 106, no. 1, pp. 135–141, 1999.

[101] B. C. Gao, “NDWI-a normalized difference water index for remote sensing of vegetation liquid water from space,” *Remote Sens. Environ.*, vol. 58, pp. 257–266, 1996.

[102] A. Gitelson and M. N. Merzlyak, “Quantitative estimation of chlorophyll-a using reflectance spectra: experiments with autumn chestnut and maple leaves,” *J. Photochem. Photobiol. B Biol.*, vol. 22, no. 3, pp. 247–252, 1994.

[103] G. Guyot, F. Baret, and S. Jacquemoud, “Imaging Spectroscopy for vegetation studies,” in *Imaging Spectroscopy: Fundamentals and Prospective Applications1*, 1992, pp. 145–165.

[104] K. L. Smith, M. D. Steven, and J. J. Colls, “Use of hyperspectral derivative ratios in the Red-edge region to identify plant stress responses to gas leaks,” *Remote Sens. Environ.*, vol. 92, pp. 207–217, 2004.

[105] J. A. Ludwig, D. J. Tongway, G. N. Bastin, and C. D. James, “Monitoring ecological indicators of rangeland functional integrity and their relation to biodiversity at local to regional scales,” pp. 1–13, 2004.

[106] L. Parras-Alcántara, B. Lozano-García, and A. Galán-Espejo, “Soil organic carbon along an altitudinal gradient

in the Despeñaperros Natural Park , southern Spain," *Solid Eart*, vol. 6, pp. 125–134, 2015.

[107] V. Kadlec, O. Holubík, E. Procházková, J. Urbanova, and M. Tippl, "Soil Organic Carbon Dynamics and its Influence on the Soil Erodibility Factor," *Soil Water Res.*, no. 3, pp. 97–108, 2012.

[108] J. Gonzalez-Perez, F. J. Gonzalez-Vila, G. Almendros, and H. Knicker, "The effect of fire on soil organic matter — a review," *Environ. Int.*, vol. 30, pp. 855–870, 2004.

[109] H. Knicker, "How does fire affect the nature and stability of soil organic nitrogen and carbon ? A review," *Biogeochemistry*, vol. 85, no. July 2007, pp. 91–118, 2007.

[110] J. E. Herselman, C. E. Steyn, and M. V Fey, "Baseline concentration of Cd, Co, Cr, Cu, Pb, Ni and Zn in surface soils of South Africa," *S. Afr. J. Sci.*, vol. 101, no. November 2005, 1997.

[111] P. H. Rathod, C. Brackhage, F. D. Van Der Meer, I. Müller, M. F. Noomen, D. G. Rossiter, and G. E. Dudel, "Spectral changes in the leaves of barley plant due to phytoremediation of metals - results from a pot study," *Eur. J. Remote Sens.*, vol. 48, pp. 283–302, 2015.

[112] M. N. Merzlyak, A. E. Solovchenko, A. a Gitelson, A. E. Solo, and A. a Gitelson, "Reflectance spectral features and non-destructive estimation of chlorophyll, carotenoid and anthocyanin content in apple fruit," *Postharvest Biol. Technol.*, vol. 27, no. 2, pp. 197–211, Feb. 2003.

[113] J. P. Darch and J. Barber, "Multitemporal remote sensing of a geobotanical anomaly," *Econ. Geol.*, vol. 78, no. 4, pp. 770–782, Jul. 1983.

[114] O. Mutanga and A. K. Skidmore, "Red-edge shift and biochemical content in grass canopies," *ISPRS J. Photogramm. Remote Sens.*, vol. 62, no. 1, pp. 34–42, May 2007.

[115] J. H. Schellekens and F. Gilbes-Santaella, "Developing a protocol to use remote sensing as a cost effective tool to monitor: Final Report," Mayagüez, 2009.

[116] C. E. Dunn, "New Perspectives on Biogeochemical Exploration," *Proc. Explor. 07 Fifth Decenn. Int. Conf. Miner. Explor.*, no. November, pp. 249–261, 2007.

[117] P. S. Hooda, "Introduction," in *Trace Elements in Soils*, First., P. S. Hooda, Ed. London: Blackwell Publishing Ltd, 2010, pp. 1–9.

[118] J. L. Hall, "Cellular mechanisms for heavy metal detoxification and tolerance.," *J. Exp. Bot.*, vol. 53, no. 366, pp. 1–11, Jan. 2002.

[119] M. D. Piwoni and J. W. Keeley, "Basic concepts of contaminant sorption at hazardous waste sites," Ada, Oklahoma, 1990.

[120] F. M. G. Tack, "Trace Elements: General Soil Chemistry, Principles and Processes," in *Trace Elements in Soils*, First., P. S. Hooda, Ed. London: Blackwell Publishing Ltd, 2010, pp. 9–38.

[121] C. J. J. Straker, I. M. Weiersbye, and E. T. F. Witkowski, "Arbuscular mycorrhiza status of gold and uranium tailings and surrounding soils of South Africa's deep level gold mines: I. Root colonization and spore levels," *South African J. Bot.*, vol. 73, no. 2, pp. 218–225, Apr. 2007.

[122] R. O'Dell, W. Silk, P. Green, and V. Claassen, "Compost amendment of Cu-Zn minespoil reduces toxic bioavailable heavy metal concentrations and promotes establishment and biomass production of Bromus carinatus (Hook and Arn.).," *Environ. Pollut.*, vol. 148, no. 1, pp. 115–24, Jul. 2007.

[123] M. M. Lasat, A. J. M. Baker, and L. V. Kochian, "Physiological Characterization of Root Zn^{2+} Absorption and Translocation to Shoots in Zn Hyperaccumulator and Nonaccumulator Species of Thlaspi.," *Plant Physiol.*, vol. 112, no. 4, pp. 1715–1722, 1996.

[124] F. Eller and H. Brix, "Influence of low calcium availability on cadmium uptake and translocation in a fast-growing shrub and a metal-accumulating herb," *AoB Plants*, vol. 7, no. December 2015, p. plv143, 2015.

[125] M. M. Lasat, “Phytoextraction of toxic metals: a review of biological mechanisms.,” *J. Environ. Qual.*, vol. 31, no. 1, pp. 109–20, 2002.

[126] S. Clemens, M. G. Palmgren, and U. Krämer, “A long way ahead: Understanding and engineering plant metal accumulation,” *Trends Plant Sci.*, vol. 7, no. 7, pp. 309–315, 2002.

[127] R. D. Reeves, “Hyperaccumulation of trace elements by plants,” in *NATO Sciences Series IV: Phytoremediation of Metal-Contaminated Soils*, 1st ed., J.-L. Morel, G. Echevarria, and N. Goncharova, Eds. The Netherlands: Springer Netherlands, 2006, pp. 25–52.

[128] “Metal tolerance • by a. j. m. b a k e r,” vol. 106, pp. 93–111, 1987.

[129] C. Reimann, F. Koller, B. Frengstad, G. Kashulina, H. Niskavaara, and P. Englmaier, “Comparison of the element composition in several plant species and their substrate from a 1 500 000-km 2 area in Northern Europe,” *Sci. TO*, vol. 278, pp. 87–112, 2001.

[130] R. John, P. Ahmad, K. Gadgil, and S. Sharma, “Heavy metal toxicity: Effect on Plant growth, biochemical parameters and metal accumulation by Brassica juncea L.,” *Int. J. Plant Prod.*, vol. 3, no. 3, pp. 65–75, 2009.

[131] H. Kupper, F. Kiipper, and M. Spiller, “Environmental relevance of heavy metal- substituted chlorophylls using the example of water plants Environmental relevance of heavy metal-substituted chlorophylls using the example of water plants,” no. February, 1996.

[132] H. Küpper, A. Parameswaran, B. Leitenmaier, M. Trtílek, and I. Setlík, “Cadmium-induced inhibition of photosynthesis and long-term acclimation to cadmium stress in the hyperaccumulator Thlaspi caerulescens,” *New Phytol.*, vol. 175, no. 4, pp. 655–674, 2007.

[133] R. E. O’Dell, J. J. James, and J. H. Richards, “Congeneric serpentine and nonserpentine shrubs differ more in leaf Ca:Mg than in tolerance of low N, low P, or heavy metals,” *Plant Soil*, vol. 280, no. 1–2, pp. 49–64, 2006.

[134] I. M. Weiersbye, “Global Review and Cost Comparison of Conventional and Phyto-Technologies for Mine Closure,” in *Mine Closure 2007*, 2007, pp. 13–29.

[135] M. R. Perrow and A. J. Davy, *Handbook of ecological restoration. Volume 1 - Principles of restoration*. Cambridge: Cambridge University Press, 2002.

[136] R. Ginocchio and A. J. M. Baker, “Metallophytes in Latin America : a remarkable biological and genetic resource scarcely known and studied in the region,” *Rev. Chil. Hist. Nat.*, vol. 77, no. 1, pp. 185–194, 2004.

[137] P. Audet and C. Charest, “Heavy metal phytoremediation from a meta-analytical perspective,” *Environ. Pollut.*, vol. 147, no. 1, pp. 231–237, 2007.

[138] M. A. Cho and A. K. Skidmore, “A new technique for extracting the Red-edge position from hyperspectral data: The linear extrapolation method,” *Remote Sens. Environ.*, vol. 101, no. 2, pp. 181–193, Mar. 2006.

[139] G. A. Blackburn, “Hyperspectral remote sensing of plant pigments.,” *J. Exp. Bot.*, vol. 58, no. 4, pp. 855–67, Jan. 2007.

[140] M. A. Cho, “Hyperspectral remote sensing of biochemical and biophysical parameters: the derivate red- edge ‘double-peak feature’, a nuisance or an opportunity?,” Wageningen University, 2007.

[141] J. Féret, C. François, and K. M. Barry, “Optimizing spectral indices and chemometric analysis of leaf chemical properties using radiative transfer modeling,” 2011.

[142] J. R. Jensen, “Remote Sensing of the Environment,” p. 544, 2000.

[143] A. A. Meharg, “Integrated tolerance mechanisms: constitutive and adaptive plant responses to elevated metal concentrations in the environment,” *Plant. Cell Environ.*, vol. 17, no. 9, pp. 989–993, 1994.

[144] B. N. Rock, “Comparison of In Situ and Airborne Spectral Measurements of the Blue Shift Associated with

Forest Decline," vol. 127, pp. 109–127, 1988.

[145] Y. Takeuchi and Y. Amao, "Light-harvesting properties of zinc complex of chlorophyll-a from spirulina in surfactant micellar media," pp. 15–21, 2005.

[146] E. W. Chappelle, M. S. Kim, and J. E. McMurtrey III, "Ratio analysis of reflectance spectra (RARS): An algorithm for the remote estimation of the concentrations of chlorophyll A , chlorophyll B , and carotenoids in Soybean leaves," *Remote Sens. Environ.*, vol. 39, pp. 239–247, 1992.

[147] A. a Gitelson, Y. Gritz, and M. N. Merzlyak, "Relationships between leaf chlorophyll content and spectral reflectance and algorithms for non-destructive chlorophyll assessment in higher plant leaves.," *J. Plant Physiol.*, vol. 160, no. 3, pp. 271–82, Mar. 2003.

[148] I. M. Weiersbye, E. M. Cukrowksa, N. Margalit, M. Govender, R. Stark, T. Feingersh, G. Revivo, Y. Zur, and O. Braun, "A remote-sensing and analytical chemistry approach to the remediation of gold and uranium mine evaporation pans in a semi-arid region," 2006.

[149] E. Tipping, C. J. Somerville, and J. Luster, "The C:N:P:S stoichiometry of soil organic matter," *Biogeochemistry*, vol. 130, no. 1–2, pp. 117–131, 2016.

[150] W. Koerselman and F. M. Meuleman, "The vegetation N:P ratio: a new tool to detect the nature of nutrient limitation," *J. Appl. Ecol.*, vol. 33, pp. 1441–1450, 1996.

[151] J. Che, N. Yamaji, J. F. Shao, J. F. Ma, and R. F. Shen, "Silicon decreases both uptake and root-to-shoot translocation of manganese in rice," *J. Exp. Bot.*, vol. 67, no. 5, pp. 1535–1544, 2016.

[152] W. J. Horst and H. Marschner, "Effect of silicon on manganese tolerance of bean plants (Phaseolus Vulgaris L.)," *Plant Soil*, vol. 50, no. 2 (October 1978), pp. 287–303, 1978.

[153] R. Salminen, M. J. Batista, M. Bidovec, A. Demetriades, B. De Vivo, W. De Vos, M. Duris, A. Gilucis, V. Gregorauskiene, and J. Halavic, "Rubidium," in *FOREGS Geochemical Atlas of Europe: Part 2*, R. Salminen, Ed. 2005, pp. 299–304.

[154] Hill Laboratories, "Assessing Soil Quality: The Organic Soil Profile," 10151 V2.

[155] C. Miller, "Understanding the carbon-nitrogen ratio," *ACRES USA - A Voicce Eco-Agriculture*, vol. 30, no. 4, pp. 20–21, 2000.

[156] J. Le Bot, M. J. Goss, M. J. G. P. R. Carvalho, M. L. Van Beusichem, and E. A. Kirkby, "The significance of the magnesium to manganese ratio in plant tissues for growth and alleviation of manganese toxicity in tomato (Lycopersicon esculentum) and wheat (Triticum aestivum) plants," *Plant Soil*, vol. 124, no. 2, pp. 205–210, 1990.

[157] G. R. Rout, S. Samantaray, and P. Das, "Aluminium toxicity in plants: a review," *Agronomie*, vol. 21, no. 1, pp. 3–21, 2001.

[158] M. S. Aulakh and G. Dev, "Interaction effect of calcium and sulphur on the growth and nutrient composition of alfalfa (Medicago Sativa L. Pers.), using ^{35}S," *Plant Soil*, vol. 50, no. 1 (August 1978), pp. 125–134, 1978.

[159] T. P. D. Association, "November 2011 Balanced nutrition shown by nitrogen : sulphur ratios .," *Potash News*, no. November. The Potach Development Association, pp. 1–2, 2011.

[160] Winfield Agri Solutions, "Nitrogen to Sulfur Ratio," p. 2011, 2011.

[161] M. K. Heenkenda, K. E. Joyce, S. W. Maier, and R. Bartolo, "Mangrove species identification: Comparing WorldView-2 with aerial photographs," *Remote Sens.*, vol. 6, no. 7, pp. 6064–6088, 2014.

[162] A. Verlič, N. ĐuriĆ, Ž. Kokalj, A. Marsetič, P. SimonČiČ, and K. Oštir, "Tree species classification using WorldView-2 satellite images and laser scanning data in a natural urban forest," *Prethod. priopćenje – Prelim. Commun.*, vol. 9–10, no. January, pp. 477–488, 2014.

[163] I. M. Weiersbye and E. T. F. Witkowski, “Impacts of acid mine drainage on the revegetation potential of highveld phreatophytes,” in *Multiple Use Management of Natural Forests and Woodlands: Policy Refinements and Scientific Progress IV.*, S. J.J. Bester, A.H.W. Seydack, Vorster, T., Van der Merwe, I.J. and Dzivhani, Ed. Department of Water Affairs and Forestry of South Africa, 2007, pp. 224–237.

[164] IPNI, “Nutri-Facts,” Georgia, 2016.

[165] B. S. Tubana, T. Babu, and L. E. Datnoff, “A Review of Silicon in Soils and Plants and Its Role in US Agriculture,” *Soil Sci.*, vol. 181, no. 9, p. 1, 2016.

[166] J. A. Rosen, C. S. Pike, M. L. Golden, and J. Freedman, “Zinc toxicity in corn as a result of a geochemical anomaly,” *Plant Soil*, vol. 50, no. 1, pp. 151–159, 1978.

[167] S. M. Reichman, “The Responses of Plants to Metal Toxicity : A review focusing on Copper , Manganese and Zinc,” Melbourne, 14, 2002.

[168] P. Lopez, E. Navarro, R. Marce, J. Ordoñez, L. Caputo, J. Armengol, J. Ordo??ez, L. Caputo, J. Armengol, J. Ordoñez, L. Caputo, and J. Armengol, “Elemental ratios in sediments as indicators of ecological processes in Spanish reservoirs,” *Limnetica*, vol. 25, no. 1–2, pp. 499–512, 2006.

[169] A. White, M. Schulz, T. Bullen, J. Fitzpatrick, D. Vivit, and R. Evett, “Use of elemental and isotopic ratios to distinguish between lithogenic and biogenic sources of soil mineral nutrients,” no. August, pp. 214–217, 2010.

[170] R. Salminen, M. J. Batista, M. Bidovec, A. Demetriades, B. De Vivo, W. De Vos, M. Duris, A. Gilucis, V. Gregorauskiene, and J. Halavic, “Geochemical Atlas of Europe. Part 1: Background Information, Methodology and Maps, Geological Survey of Finland, Espoo.” ISBN 951-890-921-3, 2005.

[171] D. P. Heenan and L. C. Campbell, “Influence of potassium and manganese on growth and uptake of magnesium by Soybeans (Glycine Max (L.) Merr. CV. Bragg),” *Plant Soil*, vol. 61, no. 3, pp. 447–456, 1981.

[172] C. Hermans, J. P. Hammond, P. J. White, and N. Verbruggen, “How do plants respond to nutrient shortage by biomass allocation ?,” vol. 11, no. 12, 2006.

[173] S. Güsewell, “N : P ratios in terrestrial plants : variation and functional significance,” *New Phytol. - Tansley Rev.*, vol. 164, pp. 243–266, 2004.

[174] S. C. Dunagan, M. S. Gilmore, and J. C. Varekamp, “Effects of mercury on visible/near-infrared reflectance spectra of mustard spinach plants (Brassica rapa P.),” *Environ. Pollut.*, vol. 148, pp. 301–311, 2007.

[175] Y. Zhu, Y. Qu, S. Liu, and S. Chen, “A reflectance spectra model for copper-stressed leaves: advances in the PROSPECT model through addition of the specific absorption coefficients of the copper ion,” *Int. J. Remote Sens.*, vol. 35, no. 4, pp. 1356–1373, Feb. 2014.

[176] J. G. P. W. Clevers, L. Kooistra, and E. A. L. Salas, “Study of heavy metal contamination in river floodplains using the Red-edge position in spectroscopic data,” *Int. J. Remote Sens.*, vol. 25, no. 19, pp. 3883–3895, Oct. 2004.

[177] L. Kooistra, E. A. L. Salas, J. G. P. . Clevers, R. Wehrens, R. S. E. W. Leuven, P. H. Nienhuis, and L. M. C. Buydens, “Exploring field vegetation reflectance as an indicator of soil contamination in river floodplains,” *Environ. Pollut.*, vol. 127, no. 2, pp. 281–290, Jan. 2004.

[178] B. Li, O. W. Liew, and A. K. Asundi, “Pre-visual detection of iron and phosphorus deficiency by transformed reflectance spectra.,” *J. Photochem. Photobiol. B.*, vol. 85, no. 2, pp. 131–9, Nov. 2006.

APPENDIX 1. SUMMARY STATISTICS FOR SOIL SAMPLES ANALYSIS BY XRF AND TEST OF NORMAL DISTRIBUTION

Statistic	*No. Of obs.*	*Minimum*	*Maximum*	*1st quartile*	*Median*	*3rd quartile*	*Mean*	*Variance (n-1)*	*Standard deviation (n-1)*	*Shapiro-wilk p-value*
Si (ppm)	72	378575.61	436631.03	408514.82	413843.58	420083.83	413250.84	101905142.19	10094.81	**0.003**
Al_2 (ppm)	72	17624.03	53401.33	26237.57	30458.34	34348.33	30591.39	49333729.73	7023.80	**0.009**
Fe_2 (ppm)	72	1818.51	3287.30	2098.28	2413.02	2727.76	2455.76	154276.88	392.78	**0.034**
Fe (ppm)	72	16090.21	29848.51	19199.43	21725.67	24562.84	22113.25	12344973.68	3513.54	0.106
Mn (ppm)	72	309.78	6195.66	542.12	697.01	2884.85	1603.77	2555997.01	1598.75	**< 0.0001**
Mg (ppm)	72	783.95	3316.70	1251.30	1386.98	1567.89	1453.99	187312.30	432.80	**< 0.0001**
Ca (ppm)	72	500.28	11935.36	768.29	1143.51	1893.93	1481.00	2034969.26	1426.52	**< 0.0001**
Na_2 (ppm)	72	0.00	1186.97	148.37	296.74	445.11	335.90	77820.09	278.96	**< 0.0001**
K_2 (ppm)	72	3569.64	23742.23	5561.99	6433.65	8010.93	7142.73	10124508.86	3181.90	**< 0.0001**
Ti (ppm)	72	2113.88	6746.80	3008.55	3454.91	3860.67	3534.03	782265.49	884.46	**< 0.0001**
P_2 (ppm)	72	174.57	2225.74	261.85	305.49	436.42	370.96	62772.12	250.54	**< 0.0001**
Cr_2 (ppm)	72	45.84	248.37	107.93	131.37	167.63	134.28	1904.23	43.64	0.423
Ni (ppm)	72	0.00	73.08	21.22	33.79	39.29	31.74	221.88	14.90	0.050
Sc (ppm)	72	3.07	17.06	7.06	8.91	10.39	8.90	6.38	2.53	**0.024**
V (ppm)	72	51.69	137.57	65.11	72.96	80.88	75.35	267.67	16.36	**< 0.0001**
Cr (ppm)	72	80.51	172.26	93.89	123.68	135.72	117.88	653.15	25.56	**0.001**
Co (ppm)	72	3.75	40.09	11.01	12.71	15.02	13.55	30.24	5.50	**< 0.0001**
Ni (ppm)	72	21.60	60.18	29.83	37.05	41.87	37.21	89.17	9.44	**0.044**
Cu (ppm)	72	10.45	56.98	18.18	22.02	29.68	24.85	83.85	9.16	**< 0.0001**
Zn (ppm)	72	14.58	1380.21	20.20	26.10	33.89	47.85	25561.43	159.88	**< 0.0001**
Ga (ppm)	72	3.73	13.25	5.59	6.36	7.88	6.72	3.19	1.79	**< 0.0001**
Rb (ppm)	72	21.54	65.36	27.06	34.65	38.92	34.47	75.93	8.71	**0.000**
Sr (ppm)	72	10.64	99.44	12.88	15.26	19.56	17.40	114.44	10.70	**< 0.0001**
Y (ppm)	72	7.93	16.96	11.38	12.10	13.46	12.33	3.53	1.88	0.736
Zr (ppm)	72	192.26	462.35	257.34	288.88	306.62	285.80	2054.87	45.33	**< 0.0001**
Nb (ppm)	72	4.08	9.66	5.39	6.11	6.86	6.08	1.27	1.13	**0.012**
Mo (ppm)	72	-0.84	2.13	0.72	0.89	1.22	0.95	0.21	0.45	**0.001**
Ba (ppm)	72	101.56	1004.21	160.97	193.41	264.22	256.22	31643.09	177.89	**< 0.0001**
Pb (ppm)	72	5.42	346.64	11.64	17.79	23.35	22.71	1572.96	39.66	**< 0.0001**
Th (ppm)	72	-1.29	7.37	1.78	2.81	3.87	2.96	3.01	1.73	0.051

APPENDIX 2. RESULTS OF THE SOILS CHARACTERISATION BY RED EARTH CC

LFT	AUGER REFERENCE	HARDNESS OR COMPACTION	SOIL FORM AND FAMILY	SURFACE FEATURES	ORGANIC CARBON RANGE	PARENT MATERIAL	EFFECTIVE ROOTING DEPTH (cm)	AMELIORATED EFFECTIVE ROOTING DEPTH (cm)	DEPTH LIMITING MATERIAL	GROUND ROUGHNESS	SLOPE (degrees)	A horizon depth	B horizon depth	C horizon depth	GL horizon depth	R horizon depth	SL horizon depth	OB Horizon	Clay %	Sand grade	Colour	COLOUR MUNSELL	STRUCTURE	COMMENTS
VLS	MMRL01	0-30	Hu3100		mh	L2	80		sl	1	2	20	80				90		30	f	R	2.5YR4/6	a	
VLS	MMAK02		Ms1100		h	T2	10		r	1	2	10				10			30	f	RB	5YR4/4	a	
VLS	MMEC03	0-30	Hu3100		mh		60		r	1	2	20	60			60			30	f	RB	5YR4/4	wb	
VLS	MMEC04	0-90	Hu3100		mh		90		r	1	2	20	90			90			40	m	R	2.5YR4/6	wb	Termite activity. Very hard dry consistence
VLS	MMAK05	0-50	Hu3100		m		90		r	1	2	20	90						40	m	RB	5YR4/4	wb	
VLS	MMRL06		Ms1100		vh	T2	10		r	1	2	10				10			20	f	DB	7.5YR3/4	a	
VLS	MMEC07	0-50	Hu3100		mh		90		r	1	2	20	90			90			40	f	RB	5YR4/4	wb	Silty
VLS	MMAK08	0-50	Hu3100		mh		90		r	1	2	20	90			90			40	f	RB	5YR4/4	wb	Silty
VLS	MMRL09	0-50	Hu3100		mh		100		r	1	2	20	100			100			50	f	RB	2.5YR3/6	wb	
VLS	MMEC10	0-50	Hu3100	<r1	mh		60		r	1	2	10	30			30			30	m	YR	5YR4/6	wb	Variable depth (isolated small rocky patch)
VLS	MMRL11	0-50	Hu3100		mh		50		r	1	2	10	50			50			35	m	RB	5YR4/4	wb	
VLS	MMAK12	0-60	Hu3100		mh		90		r	1	2	10	90			90			40	m	RB	5YR4/4	wb	
VLR	MMRL13		Hu3100	<r1	mh	T2b	10		r	1	4	10				10			25	f	RB	5YR5/4	wb	
VLR	MMEC14		Hu3100	r1	mh	T2b	10		r	1	4	10				10			20	f	RB	5YR4/4	wb	
VLR	MMAK15		Hu3100	r1	mh	T2b	10		r	1	4	10				10			20	f	RB	5YR4/4	wb	
VLR	MMRL16		Ms1100	r2	h	T2b	5		r	2	4	5				5			25	f	DB	7.5YR3/4	wb	
VLR	MMEC17		Ms1100	r2	h	T2b	5		r	2	4	5				5			25	f	DB	7.5YR3/4	wb	
VLR	MMAK18		Ms1100	r2	h	T2b	5		r	2	4	5				5			25	f	DB	7.5YR3/4	wb	
VLR	MMEC19		Ms2100	<r1-r1	h	T2b	5		r	1	4	5				5			16	f	B	5YR5/4	a	

LFT	AUGER REFERENCE	HARDNESS OR COMPACTION	SOIL FORM AND FAMILY	SURFACE FEATURES	ORGANIC CARBON RANGE	PARENT MATERIAL	EFFECTIVE ROOTING DEPTH (cm)	AMELIORATED EFFECTIVE ROOTING DEPTH (cm)	DEPTH LIMITING MATERIAL	GROUND ROUGHNESS	SLOPE (degrees)	A horizon depth	B horizon depth	C horizon depth	GL horizon depth	R horizon depth	SL horizon depth	OB Horizon	Clay %	Sand grade	Colour	COLOUR MUNSELL	STRUCTURE	COMMENTS
VLR	MMRL20		Ms2100	<r1-r1	h	T2b	5		r	1	4	5				5			16	f	B	5YR5/4	a	
VLR	MMAK21		Ms2100	<r1-r1	h	T2b	5		r	1	4	5				5			16	f	B	5YR5/4	a	
VLR	MMRL22		Ms1100	r5	h	T2b	2		r	3	4	2				2			16	f	DB	7.5YR3/4	a	
VLR	MMEC23		Ms1100	r5	h	T2b	2		r	3	4	2				2			16	f	DB	7.5YR3/4	a	
VLR	MMAK24		Ms1100	r6	h	T2b	2		r	3	4	2				2			16	f	DB	7.5YR3/4	a	
BR2	MMRL25		Ms1100	r1	mh	T2b/T2	5		r	1	2	5				5			25	m	YR	5YR5/6	a	
BR2	MMEC26		Ms1100	r1	mh	T2b/T2	5		r	1	2	5				5			25	m	YR	5YR5/6	a	
BR2	MMRL27		Ms1100	r1	vh	T2b/T2	10		r	2	2	10				10			20	m	DB	7.5YR3/4	a	
BR2	MMEC28		Ms1100	r1	vh	T2b/T2	10		r	2	2	10				10			20	m	DB	7.5YR3/4	a	
BR1	MMRL29		Ms1100	r6	vh	T2b/T2	2		r	4	4	2				2			16	f	DB	7.5YR3/4	a	Ridge scarp
BR1	MMEC30		Ms1100	r6	vh	T2b/T2	2		r	4	4	2				2			16	f	DB	7.5YR3/4	a	Ridge scarp
BR1	MMRL31		Ms1100	r5	vh	T2b/T2	2		r	3	2	2				2			16	f	DB	7.5YR3/4	a	Ridge
BR1	MMEC32		Ms1100	r5	vh	T2b/T2	2		r	3	2	2				2			16	f	DB	7.5YR3/4	a	Ridge
BR2	MMRL33		Hu3100	<r1	mh	T2b/T2	30		r	1	2	10	30			30			20	f	SB	7.5YR4/6	a	
BR2	MMEC34		Hu3100		mh	T2b/T2	30		r	1	2	10	30			30			30	m	RB	5YR3/4	wb	
BR2	MMRL35		Hu3100 and Ms1100	r1	mh	T2b/T2	40		r	1	2	10	40			40			30	m	SB	7.5YR4/6	a	Variable depth (Hu and Ms soil forms)
BR2	MMEC36		Hu3100 and Ms1100	r1	mh	T2b/T2	40		r	1	2	10	40			40			30	m	SB	7.5YR4/6	a	Variable depth (Hu and Ms soil forms)
BR1	MMRL37		Ms1100	r5	vh	T2b	5		r	3	2	5				5			20	f	DB	7.5YR3/4	a	Ridge
BR1	MMEC38		Ms1100	r5	vh	T2b	5		r	3	2	5				5			20	f	DB	7.5YR3/4	a	Ridge
BR1	MMEC39		Ms2100	b4r5	vh	T2b/T2	1		r	5	8	1				1			16	f	B	7.5YR5/4	a	Ridge, old workings vicinity
BR1	MMRL40		Ms2100	b4r5	vh	T2b/T2	1		r	5	8	1				1			16	f	B	7.5YR5/4	a	Ridge, old workings vicinity

LFT	AUGER REFERENCE	HARDNESS OR COMPACTION	SOIL FORM AND FAMILY	SURFACE FEATURES	ORGANIC CARBON RANGE	PARENT MATERIAL	EFFECTIVE ROOTING DEPTH (cm)	AMELIORATED EFFECTIVE ROOTING DEPTH (cm)	DEPTH LIMITING MATERIAL	GROUND ROUGHNESS	SLOPE (degrees)	A horizon depth	B horizon depth	C horizon depth	GL horizon depth	R horizon depth	SL horizon depth	OB Horizon	Clay %	Sand grade	Colour	COLOUR MUNSELL	STRUCTURE	COMMENTS
D1	MMEC41		Hu3100		mh	L2	181		r	1	2	20	181						20	f	DRB	2.5YR3/4	a	
D1	MMRL42		Hu3100		mh	L2	181		r	1	2	20	181						20	f	DRB	2.5YR3/4	a	
D1	MMEC43		Hu3100		mh	L2	30	80	gl/so	1	2	30		150	120				20	f	DRB	2.5YR3/4	a	Soil depth 120cm
D1	MMRL44		Hu3100		mh	L2	30	80	gl/so	1	2	30		150	120				20	f	DRB	2.5YR3/4	a	Soil depth 120cm
D1	MMEC45		Hu3100 and Ms1100		mh	L2	20	60-20	gl/r	1	2 to 4	20			100	100			20	f	DRB	2.5YR3/4	a	Variable depth (Hu and Ms soil forms)
D1	MMRL46		Hu3100		mh	L2	20	140	gl/r	1	4	20	120		150	150			16	f	DRB	2.5YR3/4	a	Soil depth 150cm
D1	MMRL47		Hu3100	r2s4	mh	L2/S	70	90	gl/so	3	4	20	70	130	100				16	m	DRB	5YR3/4	a	Soil depth 100cm. Surface rocks deposited by man
D1	MMAK48		Hu3100	r2s4	mh	L2/S	70	90	gl/so	3	4	20	70	130	100				16	m	DRB	5YR3/4	a	Soil depth 100cm. Surface rocks deposited by man
D1	MMAK49	0-60	Hu3100	o1	mh	L2	80		r	1	8	30	80			80			16	f	DRB	2.5YR3/4	a	Very hard dry consistence
D1	MMAK50		Hu3100		mh	L2	30	80	gl/so	1	2	30		150	120				20	f	DRB	2.5YR3/4	a	Soil depth 120cm
D1	MMAK51		Hu3100		mh	L2	80	110	gl/r	1	2	20	80		120	120			20	f	DRB	2.5YR3/4	a	Soil depth 120cm
D1	MMEC52		Hu3100 and Ms1100		mh	L2	80		r	1	2	20	80			80			25	f	DRB	2.5YR3/4	a	Variable depth (Hu and Ms soil forms)
D2	MMRL53		Ms1100	o4	mh	L2	20		r	2	4	20				20			16	f	DRB	5YR3/4	a	
D2	MMRL54		Hu3100	o1	mh	L2	30		r	1	2	20	30			30			20	f	DRB	5YR3/4	a	
D2	MMER55		Hu3100	o2	mh	L2	70		r	1	2	20	70			70			16	f	DRB	5YR3/4	a	
D2	MMER56		Gs		mh	L2	20	30	lc	1	2	20	30						14	m	DRB	5YR3/4	a	Next to sinkhole
D2	MMRL57		Gs		mh	L2	20	30	lc	1	2	20	30						14	m	DRB	5YR3/4	a	Next to sinkhole
D2	MMRL58		Hu3100		mh	L2	60		r	1	2	20	60			60			20	f	DRB	2.5YR3/4	a	
D2	MMER59		Hu3100		mh	L2	60		r	1	2	20	60			60			20	f	DRB	2.5YR3/4	a	
D2	MMAK60		Ms1100		m	T3	10		r	1	2	10				10			14	c	SB	7.5YR4/6	a	

LFT	AUGER REFERENCE	HARDNESS OR COMPACTION	SOIL FORM AND FAMILY	SURFACE FEATURES	ORGANIC CARBON RANGE	PARENT MATERIAL	EFFECTIVE ROOTING DEPTH (cm)	AMELIORATED EFFECTIVE ROOTING DEPTH (cm)	DEPTH LIMITING MATERIAL	GROUND ROUGHNESS	SLOPE (degrees)	A horizon depth	B horizon depth	C horizon depth	GL horizon depth	R horizon depth	SL horizon depth	OB Horizon	Clay %	Sand grade	Colour	COLOUR MUNSELL	STRUCTURE	COMMENTS
D2	MMAK61		Ms1100	r4	vh	T3	10		r	1	2	10				10			14	c	DYB	10YR3/4	a	
D2	MMAK62		Ms1100	r4	h	T3	2		r	3	2	2				2			14	m	SB	7.5YR4/6	a	
D2	MMAK63		Ms1100	o4	mh	L2	20		r	2	2	20				20			16	f	DRB	5YR3/4	a	
BR1	MMER64		Ms1100	r6	m	T2b/T2	2		r	4	2	2				2			20	f	SB	7.5YR4/6	a	Ridge
BR1	MMER65		Ms1100	r6	m	T2b/T2	2		r	4	2	2				2			20	f	SB	7.5YR4/6	a	Ridge
BR1	MMER66		Ms1100	r6	m	T2b/T2	2		r	4	2	2				2			20	f	SB	7.5YR4/6	a	Ridge
BR2	MMAK67		Wb overlying Ms1100		vh	T2b/T2	30		r	1	2	30				30		25	25	m	R	2.5YR4/6	a	Midden (glass, porcelain, screws, coal cinder, and bones in mainly ash matrix)
BR2	MMAK68		Ms1100	<r1	mh	T2b/T2	10		r	1	2	10				10			25	m	SB	7.5YR4/6	a	
BR2	MMAK69		Hu3100		mh	T2b/T2	25		r	1	2	10	25			25			30	m	SB	7.5YR4/6	a	
BR2	MMAK70		Hu3100	<r1	mh	T2b/T2	30		r	1	2	10	30			30			35	m	DB	7.5YR3/4	a	
BR1	MMAK71		Ms1100	r5	vh	T2b/T2	2		r	3	4	2				2			14	f	SB	7.5YR4/6	a	Ridge scarp
BR1	MMAK72		Ms1100	b3r3	vh	T2b/T2	2		r	4	2 to 6	2				2			16	f	DB	7.5YR3/4	a	Ridge. Square stone arrangement
BR1	MMAK73		Ms1100	r4	vh	T2b/T2	2		r	3	2	2				2			25	f	SB	7.5YR4/6	a	Ridge scarp
BR1	MMAK74		Ms1100	r3	vh	T2b/T2	5		r	2	2	5				5			20	f	DB	7.5YR4/4	a	Ridge. Old workings vicinity. Stone cattle kraal

APPENDIX 3. BOX PLOTS SHOWING XRF ANALYSIS OF SOIL ELEMENTAL CONTENT BY GEOLOGY (LEFT) AND BY LANDSCAPE FUNCTION TYPE (RIGHT) PER ELEMENT

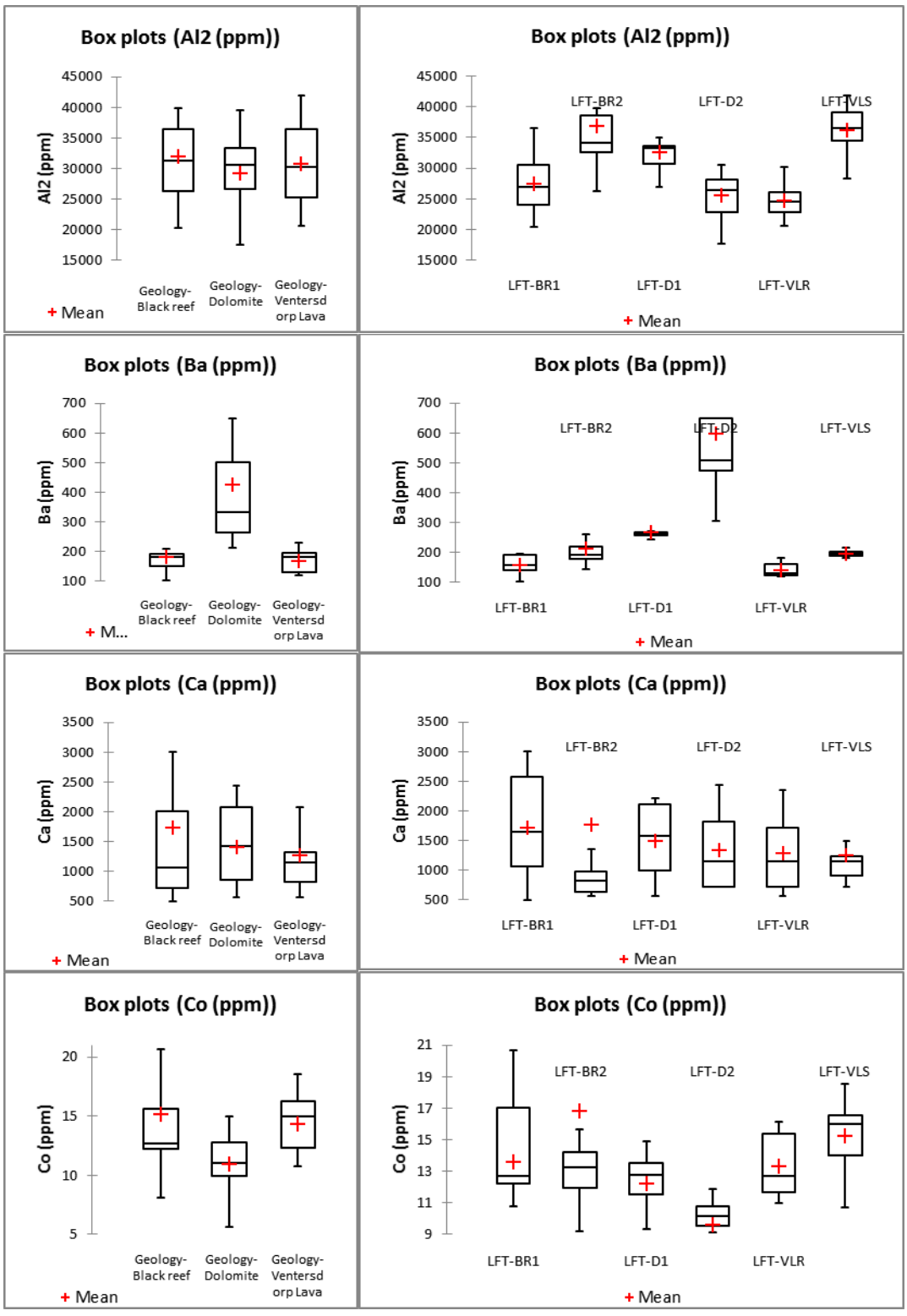

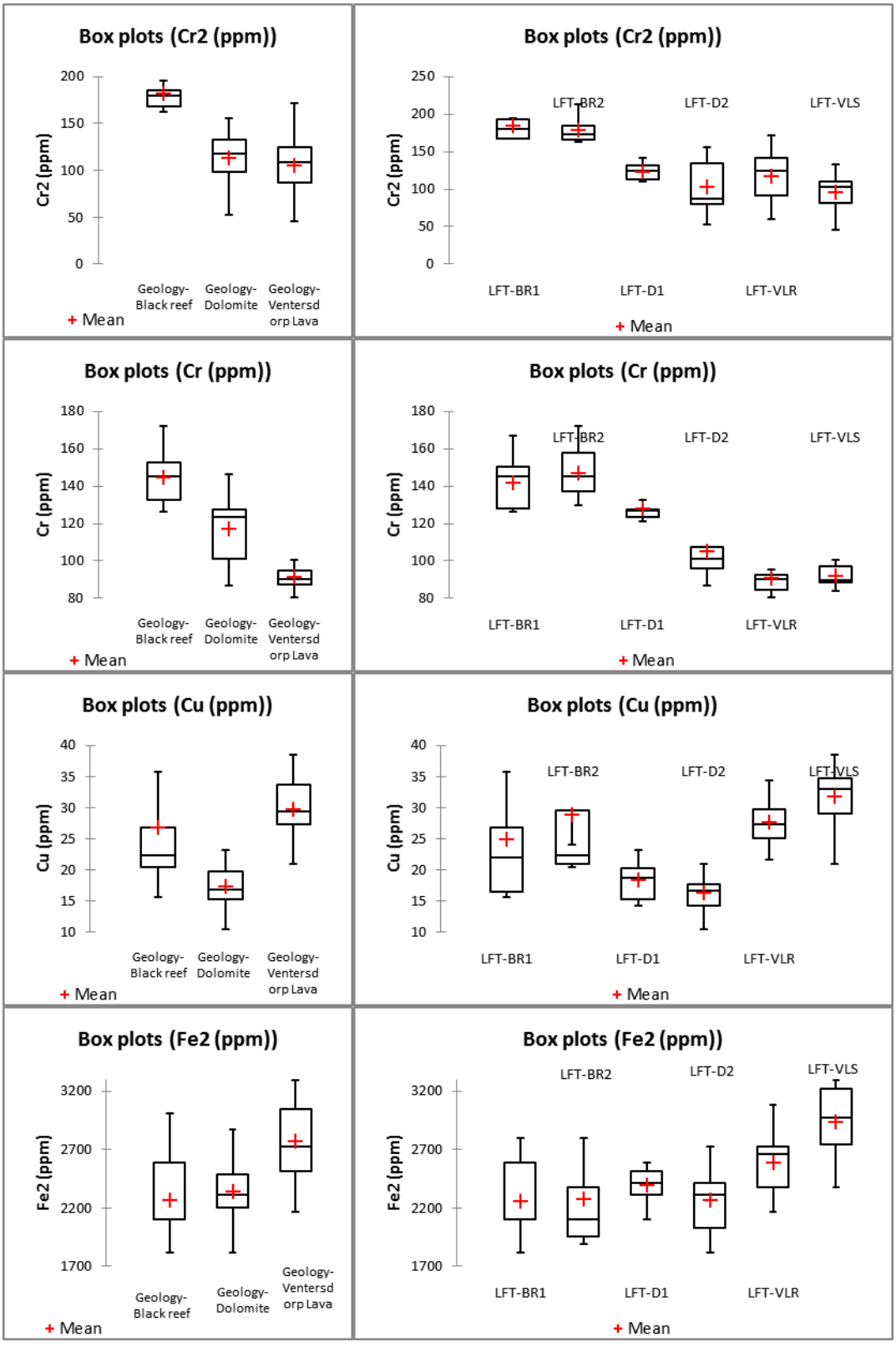
Box plots (Cr2 (ppm))
Cr2 (ppm)
200
150
100
50
0
Geology-Black reef
Geology-Dolomite
Geology-Ventersdorp Lava
+ Mean
Box plots (Cr2 (ppm))
Cr2 (ppm)
250
200
150
100
50
0
LFT-BR1
LFT-BR2
LFT-D1
LFT-D2
LFT-VLR
LFT-VLS
+ Mean
Box plots (Cr (ppm))
Cr (ppm)
180
160
140
120
100
80
Geology-Black reef
Geology-Dolomite
Geology-Ventersdorp Lava
+ Mean
Box plots (Cr (ppm))
Cr (ppm)
180
160
140
120
100
80
LFT-BR1
LFT-BR2
LFT-D1
LFT-D2
LFT-VLR
LFT-VLS
+ Mean
Box plots (Cu (ppm))
Cu (ppm)
40
35
30
25
20
15
10
Geology-Black reef
Geology-Dolomite
Geology-Ventersdorp Lava
+ Mean
Box plots (Cu (ppm))
Cu (ppm)
40
35
30
25
20
15
10
LFT-BR1
LFT-BR2
LFT-D1
LFT-D2
LFT-VLR
LFT-VLS
+ Mean
Box plots (Fe2 (ppm))
Fe2 (ppm)
3200
2700
2200
1700
Geology-Black reef
Geology-Dolomite
Geology-Ventersdorp Lava
+ Mean
Box plots (Fe2 (ppm))
Fe2 (ppm)
3200
2700
2200
1700
LFT-BR1
LFT-BR2
LFT-D1
LFT-D2
LFT-VLR
LFT-VLS
+ Mean

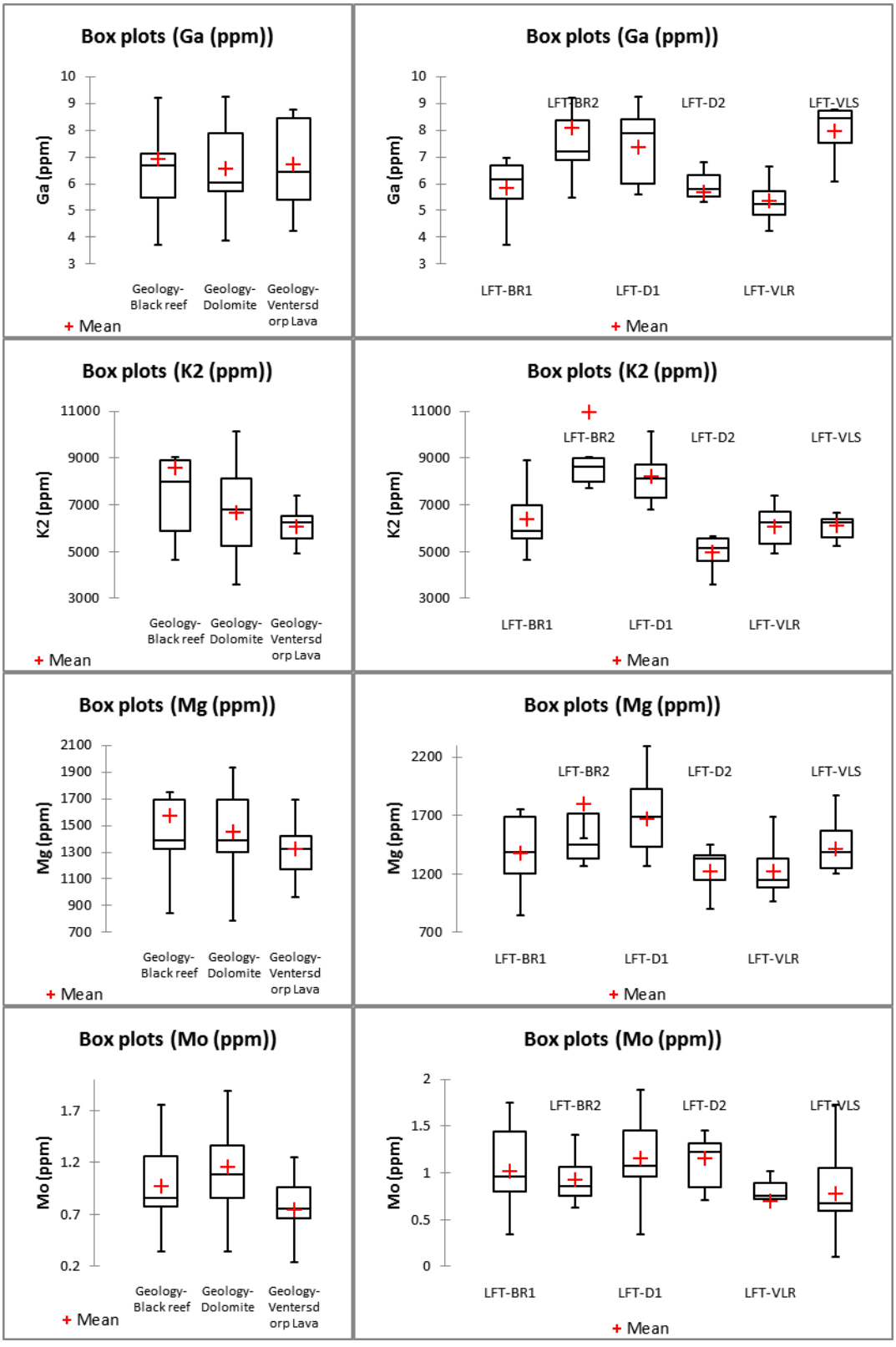
Box plots (Ga (ppm))
Ga (ppm)
10
9
8
7
6
5
4
3
Geology-Black reef
Geology-Dolomite
Geology-Ventersdorp Lava
+ Mean
Box plots (Ga (ppm))
Ga (ppm)
LFT-BR1
LFT-BR2
LFT-D1
LFT-D2
LFT-VLR
LFT-VLS
+ Mean
Box plots (K2 (ppm))
K2 (ppm)
11000
9000
7000
5000
3000
Geology-Black reef
Geology-Dolomite
Geology-Ventersdorp Lava
+ Mean
Box plots (K2 (ppm))
K2 (ppm)
LFT-BR1
LFT-BR2
LFT-D1
LFT-D2
LFT-VLR
LFT-VLS
+ Mean
Box plots (Mg (ppm))
Mg (ppm)
2100
1900
1700
1500
1300
1100
900
700
Geology-Black reef
Geology-Dolomite
Geology-Ventersdorp Lava
+ Mean
Box plots (Mg (ppm))
Mg (ppm)
2200
1700
1200
700
LFT-BR1
LFT-BR2
LFT-D1
LFT-D2
LFT-VLR
LFT-VLS
+ Mean
Box plots (Mo (ppm))
Mo (ppm)
1.7
1.2
0.7
0.2
Geology-Black reef
Geology-Dolomite
Geology-Ventersdorp Lava
+ Mean
Box plots (Mo (ppm))
Mo (ppm)
2
1.5
1
0.5
0
LFT-BR1
LFT-BR2
LFT-D1
LFT-D2
LFT-VLR
LFT-VLS
+ Mean

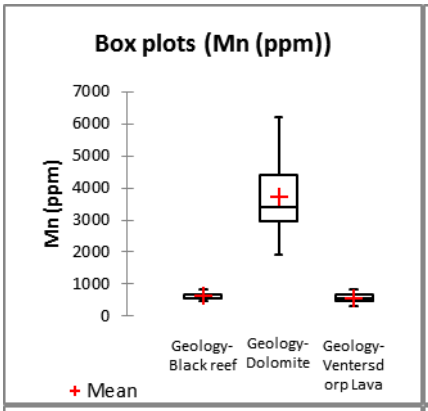
Box plots (Mn (ppm))
Mn (ppm)
7000
6000
5000
4000
3000
2000
1000
0
Geology-Black reef
Geology-Dolomite
Geology-Ventersdorp Lava
+ Mean

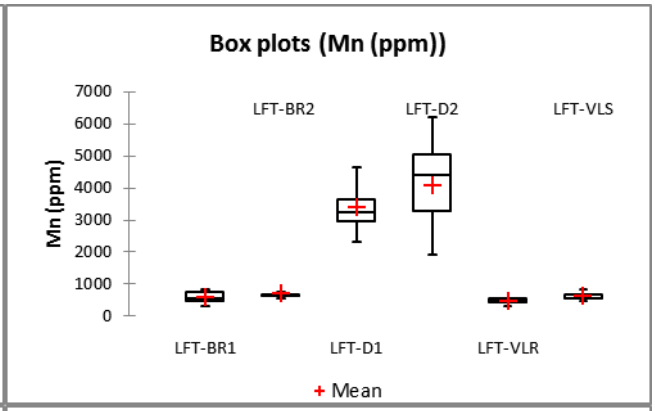
Box plots (Mn (ppm))
Mn (ppm)
7000
6000
5000
4000
3000
2000
1000
0
LFT-BR2
LFT-D2
LFT-VLS
LFT-BR1
LFT-D1
LFT-VLR
+ Mean

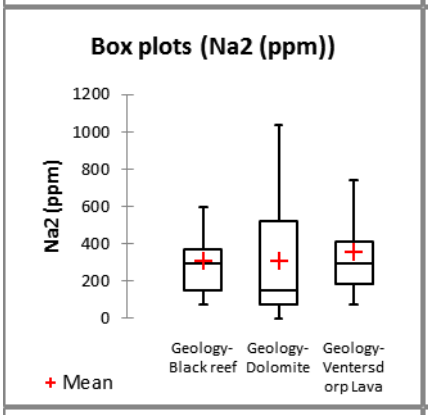
Box plots (Na2 (ppm))
Na2 (ppm)
1200
1000
800
600
400
200
0
Geology-Black reef
Geology-Dolomite
Geology-Ventersdorp Lava
+ Mean

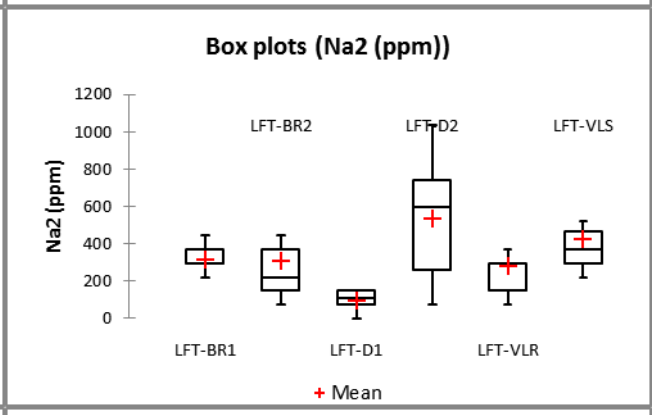
Box plots (Na2 (ppm))
Na2 (ppm)
1200
1000
800
600
400
200
0
LFT-BR2
LFT-D2
LFT-VLS
LFT-BR1
LFT-D1
LFT-VLR
+ Mean

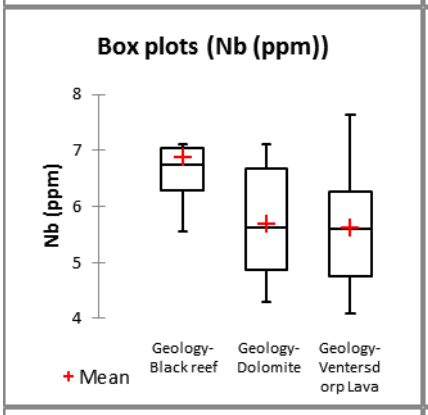
Box plots (Nb (ppm))
Nb (ppm)
8
7
6
5
4
Geology-Black reef
Geology-Dolomite
Geology-Ventersdorp Lava
+ Mean

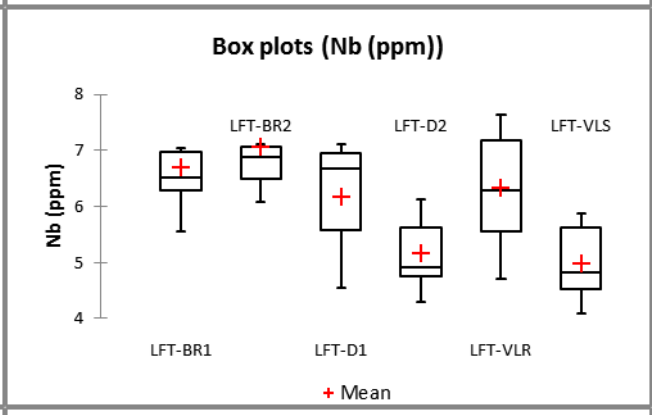
Box plots (Nb (ppm))
Nb (ppm)
8
7
6
5
4
LFT-BR2
LFT-D2
LFT-VLS
LFT-BR1
LFT-D1
LFT-VLR
+ Mean

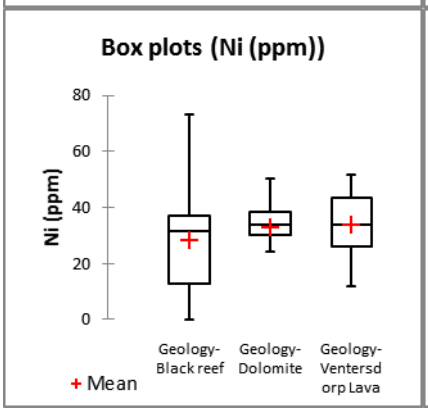
Box plots (Ni (ppm))
Ni (ppm)
80
60
40
20
0
Geology-Black reef
Geology-Dolomite
Geology-Ventersdorp Lava
+ Mean

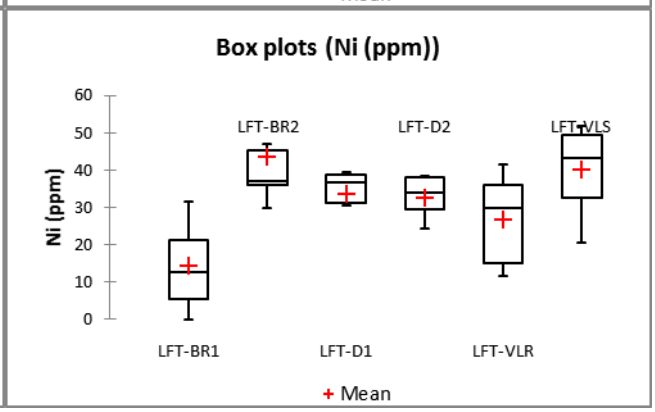
Box plots (Ni (ppm))
Ni (ppm)
60
50
40
30
20
10
0
LFT-BR2
LFT-D2
LFT-VLS
LFT-BR1
LFT-D1
LFT-VLR
+ Mean

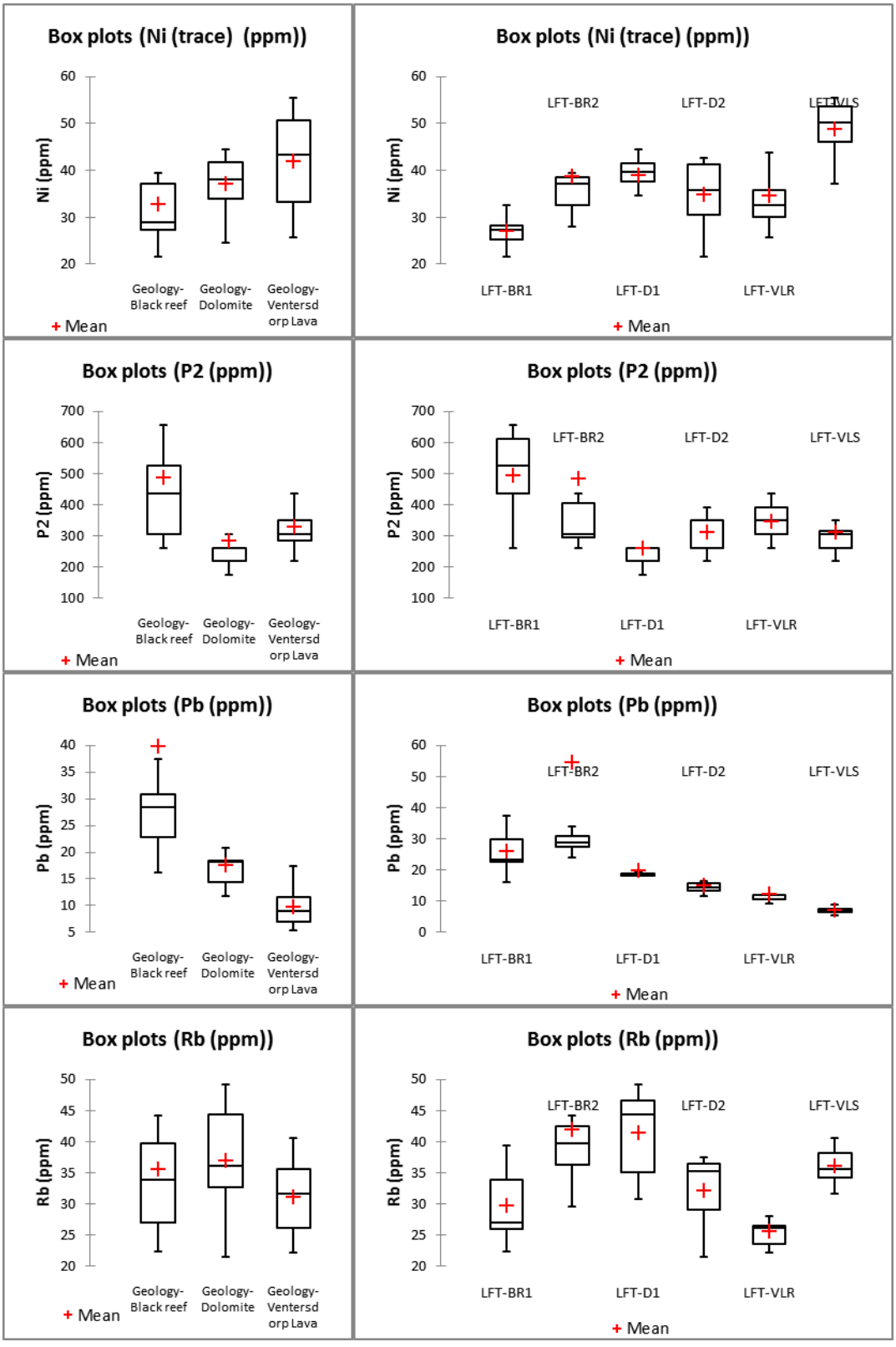
Box plots (Ni (trace) (ppm))
Ni (ppm)
60
50
40
30
20
Geology-Black reef
Geology-Dolomite
Geology-Ventersdorp Lava
+ Mean
Box plots (Ni (trace) (ppm))
Ni (ppm)
LFT-BR2
LFT-D2
LFT-VLS
LFT-BR1
LFT-D1
LFT-VLR
+ Mean
Box plots (P2 (ppm))
P2 (ppm)
700
600
500
400
300
200
100
Geology-Black reef
Geology-Dolomite
Geology-Ventersdorp Lava
+ Mean
Box plots (P2 (ppm))
P2 (ppm)
LFT-BR2
LFT-D2
LFT-VLS
LFT-BR1
LFT-D1
LFT-VLR
+ Mean
Box plots (Pb (ppm))
Pb (ppm)
40
35
30
25
20
15
10
5
Geology-Black reef
Geology-Dolomite
Geology-Ventersdorp Lava
+ Mean
Box plots (Pb (ppm))
Pb (ppm)
60
50
40
30
20
10
0
LFT-BR2
LFT-D2
LFT-VLS
LFT-BR1
LFT-D1
LFT-VLR
+ Mean
Box plots (Rb (ppm))
Rb (ppm)
50
45
40
35
30
25
20
Geology-Black reef
Geology-Dolomite
Geology-Ventersdorp Lava
+ Mean
Box plots (Rb (ppm))
Rb (ppm)
LFT-BR2
LFT-D2
LFT-VLS
LFT-BR1
LFT-D1
LFT-VLR
+ Mean

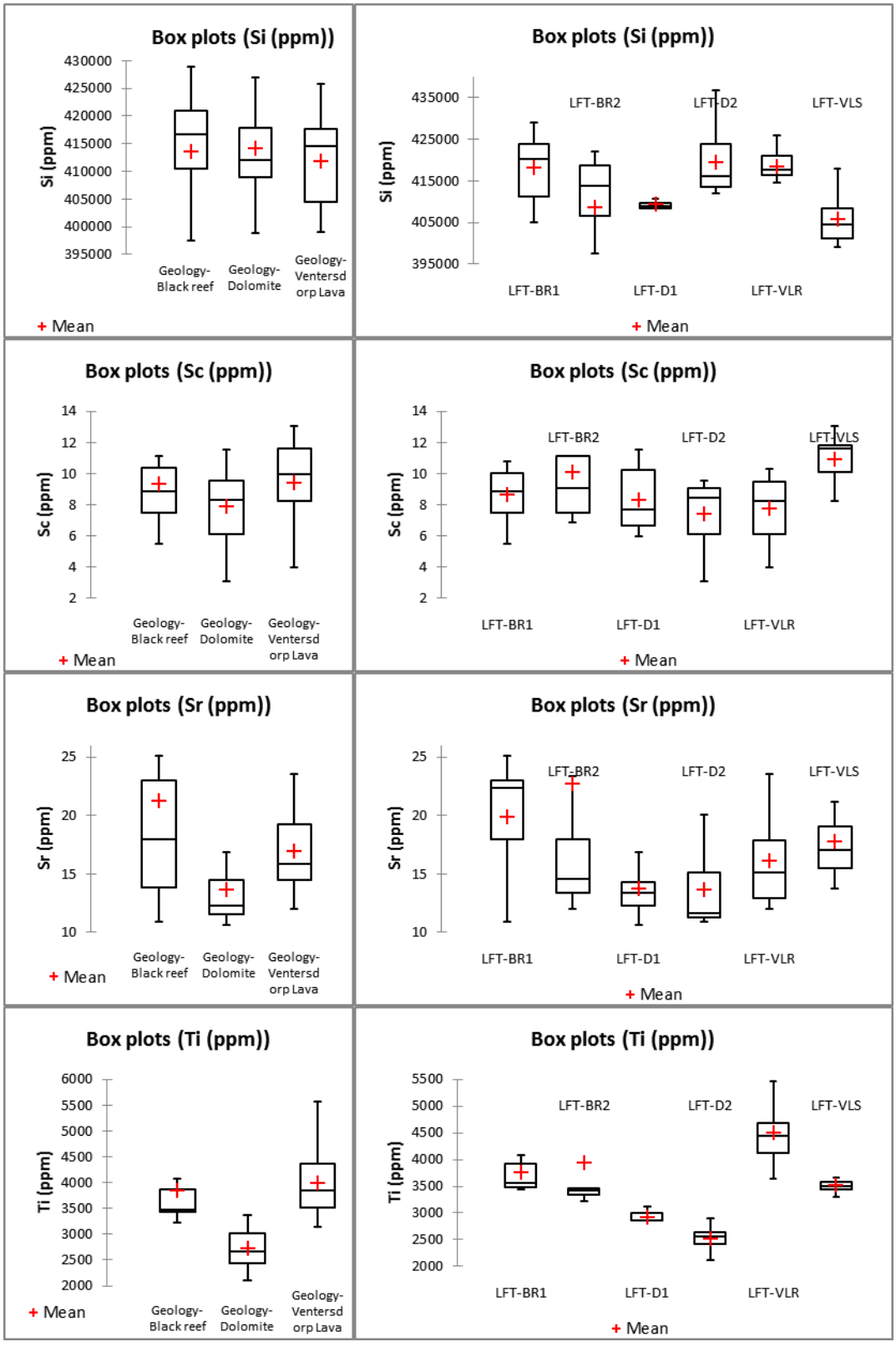
Box plots (Si (ppm))
Si (ppm)
430000
425000
420000
415000
410000
405000
400000
395000
Geology-Black reef
Geology-Dolomite
Geology-Ventersdorp Lava
+ Mean
Box plots (Si (ppm))
Si (ppm)
435000
425000
415000
405000
395000
LFT-BR1
LFT-BR2
LFT-D1
LFT-D2
LFT-VLR
LFT-VLS
+ Mean
Box plots (Sc (ppm))
Sc (ppm)
14
12
10
8
6
4
2
Geology-Black reef
Geology-Dolomite
Geology-Ventersdorp Lava
+ Mean
Box plots (Sc (ppm))
Sc (ppm)
14
12
10
8
6
4
2
LFT-BR1
LFT-BR2
LFT-D1
LFT-D2
LFT-VLR
LFT-VLS
+ Mean
Box plots (Sr (ppm))
Sr (ppm)
25
20
15
10
Geology-Black reef
Geology-Dolomite
Geology-Ventersdorp Lava
+ Mean
Box plots (Sr (ppm))
Sr (ppm)
25
20
15
10
LFT-BR1
LFT-BR2
LFT-D1
LFT-D2
LFT-VLR
LFT-VLS
+ Mean
Box plots (Ti (ppm))
Ti (ppm)
6000
5500
5000
4500
4000
3500
3000
2500
2000
+ Mean
Geology-Black reef
Geology-Dolomite
Geology-Ventersdorp Lava
Box plots (Ti (ppm))
Ti (ppm)
5500
5000
4500
4000
3500
3000
2500
2000
LFT-BR1
LFT-BR2
LFT-D1
LFT-D2
LFT-VLR
LFT-VLS
+ Mean

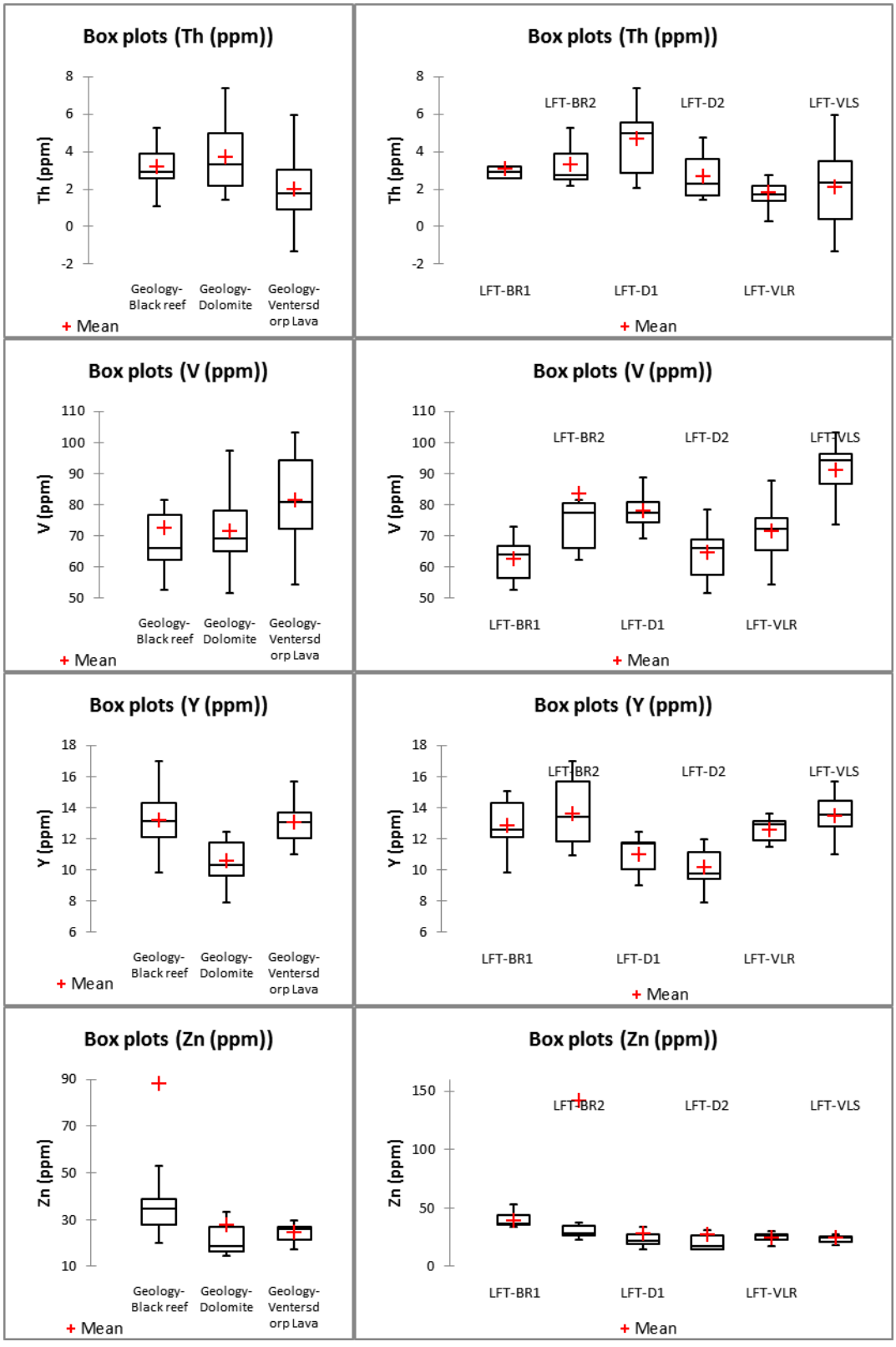
Box plots (Th (ppm))
Th (ppm)
8
6
4
2
0
-2
Geology-Black reef
Geology-Dolomite
Geology-Ventersdorp Lava
+ Mean
Box plots (Th (ppm))
Th (ppm)
LFT-BR1
LFT-BR2
LFT-D1
LFT-D2
LFT-VLR
LFT-VLS
+ Mean
Box plots (V (ppm))
V (ppm)
110
100
90
80
70
60
50
Geology-Black reef
Geology-Dolomite
Geology-Ventersdorp Lava
+ Mean
Box plots (V (ppm))
V (ppm)
LFT-BR1
LFT-BR2
LFT-D1
LFT-D2
LFT-VLR
LFT-VLS
+ Mean
Box plots (Y (ppm))
Y (ppm)
18
16
14
12
10
8
6
Geology-Black reef
Geology-Dolomite
Geology-Ventersdorp Lava
+ Mean
Box plots (Y (ppm))
Y (ppm)
LFT-BR1
LFT-BR2
LFT-D1
LFT-D2
LFT-VLR
LFT-VLS
+ Mean
Box plots (Zn (ppm))
Zn (ppm)
90
70
50
30
10
Geology-Black reef
Geology-Dolomite
Geology-Ventersdorp Lava
+ Mean
Box plots (Zn (ppm))
Zn (ppm)
150
100
50
0
LFT-BR1
LFT-BR2
LFT-D1
LFT-D2
LFT-VLR
LFT-VLS
+ Mean

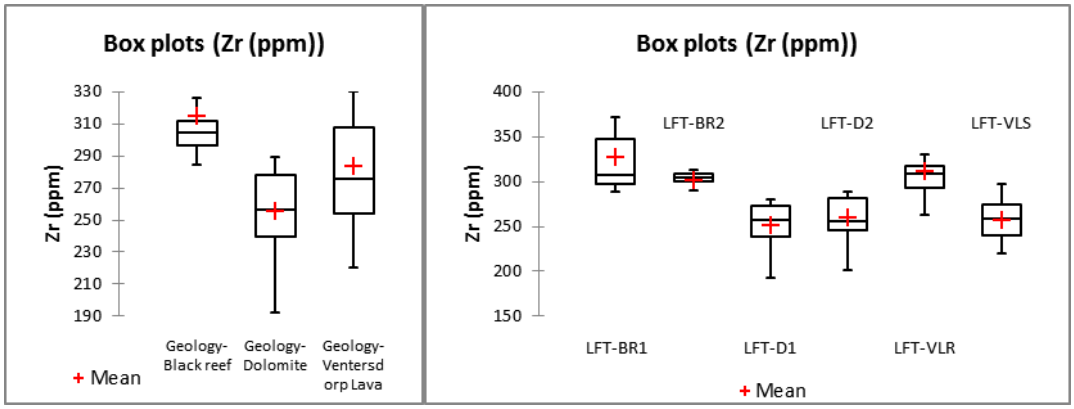
Box plots (Zr (ppm))
Zr (ppm)
330
310
290
270
250
230
210
190
Geology-Black reef
Geology-Dolomite
Geology-Ventersdorp Lava
+ Mean
Box plots (Zr (ppm))
Zr (ppm)
400
350
300
250
200
150
LFT-BR1
LFT-BR2
LFT-D1
LFT-D2
LFT-VLR
LFT-VLS
+ Mean

APPENDIX 4. RANGES OBTAINED FOR VEGETATION INDICES PER TREE SPECIES

Index	Species	No. of obs.	Minimum	Maximum	1st Quartile	Median	3rd Quartile	Mean	Variance (n-1)	Std. dev. (n-1)	Shapiro-Wilk p-value
NDVI	Combined	702	0.528	0.908	0.787	0.815	0.846	0.813	0.002	0.048	
	A. karroo	203	0.634	0.866	0.790	0.815	0.836	0.809	0.001	0.037	
	E. rigida	40	0.528	0.822	0.754	0.786	0.807	0.764	0.005	0.070	**<0.0001**
	E. crispa	209	0.668	0.860	0.768	0.790	0.810	0.787	0.001	0.035	
	S. lancea	250	0.660	0.908	0.831	0.853	0.872	0.846	0.001	0.038	
Red-edge NDVI	Combined	702	0.326	0.664	0.470	0.515	0.554	0.512	0.004	0.063	
	A. karroo	203	0.332	0.664	0.483	0.521	0.548	0.518	0.003	0.058	
	E. rigida	40	0.326	0.536	0.461	0.483	0.504	0.472	0.002	0.048	**<0.0001**
	E. crispa	209	0.335	0.583	0.430	0.469	0.507	0.470	0.003	0.052	
	S. lancea	250	0.342	0.654	0.515	0.551	0.585	0.547	0.003	0.054	
NDWI	Combined	702	-0.003	0.154	0.049	0.059	0.072	0.062	0.000	0.019	
	A. karroo	203	0.041	0.126	0.067	0.081	0.092	0.080	0.000	0.017	
	E. rigida	40	0.044	0.087	0.056	0.064	0.075	0.066	0.000	0.011	**0.000**
	E. crispa	209	0.026	0.122	0.048	0.057	0.065	0.057	0.000	0.014	
	S. lancea	250	-0.003	0.154	0.040	0.051	0.060	0.050	0.000	0.016	
PSRI	Combined	702	-0.044	0.032	-0.012	-0.001	0.004	-0.004	0.000	0.012	
	A. karroo	203	-0.044	0.004	-0.021	-0.015	-0.010	-0.016	0.000	0.009	
	E. rigida	40	-0.037	0.000	-0.022	-0.017	-0.011	-0.017	0.000	0.009	**0.001**
	E. crispa	209	-0.036	0.026	-0.002	0.002	0.007	0.003	0.000	0.008	
	S. lancea	250	-0.022	0.032	-0.001	0.002	0.006	0.003	0.000	0.007	
Red-edge Inflection point	Combined	742	0.095	0.454	0.311	0.335	0.360	0.336	0.001	0.038	
	A. karroo	223	0.269	0.454	0.338	0.364	0.381	0.361	0.001	0.035	
	E. rigida	209	0.212	0.404	0.313	0.335	0.351	0.333	0.001	0.033	**<0.0001**
	E. crispa	60	0.267	0.400	0.315	0.331	0.358	0.334	0.001	0.032	
	S. lancea	250	0.095	0.389	0.299	0.317	0.336	0.316	0.001	0.035	
Red-edge **Position**	Combined	742	727.090	738.876	729.425	730.385	731.355	730.504	2.617	1.618	
	A. karroo	223	728.537	737.818	730.248	730.966	731.638	731.118	1.858	1.363	
	E. rigida	209	728.012	736.447	730.100	730.661	731.682	731.035	1.818	1.348	**<0.0001**
	E. crispa	60	728.732	738.876	730.280	731.100	731.854	731.374	3.524	1.877	
	S. lancea	250	727.090	735.392	728.443	729.119	729.860	729.304	1.576	1.255	
725-702 Ratio of the 1st	Combined	742	0.531	2.087	0.942	1.107	1.276	1.120	0.063	0.250	
	A. karroo	223	0.721	2.087	1.081	1.226	1.388	1.247	0.062	0.249	
	E. rigida	209	0.531	1.586	0.782	0.930	1.094	0.950	0.045	0.213	**<0.0001**
	E. crispa	60	0.789	1.393	1.002	1.127	1.215	1.110	0.020	0.141	
	S. lancea	250	0.557	1.758	1.009	1.120	1.305	1.151	0.049	0.221	
725-702 Ratio of the 2nd derivative	Combined	742	-23.568	165.363	-1.382	-0.937	-0.681	-1.079	45.648	6.756	
	A. karroo	223	-23.568	37.974	-1.185	-0.768	-0.559	-1.092	11.889	3.448	
	E. rigida	209	-21.165	165.363	-2.227	-1.301	-0.895	-1.068	148.791	12.198	**<0.0001**
	E. crispa	60	-6.923	-0.574	-1.615	-1.097	-0.925	-1.364	0.761	0.872	
	S. lancea	250	-9.335	1.201	-1.090	-0.842	-0.650	-1.009	0.747	0.864	

APPENDIX 5. DESCRIPTIVE STATISTICS OF THE SPECTRAL INDICES BY SPECIES AND BY LANDSCAPE FUNCTIONAL TYPE

Spectral index	*Species*	*L F T*	*No. of obs.*	*Minimum*	*Maximum*	*1st Quartile*	*Median*	*3rd Quartile*	*Mean*	*Variance (n-1)*	*Std. dev. (n-1)*
NDVI	Combined		742	0.531	0.920	0.797	0.824	0.855	0.822	0.002	0.048
	AK	BR1	41	0.794	0.870	0.838	0.850	0.855	0.846	0.000	0.015
		BR2	40	0.714	0.860	0.799	0.818	0.837	0.812	0.001	0.036
		D1	40	0.640	0.863	0.799	0.811	0.833	0.809	0.002	0.039
		D2	40	0.725	0.861	0.808	0.826	0.841	0.823	0.001	0.026
		VLR	41	0.642	0.874	0.773	0.807	0.828	0.798	0.002	0.048
		VLS	21	0.718	0.842	0.792	0.805	0.816	0.800	0.001	0.026
	EC	BR1	40	0.717	0.814	0.750	0.768	0.785	0.767	0.001	0.025
		BR2	41	0.722	0.856	0.785	0.799	0.812	0.796	0.001	0.024
		D1	42	0.767	0.873	0.813	0.826	0.848	0.829	0.001	0.024
		VLR	41	0.740	0.835	0.780	0.794	0.805	0.794	0.000	0.021
		VLS	45	0.680	0.848	0.782	0.815	0.827	0.799	0.002	0.043
	ER	BR1	30	0.651	0.849	0.784	0.796	0.813	0.794	0.001	0.037
		D2	30	0.531	0.836	0.740	0.809	0.819	0.768	0.007	0.082
	SL	BR1	41	0.789	0.920	0.851	0.869	0.883	0.865	0.001	0.028
		BR2	41	0.767	0.898	0.833	0.852	0.875	0.851	0.001	0.028
		D1	40	0.813	0.908	0.858	0.873	0.888	0.873	0.000	0.019
		D2	40	0.670	0.909	0.861	0.870	0.880	0.866	0.001	0.037
		VLR	42	0.761	0.919	0.821	0.863	0.894	0.857	0.002	0.045
		VLS	46	0.674	0.912	0.812	0.847	0.867	0.836	0.002	0.047
NDWI	Combined		742	-0.003	0.154	0.049	0.060	0.073	0.062	0.000	0.019
	AK	BR1	41	0.041	0.086	0.053	0.059	0.070	0.062	0.000	0.012
		BR2	40	0.056	0.108	0.072	0.084	0.093	0.083	0.000	0.013
		D1	40	0.064	0.112	0.075	0.087	0.096	0.086	0.000	0.013
		D2	40	0.067	0.107	0.078	0.086	0.094	0.086	0.000	0.013
		VLR	41	0.065	0.125	0.083	0.090	0.104	0.092	0.000	0.014
		VLS	21	0.047	0.090	0.055	0.058	0.069	0.062	0.000	0.011
	EC	BR1	40	0.036	0.092	0.047	0.057	0.065	0.057	0.000	0.013
		BR2	41	0.040	0.097	0.052	0.060	0.067	0.060	0.000	0.011
		D1	42	0.026	0.094	0.046	0.052	0.065	0.056	0.000	0.017
		VLR	41	0.034	0.121	0.047	0.054	0.061	0.054	0.000	0.015
		VLS	45	0.033	0.082	0.050	0.060	0.063	0.057	0.000	0.010
	ER	BR1	30	0.043	0.079	0.056	0.060	0.067	0.062	0.000	0.009
		D2	30	0.050	0.087	0.057	0.070	0.077	0.067	0.000	0.011
	SL	BR1	41	0.020	0.080	0.038	0.049	0.060	0.048	0.000	0.015
		BR2	41	0.024	0.064	0.037	0.047	0.055	0.046	0.000	0.012
		D1	40	0.036	0.072	0.046	0.053	0.058	0.053	0.000	0.009
		D2	40	0.027	0.071	0.047	0.055	0.062	0.053	0.000	0.011
		VLR	42	-0.003	0.154	0.039	0.053	0.069	0.052	0.001	0.027
		VLS	46	0.029	0.066	0.041	0.050	0.056	0.049	0.000	0.010
	Combined		742	-0.158	0.129	-0.055	-0.009	0.017	-0.015	0.002	0.049

Spectral index	Species	L F T	No. of obs.	Minimum	Maximum	1st Quartile	Median	3rd Quartile	Mean	Variance (n-1)	Std. dev. (n-1)
PSRI	AK	BR1	41	-0.102	0.018	-0.069	-0.034	-0.004	-0.037	0.001	0.037
		BR2	40	-0.095	-0.028	-0.076	-0.068	-0.052	-0.065	0.000	0.017
		D1	40	-0.101	-0.017	-0.075	-0.056	-0.034	-0.057	0.001	0.026
		D2	40	-0.093	-0.009	-0.069	-0.056	-0.047	-0.056	0.000	0.017
		VLR	41	-0.132	-0.040	-0.104	-0.096	-0.077	-0.091	0.000	0.021
		VLS	21	-0.158	-0.045	-0.110	-0.098	-0.085	-0.096	0.001	0.023
	EC	BR1	40	-0.033	0.056	-0.003	0.008	0.024	0.010	0.000	0.019
		BR2	41	-0.037	0.075	-0.004	0.007	0.036	0.014	0.001	0.028
		D1	42	-0.027	0.081	-0.004	0.017	0.032	0.016	0.001	0.025
		VLR	41	-0.038	0.109	-0.020	0.007	0.044	0.014	0.002	0.040
		VLS	45	-0.113	0.068	-0.012	0.007	0.026	0.005	0.001	0.034
	ER	BR1	30	-0.093	-0.025	-0.071	-0.059	-0.050	-0.060	0.000	0.017
		D2	30	-0.096	-0.002	-0.072	-0.061	-0.044	-0.055	0.001	0.024
	SL	BR1	41	-0.027	0.118	0.004	0.036	0.066	0.035	0.001	0.038
		BR2	41	-0.035	0.129	0.012	0.030	0.048	0.032	0.001	0.035
		D1	40	-0.012	0.094	0.001	0.021	0.040	0.023	0.001	0.027
		D2	40	-0.052	0.082	-0.009	0.001	0.018	0.006	0.001	0.026
		VLR	42	-0.074	0.037	-0.017	-0.002	0.010	-0.005	0.001	0.024
		VLS	46	-0.069	0.084	-0.017	0.005	0.037	0.009	0.001	0.037
Red-edge NDVI	Combined		742	0.369	0.717	0.534	0.576	0.619	0.574	0.004	0.063
	AK	BR1	41	0.546	0.717	0.608	0.653	0.681	0.645	0.002	0.042
		BR2	40	0.514	0.678	0.565	0.583	0.599	0.583	0.001	0.033
		D1	40	0.419	0.630	0.550	0.575	0.592	0.568	0.002	0.040
		D2	40	0.477	0.639	0.537	0.563	0.587	0.563	0.001	0.037
		VLR	41	0.381	0.642	0.483	0.538	0.590	0.538	0.005	0.068
		VLS	21	0.499	0.613	0.536	0.542	0.577	0.555	0.001	0.029
	EC	BR1	40	0.392	0.588	0.469	0.493	0.529	0.497	0.002	0.045
		BR2	41	0.486	0.632	0.551	0.574	0.594	0.571	0.001	0.034
		D1	42	0.478	0.648	0.546	0.573	0.609	0.574	0.002	0.046
		VLR	41	0.417	0.578	0.481	0.503	0.535	0.506	0.001	0.037
		VLS	45	0.429	0.597	0.491	0.524	0.560	0.524	0.002	0.043
	ER	BR1	30	0.461	0.616	0.540	0.564	0.573	0.557	0.001	0.033
		D2	30	0.369	0.581	0.502	0.536	0.556	0.520	0.003	0.055
	SL	BR1	41	0.538	0.704	0.598	0.623	0.632	0.620	0.001	0.037
		BR2	41	0.403	0.681	0.562	0.617	0.652	0.597	0.004	0.064
		D1	40	0.588	0.715	0.632	0.665	0.681	0.656	0.001	0.035
		D2	40	0.482	0.694	0.605	0.627	0.648	0.624	0.002	0.041
		VLR	42	0.447	0.704	0.551	0.611	0.654	0.601	0.005	0.068
		VLS	46	0.471	0.688	0.566	0.590	0.623	0.592	0.002	0.045
Re d-	Combined		742	0.095	0.454	0.311	0.335	0.360	0.336	0.001	0.038

Spectral index	Species	L F T	No. of obs.	Minimum	Maximum	1st Quartile	Median	3rd Quartile	Mean	Variance (n-1)	Std. dev. (n-1)
	AK	BR1	41	0.304	0.416	0.339	0.364	0.378	0.361	0.001	0.029
		BR2	40	0.322	0.412	0.345	0.363	0.375	0.361	0.000	0.022
		D1	40	0.301	0.402	0.332	0.346	0.370	0.350	0.001	0.026
		D2	40	0.344	0.454	0.373	0.386	0.418	0.391	0.001	0.030
		VLR	41	0.314	0.434	0.347	0.370	0.388	0.370	0.001	0.029
		VLS	21	0.269	0.379	0.293	0.299	0.319	0.305	0.001	0.024
	EC	BR1	40	0.260	0.382	0.312	0.331	0.346	0.328	0.001	0.029
		BR2	41	0.253	0.401	0.317	0.332	0.345	0.330	0.001	0.030
		D1	42	0.275	0.398	0.322	0.343	0.371	0.345	0.001	0.034
		VLR	41	0.276	0.404	0.310	0.330	0.353	0.333	0.001	0.033
		VLS	45	0.212	0.378	0.306	0.333	0.350	0.326	0.001	0.035
	ER	BR1	30	0.267	0.387	0.310	0.328	0.339	0.326	0.001	0.028
		D2	30	0.277	0.400	0.319	0.342	0.371	0.342	0.001	0.034
	SL	BR1	41	0.250	0.336	0.295	0.310	0.318	0.308	0.000	0.020
		BR2	41	0.248	0.328	0.287	0.298	0.310	0.297	0.000	0.017
		D1	40	0.279	0.380	0.318	0.333	0.343	0.330	0.000	0.022
		D2	40	0.277	0.368	0.321	0.335	0.351	0.333	0.001	0.023
		VLR	42	0.095	0.375	0.302	0.322	0.353	0.315	0.003	0.057
		VLS	46	0.174	0.389	0.293	0.312	0.336	0.312	0.001	0.037
Red-edge Position	Combined		742	727.090	738.876	729.425	730.385	731.355	730.504	2.617	1.618
	AK	BR1	41	728.537	733.487	729.415	729.997	730.541	730.065	0.871	0.933
		BR2	40	729.738	734.345	730.805	731.319	731.840	731.506	1.088	1.043
		D1	40	729.577	736.343	730.528	730.992	731.568	731.188	1.416	1.190
		D2	40	729.305	733.131	730.644	731.143	731.760	731.216	0.820	0.905
		VLR	41	729.277	737.818	730.393	731.465	732.704	731.914	3.721	1.929
		VLS	21	729.034	732.731	729.916	730.446	731.145	730.557	0.730	0.855
	EC	BR1	40	729.957	736.447	731.309	732.119	732.956	732.265	1.816	1.348
		BR2	41	729.353	732.550	729.995	730.350	730.727	730.401	0.389	0.624
		D1	42	728.012	731.806	729.614	730.007	730.584	730.064	0.606	0.779
		VLR	41	729.838	734.139	730.651	731.346	732.020	731.467	1.243	1.115
		VLS	45	729.220	734.675	729.912	730.602	731.682	731.031	2.114	1.454
	ER	BR1	30	728.732	733.035	730.240	730.675	731.266	730.761	0.916	0.957
		D2	30	729.186	738.876	730.577	731.494	732.474	731.986	5.477	2.340
	SL	BR1	41	727.701	730.960	728.503	728.902	729.376	728.987	0.585	0.765
		BR2	41	727.793	735.392	728.849	729.482	730.169	729.783	2.159	1.469
		D1	40	727.495	730.813	728.149	728.700	729.463	728.818	0.680	0.825
		D2	40	728.052	734.264	728.555	728.981	729.397	729.142	1.075	1.037
		VLR	42	727.090	734.063	727.913	728.906	730.261	729.342	3.127	1.768
		VLS	46	727.886	732.973	729.090	729.521	730.383	729.687	1.224	1.106
725-702	Combined		742	0.531	2.087	0.942	1.107	1.276	1.120	0.063	0.250
	AK	BR1	41	0.994	2.087	1.333	1.525	1.688	1.527	0.077	0.277

Spectral index	Species	L F T	No. of obs.	Minimum	Maximum	1st Quartile	Median	3rd Quartile	Mean	Variance (n-1)	Std. dev. (n-1)
		BR2	40	1.106	1.851	1.243	1.337	1.462	1.350	0.022	0.150
		D1	40	0.873	1.493	1.138	1.291	1.363	1.246	0.029	0.171
		D2	40	0.874	1.431	1.016	1.159	1.251	1.138	0.020	0.140
		VLR	41	0.721	1.378	0.883	1.076	1.226	1.072	0.038	0.195
		VLS	21	0.852	1.267	0.984	1.062	1.137	1.061	0.012	0.111
	EC	BR1	40	0.591	1.208	0.726	0.861	0.959	0.859	0.025	0.158
		BR2	41	0.688	1.524	0.998	1.133	1.211	1.134	0.034	0.183
		D1	42	0.643	1.586	0.923	1.049	1.209	1.051	0.044	0.209
		VLR	41	0.553	1.116	0.719	0.794	0.904	0.820	0.021	0.143
		VLS	45	0.531	1.388	0.767	0.854	0.989	0.887	0.033	0.182
	ER	BR1	30	0.927	1.393	1.100	1.200	1.276	1.178	0.017	0.130
		D2	30	0.789	1.215	0.963	1.037	1.144	1.041	0.014	0.117
	SL	BR1	41	0.825	1.723	1.014	1.072	1.228	1.148	0.048	0.219
		BR2	41	0.557	1.486	0.897	1.153	1.355	1.111	0.064	0.253
		D1	40	1.006	1.728	1.225	1.363	1.454	1.331	0.030	0.173
		D2	40	0.879	1.758	1.090	1.173	1.272	1.199	0.039	0.199
		VLR	42	0.626	1.558	0.898	1.081	1.234	1.067	0.051	0.225
		VLS	46	0.740	1.385	0.956	1.081	1.148	1.069	0.019	0.137
725-702 Ratio of the 2nd derivative	Combined		742	-23.568	165.363	-1.382	-0.937	-0.681	-1.079	45.648	6.756
	AK	BR1	41	-1.981	-0.197	-0.617	-0.400	-0.327	-0.528	0.112	0.334
		BR2	40	-1.281	-0.242	-0.751	-0.592	-0.508	-0.653	0.055	0.234
		D1	40	-10.427	-0.440	-1.175	-0.700	-0.618	-1.152	2.533	1.591
		D2	40	-17.146	-0.579	-1.697	-1.097	-0.921	-1.941	8.346	2.889
		VLR	41	-23.568	37.974	-2.131	-0.967	-0.641	-1.177	53.918	7.343
		VLS	21	-1.908	-0.738	-1.372	-1.070	-0.887	-1.132	0.090	0.300
	EC	BR1	40	-21.165	6.386	-2.398	-1.492	-0.980	-2.548	20.264	4.502
		BR2	41	-4.818	-0.431	-1.286	-0.965	-0.739	-1.152	0.515	0.717
		D1	42	-19.213	-0.432	-1.504	-1.070	-0.788	-2.129	11.925	3.453
		VLR	41	-20.513	165.363	-3.065	-2.317	-1.254	1.440	715.686	26.752
		VLS	45	-5.963	17.145	-2.380	-1.401	-0.966	-0.969	14.266	3.777
	ER	BR1	30	-1.739	-0.574	-1.192	-0.959	-0.866	-1.037	0.088	0.296
		D2	30	-6.923	-0.762	-1.831	-1.530	-1.047	-1.691	1.239	1.113
	SL	BR1	41	-2.191	-0.357	-1.092	-0.882	-0.679	-0.920	0.162	0.403
		BR2	41	-4.297	1.201	-1.381	-0.775	-0.585	-1.112	0.948	0.974
		D1	40	-1.131	-0.352	-0.758	-0.612	-0.550	-0.670	0.037	0.193
		D2	40	-2.168	-0.357	-0.965	-0.813	-0.712	-0.876	0.128	0.358
		VLR	42	-6.749	-0.495	-1.268	-0.919	-0.754	-1.275	1.325	1.151
		VLS	46	-9.335	-0.552	-1.162	-0.931	-0.824	-1.165	1.572	1.254

APPENDIX 6. LEAF ELEMENTAL CONTENT COMPARED TO GLOBAL MEAN OF PLANT LEAF ELEMENTAL CONTENT

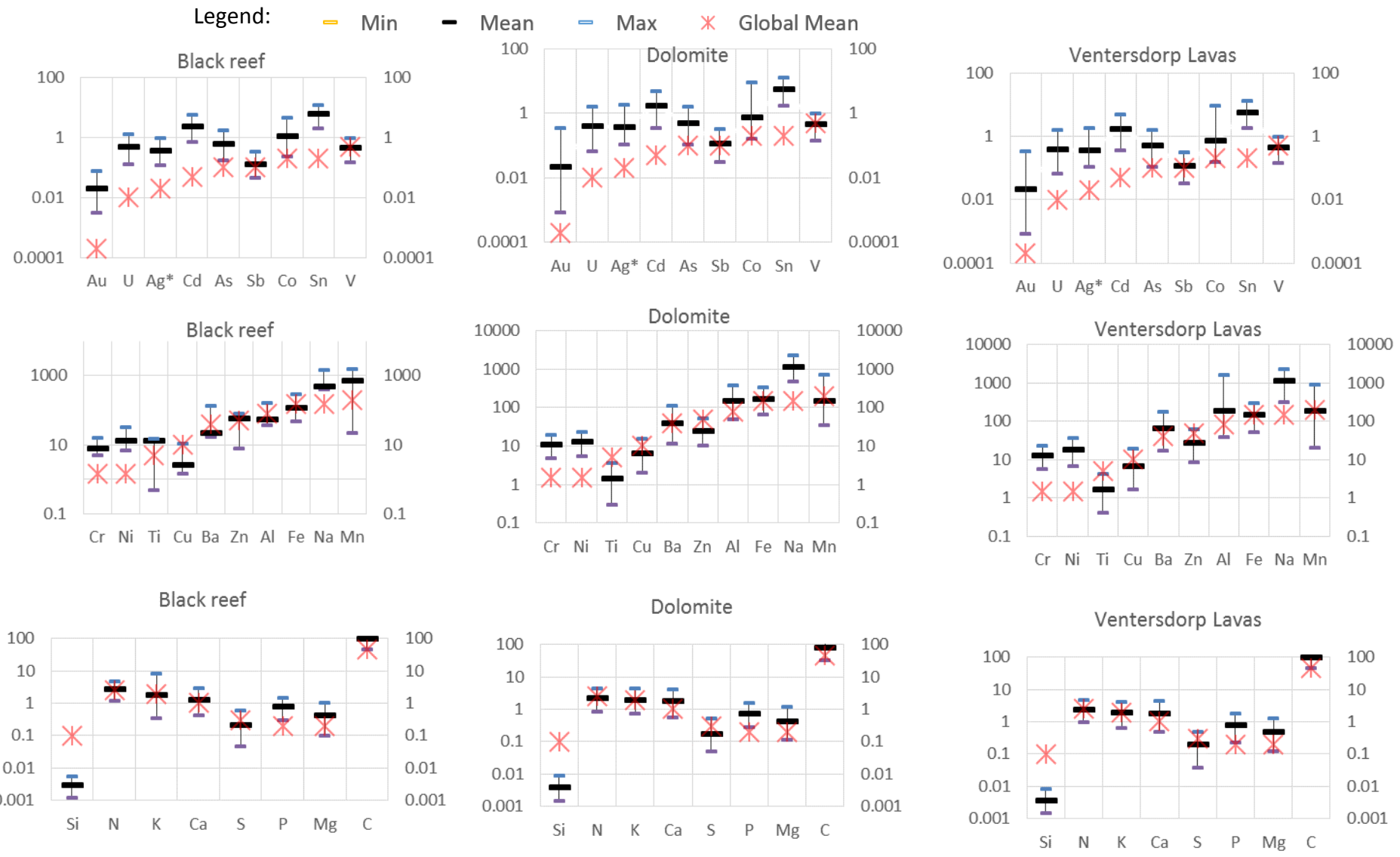

APPENDIX 7. BOX PLOTS OF LEAF ELEMENTAL CONTENT PER SPECIES AND PER GEOLOGY

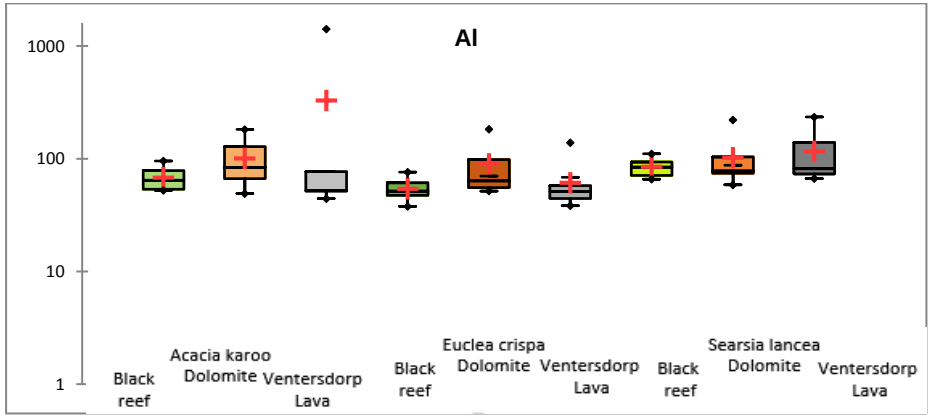

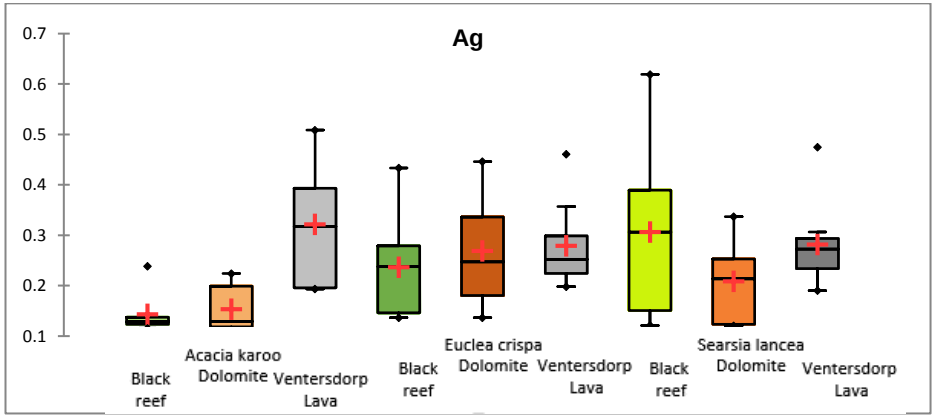

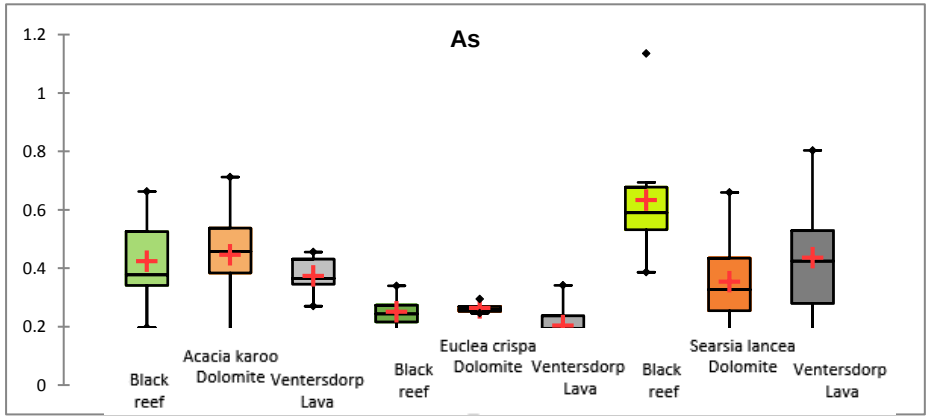

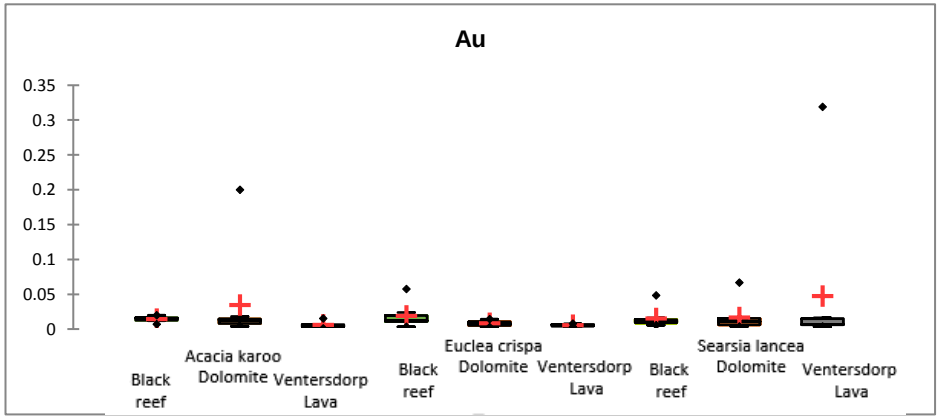

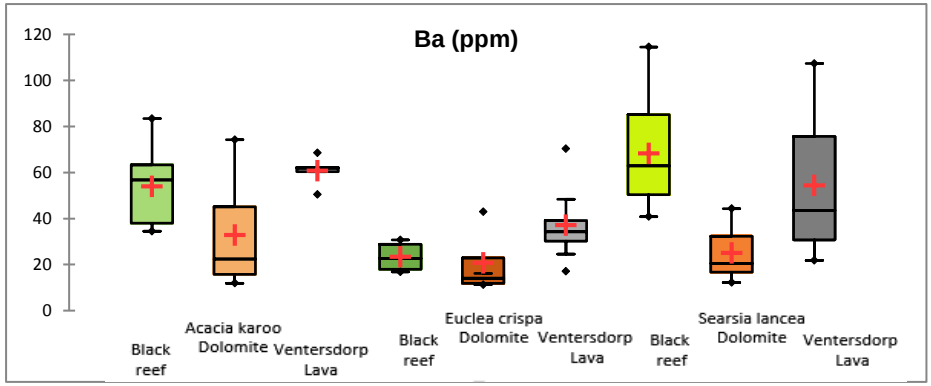
Ba (ppm)
120
100
80
60
40
20
0
Black reef
Acacia karoo
Dolomite
Ventersdorp Lava
Black reef
Euclea crispa
Dolomite
Ventersdorp Lava
Black reef
Searsia lancea
Dolomite
Ventersdorp Lava

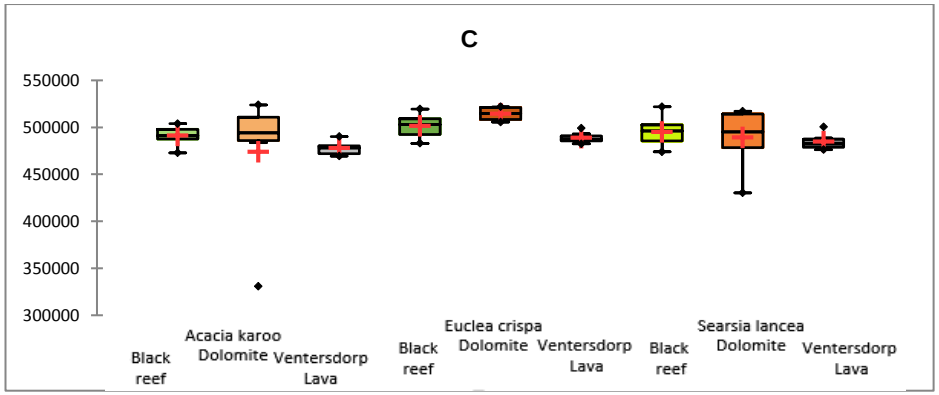
C
550000
500000
450000
400000
350000
300000
Black reef
Acacia karoo
Dolomite
Ventersdorp Lava
Black reef
Euclea crispa
Dolomite
Ventersdorp Lava
Black reef
Searsia lancea
Dolomite
Ventersdorp Lava

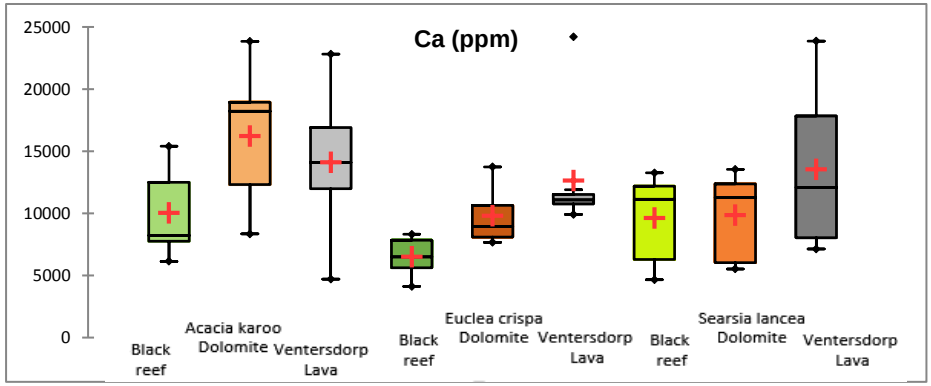
Ca (ppm)
25000
20000
15000
10000
5000
0
Black reef
Acacia karoo
Dolomite
Ventersdorp Lava
Black reef
Euclea crispa
Dolomite
Ventersdorp Lava
Black reef
Searsia lancea
Dolomite
Ventersdorp Lava

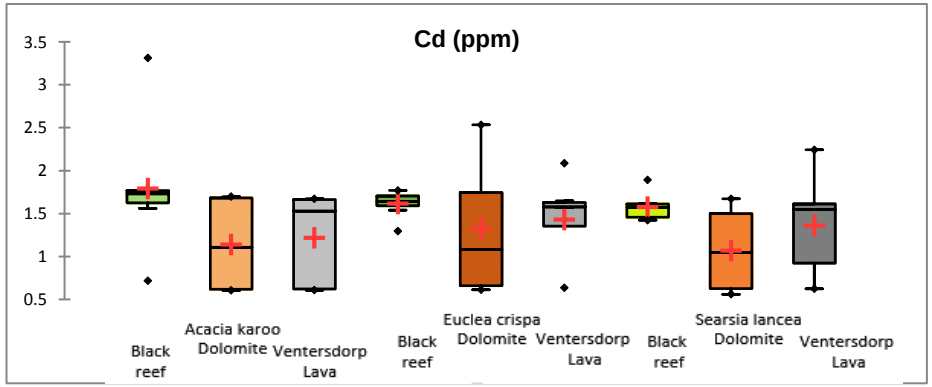
Cd (ppm)
3.5
3
2.5
2
1.5
1
0.5
Black reef
Acacia karoo
Dolomite
Ventersdorp Lava
Black reef
Euclea crispa
Dolomite
Ventersdorp Lava
Black reef
Searsia lancea
Dolomite
Ventersdorp Lava

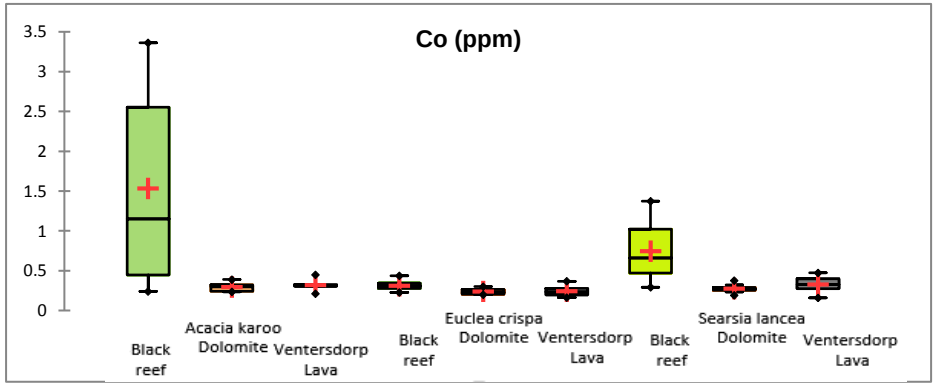
Co (ppm)
3.5
3
2.5
2
1.5
1
0.5
0
Black reef
Acacia karoo
Dolomite
Ventersdorp Lava
Black reef
Euclea crispa
Dolomite
Ventersdorp Lava
Black reef
Searsia lancea
Dolomite
Ventersdorp Lava

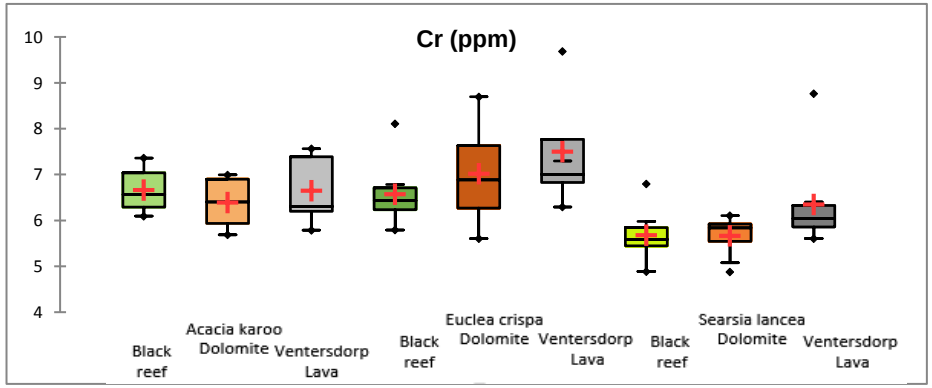
Cr (ppm)
10
9
8
7
6
5
4
Black reef
Acacia karoo
Dolomite
Ventersdorp Lava
Black reef
Euclea crispa
Dolomite
Ventersdorp Lava
Black reef
Searsia lancea
Dolomite
Ventersdorp Lava

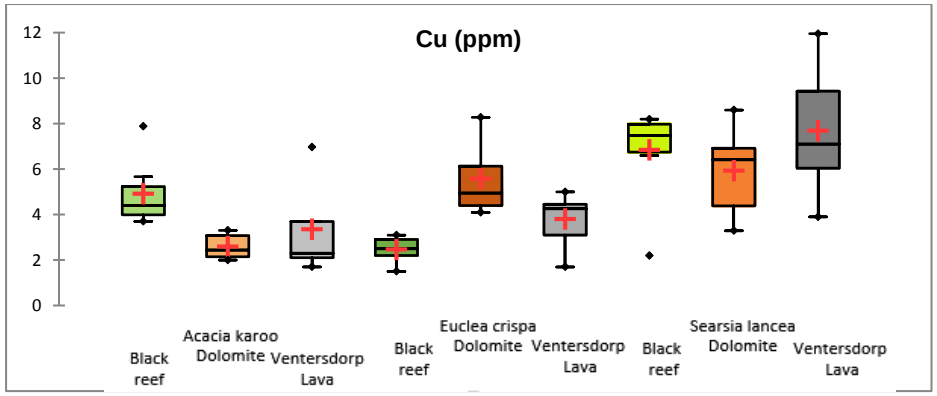
Cu (ppm)
12
10
8
6
4
2
0
Black reef
Acacia karoo
Dolomite
Ventersdorp Lava
Black reef
Euclea crispa
Dolomite
Ventersdorp Lava
Black reef
Searsia lancea
Dolomite
Ventersdorp Lava

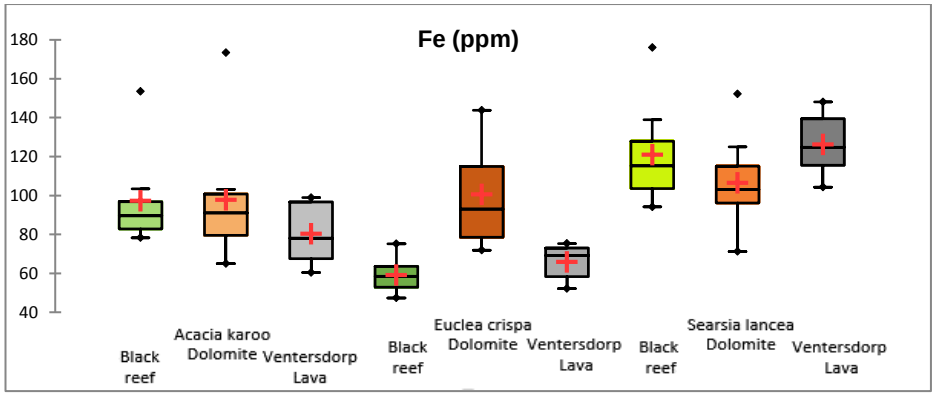
Fe (ppm)
180
160
140
120
100
80
60
40
Black reef
Acacia karoo
Dolomite
Ventersdorp Lava
Black reef
Euclea crispa
Dolomite
Ventersdorp Lava
Black reef
Searsia lancea
Dolomite
Ventersdorp Lava

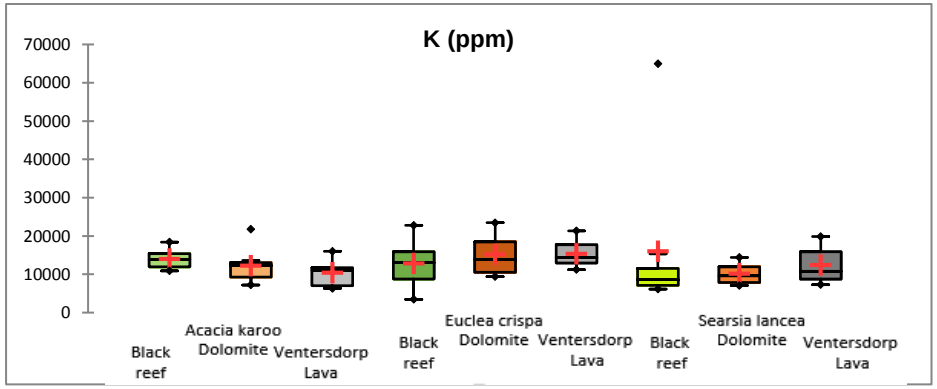
K (ppm)
70000
60000
50000
40000
30000
20000
10000
0
Black reef
Acacia karoo
Dolomite
Ventersdorp Lava
Black reef
Euclea crispa
Dolomite
Ventersdorp Lava
Black reef
Searsia lancea
Dolomite
Ventersdorp Lava

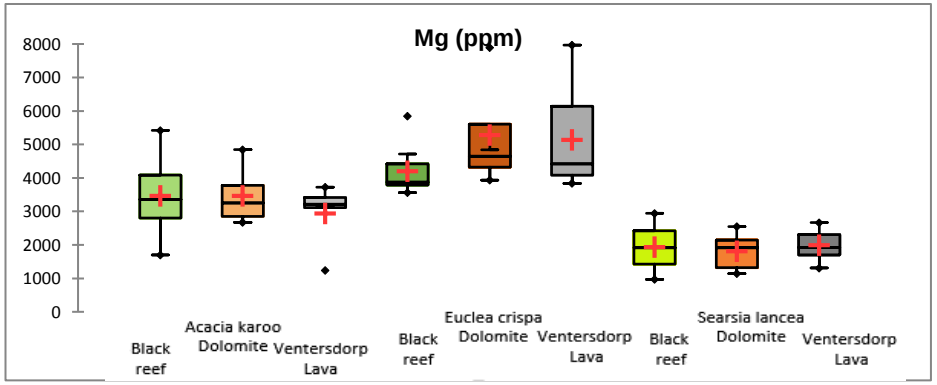
Mg (ppm)
8000
7000
6000
5000
4000
3000
2000
1000
0
Black reef
Acacia karoo
Dolomite
Ventersdorp Lava
Black reef
Euclea crispa
Dolomite
Ventersdorp Lava
Black reef
Searsia lancea
Dolomite
Ventersdorp Lava

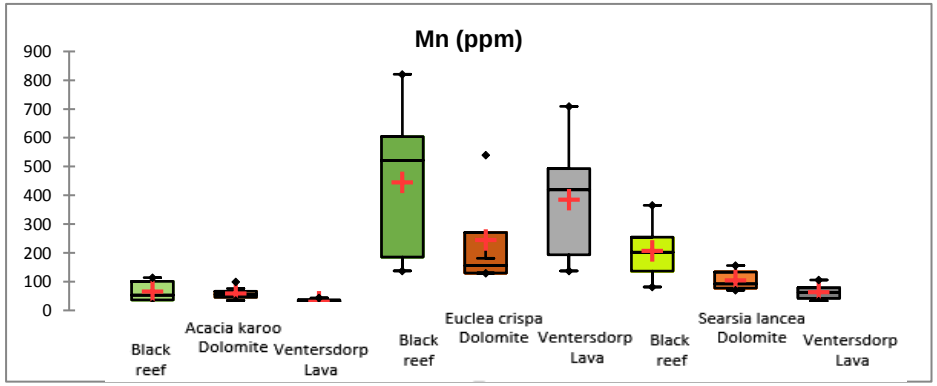
Mn (ppm)
900
800
700
600
500
400
300
200
100
0
Black reef
Acacia karoo
Dolomite
Ventersdorp Lava
Black reef
Euclea crispa
Dolomite
Ventersdorp Lava
Black reef
Searsia lancea
Dolomite
Ventersdorp Lava

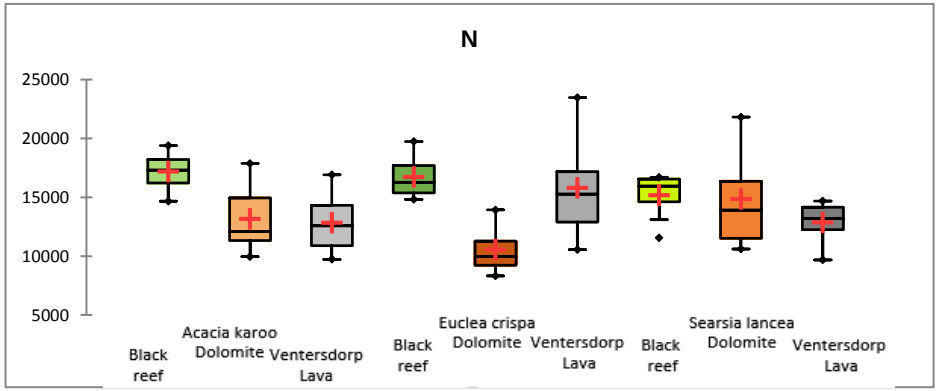
N
25000
20000
15000
10000
5000
Black reef
Acacia karoo
Dolomite
Ventersdorp Lava
Black reef
Euclea crispa
Dolomite
Ventersdorp Lava
Black reef
Searsia lancea
Dolomite
Ventersdorp Lava

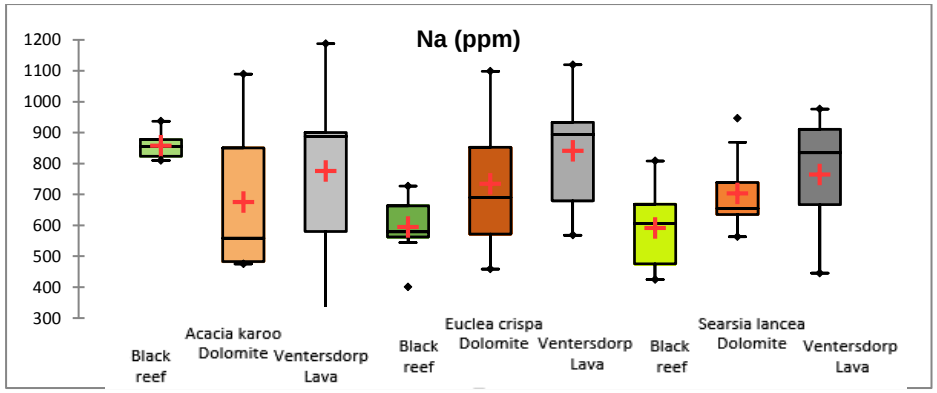
Na (ppm)
1200
1100
1000
900
800
700
600
500
400
300
Black reef
Acacia karoo
Dolomite
Ventersdorp Lava
Black reef
Euclea crispa
Dolomite
Ventersdorp Lava
Black reef
Searsia lancea
Dolomite
Ventersdorp Lava

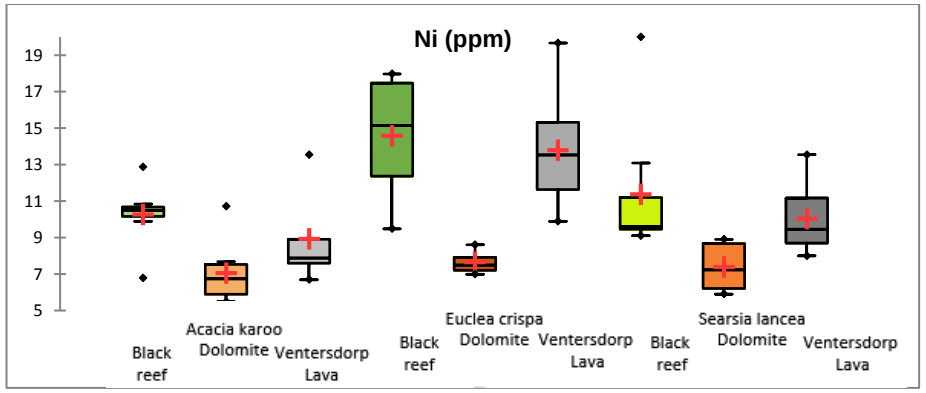
Ni (ppm)
19
17
15
13
11
9
7
5
Black reef
Acacia karoo
Dolomite
Ventersdorp Lava
Black reef
Euclea crispa
Dolomite
Ventersdorp Lava
Black reef
Searsia lancea
Dolomite
Ventersdorp Lava

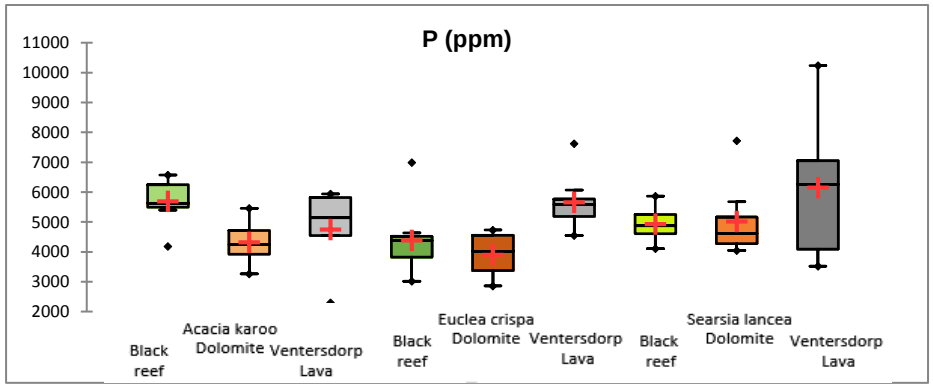
P (ppm)
11000
10000
9000
8000
7000
6000
5000
4000
3000
2000
Black reef
Acacia karoo
Dolomite
Ventersdorp Lava
Black reef
Euclea crispa
Dolomite
Ventersdorp Lava
Black reef
Searsia lancea
Dolomite
Ventersdorp Lava

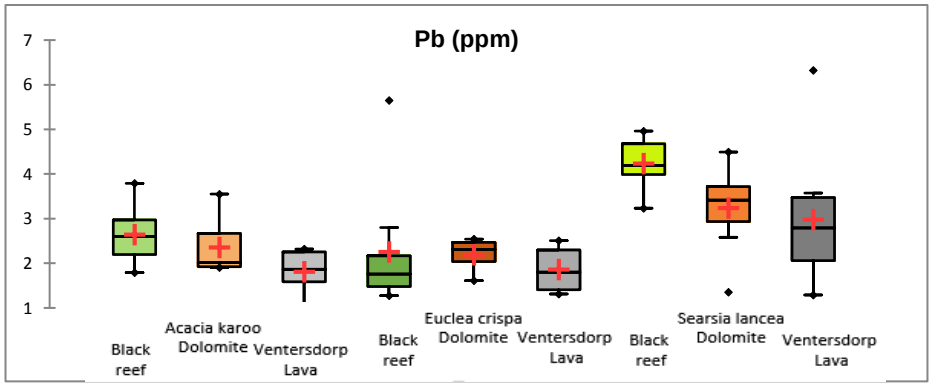
Pb (ppm)
7
6
5
4
3
2
1
Black reef
Acacia karoo
Dolomite
Ventersdorp Lava
Black reef
Euclea crispa
Dolomite
Ventersdorp Lava
Black reef
Searsia lancea
Dolomite
Ventersdorp Lava

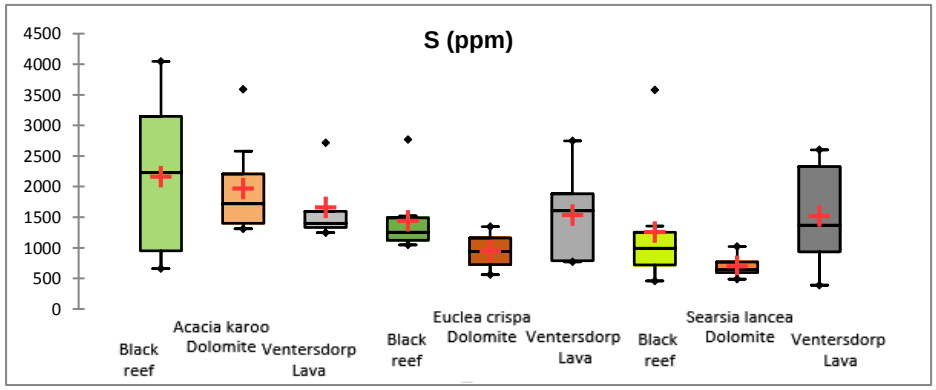
S (ppm)
4500
4000
3500
3000
2500
2000
1500
1000
500
0
Black reef
Acacia karoo
Dolomite
Ventersdorp Lava
Black reef
Euclea crispa
Dolomite
Ventersdorp Lava
Black reef
Searsia lancea
Dolomite
Ventersdorp Lava

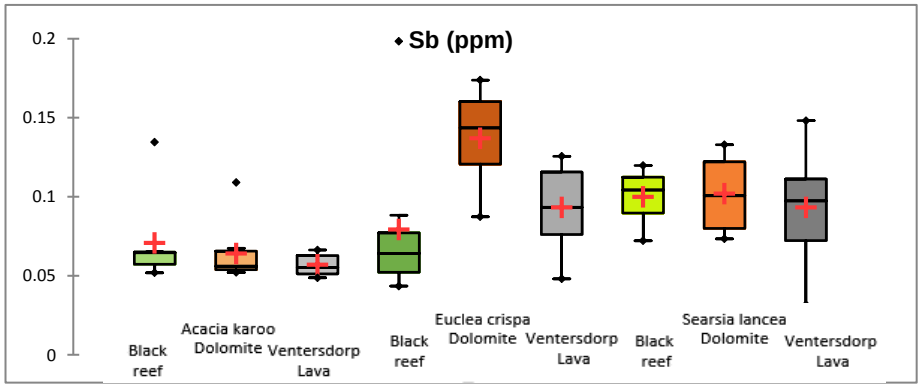
Sb (ppm)
0.2
0.15
0.1
0.05
0
Black reef
Acacia karoo
Dolomite
Ventersdorp Lava
Black reef
Euclea crispa
Dolomite
Ventersdorp Lava
Black reef
Searsia lancea
Dolomite
Ventersdorp Lava

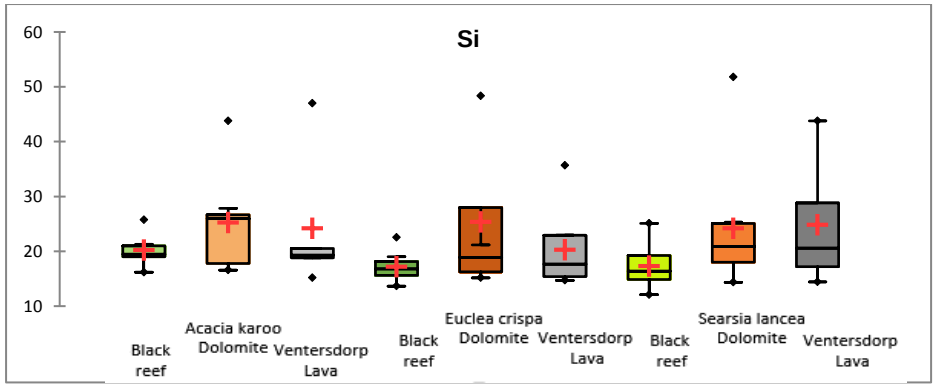
Si
60
50
40
30
20
10
Black reef
Acacia karoo
Dolomite
Ventersdorp Lava
Black reef
Euclea crispa
Dolomite
Ventersdorp Lava
Black reef
Searsia lancea
Dolomite
Ventersdorp Lava

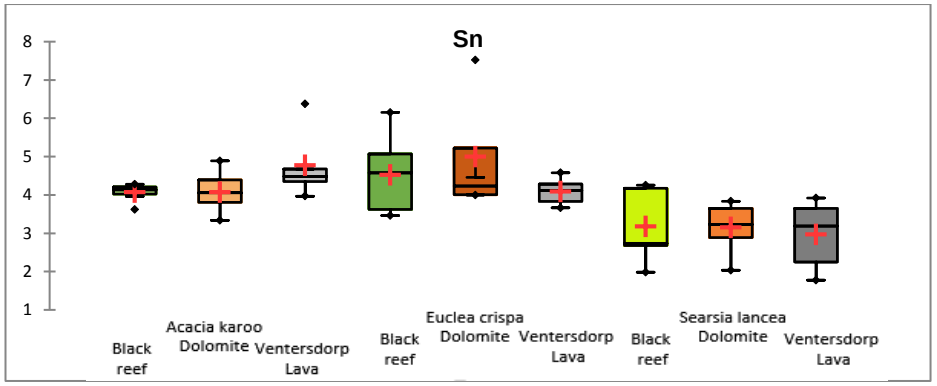
Sn
8
7
6
5
4
3
2
1
Black reef
Acacia karoo
Dolomite
Ventersdorp Lava
Black reef
Euclea crispa
Dolomite
Ventersdorp Lava
Black reef
Searsia lancea
Dolomite
Ventersdorp Lava

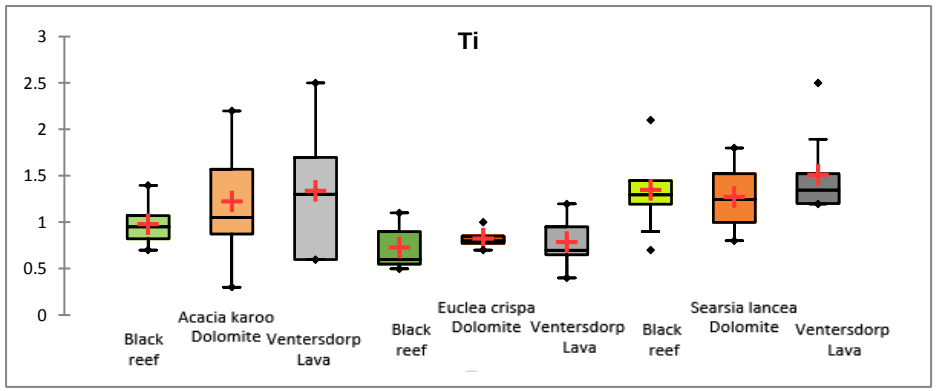
Ti
3
2.5
2
1.5
1
0.5
0
Black reef
Acacia karoo
Dolomite
Ventersdorp Lava
Black reef
Euclea crispa
Dolomite
Ventersdorp Lava
Black reef
Searsia lancea
Dolomite
Ventersdorp Lava

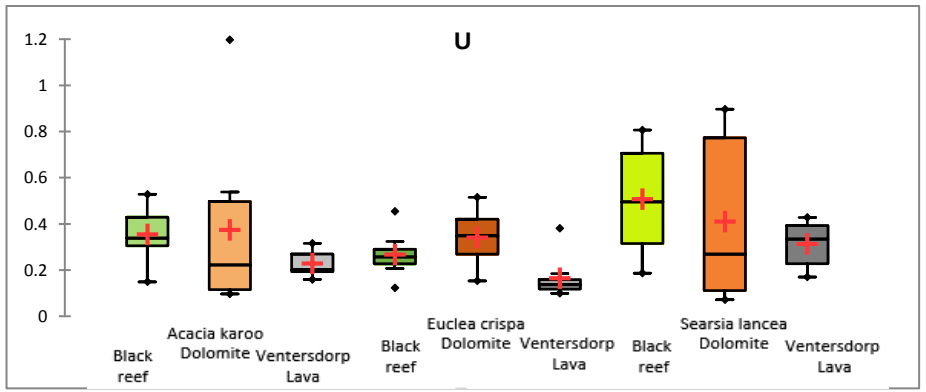
U
1.2
1
0.8
0.6
0.4
0.2
0
Black reef
Acacia karoo
Dolomite
Ventersdorp Lava
Black reef
Euclea crispa
Dolomite
Ventersdorp Lava
Black reef
Searsia lancea
Dolomite
Ventersdorp Lava

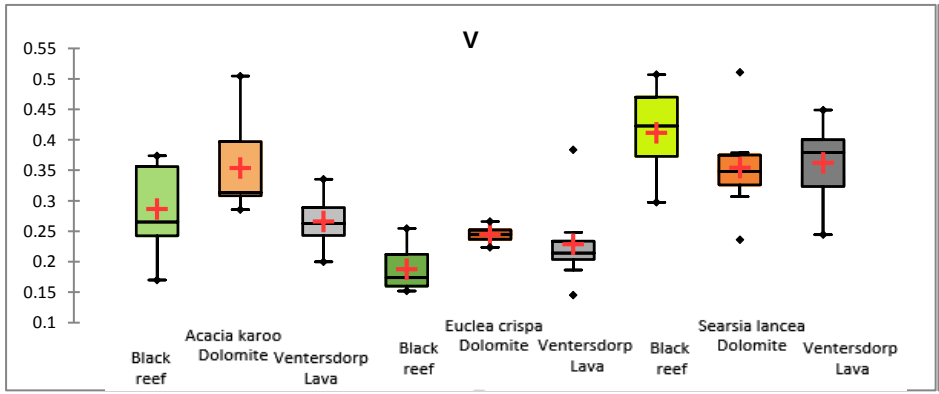
V
0.55
0.5
0.45
0.4
0.35
0.3
0.25
0.2
0.15
0.1
Black reef
Acacia karoo
Dolomite
Ventersdorp Lava
Black reef
Euclea crispa
Dolomite
Ventersdorp Lava
Black reef
Searsia lancea
Dolomite
Ventersdorp Lava

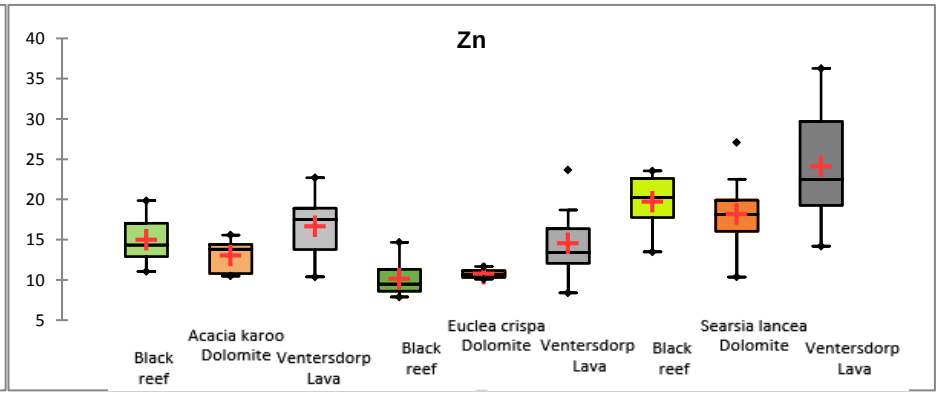
Zn
40
35
30
25
20
15
10
5
Black reef
Acacia karoo
Dolomite
Ventersdorp Lava
Black reef
Euclea crispa
Dolomite
Ventersdorp Lava
Black reef
Searsia lancea
Dolomite
Ventersdorp Lava

APPENDIX 8. VARIABLES CHARACTERISATION CORELLATION COEFFICIENTS PER VEGETATION INDEX

VI	Measure: Elemental content/ratio	AK			EC			SL			Combined		
		Element/ ratio	Correlation coefficient	p-values	Element/ ratio	Correlation coefficient	p-values	Element/ ratio	Correlation coefficient	p-values	Element/ ratio	Correlation coefficient	p-values
725-702Ratio 1st Der	Soils				Rb	0.701	0.002				Cr	0.340	0.010
											Cu	-0.439	0.001
											Fe	-0.367	0.005
											Ti	-0.428	0.001
	Leaves							Ba	-0.577	0.006	Mn	-0.437	0.001
											Ag	-0.376	0.004
											Fe	0.343	0.009
	Bioconcentration factors							Ti	0.564	0.007	Cr	-0.351	0.008
											Cu	0.425	0.001
											Fe	0.424	0.001
											Mn	-0.503	< 0.0001
	Soil:leaf ratios				Na:K leaf ratio	-0.701	0.002				Si:Ti Soil ratio	0.428	0.001
											Mg:Mn leaf ratio	0.413	0.002
											Mg:Mn soil ratio	-0.354	0.007
											Si:Mn leaf ratio	0.399	0.002
											Si:Mn leaf:soil ratio	0.465	0.000
NDVI	Soils				Zr	-0.713	0.002						
	Leaves	Ti	-0.653	0.004	Cu	0.716	0.002	Ba	-0.679	0.001	Cr	-0.359	0.006
					Mn	-0.618	0.010				Cu	0.696	< 0.0001
					Ni	-0.669	0.004				Fe	0.592	< 0.0001
					S	-0.620	0.009				Mg	-0.598	< 0.0001
											Pb	0.399	0.002
											Sn	-0.531	< 0.0001
											V	0.409	0.002
	Bioconcentration factors	Ti	-0.600	0.010	Mn	-0.762	0.001	Cu	0.546	0.009	Cu	0.750	< 0.0001
					Ni1	-0.777	0.000	Zn	0.575	0.006	Fe	0.515	< 0.0001
					Ni2	-0.706	0.002				Mg	-0.563	< 0.0001
					Zn	0.691	0.003				Zn	0.473	0.000
	Soil: leaf ratios				Mg:Mn leaf ratio	0.615	0.010				Ca:Mg leaf ratio	0.454	0.000

VI	Measure: Elemental content/ratio	AK			EC			SL			Combined		
		Element/ ratio	Correlation coefficient	p-values	Element/ ratio	Correlation coefficient	p-values	Element/ ratio	Correlation coefficient	p-values	Element/ ratio	Correlation coefficient	p-values
					Si:Mn leaf:soil ratio	0.743	0.001				Zn:Cd leaf ratio	0.442	0.001
NDWI	Soils										Sr	-0.350	0.008
		Si	-0.682	0.002				Ba	-0.665	0.001	Mn	-0.547	< 0.0001
								Pb	-0.562	0.007	Pb	-0.533	< 0.0001
	Leaves										Sb	-0.438	0.001
		Si	-0.701	0.002				Cu	0.548	0.009	Mn	-0.408	0.002
	Bioconcentration factors							Zn	0.686	0.001	Pb	-0.391	0.003
		(Leaf ca): (al: ca Soil)	0.628	0.006							Mg:Mn leaf ratio	0.591	< 0.0001
	Soil: leaf ratios	Al BCF: Ca BCF	0.628	0.006							Si:Mn leaf ratio	0.435	0.001
	Soil: plant characteristics							Leaf Water content %	0.549	0.009			
PSRI	Soils	Cu	-0.618	0.007									
		Mn	0.725	0.001				As	0.545	0.010	Mn	0.621	< 0.0001
											Pb	0.450	0.000
											S	-0.349	0.008
	Leaves										Sb	0.356	0.007
		Fe	0.662	0.003							Mn	0.397	0.002
	Bioconcentration factors												
											Si:Mn leaf ratio	-0.488	0.000
											Leaf Ca :soil Al	-0.372	0.005
	Soil:leaf ratios										Mg:Mn leaf ratio	-0.645	< 0.0001
	Soil:plant characteristics	soil pH	0.620	0.007				Leaf Water content %	-0.608	0.003	soil pH	0.379	0.004
Red-edge NDVI					K2	0.639	0.007						
	Soils				Rb	0.725	0.001						
		Ti	-0.664	0.003	Mn	-0.669	0.004	Ba	-0.609	0.003	Au	0.361	0.006
								Sn	-0.566	0.007	Cu	0.599	< 0.0001
											Fe	0.539	< 0.0001
											Mg	-0.498	< 0.0001
											Pb	0.401	0.002
											Sn	-0.483	0.000
	Leaves										Zn	0.465	0.000
		Ti	-0.672	0.003	Mn	-0.694	0.003				Cu	0.708	< 0.0001
					Na	0.640	0.007	Cu	0.621	0.003	Fe	0.513	< 0.0001
											Mg	-0.484	0.000
	Bioconcentration factors										Mn	-0.349	0.008

VI	Measure: Elemental content/ratio	AK			EC			SL			Combined		
		Element/ ratio	Correlation coefficient	p-values	Element/ ratio	Correlation coefficient	p-values	Element/ ratio	Correlation coefficient	p-values	Element/ ratio	Correlation coefficient	p-values
											Zn	0.356	0.007
		Si:Ti leaf:soil ratio	0.616	0.008	Na:K leaf ratio	-0.676	0.004				Ca:Mg leaf ratio	0.364	0.006
					Mg:Mn leaf ratio	0.652	0.006						
	Soil:leaf ratios				Si:Mn leaf:soil ratio	0.642	0.007						
REP = 700 + 40(Rre- R700:R740-R700)	Soils	Sr	-0.606	0.009	V	-0.618	0.010						
								Ba	0.582	0.005	Cu	-0.685	< 0.0001
								Cu	-0.564	0.007	Mg	0.490	0.000
								Zn	-0.614	0.003	Fe	-0.539	< 0.0001
											Pb	-0.401	0.002
	Leaves										Sn	0.538	< 0.0001
											Zn	-0.550	< 0.0001
					Mn	0.713	0.002	Zn	-0.548	0.009	Cu	-0.653	< 0.0001
					Ni1	0.674	0.004				Fe	-0.436	0.001
					Ni2	0.650	0.006				Mg	0.547	< 0.0001
	Bioconcentration factors										Zn	-0.405	0.002
		Si:Ti leaf:soil ratio	-0.614	0.008	Si:Mn leaf:soil ratio	-0.664	0.005				Zn:Cd leaf ratio	-0.368	0.005
											Ca:Al Leaf	0.348	0.008
	Soil:leaf ratios										Leaf Ca:Al :Soil al	-0.431	0.001
Rre = (R670 + R780):2	Soils										Sr	-0.404	0.002
		As	-0.633	0.006				As	-0.762	< 0.0001	Ag	-0.382	0.004
		Fe	-0.713	0.001				Ba	-0.730	0.000	Al	-0.407	0.002
		U	-0.707	0.001				U	-0.556	0.008	As	-0.384	0.003
											Mn	-0.423	0.001
											Pb	-0.459	0.000
											Sn	0.370	0.005
											Ti	-0.359	0.006
	Leaves										U	-0.374	0.004
								Ba	-0.635	0.002	Mn	-0.409	0.002
								Mn	-0.625	0.002	Pb	-0.366	0.005
	Bioconcentration factors							Zn	0.605	0.003			
								Si:Mn leaf:soil ratio	0.597	0.004	Mg:Mn leaf ratio	0.489	0.000
								Rb:K soil ratio	0.583	0.005	Si:Mn leaf:soil ratio	0.353	0.007
											Si:Mn leaf ratio	0.353	0.007
	Soil:leaf ratios												

APPENDIX 9. BOX PLOTS SHOWING LEAF AND SOIL ELEMENTAL RESULTS BY VEGETATION INDEX GROUP AND BY SPECIES

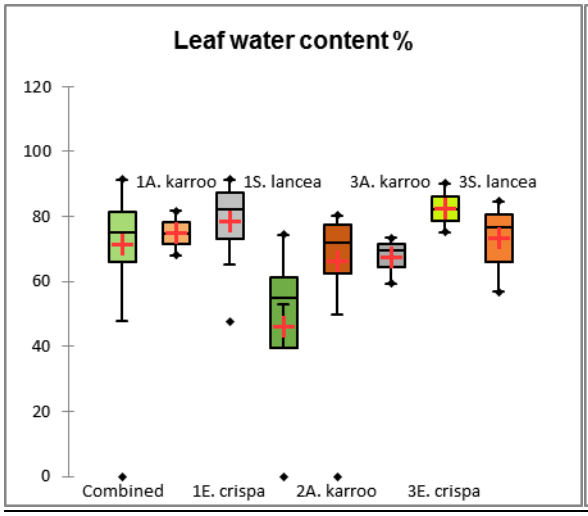

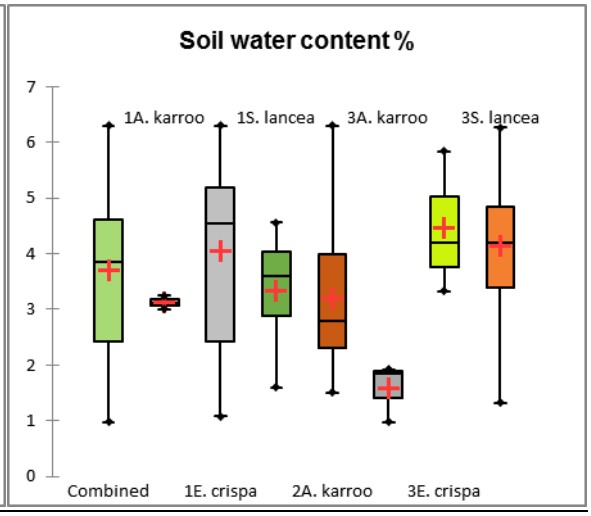

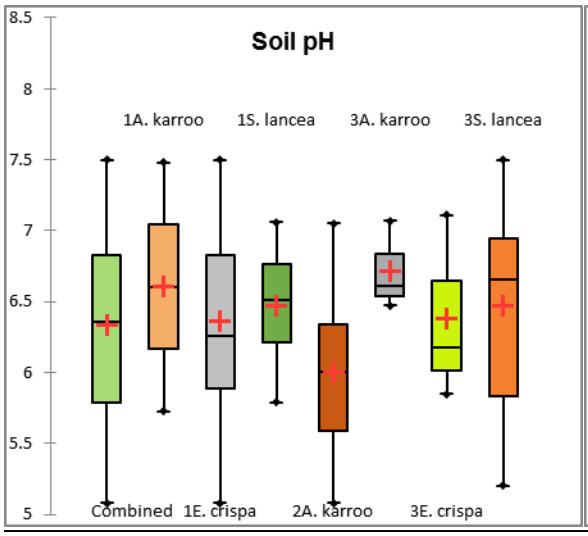

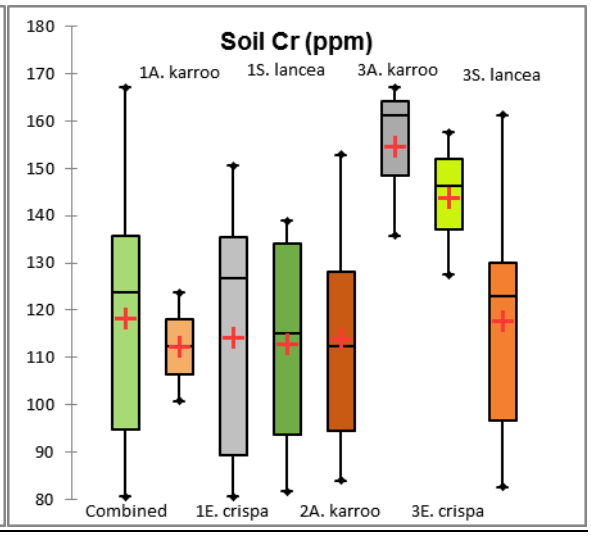

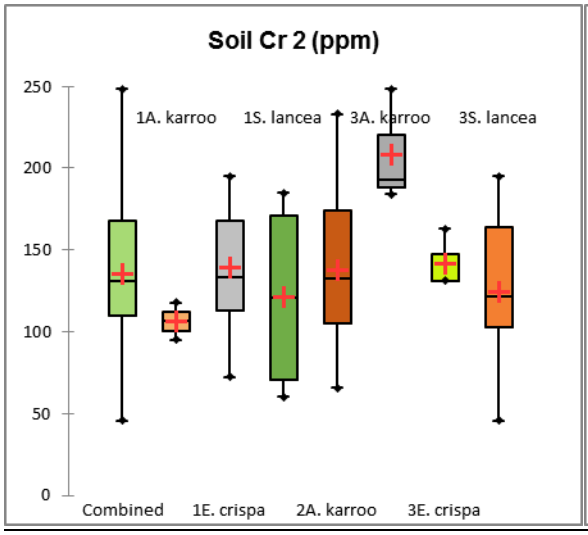

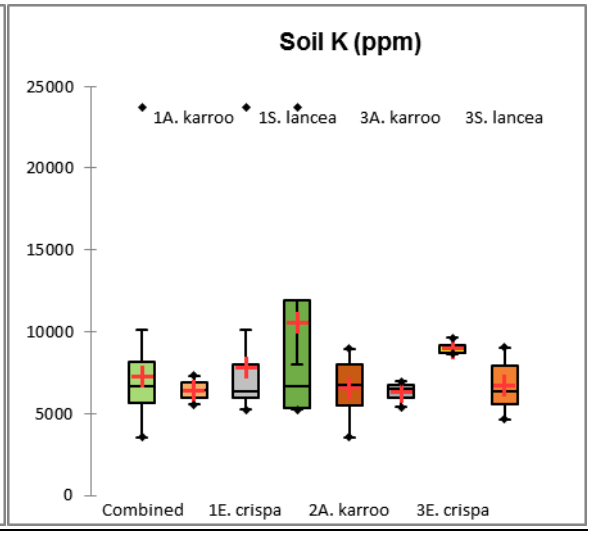

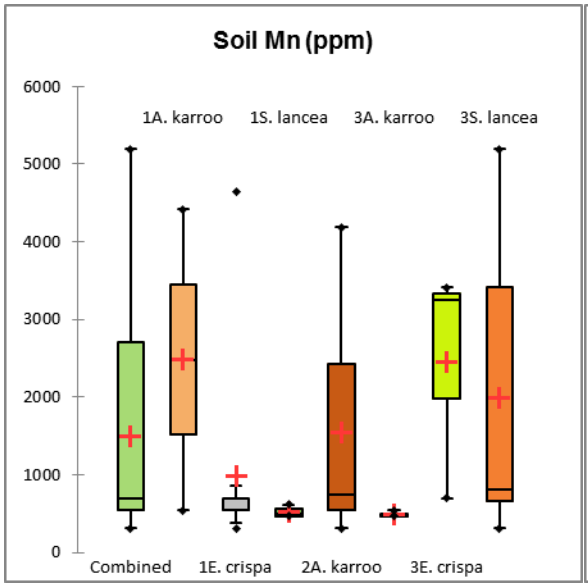
Soil Mn (ppm)
6000
5000
4000
3000
2000
1000
0
1A. karroo
1S. lancea
3A. karroo
3S. lancea
Combined
1E. crispa
2A. karroo
3E. crispa

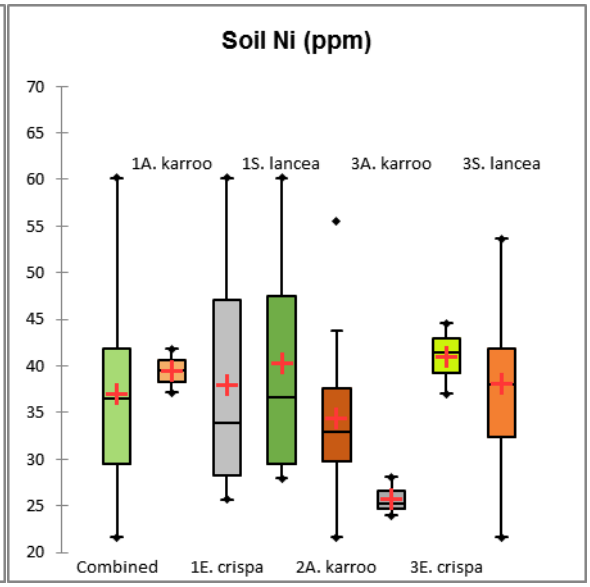
Soil Ni (ppm)
70
65
60
55
50
45
40
35
30
25
20
1A. karroo
1S. lancea
3A. karroo
3S. lancea
Combined
1E. crispa
2A. karroo
3E. crispa

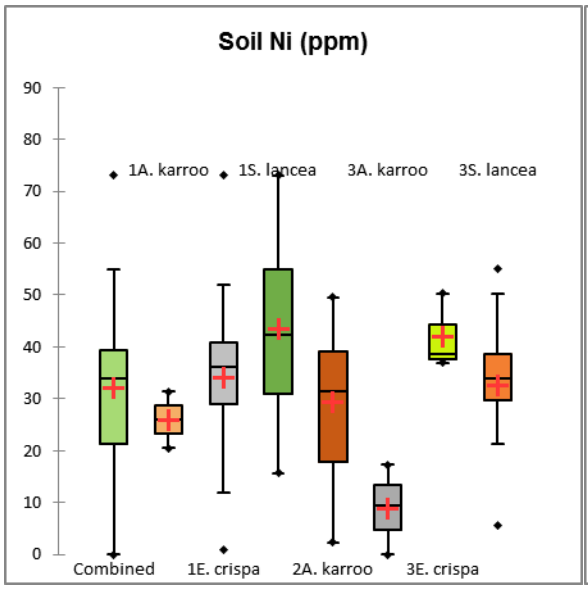
Soil Ni (ppm)
90
80
70
60
50
40
30
20
10
0
1A. karroo
1S. lancea
3A. karroo
3S. lancea
Combined
1E. crispa
2A. karroo
3E. crispa

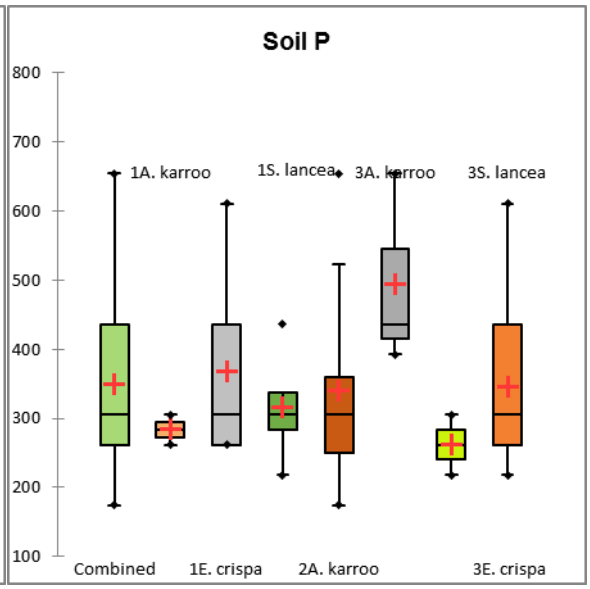
Soil P
800
700
600
500
400
300
200
100
1A. karroo
1S. lancea
3A. karroo
3S. lancea
Combined
1E. crispa
2A. karroo
3E. crispa

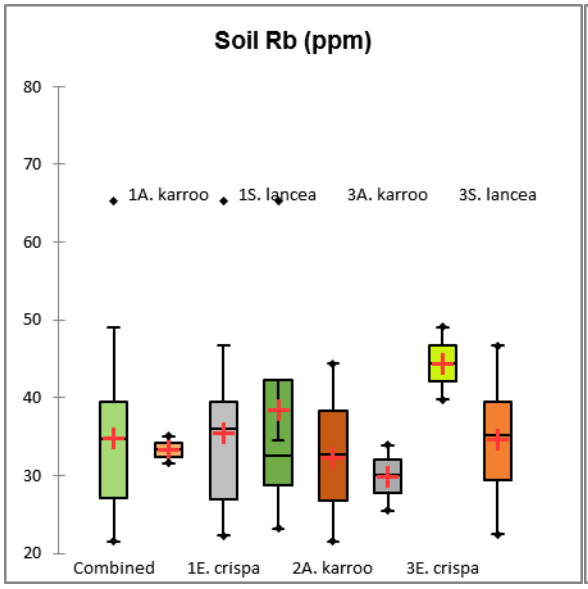
Soil Rb (ppm)
80
70
60
50
40
30
20
1A. karroo
1S. lancea
3A. karroo
3S. lancea
Combined
1E. crispa
2A. karroo
3E. crispa

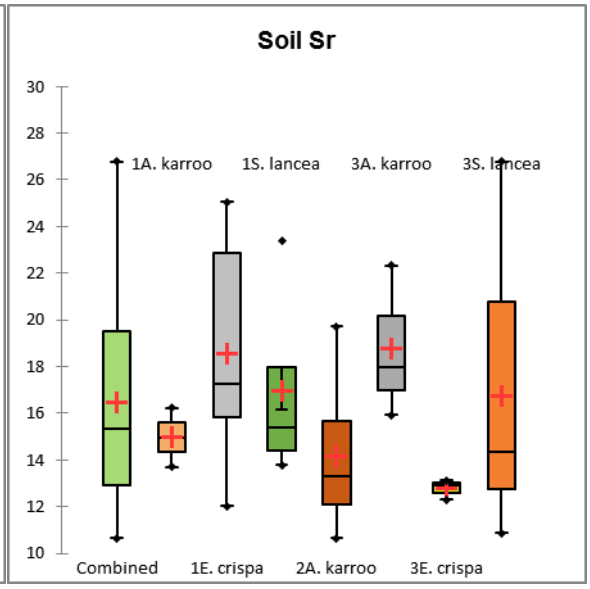
Soil Sr
30
28
26
24
22
20
18
16
14
12
10
1A. karroo
1S. lancea
3A. karroo
3S. lancea
Combined
1E. crispa
2A. karroo
3E. crispa

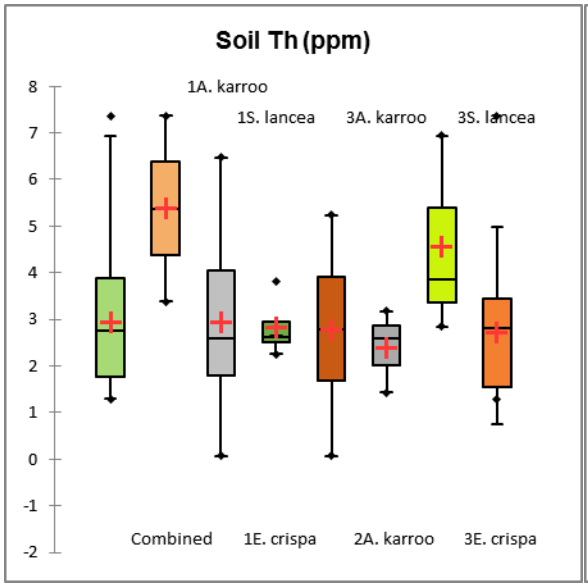
Soil Th (ppm)
8
7
6
5
4
3
2
1
0
-1
-2
1A. karroo
1S. lancea
3A. karroo
3S. lancea
Combined
1E. crispa
2A. karroo
3E. crispa

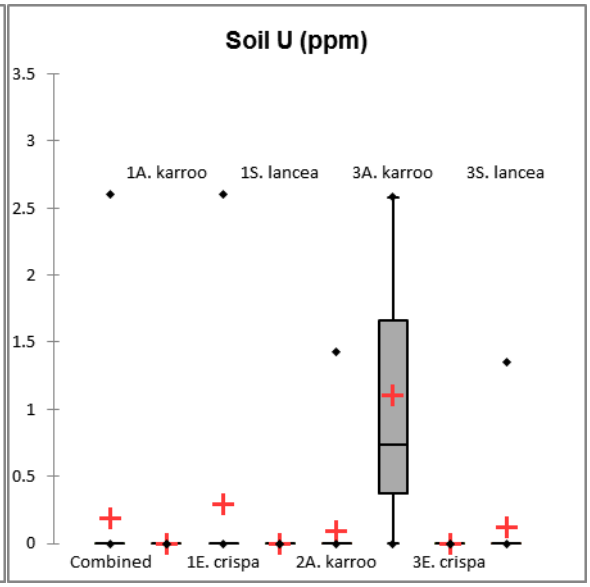
Soil U (ppm)
3.5
3
2.5
2
1.5
1
0.5
0
1A. karroo
1S. lancea
3A. karroo
3S. lancea
Combined
1E. crispa
2A. karroo
3E. crispa

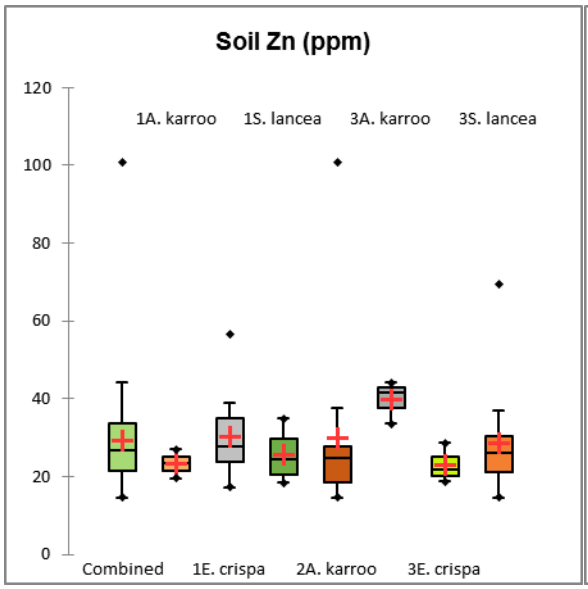
Soil Zn (ppm)
120
100
80
60
40
20
0
1A. karroo
1S. lancea
3A. karroo
3S. lancea
Combined
1E. crispa
2A. karroo
3E. crispa

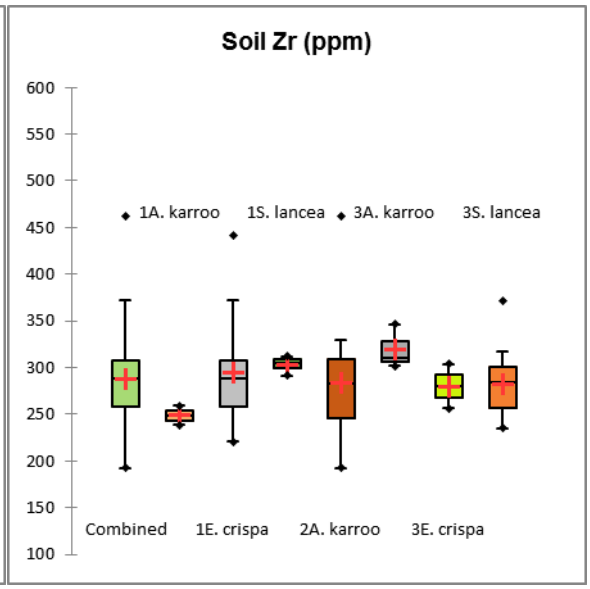
Soil Zr (ppm)
600
550
500
450
400
350
300
250
200
150
100
1A. karroo
1S. lancea
3A. karroo
3S. lancea
Combined
1E. crispa
2A. karroo
3E. crispa

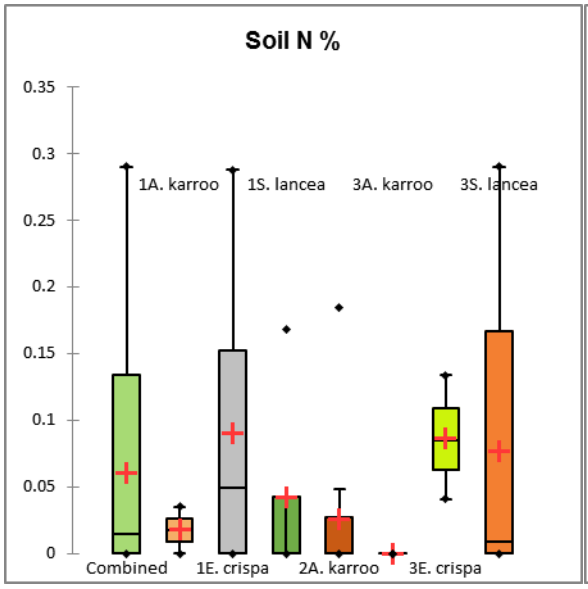
Soil N %
0.35
0.3
0.25
0.2
0.15
0.1
0.05
0
1A. karroo
1S. lancea
3A. karroo
3S. lancea
Combined
1E. crispa
2A. karroo
3E. crispa

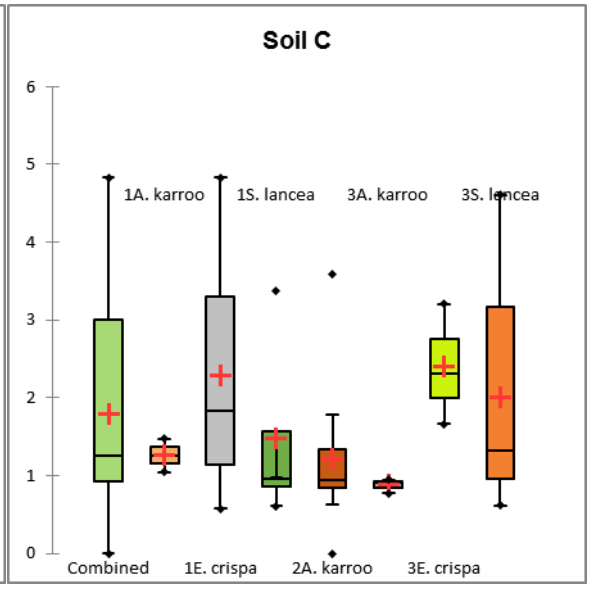
Soil C
6
5
4
3
2
1
0
1A. karroo
1S. lancea
3A. karroo
3S. lancea
Combined
1E. crispa
2A. karroo
3E. crispa

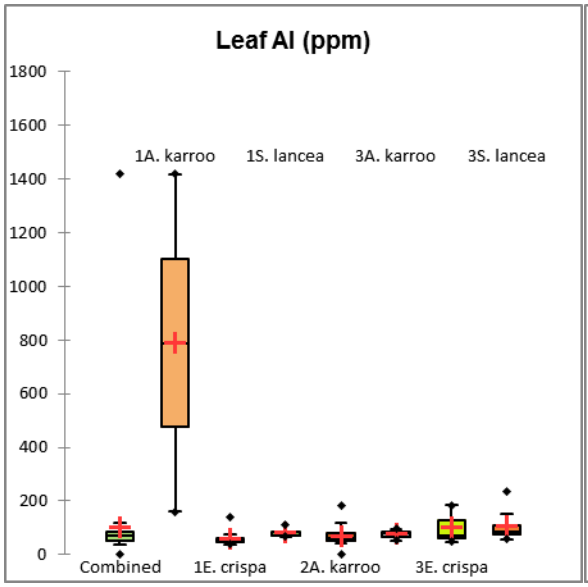
Leaf Al (ppm)
1800
1600
1400
1200
1000
800
600
400
200
0
1A. karroo
1S. lancea
3A. karroo
3S. lancea
Combined
1E. crispa
2A. karroo
3E. crispa

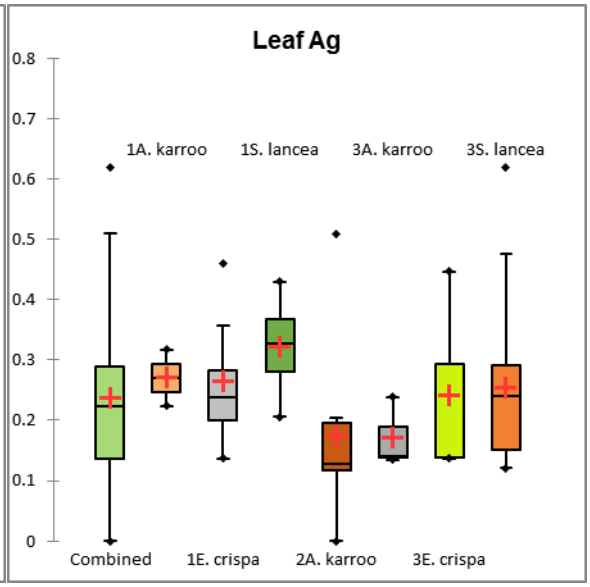
Leaf Ag
0.8
0.7
0.6
0.5
0.4
0.3
0.2
0.1
0
1A. karroo
1S. lancea
3A. karroo
3S. lancea
Combined
1E. crispa
2A. karroo
3E. crispa

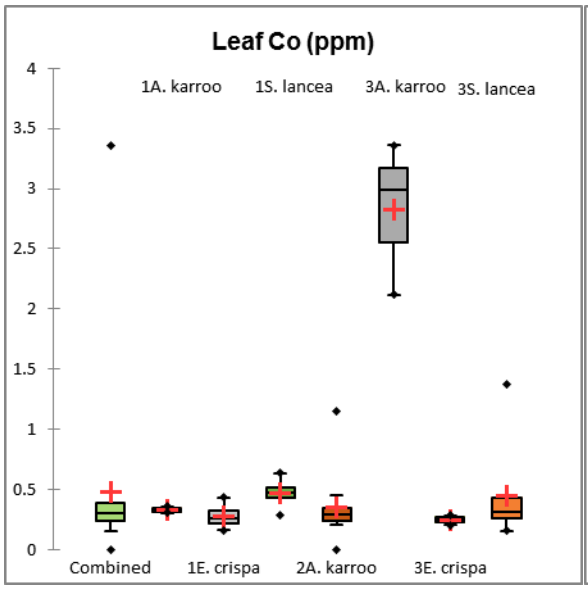
Leaf Co (ppm)
4
3.5
3
2.5
2
1.5
1
0.5
0
1A. karroo
1S. lancea
3A. karroo
3S. lancea
Combined
1E. crispa
2A. karroo
3E. crispa

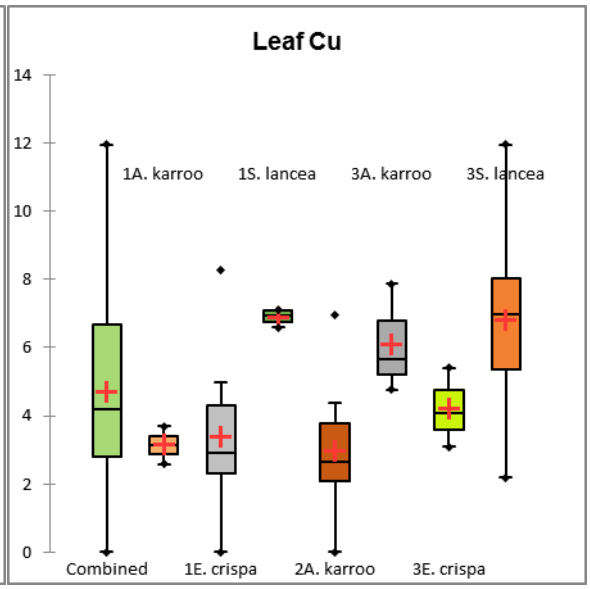
Leaf Cu
14
12
10
8
6
4
2
0
1A. karroo
1S. lancea
3A. karroo
3S. lancea
Combined
1E. crispa
2A. karroo
3E. crispa

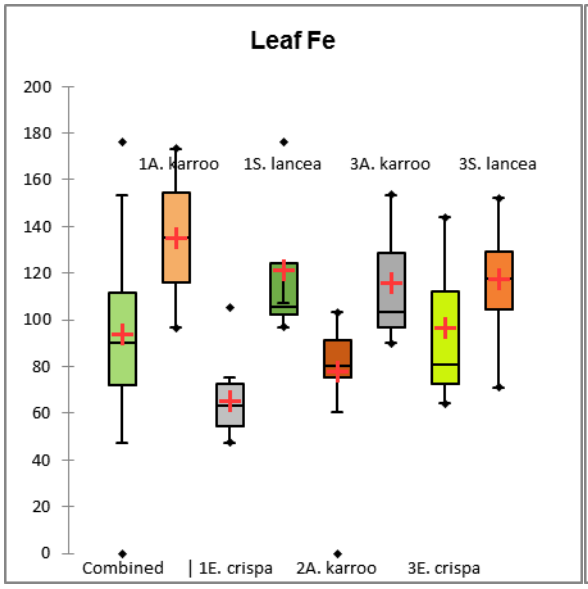
Leaf Fe
200
180
160
140
120
100
80
60
40
20
0
1A. karroo
1S. lancea
3A. karroo
3S. lancea
Combined
1E. crispa
2A. karroo
3E. crispa

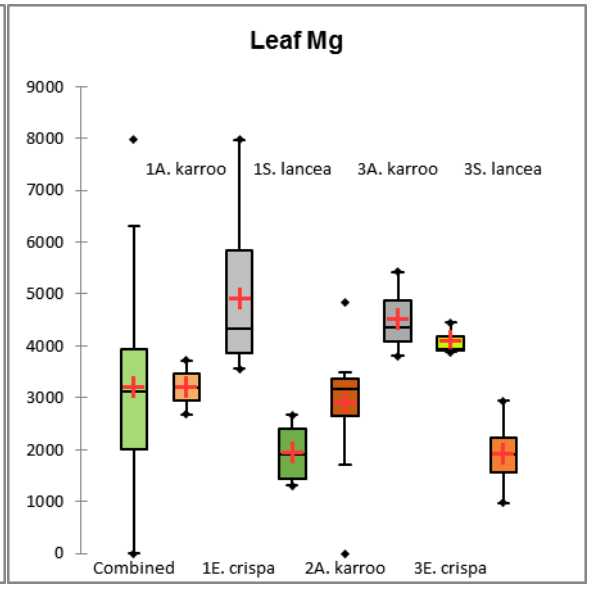
Leaf Mg
9000
8000
7000
6000
5000
4000
3000
2000
1000
0
1A. karroo
1S. lancea
3A. karroo
3S. lancea
Combined
1E. crispa
2A. karroo
3E. crispa

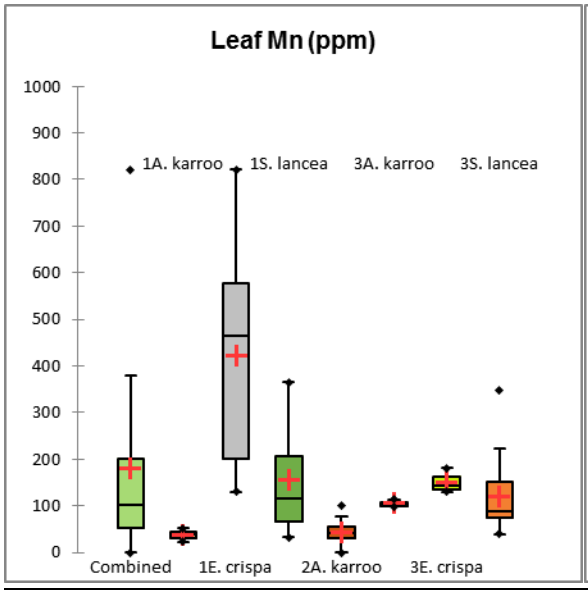
Leaf Mn (ppm)
1000
900
800
700
600
500
400
300
200
100
0
1A. karroo
1S. lancea
3A. karroo
3S. lancea
Combined
1E. crispa
2A. karroo
3E. crispa

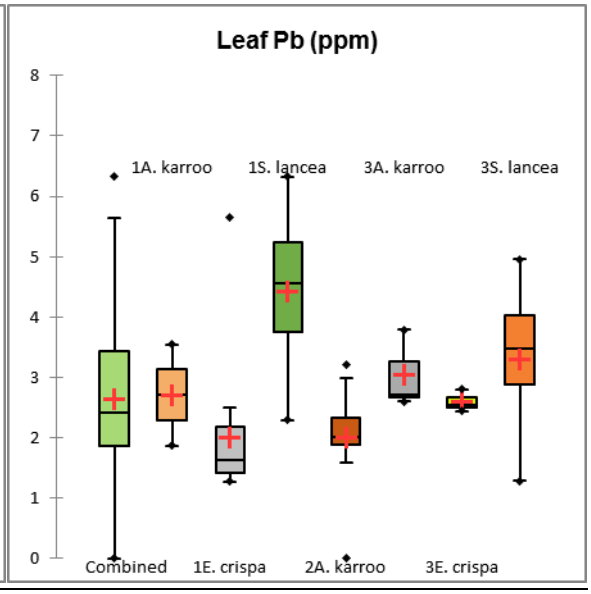
Leaf Pb (ppm)
8
7
6
5
4
3
2
1
0
1A. karroo
1S. lancea
3A. karroo
3S. lancea
Combined
1E. crispa
2A. karroo
3E. crispa

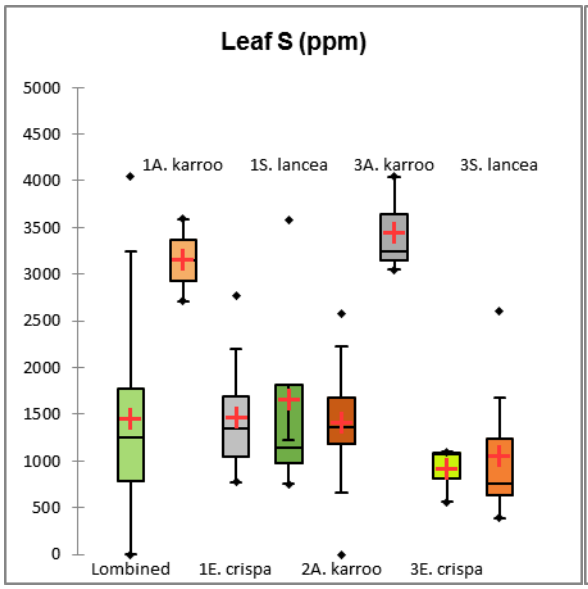
Leaf S (ppm)
5000
4500
4000
3500
3000
2500
2000
1500
1000
500
0
1A. karroo
1S. lancea
3A. karroo
3S. lancea
Lombined
1E. crispa
2A. karroo
3E. crispa

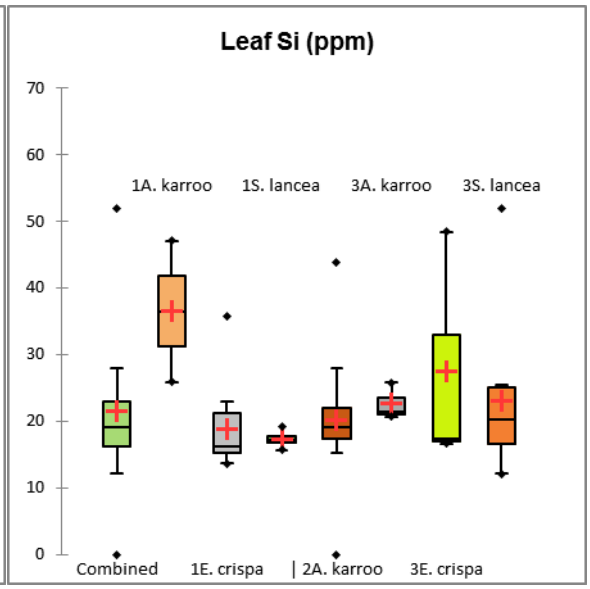
Leaf Si (ppm)
70
60
50
40
30
20
10
0
1A. karroo
1S. lancea
3A. karroo
3S. lancea
Combined
1E. crispa
2A. karroo
3E. crispa

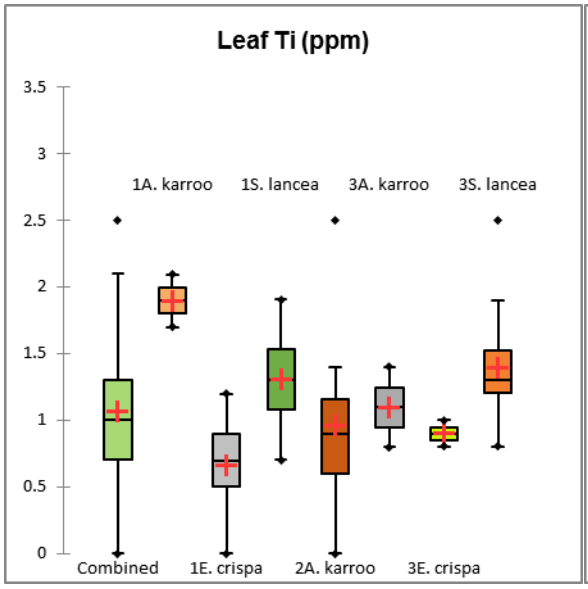
Leaf Ti (ppm)
3.5
3
2.5
2
1.5
1
0.5
0
1A. karroo
1S. lancea
3A. karroo
3S. lancea
Combined
1E. crispa
2A. karroo
3E. crispa

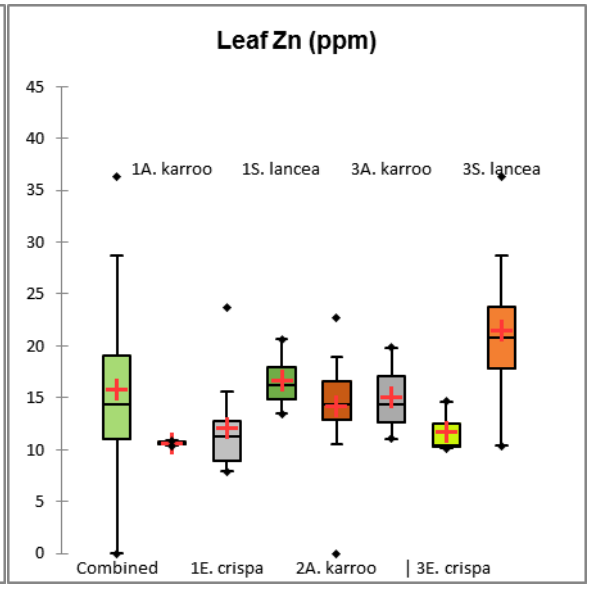
Leaf Zn (ppm)
45
40
35
30
25
20
15
10
5
0
1A. karroo
1S. lancea
3A. karroo
3S. lancea
Combined
1E. crispa
2A. karroo
3E. crispa

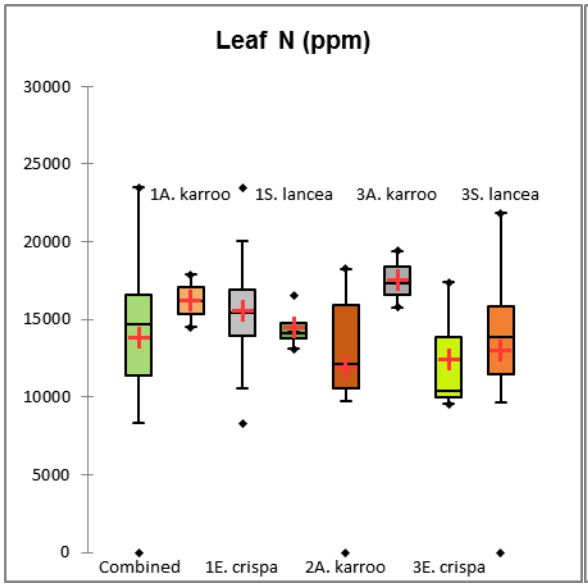
Leaf N (ppm)
30000
25000
20000
15000
10000
5000
0
1A. karroo
1S. lancea
3A. karroo
3S. lancea
Combined
1E. crispa
2A. karroo
3E. crispa

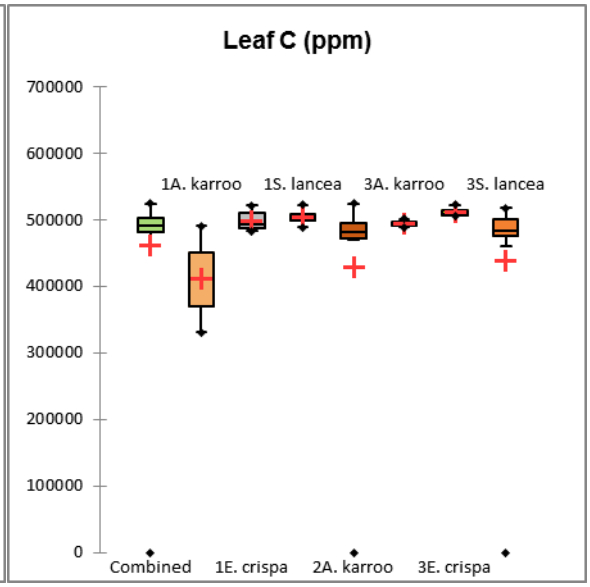
Leaf C (ppm)
700000
600000
500000
400000
300000
200000
100000
0
1A. karroo
1S. lancea
3A. karroo
3S. lancea
Combined
1E. crispa
2A. karroo
3E. crispa

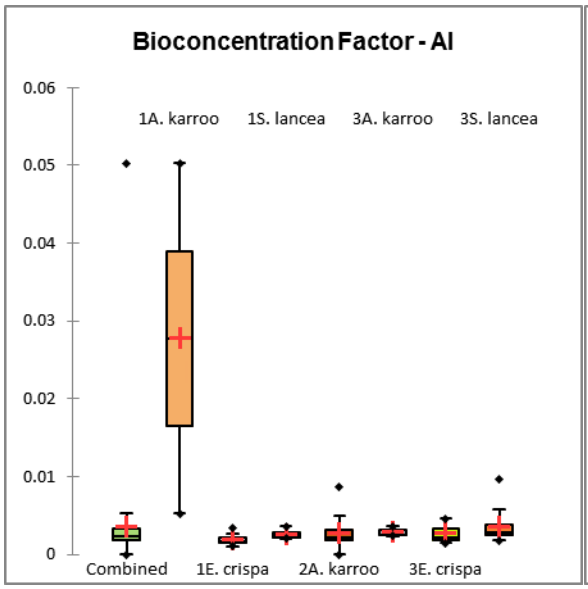
Bioconcentration Factor - Al
0.06
0.05
0.04
0.03
0.02
0.01
0
1A. karroo
1S. lancea
3A. karroo
3S. lancea
Combined
1E. crispa
2A. karroo
3E. crispa

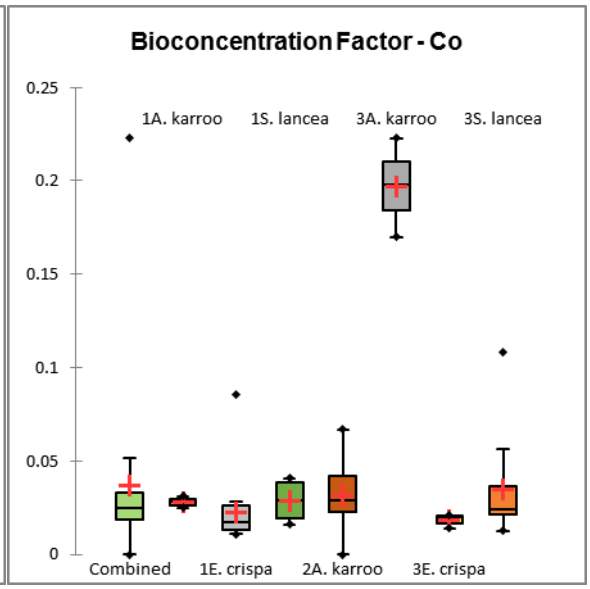
Bioconcentration Factor - Co
0.25
0.2
0.15
0.1
0.05
0
1A. karroo
1S. lancea
3A. karroo
3S. lancea
Combined
1E. crispa
2A. karroo
3E. crispa

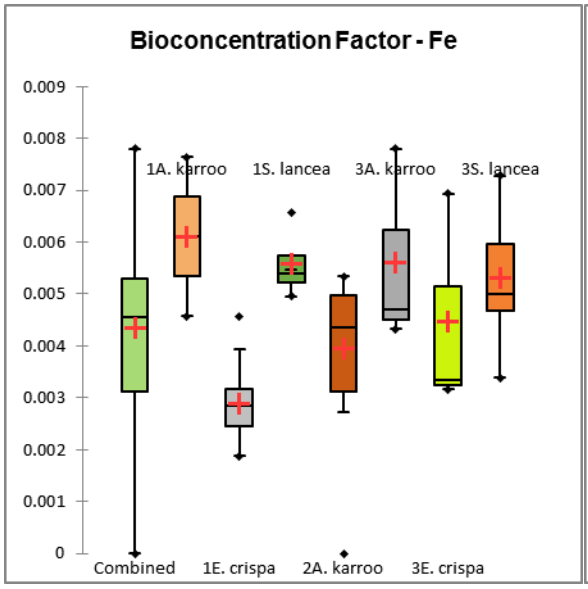
Bioconcentration Factor - Fe
0.009
0.008
0.007
0.006
0.005
0.004
0.003
0.002
0.001
0
1A. karroo
1S. lancea
3A. karroo
3S. lancea
Combined
1E. crispa
2A. karroo
3E. crispa

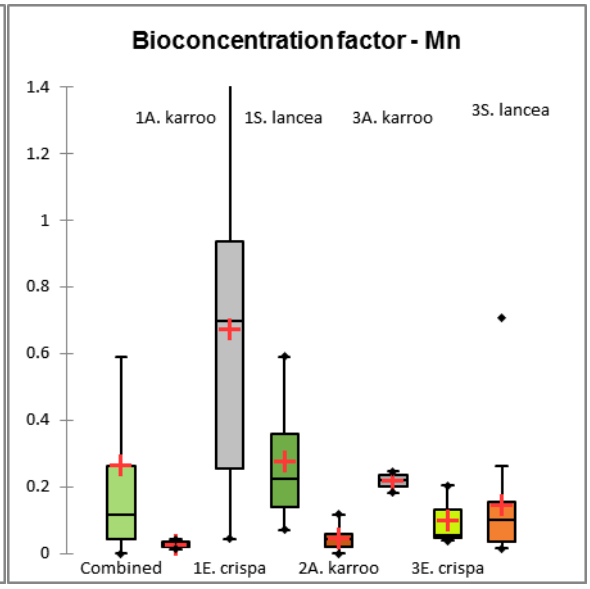
Bioconcentration factor - Mn
1.4
1.2
1
0.8
0.6
0.4
0.2
0
1A. karroo
1S. lancea
3A. karroo
3S. lancea
Combined
1E. crispa
2A. karroo
3E. crispa

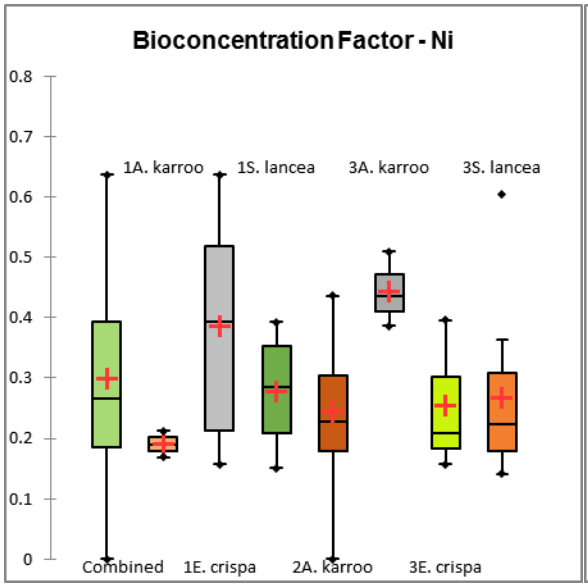
Bioconcentration Factor - Ni
0.8
0.7
0.6
0.5
0.4
0.3
0.2
0.1
0
1A. karroo
1S. lancea
3A. karroo
3S. lancea
Combined
1E. crispa
2A. karroo
3E. crispa

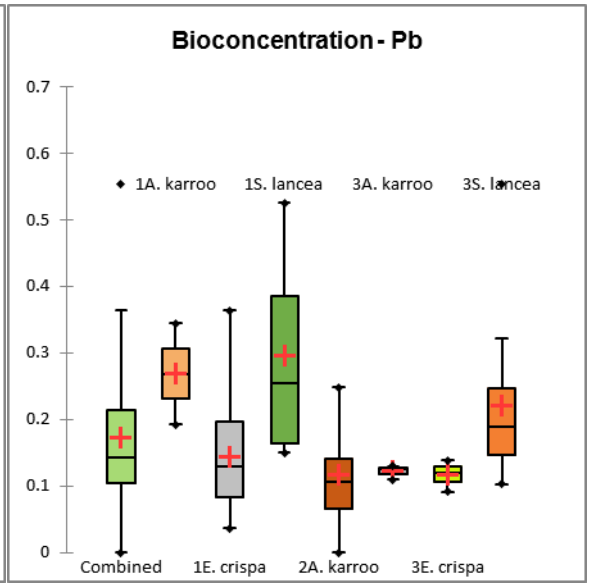
Bioconcentration - Pb
0.7
0.6
0.5
0.4
0.3
0.2
0.1
0
1A. karroo
1S. lancea
3A. karroo
3S. lancea
Combined
1E. crispa
2A. karroo
3E. crispa

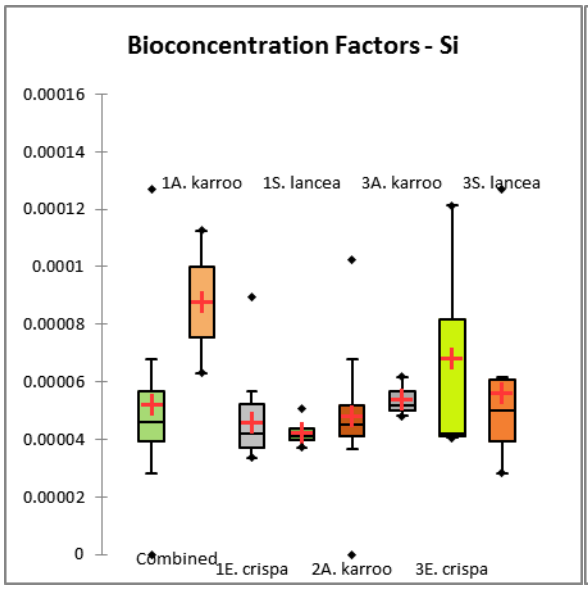
Bioconcentration Factors - Si
0.00016
0.00014
0.00012
0.0001
0.00008
0.00006
0.00004
0.00002
0
1A. karroo
1S. lancea
3A. karroo
3S. lancea
Combined
1E. crispa
2A. karroo
3E. crispa

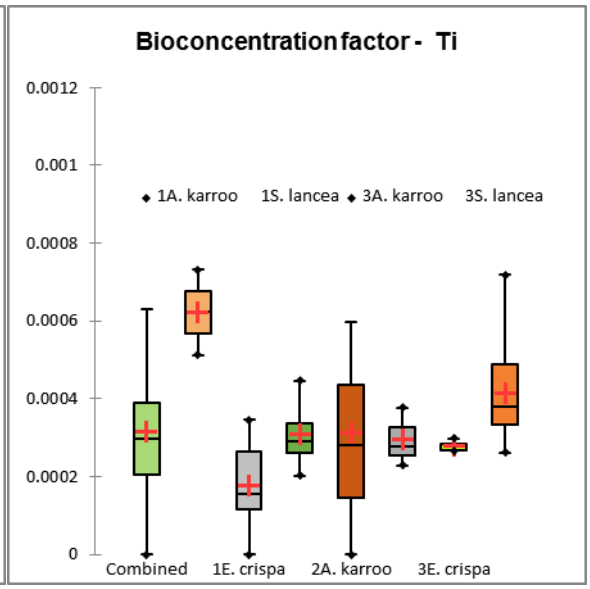
Bioconcentration factor - Ti
0.0012
0.001
0.0008
0.0006
0.0004
0.0002
0
1A. karroo
1S. lancea
3A. karroo
3S. lancea
Combined
1E. crispa
2A. karroo
3E. crispa

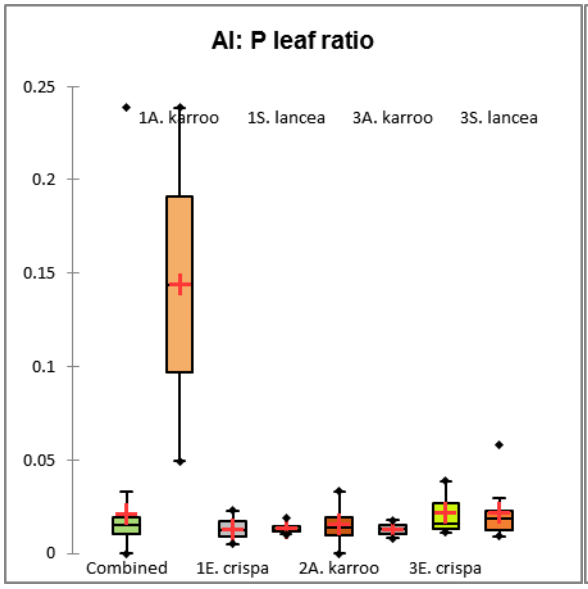
Al: P leaf ratio
0.25
0.2
0.15
0.1
0.05
0
1A. karroo
1S. lancea
3A. karroo
3S. lancea
Combined
1E. crispa
2A. karroo
3E. crispa

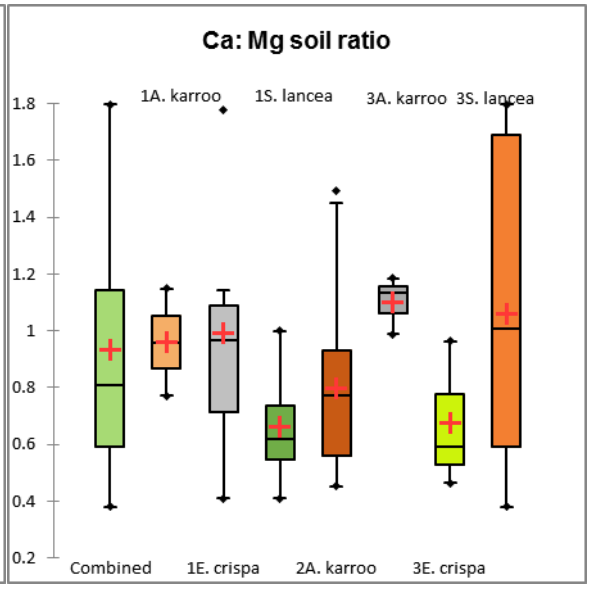
Ca: Mg soil ratio
1.8
1.6
1.4
1.2
1
0.8
0.6
0.4
0.2
1A. karroo
1S. lancea
3A. karroo
3S. lancea
Combined
1E. crispa
2A. karroo
3E. crispa

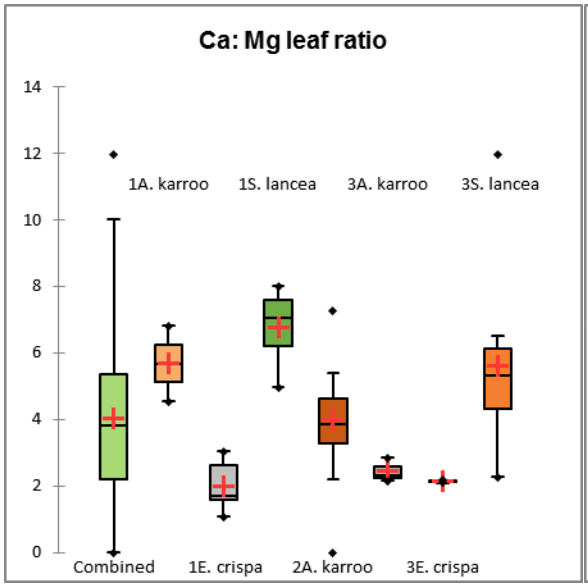
Ca: Mg leaf ratio
14
12
10
8
6
4
2
0
1A. karroo
1S. lancea
3A. karroo
3S. lancea
Combined
1E. crispa
2A. karroo
3E. crispa

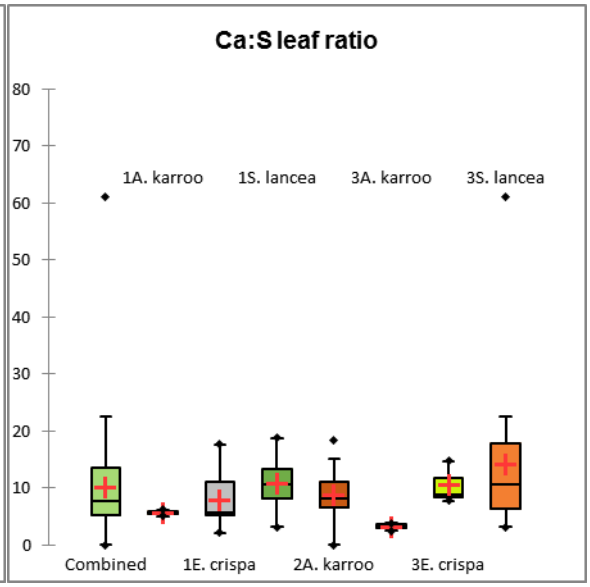
Ca:S leaf ratio
80
70
60
50
40
30
20
10
0
1A. karroo
1S. lancea
3A. karroo
3S. lancea
Combined
1E. crispa
2A. karroo
3E. crispa

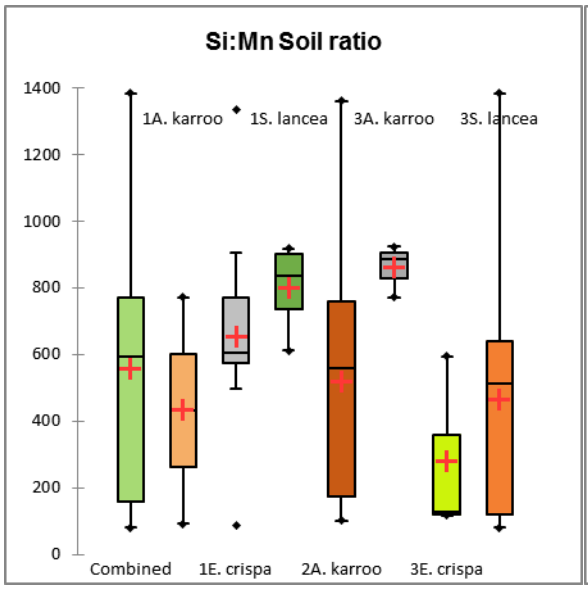
Si:Mn Soil ratio
1400
1200
1000
800
600
400
200
0
1A. karroo
1S. lancea
3A. karroo
3S. lancea
Combined
1E. crispa
2A. karroo
3E. crispa

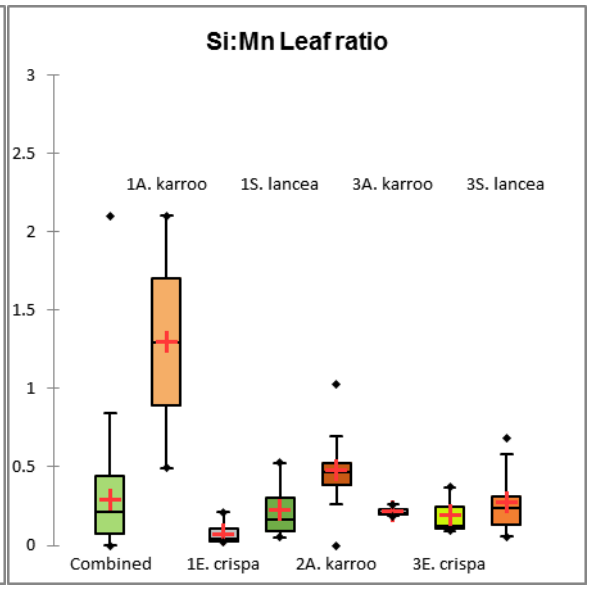
Si:Mn Leaf ratio
3
2.5
2
1.5
1
0.5
0
1A. karroo
1S. lancea
3A. karroo
3S. lancea
Combined
1E. crispa
2A. karroo
3E. crispa

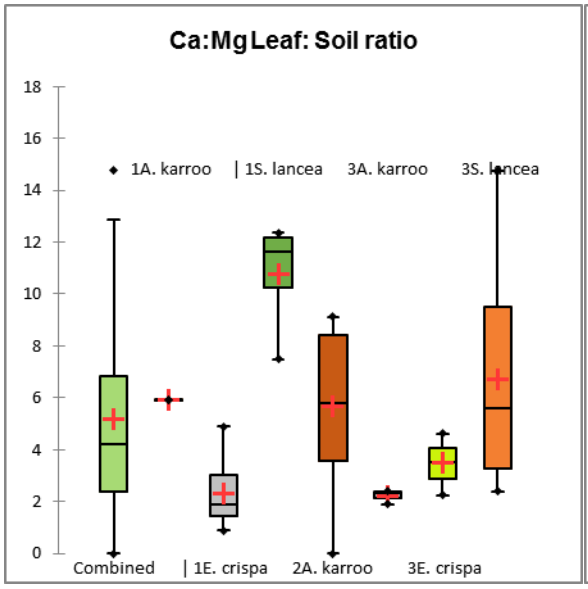
Ca:Mg Leaf: Soil ratio
18
16
14
12
10
8
6
4
2
0
1A. karroo
1S. lancea
3A. karroo
3S. lancea
Combined
1E. crispa
2A. karroo
3E. crispa

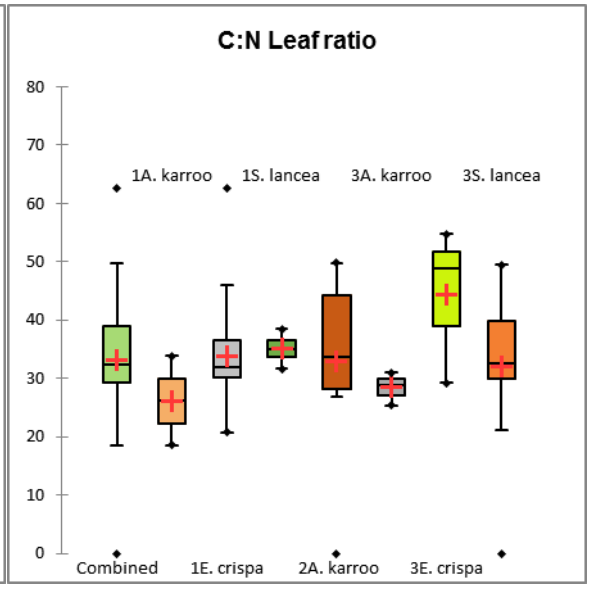
C:N Leaf ratio
80
70
60
50
40
30
20
10
0
1A. karroo
1S. lancea
3A. karroo
3S. lancea
Combined
1E. crispa
2A. karroo
3E. crispa

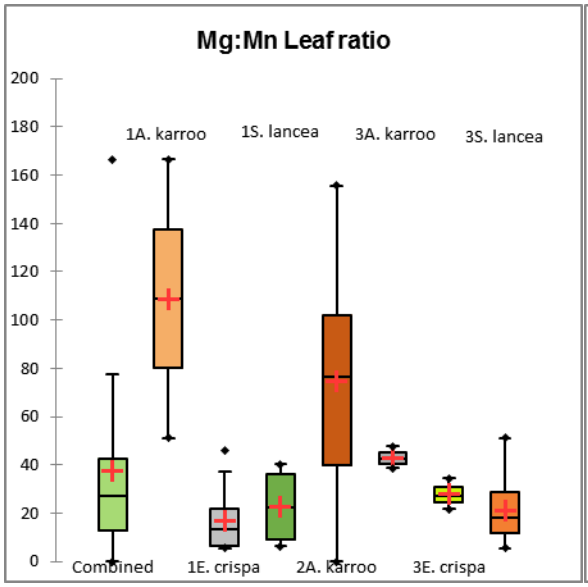
Mg:Mn Leaf ratio
200
180
160
140
120
100
80
60
40
20
0
1A. karroo
1S. lancea
3A. karroo
3S. lancea
Combined
1E. crispa
2A. karroo
3E. crispa

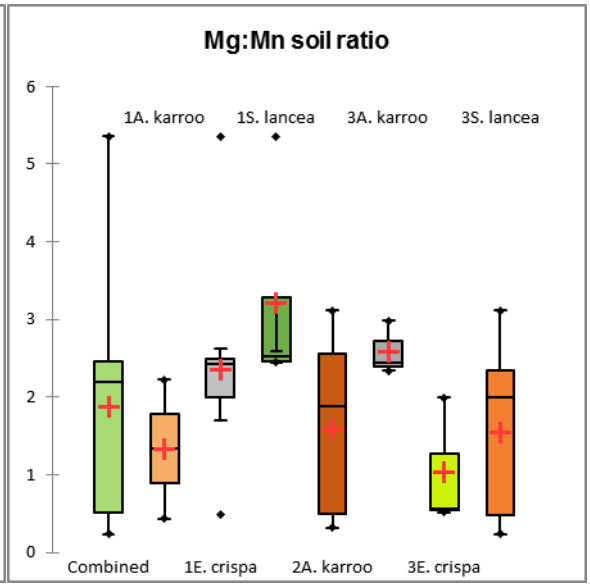
Mg:Mn soil ratio
6
5
4
3
2
1
0
1A. karroo
1S. lancea
3A. karroo
3S. lancea
Combined
1E. crispa
2A. karroo
3E. crispa

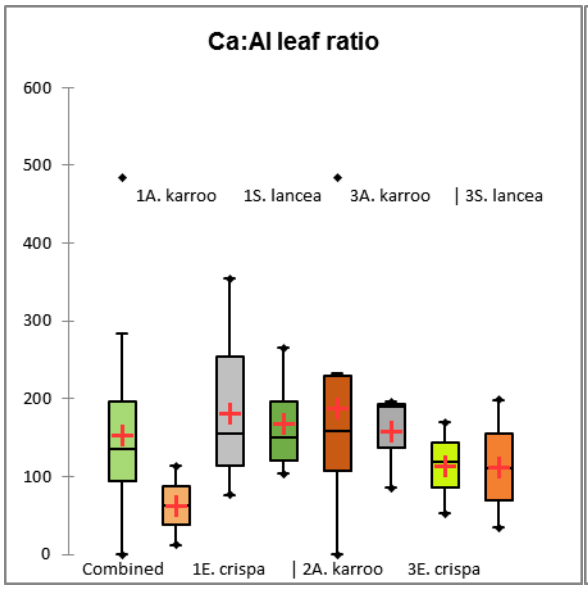
Ca:Al leaf ratio
600
500
400
300
200
100
0
1A. karroo
1S. lancea
3A. karroo
3S. lancea
Combined
1E. crispa
2A. karroo
3E. crispa

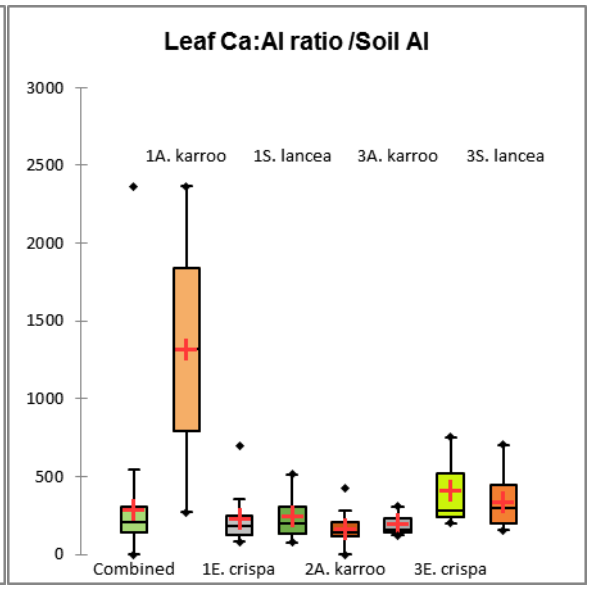
Leaf Ca:Al ratio /Soil Al
3000
2500
2000
1500
1000
500
0
1A. karroo
1S. lancea
3A. karroo
3S. lancea
Combined
1E. crispa
2A. karroo
3E. crispa